Nucleic acids and SNP detection via template-directed native chemical ligation and inductively coupled plasma mass spectrometry

Dissertation

zur Erlangung des akademischen Grades

doctor rerum naturalium

(Dr. rer. nat.)

im Fach Chemie: Angewandte Analytik und Umweltchemie

eingereicht an der

Mathematisch-Naturwissenschaftlichen Fakultät

der Humboldt-Universität zu Berlin

von

M. Sc. Pablo Lores Lareo

Präsidentin der Humboldt-Universität zu Berlin

Prof. Dr.-Ing. Dr. Sabine Kunst

Dekan der Mathematisch-Naturwissenschaftlichen Fakultät

Prof. Dr. Elmar Kulke

Gutachter:

1. Prof. Dr. Oliver Seitz
2. Prof. Dr. Michael W. Linscheid
3. Prof. Dr. Ilko Bald

Tag der mündlichen Prüfung: 26.03.2019

Die vorlegende Arbeit wurde von April 2013 bis März 2017 in den Arbeitskreis von Prof. Dr. Oliver Seitz und von Prof. Dr. Michael W. Linscheid am Institut für Chemie der Humboldt-Universität zu Berlin angefertigt.

Kurzzusammenfassung

In den letzten Jahren gab es rasche Weiterentwicklungen auf dem Gebiet der Nukleinsäure-Erkennung. Von microRNA-Quantifizierung zur Untersuchung von Zelltods, --Teilung und -Regulation bis zur Bewertung genetischer Variabilität in Hinblick auf Krankheitsentstehung und -Behandlung: Die Analyse von Nukleinsäuren wird in der zukünftigen Medizin eine zentrale Rolle zukommen. Vor allem die Erkennung von SNPs als Hauptquelle der genetischen Vielfalt, aber aus Analysesicht auch eine der herausforderndsten Mutationen, stellt in dieser Hinsicht einen wesentlichen Aspekt dar. Methoden zur SNP-Erkennung müssen nicht nur sensibel, selektiv und stabil, sondern auch vielfältig sein und eine der wachsenden Analyseanzahl gerecht werdende hohe Verarbeitungsmenge bieten.

Im Rahmendieser Arbeit wurde ein chemisches Prüfverfahren zur Erkennung von Nukleinsäuren und Einzelnukleotid-Polymorphismen (SNPs) entwickelt. Das Reaktionssystem zur Nukleinsäuren-Erkennung beruht hierbeiauf der Interaktion zweier modifizierter Peptid-Nukleinsäure (PNS) Oligonukleotiden. Das Erste beinhaltet einen C-terminalen Thioester (Donor-Sonde), die zweite einen N-terminalen Cysteinyl-Rest (Akzeptor-Sonde). Zusätzlich ist die Donor-Sonde durch einen makrocyclischen Metall Chelatkomplex aus 1,4,7,10-tetraazacyclododecan-1,4,7,10-tetraessigsäure (DOTA) mit einem gebundenen lanthanoid-tag funktionalisiert. In die Akzeptor-Sonde wurde, zur Reinigung mit magnetischen Streptavidin Partikeln, Biotin integriert. Der Ziel-DNA-Strang bringt beide Sonden in räumliche Nähe zueinander und ermöglicht so eine chemische Reaktion. Das so gewonnene Ligationsprodukt beinhaltet den Lanthanoid-Tag und Biotin, über welches das Produkt gereinigt wird, bevor die Detektion mittels ICP-MS erfolgt. Die Lanthanoid Konzentration dient als Indikator des Ligationsprodukts welches wiederum den Reporter des Ziel-DNS-Strangs darstellt. Die, mithilfe dieses Systems erreichte, methodische Nachweisgrenze lag bei 29 pM mit einem RSD von 6,8% bei 50 pM (n=5).

Zur Erkennung von SNPs wurde das Experiment mit einer Kombination zweier-Sets PNS Sonden mit unterschiedlichen Lanthanoid Tags durchgeführt. Das erste Set zielte auf die SNP beinhaltende Sequenz (Reportersystem) ab, während das zweite an eine benachbarte Sequenz (Kontrollsystem) binden sollte. Zur Erkennung der SNP wurden die Signale bei der Lanthanoide wurden ins Verhältnis gesetzt. Mithilfe dieses Verfahrens konnte durch Messung von sechs Lanthaniden bei einer Konzentration von 5 nM erfolgreich simultan zwischen den Allelen dreier SNPs unterschieden werden.

Abstract

The field of nucleic acid detection has evolved swiftly in recent years. From quantification of micro RNA for the study of cell death, proliferation, and regulation, to the assessment of the influence of genetic variability towards disease development and treatment, the analysis of nucleic acids will play a central role in future medicine. In that regard, the detection of SNPs, as the primary source of genetic variability and the most challenging mutation from the analytical point of view, will be at the forefront of the discussion. Methods for the detection of SNPs not only require sensitivity, selectivity and robustness, but they should also allow multiplexing and offer high throughput in order to face the growing analysis demand

In this work an assay for the detection of nucleic acids and single nucleotide polymorphisms (SNPs) was developed. The reaction system for the detection of nucleic acids is based on the interaction between two modified peptide nucleic acid (PNA) oligonucleotides. The first incorporated a C-terminal thioester (donor probe), and the second one a N-terminal cysteinyl residue (acceptor probe). In addition, the donor probe is functionalized with a metal-tag, which consist of a macrocyclic metal chelate complex of 1,4,7,10-tetraazacyclododecane-1,4,7,10-tetraacetic acid (DOTA) with a chelated lanthanoide. A biotin tag for purification by streptavidin magnetic particles was incorporated in the acceptor probe. The target DNA strand brings together the reporter probes allowing the chemical reaction. The resulting ligation product contains the metal-tag and the biotin, which is used to purify the product before measurement in the ICP-MS system. The lanthanoid concentration is used as an indicator of the ligation product, which at the same time serves as reporter of the target template. The methodological limit of detection achieved with this system was 29 pM with RSD of 6.8% at 50 pM (n=5).

Detection of SNPs was performed using a combination of two sets of PNA probes labeled with different lanthanoid metal tags. The first probe set targeted the sequence where the SNP was present (reporter probe system), while the second set of probes was designed to bind to a neighboring sequence (control probe system). The signals of both lanthanides were used to establish a ratio that allowed the detection of the SNP. This assay was successfully used to simultaneously differentiate between alleles of 3 SNPs by measuring six lanthanoids at 5 nM concentration.

Contents

List of Abbreviations

ε	Extinction coefficient
ΔG	Gibb's free energy
ΔH	Enthalpy
ΔS	Entropy
λ	Wavelength
DNA	Deoxyribonucleic acid
dsDNA	Double stranded DNA
ssDNA	Single stranded DNA
et al.	*et alia*
k	Rate constant
K	Equilibrium constant
Ln	Lanthanide
LOD	Limit of detection
LOQ	Limit of quantification
MeCAT	Metal-coded affinity tag
MDL	Methodological limit of detection
MW	Molecular weight
m/z	mass to charge ration
NCBI	National Center for Biotechnology Information
NCL	Native chemical ligation
NGS	Next generation sequencing
NTP	Nucleside Triphosphate
dNTP	Deoxynucleotidetriphosphate
ddNTP	di-deoxynucleotidetriphosphate
NTC	Non-templated control
OR	Odds ration
PCR	Polymerase chain reaction
qPCR	Real-time PCR
pH	Potential of hydrogen
PNA	Peptide nucleic acid
RF	Radio frequency
RNA	Ribonucleic acid
RSD	Relative standard deviation
SNP	Single nucleotide polymorphism
SPPS	Solid-phase peptide synthesis
T_m	Melting temperature
v	volume

Units

%	percentage
s	second
min	minute
h	hour
m	meter
M	molar
L	litter
cps	counts per second
eV	Electronvolt
Torr	1/760 of a standard atmosphere
amu	unified atomic mass unit
ppm	parts per million
ppb	parts per billion
ppt	parts per trillion
Hz	Hertz

Instrumentation

ESI	Electrospray ionization
HPLC	High-performance liquid chromatography
ICP	Inductively-coupled plasma
MALDI	Matrix assisted laser desorption/ionization
MS	Mass spectrometry
UPLC	Ultra-performance liquid chromatography

Chemicals

Boc	*tert*-Butyloxycarbonyl protecting group
BSA	Bovine serum albumin
CbZ	Carboxybenzyl protecting group

Contents

CHAPS	3-[(3-Cholamidopropyl) dimethylammonio]-1-propanesulfonate
DCM	Dichloromethane
DIPEA	*N*-Ethyl-*N*-(propan-2-yl)propan-2-amine
DMF	*N*,*N*-Dimethylformamide
DOTA	1,4,7,10-Tetraazacyclododecane-1,4,7,10-tetraacetic acid
EDTA	2,2′,2″,2‴-(Ethane-1,2-diyldinitrilo)tetraacetic acid
FA	Formic acid
Fmoc	Fluorenylmethyloxycarbonyl protecting group
HCl	Hydrogen chloride
H_2O_2	Hydrogen peroxide
H_2SO_4	Sulfuric acid
MeCN	Acetonitrile
MPA	3-Mercaptopropionic acid
MPAA	4-Mercaptophenylacetic acid
MESNa	Sodium 2-mercaptoethanesulfonate
MOPS	3-Morpholinopropane-1-sulfonic acid
NaCl	Sodium chloride
NaOH	Sodium hydroxide
NMP	1-Methylpyrrolidin-2-one
PyBOP	(Benzotriazol-1-yloxy)tripyrrolidinophosphonium hexafluorophosphate
TFA	Trifluoroacetic acid
TFMSA	Trifluoromethanesulfonic acid
TCEP	3,3′,3′′-Phosphanetriyltripropanoic acid
Trt	Trityl protectinc group
Tris	2-Amino-2-(hydroxymethyl)propane-1,3-diol

Bases

A/a	DNA/PNA	Adenine
C/c	DNA/PNA	Cytosine
G/g	DNA/PNA	Guanine
T/t	DNA/PNA	Thymine

Amino Acids

G	Gly	Glycin
K	Lys	Lysin
C	Cys	Cystein

Prefix

k	10^{3}	kilo
c	10^{-2}	centi
m	10^{-3}	milli
µ	10^{-6}	micro
n	10^{-9}	nano
p	10^{-12}	pico
f	10^{-15}	femto
a	10^{-18}	atto

List of Figures

Contents

List of Schemes

List of Tables

1 Foreword

The longest run home

I would like to start my dissertation with one simple question: how much do we actually know that we can measure? I mean it in a pure way. As a scientist in training, I go to the laboratory and I take several facts for granted that "others" have tested: reactions happen, there is an explanation for most phenomena, instruments measure, and chemicals are pure. When I write "others" I mean previous generations of people on whose work we rely; however, when and how does it all start? How are things explained when there is no previous knowledge on reactions, when the instruments are as simple as the tools that we can build with our hands, and phenomena are still limited to what it can be seen, heard, tasted, and touched? For example, let us go back in time to ancient Greece, for the sake of the narrative, to the 6th century before Christ. How could you then explain the physical similitude among members of the same lineage? When people mate, descendants take some of their physical features, and siblings look alike in some cases they are even identical.

It is common knowledge, that one of the first theories that we keep record of to explain such phenomenon is from Pythagoras. In addition to his contributions to mathematics and geography, Pythagoras applied his famous right-angled triangles to solve the inheritance question: the hereditary information was carried in male semen, which matured in a fetus after being transferred into the female's womb through intercourse. The semen compiled all the information while traveling through the male's body. As in the right-angle triangle that gave Pythagoras his fame, one of the sides in heredity is greater; in this case, it is the male contribution, who in theory had all the information, while the mother only provided the nutrition and nourishment. The basis of such theories prevailed over time. In the middle age, the reigning theory in Europe was the preformation, which was based on the existence of a fully formed and shrunk fetus. Such fetus would be passed from male to female in whose womb it would grow into a fully matured human.

It is difficult to imagine how to approach the inheritance question with only our eyes and hands. Although the first revolution in the field came with an outstanding application of the scientific method by Gregor Johann Mendel, when he discovered that inheritance involves passing of discrete units of information (genes) from parents to offspring, further advances required the conjunction of chemistry and physics for the development of the proper analytical methods. For example, the determinations that genes were located into chromosomes would not have been possible without DNA staining and improvements in optics. In the same line, the DNA structure elucidation would not have been possible without neither information from the X-ray diffraction images of Rosalind Franklin, nor the molecular models from James Watson and Francis Crick. A race for knowledge that started hundreds of years ago, could not be solved until the right tools were developed. In the same manner, future advances should only arise if the right fields are combined, and synergies are exploited to their maximum exponential. If we are ever to fully understand our own nature, and finish this race, we cannot study its separate parts, we will need to combine technologies and techniques to visualize the whole reality and uncover the knowledge that resides under the limit of detection.

2 Fundamentals

The international Human Genome Sequencing consortium published the finished euchromatic sequence of the human genome in 2004 as one of the biggest research collaboration in human history.[1] From the sequence of 2,85 billion nucleotides we learned afterwards that 4,1 to 5,0 million sites are responsible for the genetic variance among Humans.[2] Not only our eye and hair color but also a large number of diseases and metabolic variations are determined by a minimal fraction of the whole sequence, making genome study and profiling an indispensable tool in drug discovery.[3-4] Most of this variability comes from single nucleotide polymorphisms (SNPs), with 84.7 million variations, followed by short insertions and deletions (indels) with an estimate number of 3.6 million variations, and finally, 60.000 structural variants.

2.1. Single Nucleotide Polymorphism (SNP)

A single nucleotide polymorphism (SNP) is a variation in a single nucleotide that occurs at a specific position in the genome, with the rarer allele having a frequency of at least 1% in a random set of individuals in a population. This variation can be either a substitution, a deletion, or an insertion of a base pair. The most abundant in a population is usually known as wild-type allele and among distinct populations the most common allele might diverge. SNPs are accountable for 96% of the human genetic variability,[2] and their presence may not only lead to the development of diseases,[5] but they can also affect how diseases develop,[6] and the effectiveness of the treatment used.[7]

In the latest SNP-build released of the National Center for Biotechnology Information (build 150 from February 3rd, 2017), a total number of 325.7 million SNPs had been reported.[8] Despite the great number, not all have the same effect. SNPs can occur in non-coding regions or coding regions, and while in a coding region, they can affect the sequence of the encoding protein or leave it unchanged due to the degeneracy and redundancy of the genetic code (several three-base pair combinations can code for the same amino acid). At the same time, once there is a change in the sequence, the effect can vary depending on the mutagenic SNP to code for a change in the translated amino acid (missense mutation) or a stop in the translation process (nonsense mutation). The effect on a different amino acid can be limited, while the interruption in the sequence can have a more severe outcome. For example, the third most common cystic fibrosis mutation is caused by a glycine-to-aspartic acid missense mutation at codon 551 (G551D),[9] whereas the substitution of adenine by uracil in the mRNA for β-globin results in the

lysine-to-termination missense mutation which in consequence leads to the development of β^0 thalassemia.[10]

SNPs are not only directly associated to several Mendelian diseases, conditions caused by one or more abnormalities in the genome, but they are also a risk factor, which in associative combination with other parameters, leads to the development of a more complex disease. The usual unit to report the effect of an SNP is called odds ratio (OR). The odds ratio in this context is defined as the ratio of the odds of having a disease for individuals carrying the allele and the odds of having the disease for individuals not carrying the allele.

$$Odds\ Ratio = OR = \frac{Odds\ with\ SNP_{mutagenic}}{Odds\ with\ SNP_{wild}}$$

When OR>1 there is a direct dependency on the wild SNP and the disease, while a value lower than 1 reflects an enhanced resistance. The greater the divergence from 1, the stronger the relationship between the SNP and the disease. Selected SNPs with their OR value and the disease they are associated with can be seen in Table 1.

Table 1: Selected SNPs with their odds ratio for the correspondent disease.

SNP	OR	Region	Disease	Reference
rs10974944	3,10	9p24.1	Myeloproliferative neoplasms	[11]
rs11218343	0,77	11q.24.1	Alzheimer's disease	[12]
rs9271640-G rs3135388-A rs3957148-A	2,23	6p21.32	Multiple Sclerosis	[13]
rs7504990-A	6,95	18q21.2	Gallbladder cancer	[14]
rs12568010-A rs1125777-C rs41453448-G	2,50	1p31.3	Bipolar disorder	[15]
rs12317459-? rs16901979-?	2,06	12q21.31	Prostate cancer	[16]
rs12632235-T	2,11	1q25.2	Alcohol dependence	[17]

The relationship between SNPs and complex diseases has been widely studied and reported, but the synergistic effect due to the presence of several SNPs is a phenomenon studied to a lesser extent. For example, Chang *et al.*[18] found that combinations of 2, 3, and 5 different SNPs that individually were not significantly associated with breast cancer, had a higher risk once associated, elevating the odds ratio to 1.357, 1.689, and 13.148 respectively. The susceptibility towards some other major diseases such as coronary artery disease, [19] glaucoma,[20] and schizophrenia,[21] or the aggressiveness on the development of others such as prostate cancer[22] have also been reported to have a significant SNP-SNP interaction. It is because of this fact, that the analysis of a SNP cannot be taken as an individual and isolated mutation, but it should be studied as a combination of several biomarkers, and methods targeting SNPs should provide means to detect an array of SNPs simultaneously (multiplexing).

2.1.1. SNP discovery

Methods for the discovery and detection of SNPs have developed along and by the hand of the Human Genome Sequence project. Initially, the Consortium used the Sanger sequencing method,[23] which is based on the selective incorporation of chain-terminators containing a reporter group by a DNA polymerase during *in vitro* DNA replication (Figure 1). The chain terminators are di-deoxynucleotidetriphosphates (ddNTPs) that lack a 3'-OH necessary for the formation of the phosphodiester bond between two nucleotides, so when a ddNTP is incorporated instead of a normal deoxynucleotidetriphosphate (dNTPs), the extension process by the polymerase is stopped. The same DNA sequence is divided into four separate sequencing reactions each of them incorporating all four dNTPs, and only one of the ddNTPs in a 1:100 ratio. This ratio difference allows the formation of fragments of different length with a termination at each point where the base complementary to the ddNTP is present. Fragments are separated by gel electrophoresis, and the results of the four reactions are compared to recreate the sequence. This method was further refined with the introduction of the so-called shotgun sequencing,[24] which applies Sanger sequencing to randomly generated DNA fragments, and with the help of bioinformatic tools, combine all reads to generate the continuous sequence. Although shotgun sequencing is an improvement over the Sanger method, allowing to move from strands of 100 to 1000 base pairs of Sanger sequencing to fragments of 200.000-300.000 base pairs on shotgun sequencing, both techniques are limited and cannot fully map for SNPs.

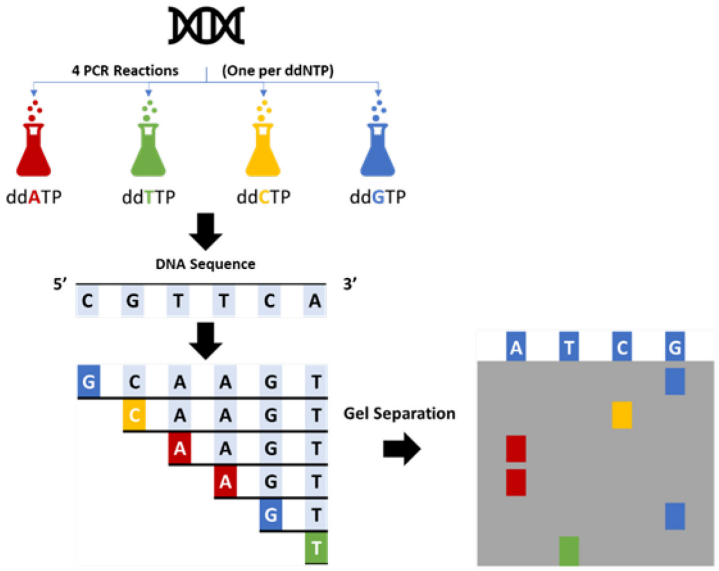

Figure 1: Sanger Sequencing method. Four parallel PCRs are performed each with different chain terminators, ddNTPs, that lack a 3'-OH necessary for the formation of the phosphodiester bond between two nucleotides. Incorporation on the extension step stops further elongation. Fragments are separated by gel electrophoresis and the results of the four reactions are compared to recreate the sequence.

The Human Genome Project gave rise to genome-wide association studies trying to link molecular causes to diseases, their development, and treatment, increasing the demand for fast and accurate analysis of large amounts of genomic DNA with a low price.[25] This high demand fostered the development of the technology known as next generation sequencing (NGS), which is a term that englobes a collection of techniques. All techniques are based on the array-based sequencing of millions of reactions in parallel by combination of different methods for template preparation, sequencing and imaging, and data analysis. The combination of protocols has

stimulated the emergence of different commercial platforms, but they all share some common features and their workflows are conceptually similar. The target DNA is randomly fragmented and ligated with a custom adaptor sequences to generate a library. These fragments are then clustered to either a single location on a planar substrate or to the surface of a bead, and through alternating cycles of enzyme-driven reactions and imaging, sequencing is achieved. The main commercial sequencing methods are i) 454 pyrosequencing, ii) ion torrent semiconductor sequencing, iii) sequencing by ligation (SOLiD), and iv) reversible terminator sequencing (Illumina). There are several reviews covering their specific technical performance and comparing their data quality,[26-28] but their main point in this discussion, is that these techniques have made possible to sequence an entire human genome in a matter of hours at low cost, and by comparing the resulting sequence to a reference, it is possible to identify a great number of SNPs at once.

From an analytical point of view, sequence length comes at the expense of sequence fidelity. Sanger sequencing is a reliable and robust technique if limited to short fragments, while NGS are fast and cheap methods which can work with whole genomes, but they offer lower specificity. Not only have polymerases shown bias and the formation of artifacts with multi-template PCR,[29] but on average, 0.1 to 1 % of the bases are named incorrectly during the cluster amplification, sequencing cycles, and image analysis with NGS.[30] In some cases, and when the sample is homogeneous, these errors can be corrected via a bioinformatic approach, by establishing the correct sequence as product of the base most frequent at each position (consensus sequence). However, when several templates are present, the consensus sequence is not an option anymore, and enhanced analytical methods must be developed to make up for the limitations of bioinformatics. Prenatal screening, detection of circulating tumor DNA, and forensics are typical applications where two or more templates might be present, and identification and differentiation is the main issue.

2.1.2. Methods for SNP Detection

The current method of choice to analyze a known SNP is the TaqMan 5'-nuclease assay[31] which is summarized in Figure 2. A forward and reverse primers are set to amplify the area where the SNP is present via real time PCR. To the normal PCR mixture, two hybridization probes, TaqMan probes, are added. These probes are each complementary to one allele, and they carry a fluorophore on the 5'-end and a quencher on the 3'-end. During the elongation step, only the complementary hybridization probe has sufficient affinity to bind the sequence, and it will get degraded due to the 5'-nuclease-activity of the Taq polymerase. Degradation of the hybridization probe separates the quencher from the fluorophore, increasing fluorescence. The sequence of the hybridization probe must be carefully optimized to yield selective probes, and primers have to be selected to ensure the performance of the PCR. This laborious and complicated optimization makes the TaqMan approach strongly dependent on each SNP. Moreover, the concentration of target is also a factor to consider. Lower concentrations of target sequence will require longer primers and hybridization probes; therefore, there is a dependency on the concentration with the size of the sequence to measure. The multiple experimental considerations that each SNP requires, together with the relatively high cost of TaqMan probes, has driven research to look for alternative methods. These methods are either based on hybridization, enzymatic discrimination, or thermal denaturation, and they have come to challenge the performance of the TaqMan approach. It should also be noted that in recent years, nanopore sensors have been thought to be the future of sequencing and SNP detection;[32]

however, their application has moved towards the detection of substrates rather than sequencing,[33] and accordingly, they have been excluded from this discussion.

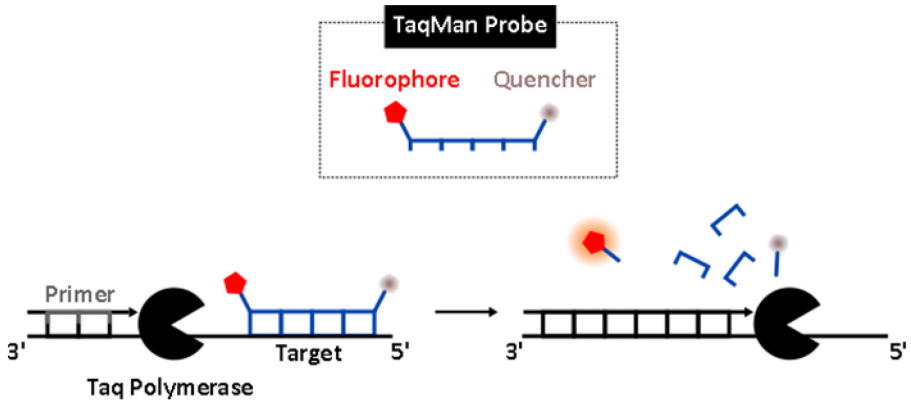

Figure 2: TaqMan approach. The Taq polymerase has a 5'-nuclease-activity which separates the fluorophore from the quencher along the extension step. The separation between fluorophore and quencher results in an increase of fluorescence that can be directly linked to the presence or absence of the SNP to which the probe is complementary.

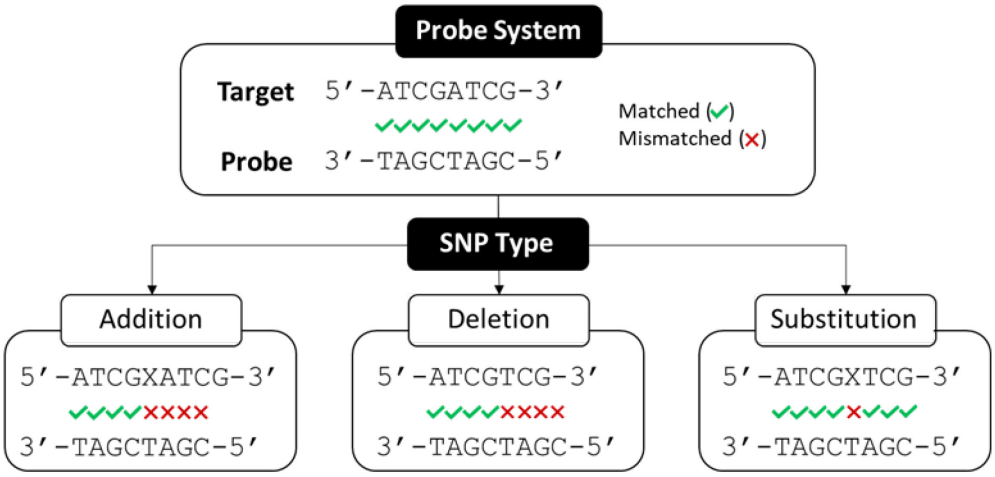

Figure 3: Types of SNPs and probe base pairing. Probes for addition and deletion SNPs can be designed so repulsion is maximized, while the effectivity of probes that target substitution SNPs are limited to the effect of one base.

The sequence fidelity of the Watson-Crick base paring is the cornerstone of SNP detection. As a simplification, the basic principle for SNP detection is to expose the target sequence to the fully matched and/or mismatched probe: on the matched duplex all bases contribute positively to its stability, while in the mismatched there is a pair of bases with a negative contribution to the duplex stability. This destabilization translates in a decrease in affinity and structural deformation of the duplex which is detected. In this regard, the kind of SNP to be analyzed is critical in the performance of the method (Figure 3). In an addition or deletion SNP, half of the probe can be unpaired if the probes are properly designed, making the negative contribution that strong that there is no binding whatsoever. On the other hand, substitution SNPs are the most challenging mutation kind, since only one base pair bares the negative contribution regardless of the position. The limited effect that one pair of bases can have on the total stability of the duplex is one of the main limitations, and several approaches have been offered to increase the effect of such small differences.

Hybridization Assays

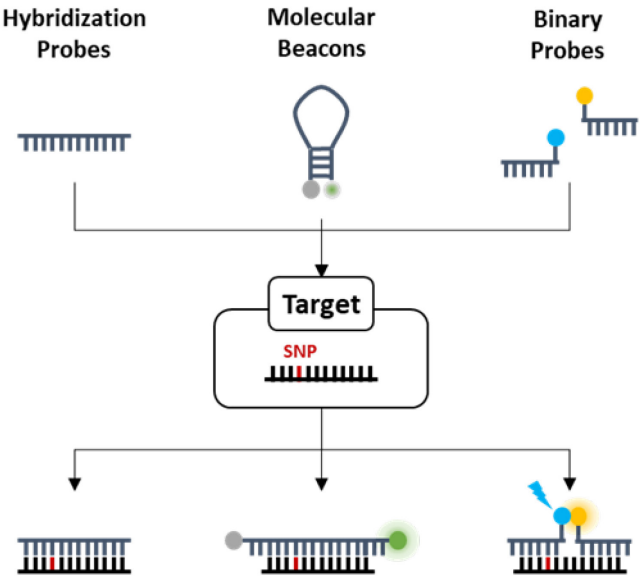

Figure 4: Most common approaches for the design of hybridization probes.

The utilization of hybridization probes is based on the difference in affinity of a sequence for its fully complementary or mismatched target when a SNP is present (Figure 4). The limited effect of one base pair in the total affinity is the greatest drawback. Consequently, the hybridization process is controlled to improve selectivity for the complete faithful sequence; this can be achieved in a direct way via alterations in temperature, ionic strength, and concentration of probes, making each analysis dependent on a set of previously optimized conditions. Alternatively, the so-called Force intercalation probes (FIT-probes) can also be used.[34-38] This probes rely on the forced intercalation of a cyanine dye such as thiazole orange (TO) as replacement of a canonical nucleobase (Figure 5). The restriction of the torsional flexibility of the dye when intercalated in the probe-target duplex, is translated in a fluorescence enhancement.[39] The intercalator dye can be attached through a flexible linker to one end of the probe, or it can be attached to the backbone of the probe. Fluorescence depends in the fully hybridization of the adjacent probes, and therefore FIT-probes can be used in the detection of SNPs.

An indirect way to increase control over hybridization process is to introduce a secondary structure. One example would be the utilization of molecular beacons,[40] which are probes that present a secondary structure, that must be broken in order to hybridize the target. This secondary structure is achieved by placing self-complementary sequences at each side of the recognition sequence (sequence complementary to the target). The duplex with the target is thermodynamically more favorable, but the need for breakage of its secondary structure allows for a second layer of specificity.[41] Usually, a fluorophore and a quencher are attached to each side of the beacon; therefore, in the absence of the target sequence, the fluorophore and quencher bear together, while when the template is present, the unfolding of the hairpin structure separates them, and fluorescence is enhanced. This approach has been widely used in the detection of SNPs; Tyagi *et al.*[42] reported a multiplexing method for the detection of closely spaced SNPs with the use of molecular beacons which coupled a set of fluorophores suited for fluorescence resonance energy transfer (FRET) coupled to each probe. Although research has been focused on enhancing recognition performance (specificity and sensitivity) of the

probes,[43] the main limitation of molecular beacons is the severe thermodynamic optimization needed in order for the probes to perform properly at room temperature.[44]

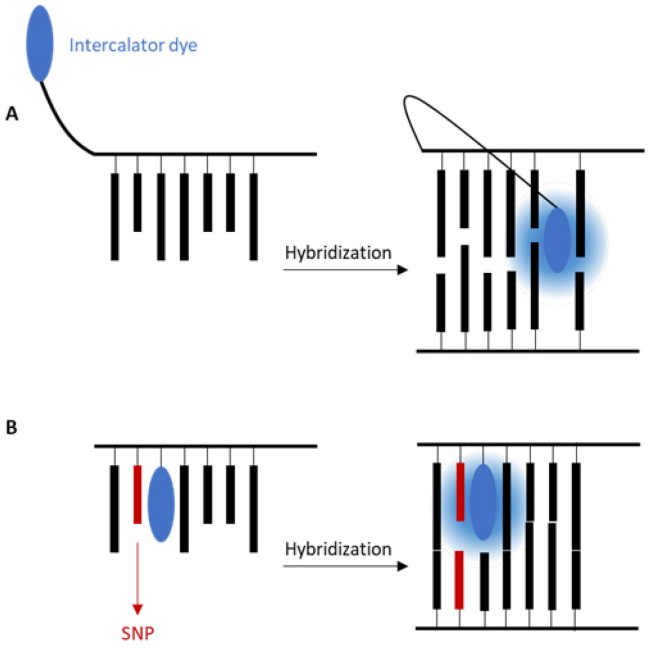

Figure 5. FIT-probes described by Seitz et al.[34] **A.** In the first construction the intercalator dye is attached thorough a flexible linker to the end of the probe. Upon hybridization of the probe with the target the intercalator dye can fold back and intercalate between base pairs. **B.** The intercalator can be directly linked to the backbone of the probe. Upon hybridization with the target, the precise hybridization of the adjacent probes determines the intensity of the fluorescence.

One way to increase the total contribution of the SNP to the affinity difference between alleles is to divide the sequence of the probe in two and combine them in what is called a binary-probe assay. Binary-probes are based on the use of two probes that produce a signal once brought together by the target. Binary probes for the detection of nucleic acids were introduced by Cardullo et al. in 1988.[45] Their approach was based on the attachment of fluorescein and rhodamine to the 5' ends of complementary oligodeoxynucleotides. Upon hybridization of the probes with the complementary target energy transfer was detected. There are a great number of other examples available in the literature. From straight forward binary probes carrying a ruthenium complex and organic fluorophore suited for FRET,[46] to more convoluted approaches, such as a system where each binary probe carries one part of the sequence complementary of a molecular beacon whose hybridization results in an increase on fluorescence.[47] Ribozymes, DNA/RNA sequences with an enzymatic activity, are also common in the field. Kolpashchikov *et al.*[48] developed an assay in which each binary-probe is coupled with a section of a functional peroxidase ribozyme that catalyzes the oxidation of diaminobenzidine tetrahydrochloride, resulting in the change from a colorless substrate to a colored product.

In conclusion, there are many approaches based on hybridization probes that can be used to detect SNPs. Their performance and limit of detection greatly depends on the procedure and detection system. Since most methods measure fluorescence, the limit of detection depends on the noise and background reactions, while their ability to multiplex is limited to the spectral overlap between fluorophores.

Enzymatic assays

There are several enzymatic methods for the detection of SNPs, which make use of either the recognition capacity of the protein MutS,[49] the match specificity needed for binding with a ligase,[50] or the recognition of specific sequences of nicking enzymes.[51] The MutS protein is a component of the DNA mismatch repair system in many organisms, and it can recognize and bind all possible single-base mismatches. The superior selectivity of the MutS protein towards wrong base pairing is limited by its inability to discriminate among different mutations, and it cannot identify multiple mutations in one strand. On the other hand, nicking endonucleases, which are enzymes that cuts one strand of a double stranded DNA (dsDNA) at a specific recognition nucleotide sequence, are also limited in the number of specific sequences they can recognize. Such limitations in applicability leave ligases as the main enzymes in the field. Ligases are universal and can be used for several targets simultaneously. They covalently join two adjacent oligonucleotides when the nick is located on a duplex between matched nucleotides. The combination of short hybridization probes with a ligase can therefore assure a high degree of specificity. Landegren *et al.*[52] introduced the first assay based on a ligase for gene and SNP detection. Their method is based on the covalent linkage by a ligase of two oligonucleotides complementary to the target DNA. In the presence of a SNP at the junction inhibits the reaction, and therefore, mutations can be detected. There are many examples on the use of ligase enzymes for the detection of SNPs.[53] In recent years, the universality of ligation enzymes has elevated its application in combination with gold nanoparticles. Yang *et al.*[54] exploited the fluorescence quenching of gold nanoparticles for organics dyes, the difference in noncovalent interactions of nanoparticles with single stranded DNA (ssDNA) and dsDNA to develop a ligation assay. Gold nanoparticles have a higher affinity ssDNA than dsDNA. Their method was based on the ligation of two probes, one of them carrying a fluorophore, when the complementary template was present. In the absence of template, both probes bind to the nanoparticle and florescence is quenched. On the contrary, once the template is present, the probes are ligated, and they form a dsDNA duplex with lower affinity for the gold nanoparticle, which results in an enhanced fluorescence. Similar approaches have been used for point-of-care approaches and in combination with rolling circle amplification[55] or ligation chain reaction[56] to increase sensitivity down to the low pM range.

Thermal Assays

The sequence of a DNA double strand determines its thermodynamic stability. The temperature at which half the concentration of the duplex is denatured is known as melting temperature (T_m). Since the thermodynamic stability of a double strand is determined by its sequence, variations on T_m can be used to detect SNPs. The low impact of a single base on the total T_m variation limits its sensitivity, but its feasibility to be directly used after PCR has spread its use. There are two different ways to apply the technique, in liquid phase and on surface. Gains in automatization are usually at the expenses of sensitivity, and neither liquid nor solid phase method offer sensitivities that can rival those of enzymatic or hybridization probes, but in general, they are less convoluted and easier to apply. For example, Wienken et al.[57] were able not only to detect SNPs but also DNA methylation with a simple all-optical set-up. The minuscule sample volume needed (250 nL) contrasts with the relatively high measured concentration (1 µM). In any case, the sensitivity needed in SNP detection is incompatible with most approaches based on thermal denaturation.

In conclusion, methods for the analysis of SNPs should be specific, sensitive, and robust by default. Moreover, due to the nature and properties of SNPs, the ideal method should cover

certain additional parameters: first, it should allow simultaneous detection of several SNPs, since isolated SNPs have a limited effect and they might manifest synergistic properties. Additionally, the high demand of data needed requires a high throughput method. Despite the fast development in the field over the last years, these requisites for multiplexing capabilities, high throughput, and allele discrimination have not been successfully address in a compelling way,[58] and it is where this work sets its ambitions. In the next two chapters, the foundations of our approach will be laid: mass spectrometry, specifically, inductively coupled plasma mass spectrometry (ICP-MS) will be considered as the technique of choice to satisfy the sensitivity, throughput, and multiplexing needs, while template-directed native chemical ligation (NCL) in combination with peptide nucleic acids (PNA) will provide the specificity and discrimination demands.

2.2. Inductively coupled plasma mass spectrometry

The induction-coupled plasma was introduced by T. B. Reed in 1961,[59] but it was not until the works of Houk *et al.* in 1980 that it was used as ion source for a mass spectrometer.[60] ICP-MS was commercially introduced in 1983, and over the years, the instrumentation has been improved, optimized, and compacted. Its technical performance with low detection limits for most elements across the periodic table, high throughput and dynamic range, low matrix effect, and the possibility to obtain isotopic information have fostered the adoption of the technique in different fields. Along the following chapter, a general description of the technique will be covered in order to address the strengths and limitations of the technique for SNPs detection.

2.2.1. Instrumental description

Liquid samples are introduced into the ICP-MS system by pumping the solution through a nebulizer. The spray chamber separates small droplets that go into the plasma through the injector, from bigger ones which get discharged. The plasma is formed by application of a high voltage spark to a tangential flow of argon gas, which causes electrons to be stripped from their argon atoms. Electrons are caught up and accelerated into a magnetic field generated by a radio frequency energy applied on a RF coil surrounding the plasma torch. This stripping, reclusion, and acceleration of electrons generates a collision-induced chain reaction that causes the ICP discharge which can reach temperatures as high as 10000 Kelvin. The aerosol passes through the middle of the plasma, where it undergoes several physical changes to yield mostly positive atomic ions, deleting all traces of molecular information. Ions are transferred from atmospheric pressure to the high vacuum of the mass analyzer, where they are separated based on their mass to charge ratio (m/z) through an interface. The ion flow is converted into an electrical signal at the detector, in order to quantify the amount of analyte present in the sample. Solid samples can also be directly ionized with a laser ablation unit to avoid digestion and sample preparation. In this case, the sample surface is irradiated with a deep-UV laser that generates an aerosol that goes directly into the plasma. Due to the focus of this work, laser ablation will not be discussed, and the review will focus on liquid samples.

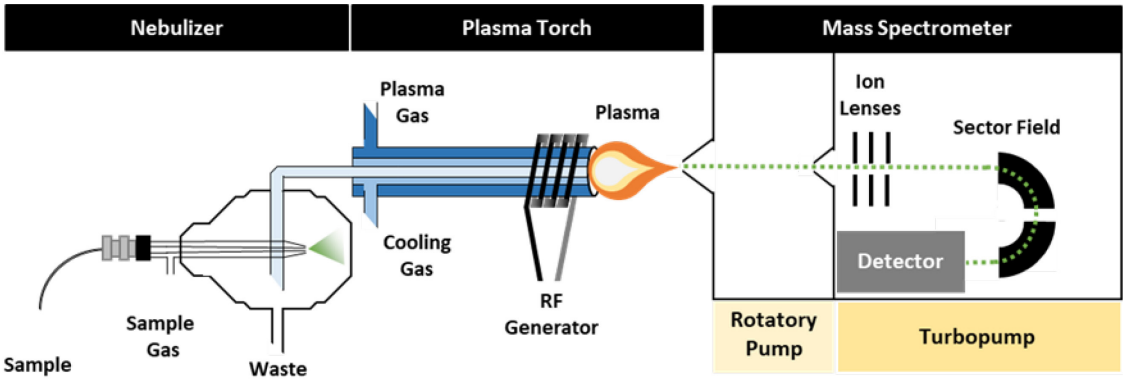

Figure 6: ICP-MS system with a concentric nebulizer, cyclonic spray chamber, and sector field mass analyzer.

Sample Introduction

The aim of the sample introduction system is to generate a fine aerosol of the sample, so that it can be efficiently ionized in the plasma discharge. For that purpose, a combination of a nebulizer and spray chamber is used for liquid samples, while, as mentioned before, a laser ablation unit can be used to directly atomize solid samples. This step is one of the main limiting factors of ICP-MS since only a small percentage of the sample passes to the plasma while most of it is discharged.

There are several nebulizer designs and materials available to allow the injection of different matrices and sample volumes, but they are all based on the same principle of passing the sample through a small capillary to generate the aerosol in combination with a sample gas. The main used nebulizers are: the concentric nebulizer, which is the standard for clean samples generating a fine droplet aerosol of around 1 mL min^{-1}, the cross-flow nebulizer, allowing more complex samples with undissolved matter, and the microflow nebulizer, thanks to a much thinner capillary generates a higher fraction of smaller droplets with flows as low as 100 µL min^{-1}. The reduced size of the capillary limits the array of matrices that can be used, thus efficiency of the process comes at expenses of matrix tolerance.

The amount of sample that goes into the plasma strongly depends on the nebulizer used. The efficiency on making an aerosol of the sample ranges from the 2% of the concentric nebulizers to the 50% efficiency of the microflow nebulizers. Since the plasma discharge is not efficient at dissociating large droplets, once the aerosol has been generated, bigger droplets are separated from smaller ones on the spray chamber. There are two main designs, the double-pass and the cyclonic spray chamber. The first one is based on a long tube where the aerosol is directed. Larger droplets emerge from the tube and exit through a drain that generates a positive pressure that leads small droplets into the sample injector. The cyclonic chamber operates by centrifugal forces. A tangential flow of the sample aerosol creates a vortex where larger droplets collide with the chamber walls, while smaller droplets get into the injector.

Plasma Source

The plasma source consists of the plasma torch with a radiofrequency (RF) coil surrounding it, and a power supply to feed it. The plasma torch is a set of three concentric tubes (outer, middle and sample injector) made of quartz. Three different gas flows are used to generate and control the plasma: The plasma gas (usually argon) which is the main feed of the plasma, and it is passed between the two most outer tubes at a flow rate of 12 to 17 L min^{-1}. The second gas flow passes between the middle and injector tube at approximately 1 L min^{-1} (depending on operational conditions), and it is set to control the position of the base of the plasma. Finally, the sample gas, which flows through the injector carrying the sample, and it physically punches a channel through the center of the plasma for the sample to reach the MS system.

A load coil surrounds the top end of the torch, and it is connected to a RF generator. When RF power is applied, an alternating current oscillates within the coil at a rate corresponding to the frequency of the generator, generating a strong electromagnetic field in the process. A high-voltage spark is applied to the flowing plasma gas stripping several electrons, which then get caught up and accelerated in the electromagnetic field. This highly energetic electrons collide with other atoms stripping even more electrons, forming what is known as the ICP discharge. The discharge is then stabilized within the torch and sustained with the RF energy continually transferred to it through the inductive coupling process. Due to its availability in high purity, high ionization energy, and inert character, the most common plasma gas is Argon. The amount of

energy required to generate argon ions is of 15.8 eV which is enough to ionize most of the elements in the periodic table (only helium, fluoride, and neon have higher first ionization energies).

Due to the geometry of the magnetic field, the largest current flow occurs on the periphery, generating a torus-shaped plasma. The aerosol from the injector passes through the middle of the central channel, where temperatures range from 8000 to 6000 Kelvin. In the process the sample undergoes several physical changes. First, the droplet desolvates into a solid particle, which is then vaporization into a ground-state atom. The ground-state atom is excited and ionized by losing of an electron due to a collision with an energetic argon electron and to a lesser extent with and argon ion. The ion emerges from the plasma into the interface of the mass spectrometer.

Ionization in the plasma has a clear disadvantage when compared to electrospray ionization (ESI) or matrix assisted laser desorption ionization (MALDI). The process eliminates all short of molecular information. However, that effect is compensated with a more accurate and reliable information on the absolute elemental content, which in turn reflects the concentration of biomolecules.

Interface and Ion Focusing

The interface consists of a set of two cones, the first one with an internal diameter from 0.8 to 1.2 mm called the sample cone, and a second one with an internal diameter from 0.4 to 0.8 mm called the skimmer cone. Some configurations incorporate a third one called hyper skimmer cone that allows a more gradual pressure reduction which results in a lower ion dispersion. The cones are set with their orifices aligned, to allow only the center of the ion beam coming from the plasma to pass through, increasing the fraction of ions coming from the sample, thus reducing those from the plasma. The interface is operated at a reduced pressure of around 1 to 2 torr. It has the role of efficiently transporting the ions from the atmospheric pressure at which the plasma is operated (760 torr) to the mass spectrometer analyzer which is operated at high vacuum (10^{-7} torr), while keeping the electrical integrity of the ions. The reduced size of the cones orifices limits the amount of total dissolved solids, TDS, in the sample that the ICP-MS system can tolerate. The recommended value of TDS is of 0.2%, with greater values having the risk of clogging the entrance to the mass spectrometer, and therefore, reducing the sensitivity of the instrument. The same limitation applies to organics on the sample, since incomplete combustion in the plasma leads to the deposition of debris on the cones.

Most generated ions are related to the plasma itself and not to the sample. Sampling of the center of the plasma improves such ratio, but there is still a greater number of species belonging to the matrix than to the analyte itself. This disadvantageous ratio has the effect of defocusing the ions, and it alters the transmission characteristics of the ion beam. Moreover, when passing from a region of low vacuum to a region with high vacuum, there is a rapid expansion of the ion beam. This is a process controlled by gas dynamics and not electrodynamics, thus smaller size electrons diffuse further from the beam; in other words, electrons which are much smaller than the positively charged ions, diffuse faster, generating a net positive charge in the ion beam that further increases repulsion among ions, and therefore defocusing. The role of ion lenses is to transport the maximum number of analyte ions from the interface region to the mass separation device, while increasing even further the vacuum. This is accomplished with the use of a set of electrostatically controlled lens components maintained at a vacuum of approximately 10^{-3} torr with a turbomolecular pump.

Mass Analyzer and Detector

Once the ions produced into the plasma reach the mass analyzer, they are separated based on their mass to charge, m/z, ratio. In the process, ions are directed towards the detector where ion flows are translated into electric currents that allow quantification of the species.

For most ICP-MS applications, a quadrupole is the mass analyzer of choice. A quadrupole consists of four parallel cylindrical rods arranged symmetrically and connected in pairs with the opposite one. A radiofrequency voltage with a direct current offset voltage is applied between one pair of rods and the other. Ions, except those with the adequate m/z ratio, will collide with the rods. Therefore, by scanning the voltages applied to the rods, it is possible to control which m/z ratio passes at each time. The quadrupole mass analyzer provides fast scans at low cost with resolution of 0.7 to 1.0 amu, and resolving power in the order of 800, which is sufficient for most applications. Several elements such as iron, potassium, arsenic, vanadium, and chromium present polyatomic interferences that need higher resolution to be resolved, and this niche has foster the introduction of sector field mass analyzers.

A sector field mass analyzer uses an electric and magnetic sector to separate ions according to their m/z. There are two main approaches for sector field instruments: the standard Nier-Johnson configuration, where the electrostatic analyzer is before the magnetic, and the reverse Nier-Johnson configuration, where the magnet is positioned before the electrostatic analyzer. The magnetic field is dispersive with respect to ion energy and mass, while the electrostatic analyzer is only dispersive with respect to ion energy. Therefore, if dispersion of both sectors is equal but in reverse direction, they will focus both ion angles and ion energies when combined.

A double-focusing magnetic sector instrument involves focusing ion angles and ion energies; therefore, the greater the dispersion at the entrance, the higher the dispersion at the exit. This translated in an inverse dependency between the size of the entrance and exit slits and resolution: the smaller the entrance and exit slit, the greater the resolution. Reducing the slits reduces ion transmission, therefore, increasing resolution lowers sensitivity, and therefore the LOD. Since most applications do not require high resolution, sector field instruments are usually set at low resolutions, where they have an exceptionally high sensitivity (low ppt range for most heavy metals). Detection limits, especially for high-mass elements where high resolution is not required, are typically 5 to 10 times better than a quadrupole-based instrument.[61] Moreover, sector field detectors present great precision, which makes them suitable for applications such as isotope ratio determinations.

2.2.2. ICP-MS for biological applications

Along the years ICP-MS has expanded the range of routine applications, replacing other techniques due to its superior analytical performance. For example, the maximum concentration of several metals in drinking water have been set according to the limit of detection of ICP-MS, making other analysis techniques obsolete in the process. This superior sensitivity has also driven its use in fields where concentrations are low, and sample amount is limited, such as the determination of nutritional and toxic elements in biological samples.

First applications of ICP-MS on biological samples started with a direct measurement of an element representative of the biomolecule, such as ^{31}P for the detection of adenosine phosphate, or ^{34}S for the detection of sulfur-containing amino acids.[62] Although several biomolecules contain elements that can be detected via ICP-MS, the real development of the field came with the study of platinum and ruthenium adducts, due to the introduction of

cisplatin as anticancer agents.[63] Research in this area has been focused either on the identification, or quantification of adducts. [64-65] Speciation can be carried by hyphenation to HPLC, and after identification of the species, quantification can be performed without the need of standards, since ICP-MS is an elemental technique.

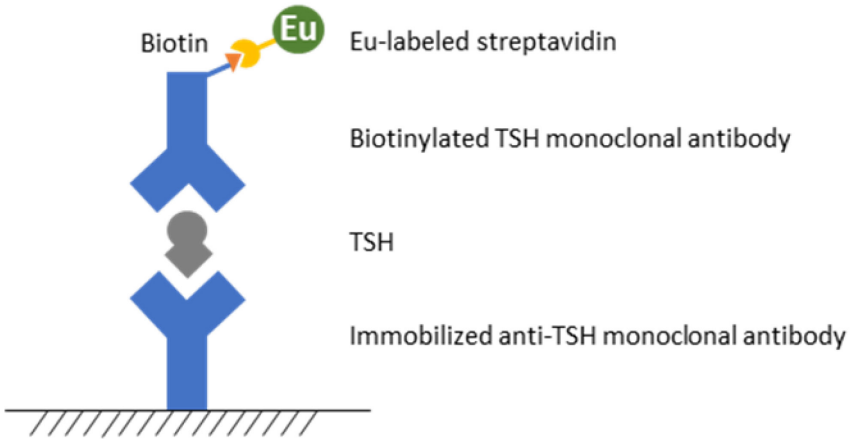

Figure 7: Immunoassay with europium as reporter group suggested by Zhang *et al.*[69] The assay consists of two antibodies selective for the thyroid-stimulating hormone (TSH). One of the antibodies is immobilized on a solid support while the second antibody is biotinylated. Quantification was performed via ICP-MS based on the signal of europium which was added to the sandwich assay via an europium-labeled streptavidin.

None of the major elements found in proteins (carbon, hydrogen, oxygen, nitrogen, and sulfur) are especially suited for the analysis with ICP-MS. Sulfur has been targeted as possible marker for the quantification of proteins,[66] but the real analytical potential was unleashed on the analysis of metalloproteins. Since sensitivity is much higher for metals, using the metal ion cofactor as reporter of the biomolecule results in an increase of the LOD,[67] especially when using isotope dilution analysis.[68] Therefore, the natural evolution of the field was to introduce metal labels that would increase the range of application from metalloproteins to any protein suitable for labeling. In such manner, the first immunoassay based on ICP-MS reported used an europium-tagged streptavidin on a sandwich immunoassay with one monoclonal antibody coated to a surface, and one with a biotin attached to its structure (Figure 7). The antibodies provided the selectivity for the thyroid-stimulating hormone (TSH), while the europium tag was used to quantify the amount of protein.[69] Secondary labeling was avoided by direct coupling of the lanthanide to the reporter antibody via a water-soluble polymer bearing multiple-chelating ligands.[70] In addition to the enhanced sensitivity, the use of lanthanide-based immunoassays had some other advantages, such as the possibility of quantification with high precision, large dynamic range, lower matrix effect, and lower contamination sources due to the practical inexistence of lanthanide in biological samples and plastic ware. The scarcity of external sources of lanthanides makes such labels independent of non-specific background an analytical response from incubation or storage times. Moreover, lanthanide-based immunoassays offer the possibility of multiplexing.[71]

Due to their versatility, lanthanide tags of 1,4,7,10-tetraazacyclododecane-1,4,7,10-tetraacetic acid (DOTA) have become widespread as labels for the quantification of proteins. Their suitability as labels relies on the low biological relevance of lanthanides,[72] which results in a low background, and the high affinity and low exchange rate of their complexes with DOTA,[73-74] which confers robustness to the label. The combination of a DOTA-macrocyclic metal-chelate

with an affinity tag and a reactive group for reaction with amino acids, generally known as metal-coded affinity tag (MeCAT), has demonstrated not only its usefulness to label peptides and proteins,[75] but also its suitability for either absolute quantification[76] or quantification via isotope dilution analysis.[77] As it can be seen in Figure 8, MeCATs are configurated with different parts to fulfill different purposes. First, it is the metal tag per se, which is the detectable part in ICP-MS (green moieties in Figure 7). The metal tag also incorporates a reactive site, which reacts with the targets and links to it (i.e. maleimide and iodoacetamide groups in red in Figure 7). In some cases, an affinity tag for purification (i.e. biotin in blue in Figure 7) is attached, and all them held together by a linker (i.e. black in Figure 7). The selection of the reactive group depends on the target, and it determines the specificity of the analysis. Amino groups can be targeted with a MeCAT with N-(p-isothiocyanatobenzyl) functionality[78] or N-hydroxysuccinimide,[79] while maleimide[80] or iodoacetamide groups[81] are used to target reduced cysteinyl residues. More recently, other approaches based on click-chemistry have been suggested, although they include an extra step in order to introduce the functional group needed for such a reaction (azide, or alkine).[82] In either case, ICP-MS has allowed the introduction of absolute quantification of proteins based on the concentration of a metal: this label approach has benefited from the low background of lanthanides on biological samples, and it has simplified analytical procedures; quantification can be performed in comparison with an elemental lanthanide solution instead of the reference protein material, or by isotopic ratio comparison.

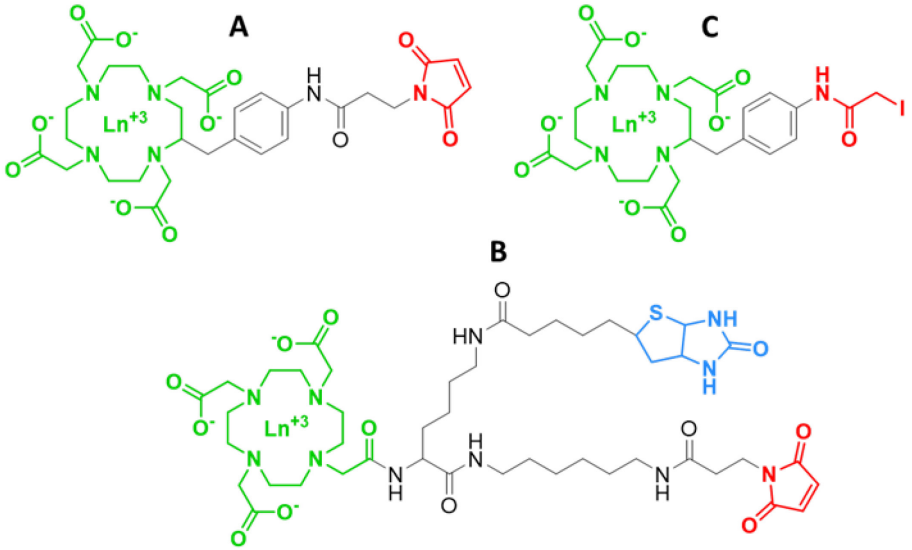

Figure 8: Metal code affinity tags. **A** and **B**, first generation MeCAT, MeCAT-MA, with a maleimide group as reactive group and B with a biotin group for purification by Ahrends *et al.*[80] **C**, second generation MeCAT, MeCA-IA, with an iodoacetamide moiety for cysteinyl group labeling by Schwarz *et al.*[81]

2.2.3. ICP-MS in nucleic acid research

Research in the nucleic acid field followed a similar patter as proteins; the lack of sensitivity when using phosphorous as a reporter moved the focus on metal-intercalators, metal tags, and nanoparticles. Indirect approaches such as the use of a nanoparticle modified with an antibody for the detection of trace oligonucleotides carrying an antigen-peptide,[83] or the use of streptavidin-modified gold nanoparticles for the detection of biotinylated oligonucleotides[84] soon moved into more direct approaches. For example, metal DNA intercalators (transition-metal complex that can insert between nucleotide pairs of DNA) of iridium and rhodium were used as a rapid and sensitive measurement of cell numbers by ICP-MS.[85]

Metal-intercalators tackled sensitivity, but their lack of sequence information gave metal tags, by then an established protein analysis tool, the edge in the field. The first works in this direction were carried out by Han *et al.*[86] with the simultaneous detection of 15 DNA targets 28 to 30 bases long. The assay was developed by functionalizing the surface of a magnetic microparticle with the thiolated capture probes that were complementary to one half of the region of the target of interest, and then addition of the second probe, reporter probe, which was complementary to the second half. Each target was associated with a reporter probe with a different metal (Y, La, Ce, Pr, Nd, Sm, Eu, Gd, Tb, Dy, Ho, Er, Tm, Yb, and Lu), so each lanthanide signal on the ICP-MS spectrum could be associated with a different DNA target. Quantification was performed via direct comparison with an elemental standard, but it was also shown that multi-isotopic species could be measured by isotopic dilution. The low background of lanthanides combined with the high sensitivity in ICP-MS resulted in limits of detection ranging from 5 to 20 nM.

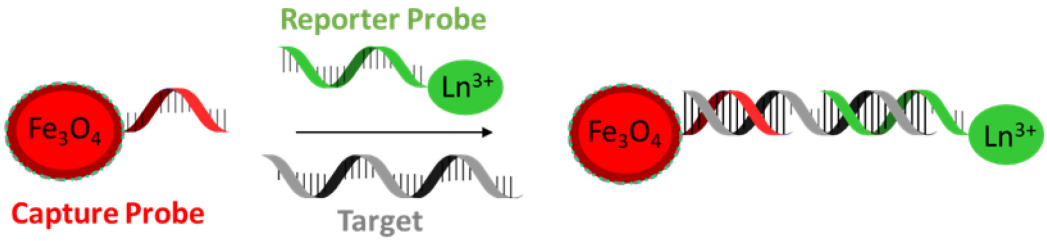

Figure 9: Hybridization assay for ICP-MS detection of nucleic acids by Lou et al.[87] The assay consists of a capture DNA-probes (red) complementary to one half of the target template (grey) bound to a magnetic microparticle and a second DNA-probe, reporter probe (green), complementary to the other half of the template carrying the lanthanide label.

A similar system was developed by Lou et al.[87] to detect viral DNAs. A magnetic nanoparticle with an attached single-stranded capture DNA complementary to half of the sequence of a DNA target, 30 to 33 bases long, was used in combination with a reporter single-stranded DNA probe complementary to the other half and carrying a lanthanide-DOTA complex (Figure 9). The capture probe was used to fish out the target, while the reporter probe was used to quantify the amount of target after release at high temperature. By taking advantage of the concurrent isotope detection in ICP-MS, three different sets of capture and reporter probes were used to quantify three different viral-DNA targets at concentrations ranging from 10 pM to 500 nM. Moreover, to increase sensitivity even further, they introduced a rolling cycle amplification system. This cycle amplification is based on the addition of a bridge DNA consisting of a complementary DNA sequence for specific hybridization with the targeted DNA, and a primer sequence, which is complementary with the reporter probe, so more reporter probes can be attached, increasing the sensitivity of the method three more orders of magnitude. On the same direction, Brückner et al.[88] introduced a sandwich assay with a limit of detection of 6 pM of template and a ligase chain reaction method which resulted in a 6000-fold increase in sensitivity. The approach targets single DNA strands of 50 bases with a capture probe that contains a biotin that binds to a streptavidin plate, and a reporter probe with a lanthanide-DOTA complex. After hybridization, the reporter probe is either eluted to detect on ICP-MS in the direct approach or subjected to a thermal cycle of hybridization-binding-denaturation and ligation. SNPs placed into the ligation site decreased the yield of product, which pointed to the suitability of this approach to the SNP analysis.

Rolling circle amplification combined with metal tags has been widely used, and it is an effective way of strengthening sensitivity breaking the 1:1 metal:product stoichiometry. Such stoichiometry can also be altered with metal tags carrying several metal atoms,[89] and with the use of nanoparticles as reporter groups. With multi metal tags the increase in sensitivity is limited to the number of metal tags attached, while the use of nanoparticles has the potential of a greater enhancement. Zhang *et al.*[90] used nanoparticles of gold, silver, and platinum to detect three different strands associated with the HIV virus. The principle is analogous to those presented before, with a capture probe linked to a solid support, and a reporter probe in this case attached to the nanoparticle. Each probe was complementary to a different half of the target sequence. Despite the potentially superior sensitivity of nanoparticles due to the higher number of metal atoms, limits of detection were of 1 pM of target sequence, emphasizing the lack of a single universal solution. More sensitive labels require stronger washing steps to avoid background. Sandwich assays are limited on the stringency of the washing steps due to the weakness of the intermolecular forces holding together the reporter probe. On the other hand, methodologies covalently binding reporter and capture probes, which allow harsher washing steps and present limits of detection exceptionally low, are restrained by the conditions needed for the enzymes to properly function. Therefore, new developments need to offer not only advances on label performance but also suitable approaches for background reduction while maintaining simplicity to avoid over reduction of the scope of applicability.

In conclusion, ICP-MS is a technique that can address sensitivity and multiplexing in SNP analysis. Since all traces of molecular information are removed during the analysis, its superior analytical performance has to be combined with the suitable probe system to provide selectivity. The probe system must be robust and able to provide a way to tackle the background. In accordance with such thinking, peptide nucleic acids (PNA) and native chemical ligation (NCL) will be discussed in the next chapter as means for providing selectivity and robustness respectively.

2.3. Peptide nucleic acid (PNA)

Peptide nucleic acid (PNA) is a DNA analog which instead of a deoxyribose-phosphodiester backbone, presents repeating N-(2-aminoethyl)glycine units linked by peptide bonds, forming a chain onto which bases are bound by methylene carbonyl linkages as shown in Figure 10.[91] The PNA backbone sets itself apart from DNA in that it is acyclic, achiral, and neutral. PNA binds to complementary nucleic acids obeying the Watson-Crick base pairing rules.[92] Contrary to DNA, which always binds in an antiparallel orientation, adducts can be formed in either parallel or antiparallel orientation even though the antiparallel is preferred. By convention, PNA is depicted like peptides from N-terminus to C-terminus, and in the preferred antiparallel orientation the N-terminus is facing the 3'-end.

Due to the lack of charge on the PNA backbone, in a PNA/DNA, PNA/RNA or PNA/PNA duplex affinity of the nucleobases is not hindered by the repulsion that the phosphodiester backbones of a DNA/DNA duplex would have. This fact confers a set of properties that make it interesting for several applications. First, thermal stability of duplexes with DNA is, not only higher, but also independent of the salt concentration,[93] and thermal stability is even higher on PNA/RNA duplexes. This enhanced thermal stability translates into a higher selectivity towards mismatches; for example, the average mismatch effect on a PNA/DNA duplex is of 15 °C while on a DNA/DNA duplex it is of 11°C.[94] The extreme case was reported with a T-G substitution which caused a decrease of only 4°C on a DNA/DNA duplex, but for the PNA/DNA in antiparallel orientation the decrease was of 13°C. In addition, the artificial structure of PNA makes it difficult for nucleases or proteases to recognize it[95] and confers a high stability over a wide pH range, making it a suitable candidate for either *in vivo* or *in vitro* applications.[96]

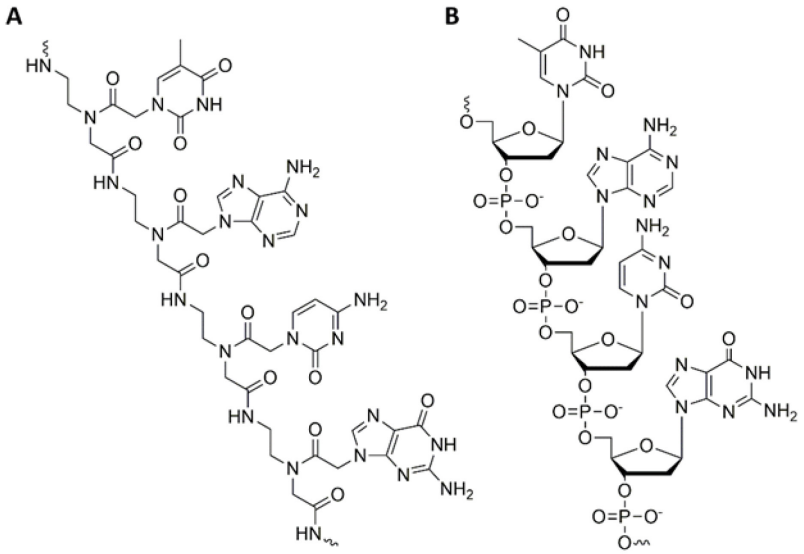

Figure 10: DNA and PNA structure. **A**, PNA chain. **B**, DNA chain.

PNA oligomers also experience some limitations. First, the lack of a charged backbone results in a lower water solubility when compared to other oligonucleotides. Its solubility is especially dependent on the length of the oligomer and the purine/pyrimidine ratio.[96] Approaches to increase PNA hydrophilicity have been based on either conjugation with solubilizing groups such as cell penetrating peptides,[97] poly-arginine or poly-lysine residues,[98-99] or on the chemical modification on either the PNA backbone[100] or nucleobase[101] to introduce charges or structural constrains.

2.3.1. PNA-Backbone Modifications: γ-PNA

Affinity of PNA can be tackled with the introduction of modifications on the backbone structure that pre-organizes PNA's structure, adopting a conformation which minimizes entropy loss of the binding. If the PNA backbone is too flexible, the entropy loss of the hybridization process would be too big to overcome, on the contrary, if it is too rigid, PNA would not be able to fit into the DNA structure. This was first studied by Hyrup *et al.*[102] when the introduction of a methylene group between the nucleobase and backbone resulted in a destabilization of the PNA/DNA duplex. Kumar and Ganesh went a step further in the study of structural preorganization of the PNA backbone.[103] They further explored the chemical, structural, and configurational diversity of the piperidine heterocyclic nucleus and expanded the repertoire of modified PNA structures. Their synthetic efforts yielded five- and six-member rings on and onto the PNA backbone. The aim was to achieve a higher binding with the introduction of structural constrains that would preorganize the PNA molecule. Pokorski et al.[104] have also studied constructions with the replacement of the ethylenediamine portion of aminoethylglycine PNAs with one or more (S,S)-*trans*-cyclopentane units. The modified PNA formed PNA/DNA duplexes with an average increase of melting temperature of 5 °C. The effect resulted to be additive and independent on the position of the modified base. Stereochemistry on the other hand resulted to be crucial since no melting transition could be detected with the (R,R)-form, highlighting the importance of geometry and preorganization in DNA hybridization.

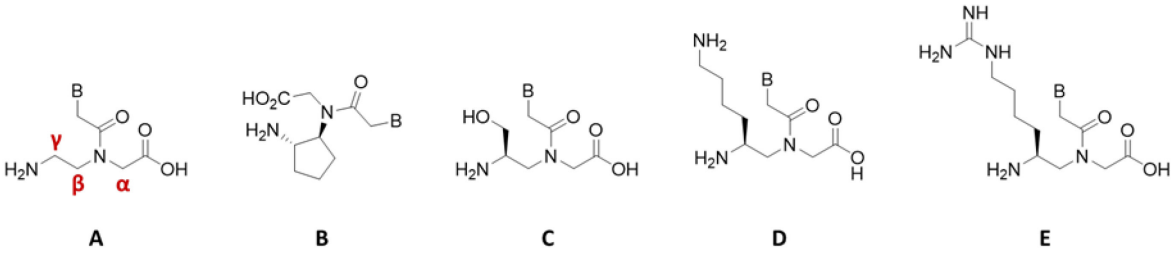

Figure 11: Selected backbone modifications of PNA. **A**, PNA monomer. **B**, cyclic PNA monomer by Pokorski *et al.*[104] **C**, Serine-based γ-PNA monomer by Andrasi *et al.*[105] **E**, Lysine-based γ-PNA monomer by Englung *et al.*[106] **F**, Guanidine-based γ-PNA by Sahu *et al.*[112]

It was first discovered by Andrasi et al.[105] that the introduction of modification (such as L-serine side chain) on the γ-position of the PNA backbone conferred a sterically driven helical structure from the C- to N-terminal direction to unfolded PNA. Consequently, the γ-position has since become a recurrent place to introduce modifications on the PNA backbone. In addition to the conformational effect, functional groups that interact with the negatively charged DNA backbone can be introduced to increase duplex stability. E. A. Englund and D. H. Appella,[106] synthesized a γ-substituted PNA constructed from L-Lysine and studied duplex stability of several PNA probes. The incorporation of L-Lys-γ-monomers into the PNA sequence increased the melting temperature an average of 2.4 °C. An acetamide group attached on the same position or even a small peptide bound to the Lys group resulted in a similar stabilization of the duplex. On the contrary, D-γ-monomers showed a destabilization effect, highlighting the importance of preorganization on the hybridization process.

The Ly group has focused on enhancing cellular uptake of PNA. Inspired by the success of the HIV-1 TAT transduction domain in increasing mammalian cellular uptake of proteins and nanoparticles,[107-109] and on the substitution of it by a homoarginine peptoid,[110] they first attempted to modify the α-position of the PNA monomer with guanidinium groups.[111] The increase in duplex stability was accompanied by an increase in cellular uptake. Later work carried

by Sahu *et al.*[112] coupled the same guanidinium group on the γ-position to revealing and even greater efficiency on cellular uptake and duplex stability partly due to the right-handed helix preorganization of the γ-PNA.

PNA forms very stable duplexes with ssDNA, but invasion of ds B-DNA is limited to homopurine or homopyrimidine probes in high concentrations. Rapireddy *et al.*[113] have used γ-PNA with an acridine moiety to solve this problem, achieving hybridization in 1:1 DNA:PNA ratios with selected sequences. In a similar manner, the replacement of cytosine with a more favorable synthetic analogue in combination with γ-PNA has also proved to be beneficial for hybridization to dsDNA.[114] These are two examples where the enhanced binding capacity of γ-PNA was combined with the fact that displacement depends on probes having sufficient binding free energy. Affinity is directly proportional to probe size, and thus γ-PNA probes of at least 15-20 bases can indeed hybridize dsDNA when in excess and enough time.[115] Universalization of dsDNA strands hybridization was not possible until the introduction of γ-PNA modified with diethylene glycol,[116] which in combination with an electrophoretic technique was successfully used to detect SNPs in 22 nucleotide dsDNA.[117]

In conclusion, γ-modified PNA has proven its potential to enhance some of the drawbacks of PNA. The introduction of charged functional groups can be used to increase the solubility of the oligomers, and several groups can not only increase cell permeability, but also allow hybridization of dsDNA.

2.3.2. PNA in the detection of SNP: hybridization

PNA has a higher affinity for DNA at low ionic concentration than DNA per se. Stronger affinity also means stronger destabilization in presence of a mismatch and therefore, PNA was naturally considered as a candidate for hybridization probes for SNP detection. The development of methodologies implementing PNA evolved in a similar fashion to those using DNA; from simple hybridization probes, to enzyme-based assays and binary probes. Initially, the presence of the target SNP was assessed by detection of either the matched or mismatched probe via MALDI-MS after several incubation wash cycles of the immobilized target,[118] or after capturing the PNA-target duplex on a strong anion exchanger.[119] In contrast to enzyme-based DNA methodologies which use ligases, enzyme-based PNA methods take advantage of the enzymatic resistance of PNA. Detection via spectrometric methods (usually MALDI-MS) targets the hybridization product of a PNA probe after treatment with nucleases or exonucleases.[120-121] Since the point ligation specificity of ligases is lost, selectivity is then dependent on the enhanced recognition of the PNA probe, which although greater, it has been the focus of research carried out in the area, and it has been usually addressed by exploring chemical modification of the recognition point.[122]

Point-of-care (POC) testing, medical diagnostic testing at the time and place of patient care, has become more widespread in the latest decade. In the quest for the ideal detection method on POC devices, the enhanced selectivity of PNA has also been a natural partner for the high sensitivity, compatibility with miniaturization, easy operation, and low cost of electrochemical analysis. The requirement of multiplexing on the SNP detection in this kind of biosensors is usually achieved by direct labeling of the electrode or by labeling of each probe with different indicators that produce signals at different potentials. Focusing on the electrode increases the complexity of the system not only by introducing laborious and time-consuming immobilization steps, but also by enhancing the complexity of the biosensor construction with the addition of more electronic measurement circuits. The introduction of different indicators entails an

increase in the number of chemistries needed for the labeling process, or the low resolution that results on the use of similar species.[123] To eliminate the immobilization step all together, Luo and Hsing[124] coupled two different electroactive indicators (ferrocene and methylene blue) to two different reporting PNA probes. The suppression on the signal on a negatively-charged electrode due to the formation of the also negatively-charged PNA/DNA duplex was successfully used to detect two targets at concentrations as low as 200 nM.

Fluorescence has been recurrently used in combination with PNA probes for the detection of SNPs. For example, the assay from Gaylord *et al.*,[125] coupled an acceptor chromophore in a PNA probe complementary to the target. The method was based on the use of a positively-charged optically-amplifying polymer that acted as donor chromophore. Once the negatively-charged DNA/PNA duplex was formed, fluorescence was enhanced due to capture by the polymer. As mentioned before, another example of the use of fluorescence in combination with PNA has been the forced intercalation probes (FIT-probes). FIT probes are modified PNA oligos in which an intercalator such as thiazole orange serves as a replacement of a nucleobase. When the probe is fully hybridized to its complementary target the dye loses its torsional flexibility, and hence fluorescence increases. This torsional flexibility is dependent on the immediate environment, so it is sensitive to mismatches in the adjacent position.[34,126] The applications of this kind of probes ranges from the detection on SNPs in combination with qPCR[36] to the imaging of viral mRNA in living infected cells,[127] or more recently on the SNP detection in living cancer cells by fluorescence microscopy.[128]

Most of the technologies are a compensation of the drawbacks of the detection with the use of PNA or the other way around, but none of them really captures the possibilities that PNA can offer to justify its use. Hybridization probes in combination with spectrometric method promise great multiplexing, but they lack the limits of detection and selectivity needed. Enzymatic methods based on the enzymatic resistance and enhanced recognition of PNA pale in comparison with the specificity of ligase assays and finally, hybridization approaches in combination with fluorescence lack the multiplexing characteristics needed in the field. Besides, most of these approaches rely on discrimination by the establishment of an equilibrium which should balance sensitivity and selectivity but not both at the same time: longer probes can detect targets at lower concentration but limit the contribution of the mismatch to the total affinity of the probe. As mentioned before, there is a high degree or parallelism between PNA and DNA-based assays, and as such, binary probes have been contemplated as the possible solution to the probe size problem and native chemical ligation (NCL) to the need of a biocompatible and high chemoselective reaction to bind both probes together.

Another field where the properties of PNA have been exploited towards SNP detection is the field of gene microarrays.[129] A microarray is an analytical device that presents a great number of functionalized probes on a solid support, and PNA makes such probes more sensitive towards SNPs and assays independent of ionic strength. Construction of the microarray depends on the length of probe needed. Short probes can be directly synthesized on the surface of the microarray,[130] while longer probes are usually directly bound to the surface yielding lower density microarrays.[131] In most cases, a fluorescent label or FRET pair is introduced into the system for detection of the hybridization product,[132-133] but the requirement of modifying the target and the increased cost and time of sample preparation has fostered the development of label free approaches which are based mostly on the direct detection of the hybridization product via MALDI-MS.[134] PNA microarrays have been used on the detection of genes[135] and

SNPs,[136] but they remain a niche application mostly due to the challenging absolute quantification and bias towards detecting low abundant genes.[137]

2.3.3. PNA in the detection of SNP: native chemical ligation

Native chemical ligation was first introduced as a technique that allows the direct synthesis of native backbone proteins of moderate size.[138] This reaction conjugates two unprotected peptide segments, one carrying a C-terminal thioester and one with a N-terminal cysteine with a peptide bond, in water, mild conditions, and without the use of enzymes. As shown in Figure 12, the native chemical ligation is a two steps process. First, there is a thiol exchange between the thioester on the C-terminal residue and the sulfhydryl group of the N-terminal cysteine residue. This transthioesterification is a reversible reaction which is chemoselective. The second step, and reaction driver, is an intramolecular nucleophilic attack by the α-amino group of the N-terminal cysteine (S→N acyl rearrangement) to form the final amide bond in a regioselective reaction. This second step is irreversible at physiological conditions and kinetically accessible because of the five-member transition state. The thioesters involved in native chemical ligation are prone to hydrolysis, therefore, appropriate reaction conditions such as pH and temperature need to be chosen.

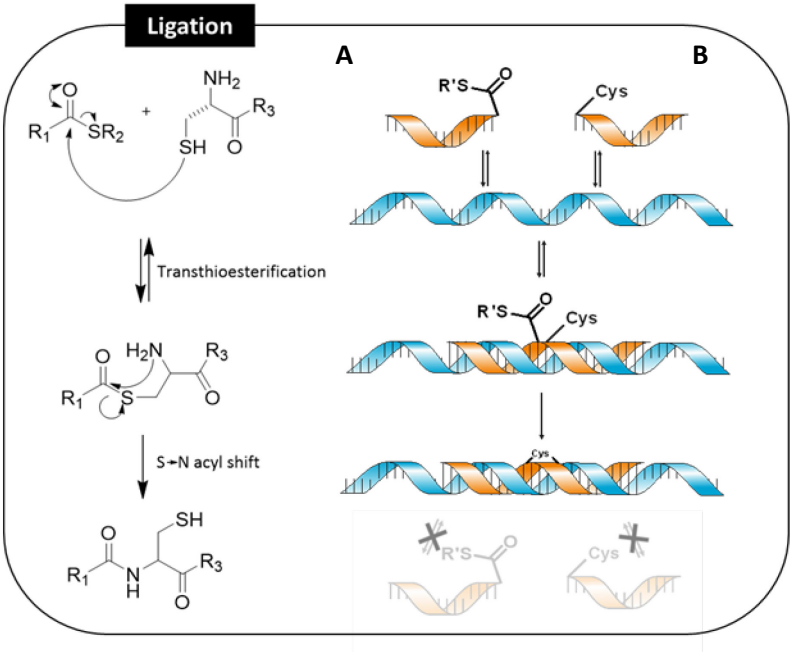

Figure 12: Native chemical ligation mechanism and combination with templated reaction. The reaction has two steps, first the transthioesterification between the thioester on the C-terminal residue and the sulfhydryl group on the N-terminal cysteine residue, secondly an intermolecular nucleophilic attack by the α-amino group of the N-terminal cysteine (S→N acyl rearrangement) to form the final amide bond.

Native chemical ligation has been successfully combined with nucleic acid templated reactions.[139-140] The use of PNA oligos that complementary bind to a template causes the alignment of the reactive groups, increasing the effective molarity, and therefore, allowing the reaction to proceed in a similar fashion to an intramolecular reaction (Figure 15 B). In other words, the use of a template in combination with native chemical ligation has two effects. First, it increases the effective molarity which yields product at lower concentrations than non-

templated reactions, and second, the need for alignment introduces an extra layer of chemoselectivity.

Templated native chemical ligation with PNA probes has proven high sequence selectivity, especially with the introduction of an abasic site.[139] Abasic means that the backbone does not contain neither purine nor pyrimidine base. In this case, an abasic site is achieved by designing the probes in such way that the reactive groups are surrounding a base that is not complementary to any of the probes. Its inclusion in the probe design makes template NCL as selective against SNP as several DNA ligases, exceeding fidelity of other chemical DNA ligation methods.[140] This added to the fact that ligation rates rival those of ligase-mediated reactions of oligodeoxynucleotides,[141] has made templated NCL of binary PNA probes the perfect candidate for SNP detection.

In contrast to the similar reaction rates of template-directed NCL and enzymatic reactions, template-directed NCL does not achieve the same degree of turnover than some enzymatic reaction can reach. The sequence of the ligation product is the result of the addition of the two individual probes. Affinity is directly proportional to probe length; therefore, the product has a much higher affinity for the target than the reactants, preventing other probes from hybridizing, and therefore, reacting. This self-inhibition results in a one to one stoichiometry product to target, and constitutes the main limitation of NCL, especially in the field of nucleic acid detection. From a methodological point of view, this problem can be addressed by either reducing the strength of the product/target duplex, or by avoiding the formation of longer products.

One example on the product front would be the use of isocysteine (*i*Cys) instead of cysteine on the acceptor probe.[142] *i*Cys presents the position of the amino and thiol groups interchanged and it leads to the formation of a ligation product with an extra carbon in the aminoethylghlycine PNA backbone which is shown to destabilize the PNA/DNA duplex.[143] Although the use of *i*Cys enhanced the turnover of the ligation reaction while reducing the rate of the off-template background reaction without compromising the speed and selectivity of the templated reaction, the real enhancement on the turnover front is the introduction of the so-called transfer reactions. [144]

In transfer reactions a reporter group is covalently bound to the donor probe as thioester, which can then be ligated in a native chemical ligation-like fashion once the template is present as shown in Figure 13. In other words, the tertiary complex between both probes and target results in the transthioesterification and S→N acyl migration of the reporter group from the donor to the acceptor probe. The change is in the position of the reporter group, leaving reactants and products with the same sequence. The identic sequence results in a similar template affinity as molecules before reaction, enabling strand exchange. The result of this reactant and product exchange is an increased turnover, conferring catalytic activity to templated native chemical ligation reactions. Moreover, besides the focus on turnover,[144] not only several reporter groups such as fluorescence quenchers, [145] biotin moieties[146] or amino acids[147] have been reported, but also several other chemistries have been used with the same concept in mind to expand the scope and applicability of such reactions in the nucleic acid detection field.[148-149]

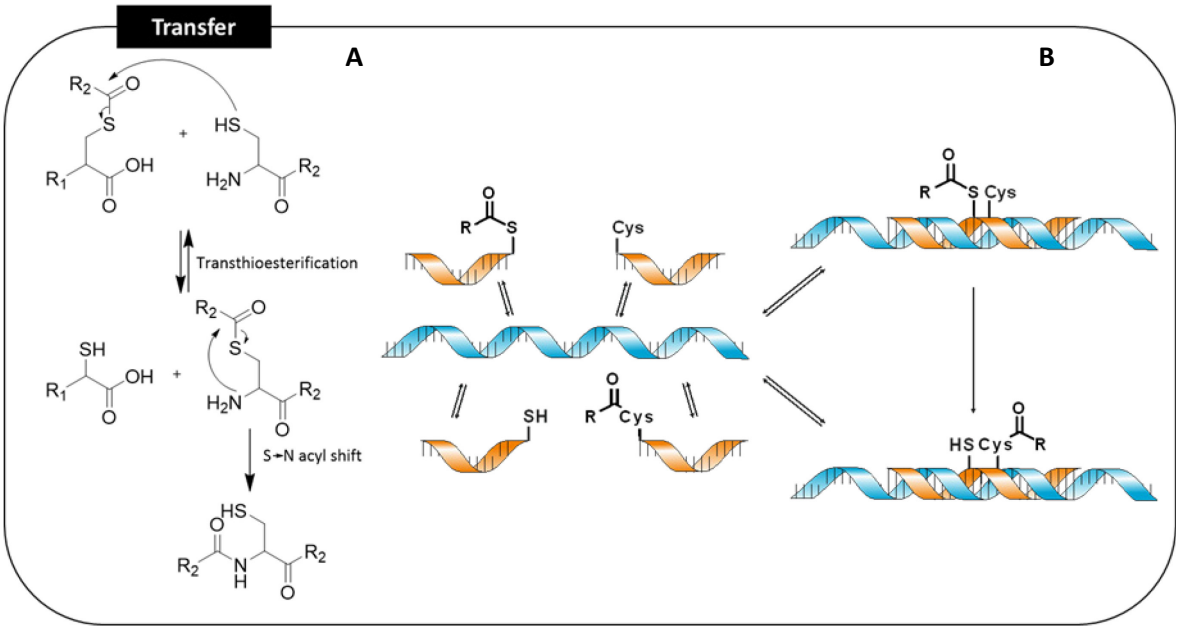

Figure 13: Transfer mechanism and templated transfer. In this case the reporter group is set as thioester on the donor probe. The probe configuration results in migration of the reporter group from the donor to the acceptor probe through the same transthioesterification and S→N acyl rearrangement as explained before.

3 Aim

The field of nucleic acid detection has evolved swiftly in recent years. NGS methods are nowadays able to sequence whole genomes in a few hours at low cost. From quantification of micro RNA for the study of cell death, proliferation, and regulation, to the assessment of genetic variability towards disease development and treatment, the analysis of nucleic acids will be at the center of future medicine. In that regard, SNPs, as the primary source of genetic variability and the most challenging mutation from the analysis point of view, will be at the forefront of the discussion. Methods for the detection of SNPs should not only be sensitive, selective and robust, but they should be suitable to multiplex and offer high throughput to face the increase number of analysis needed.

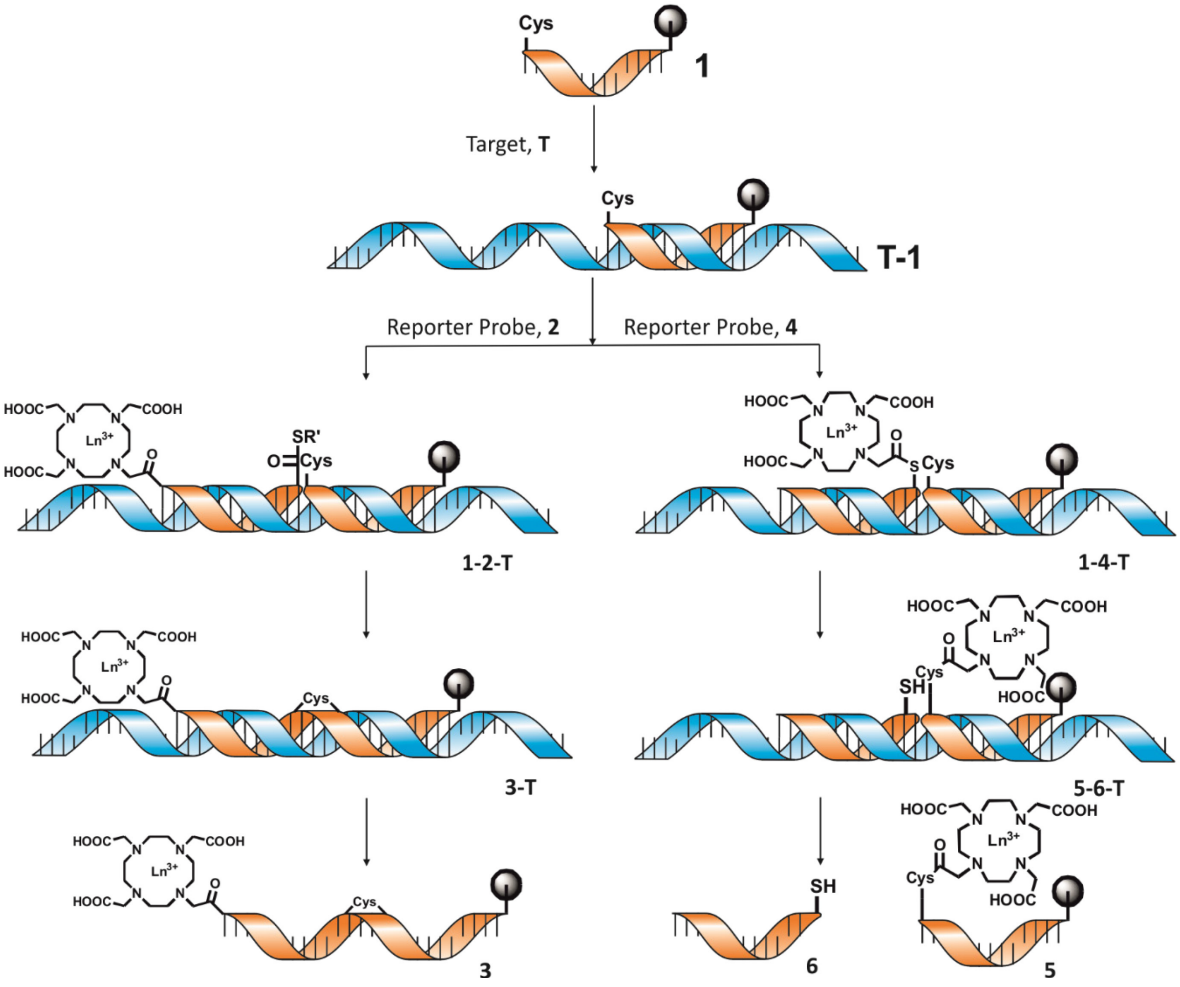

Figure 14: Nucleic acid detection via template-directed NCL and ICP-MS detection: Cysteine-bearing PNA probe, **1**, hybridizes the nucleic sequence, **T**, of interest. On the left, binding of PNA probe **2**, bearing the reporter group N-terminal, and allowing the native chemical ligation reaction yielding o the product **3**. On the right, binding of PNA probe **4**, bearing the reporter group as thioester, leading to transfer of the reporter group to **1**, and yielding to product **5**. The reporter group is a lanthanide chelated by DOTA.

The goal of this work is the combination of two established research lines to present a new approach for the analysis of SNPs. The first method is based on PNA capture probes for strand invasion into folded DNA that react in presence of a target DNA sequence following a native chemical ligation. As it has been previously discussed, PNA conjugates allow the fashioning of

highly chemo- and sequence-selective nucleic acid directed native chemical PNA-ligation reactions with reaction rates that reach those of enzyme-catalyzed oligodeoxynucleotide reactions.[139-140] The second approach is the ligation or transfer reaction that result in the immobilization of a lanthanide-containing reporter group also known as MeCAT,[75-76] that will later on be analyzed by ICP-MS (Figure 14).

The target DNA strand, **T**, will bring together the hybridization probe **1** and **2**, or **1** and **4** increasing the effective molarity of the probes and allowing the chemical reactions: ligation for **1** and **2**, and transfer for **1** and **4**. The product of the reaction with probe **2** will result in a ligation product **3**, which has a higher affinity for the template than reactants, while the transfer product, **5**, of the reaction with probe **4** will have a similar affinity to reactants theoretically allowing higher turnovers. The capture probe **1** includes a biotin in its structure that allows the introduction of a clean-up procedure based on the biotin-streptavidin interaction.

The reporter group is a Metal-coded affinity tag (MeCAT) which consists of a macrocyclic metal chelate complex of 1,4,7,10-tetraazacyclododecane-1,4,7,10-tetraacetic acid (DOTA) with a lanthanide. The MeCAT act as a chelate of a lanthanide metal and as an anchor to fix that metal to the PNA probe; therefore, evidence of the probe presence can be detected by measuring the signal of the chelated lanthanide. The instrumental limit of detection (LOD) of lanthanides by ICP-MS is in the order of 0.1 to 0.5 ppt and it is much greater than the LOD of any other element contained in the PNA probe, thus coupling of the MeCAT significantly enhances detection via ICP-MS.

Combination of both approaches will be the first challenge of this work, exploring and exploiting the synergies that might arise from the combination is the ultimate goal.

4 Experimental

4.1. Reagents and Materials

For PNA synthesis, DMF, NMP, and TFA were purchased from *Alfa-Aesar* (Karlsruhe, Germany) in peptide synthesis grade. Coupling agents PyBOP® and Oxima Pure™ were supplied by *Carbolutions Chemicals* (St. Ingbert, Germany). MBHA resin was acquired from *NovaBiochem* (Schwalbach, Germany) and Tentagel® Rink Amid resin from *RappPolymere* (Tubingen, Germany). Boc/Cbz-protected PNA monomers and Fmoc and Boc protected amino acids were purchased from *ASM Research Chemicals* (Hannover, Germany). Fmoc/Bhoc protected PNA monomers were acquired from *Link Technologies* (Lanarkshire, United Kingdom). DOTA-NHS ester was supplied by *CheMatech* (Dijon, France). Lanthanoid chloride of praseodymium, gadolinium, terbium, holmium, thulium, and lutetium were purchased from *Sigma-Aldrich* (St. Luis, USA). Dysprosium was acquired as the oxide from *Sigma-Aldrich*.

Single-element ICP-standard solutions of lanthanides and bismuth were purchased from *Carl Roth* (Karlsruhe, Germany). Tuning of the ICP-MS was performed with a 1 ppb dilution of the 500 ppm/element lanthanide metals standard solution from *Alfa Aesar* (Karlsruhe, Germany). Mass calibration of the ICP-MS was performed using the tune-up solution *ELEMENT®* from *Thermo Fischer Scientific* (Bremen, Germany). Nitric acid 69 %, used as carrier solution in a 3.5% (v:v) dilution into the ICP-MS, and hydrochloric acid 36,5-38,0 %, used to adjust the pH of the elution solution, were purchased from *Carl Roth* (Karlsruhe, Germany) in ultra-quality purity grade (*Rotipuran® Ultra*).

HPLC-purified DNA templates were purchased from *BioTeZ* (Berlin, Germany). A compendium of all the sequences used is shown in Table 2. Several different streptavidin magnetic particles were tested: the streptavidin magnetic particles and *StreptaWell®* from *Roche* (Mannheim, Germany), and *Dynabeads® MyOne™ Streptavidin C1* from *Thermo Fischer Scientific* (Massachusetts, USA). The *Dynabeads® M-270 Streptavidin* from *Thermo Fischer Scientific* magnetic particles were the ones incorporated into the purification method.

Reagents and solvents for synthesis of γ-modified PNA were purchased from *Acros* (Geel, Belgium), *Alfa-Aesar* (Karlsruhe, Germany), and *Merck* (Darmstadt, Germany) in synthesis purity grade. Solutions were prepared with deionized water from a *MembraPure Milli-Q water purification system* from Astacus (Berlin, Germany).

For the preparation of buffers, 3-(N-morpholin)propanesulfonic acid (MOPS) and 2-amino-2-(hydroxymethyl)propane-1,3-diol (TRIS) were acquired from *Sigma-Aldrich*. Sodium 2-sulfanylethanesulfonate (MESNa) was supplied by *Tokyo Chemical Industry* (Tokyo, Japan) and 3-[(3-cholamidopropyl)dimethylammonio]-1-propanesulfonate (CHAPS) was purchased from *Alfa Aesar*.

Name	Sequence
T1 m	5'-GTC GGC GCT G**T**A GGT GTG GGG AAG AGT GCC-3'
T1 w	5'-GTG GGC GCT G**G**A GGT GTG GGG AAG AGT GCC-3'
T2	5'-CCT GAC CAT CCA GCT TAT CCA GAA CCA CTT-3'
T3	5'-CTT TGT GGA TGA GTA CGA CCC CAC CCA TAG A-3'
T4	5'-CAT AGA GGA CTC CTA CCG GAA GCA AGT GTG-3'
T5	5'-CTT GCT GCA C**T**T CTA TCA CAC CTG TGC CTT-3'
T5 m	5'-CTT GCT GCA C**C**T CTA TCA CAC CTG TGC CTT-3'
T6	5'-CTT CCT TGA TG**G** GGA AGG GGC CCT AGT GAT-5'
T6 m	5'-CTT CCT TGA TG**A** GGA AGG GGC CCT AGT GAT-3'
T7	5'-CTA GAT GGT GC**T** GAA CCT ATC ACT TAG TCT CAC-3'
T7 m	5'-CTA GAT GGT GC**C** GAA CCT ATC ACT TAG TCT CAC-3'
T8	5'-TTC TCT ATC ATG ACA CTT AAT CTA CCG TCC TGT-3'
T9	5'-TGA AAA TAT AGA GAA AAG CCA GTT ACA TTA CAG AAC-3'
T10	5'-TTT GAA ACC AAT AGA CTG TGG CTT TTG CTA AC-3'

Table 2: Sequences of DNA templates. The nucleobase that differentiates the mutagenic from the wild allele has been highlighted in bold.

4.2. Instrumentation

Semi-preparative HPLC: purification of synthesized products was carried out on a *1100 Series* HPLC from *Agilent* equipped with an UV detector set at λ= 260nm slit. Two different columns were used depending on the scale of the synthesis. For synthesis performed in a 5 µmol scale a *C18 Gravity* (5 µ, 250x21 mm, pore size: 110 Å) column from *Macherey-Nagel* (Berlin, Germany) was used. For synthesis performed in a scale up to 2 µmol a *Polaris C18 A* (5 µ, 250x10 mm, pore size: 220 Å) analytical column from *Varian* (Palo Alto, USA) was used. A combination of mobile phase A (water: acetonitrile: TFA in 989:10:1, *v:v:v*) and B (acetonitrile: water: TFA in 989:10:1, *v:v:v*) with gradients specified below was used for separation:

Gradient 1: from 3 % to 20 % B in 20 min

Gradient 2: from 3 % to 40 % B in 20 min

Flow rates were set at 12 mL min^{-1} and 6 mL min^{-1} for the *C18 Gravity* and *Polaris C18 A* respectively.

Analytical UPLC®: photometric spectra of synthesized and reaction products were obtained on an *Acquity UPLC®* System from *Waters* (Miliford, USA) equipped with an UV-Detector set at λ= 260 nm and a quadrupole MS. Separation was performed at 50 °C with an *X-Bridge C18 BEH/CSH 130* (1.7 µ, 50x2.1 mm, pore size: 130 Å) column from *Waters*. As mobile phase, a combination of eluent A (water: acetonitrile: TFA 989:10:1, in *v:v:v*) and B (acetonitrile: water: TFA in 989:10:1, in *v:v:v*) with the gradient specified below was used:

Gradient 3: from 3% B to 30% B in 4 minutes (flowrate 0.5 mL min^{-1})

Analytical HPLC-DAD: reactions were followed using an *Elite LaChrom Series* HPLC from *Merck Hitachi* (Tokyo, Japan) equipped with a diode-array detector set to measure at λ= 260 nm. Separation was performed at 55 °C with a *Polaris C18 A* (5 µ, 250x4,6 mm, pore size: 220 Å) from *Agilent*. A combination of mobile phase A (water: acetonitrile: TFA in 989:10:1, *v:v:v*) and B (acetonitrile: water: TFA in 989:10:1, *v:v:v*) with gradients specified below was used for separation:

Gradient 4: from 3% to 30% B in 30 min (flowrate: 1,0 mL min^{-1})

Gradient 5: from 3% to 25% B in 25 min (flowrate: 1,0 mL min^{-1})

UV/Vis-Spectroscopy: UV-Vis spectroscopy was used for SPPS monitoring, concentration determination, and PNA-DNA melting temperature determination. In each case, triplicates of the absorption were measured and averaged. DNA extinction coefficients were calculated via the nearest neighbor model with the online tool from *Atdbio*,[150] and quantification was performed using the Lambert-Beer law.

SPPS monitoring: The *Carey 100 Bio* from *Varian* was used for the determination of resin loading and control of successful coupling in SPPS by measuring absorption at λ= 300 nm in quartz cuvettes.

PNA or DNA stock concentration: for the determination of the concentration of either PNA probes or DNA templates, absorption was measured at λ= 260 nm in a 1 mL quartz cuvette (d= 1 cm) on *Smart Spect™* Plus spectrophotometer from *Bio-Rad* (Munich, Germany).

Stock monitoring: before every experiment concentrations were reevaluated by measuring absorption of stock solutions at λ= 260 nm on a *NanoDrop™ 1000* from *peqLab* (Radnor, USA).

Melting temperature: for the determination of DNA/PNA-duplex melting temperatures, a *Jasco V-750* spectrophotometer from *Jasco Inc* (Easton, USA) was used. Samples were measured in a 1 mL quartz cuvette (d= 1 cm) with four cycles of: 20 to 90 °C at rate of 1 °C min^{-1} with absorbances recovered every 0,2 °C.

Hyphenated nanoHPLC ICP-MS: the ICP-MS system was hyphenated to an *Agilent 1100 Series* nanoHPLC from *Agilent* via an *MCN-6000* from *CETAC with sweep gas flow of 3.0 L* min^{-1}. Separation was performed with a Polaris 3 C18-Ether (3 µ, 150x1,0 mm, pore size: 180 Å) from *Varian* (Palo Alto, USA). A combination of mobile phase A (water: methanol: FA in 989:10:1, *v:v:v* ratio) and B (methanol: water: TFA in 989:10:1, *v:v:v* ration), or mobile phase C (water: acetonitrile: TFA in 989:10:1, *v:v:v*) and D (acetonitrile: water: TFA in 989:10:1, *v:v:v*) with gradients specified below was used for separation:

Gradient 6: 3 % B for 4 min, to 5 % B in 6 minutes, and to 15 % B in 5 min rest of fraction A (flowrate: 1,0 mL min^{-1})

Gradient 7: 3 % D for 4 min, to 5 % D in 6 minutes, and to 15 % D in 5 min rest of fraction C (flowrate: 1,0 mL min^{-1})

ICP-MS: detection was performed with a sector field mass spectrometer *Element XR* from *Thermo Fisher Scientific*. Measurements were either performed with direct aspiration with a *MicroMist* nebulizer of 100 µL min^{-1} and *Scott* spray chamber or hyphenated to a HPLC via a membrane nebulizer *MCN-6000* from *CETAC* (Walthman, USA) to reduce the fraction of organic solvent going into the system. Table 3 summarizes set-up conditions of the ICP-MS system.

Parameter	Magnitude
Cooling gas	15,0 L min^{-1}
Auxiliary gas	1,0 L min^{-1}
Sample gas	1,3 L min^{-1}
Plasma power	1250 W
Sampler and skimmer cone	Nickel

Table 3: Operation conditions of ICP-MS

Tune-up of the equipment was performed daily to reach a minimum 10^7 counts per second of Holmium, ^{165}Ho, with relative standard deviation (RSD) of 12 samples lower than 1,0 % with a 1 ppb multi-element solution. Bismuth, ^{209}Bi, was used as internal standard in a concentration of 500 ppt which was either spiked into 3,5 % nitric acid or into the elution solution (see biotin streptavidin clean-up). Along the execution of the project the instrumentation suffered several issues that resulted in decreased sensitivity and lower signal stability. In most of the qualitative results the instrument performance was not an issue, but for the sensitivity results and SNP detection a tune up of the instrument with the thermos multielement solution was performed until the iridium counts per second were higher than $1 \cdot 10^6$ and RSD with 12 sample points was lower than 1,0%. For quantification, peak areas under the ion intensity curves were integrated. In order to assess matrix effects several samples were digested with H_2SO_4: H_2O_2 (4:1, *v:v*) at 90 °C overnight. The digestion mixture was evaporated, and the product was re-dissolved in 3.5 % nitric acid.

Experimental

Three different methods were used to measure on the ICP-MS:

Method 1

- Isotopes: ^{159}Tb, ^{165}Ho, ^{169}Tm, ^{175}Lu, and ^{209}Bi
- Mass window: 100
- Sample time: 0,02
- Samples per peak: 20
- Search/Integration window: 0/50
- Integration type: Integral
- Runs/Passes: 3/3

Method 2

- Isotopes: ^{165}Ho and ^{209}Bi
- Mass window: 50
- Sample time: 0,01
- Samples per peak: 20
- Search/Integration window: 100/50
- Integration type: Integral
- Runs/Passes: 3200/1

Method 3

- Isotopes: ^{141}Pr, ^{157}Gd, ^{159}Tb, ^{163}Dy, ^{165}Ho, ^{169}Tm, and ^{209}Bi
- Mass window: 50
- Sample time: 0,01
- Samples per peak: 20
- Search/Integration window: 100/50
- Integration type: Integral
- Runs/Passes: 3/3

4.3. Buffers and solutions

Buffers and dissolutions used are summarized in Table 4.

Name	Composition
Reaction Buffer	10 mM MOPS 150 mM NaCl 0,1 % CHAPS 100 µM TCEP pH = 7,0 (adjusted with HCl conc.)
Preparation Buffer	10 mM MOPS 150 mM NaCl 0,1 % CHAPS pH = 7,0 (adjusted with HCl conc.)
TCEP Buffer	10 mM MOPS 150 mM NaCl 0,1 % CHAPS 2 mM TCEP pH = 7,0 (adjusted with HCl conc.)
MESNa Buffer	5 mM MESNA 10 mM MOPS 150 mM NaCl 0,1 % CHAPS 100 µM TCEP pH = 7,0 (adjusted with HCl conc.)
MESNa Incubation Buffer	5 mM MESNA 10 mM MOPS 150 mM NaCl 100 µM TCEP 0,1 % CHAPS pH = 7,0 (adjusted with HCl conc.)
Incubation Buffer	10 mM EDTA 100 mM Tris base 100 mM NaCl 1,0 % BSA pH= 7.0 (adjusted with HCl conc.)
Wash Buffer	10 mM EDTA 100 mM Tris base 1 M NaCl 0,1% BSA pH= 7,0 (adjusted with HCl conc.)
Elution Solution	0,1M Glycine 0,1 % CHAPS 500 ppt Bi

Table 4: Summary of buffers and solutions.

Fmoc Deprotection	80 % DMF 20 % Piperidine
Boc Deprotection	95 % TFA 5 % m-cresol
Boc Wash	99 % DMF 1 % NMM
Coupling	4 eq. monomer 4 eq. PyBOP® 8 eq. NMM 300 µL DMF
Capping	89 % DMF 6 % 2,6-Lutidine 5 % Acetic anhydride
Cleavage Tentagel®	90 % TFA 5 % Water 5 % TIS
Cleavage MBHA	80 % TFA 15 % TFMSA 5 % m-cresol
Deprotection Trt	90 % TFA 10 % TIS
Deprotection Fm	76 % DMF 20 % Piperidine 2 % DBU 2 % 2-Mercaptoethanol
Deprotection Mtt	90 % DCM 5 % TFA 5 % TIS
Re-Dissolution Solution	98,9 % Water 1,0 % Acetonitrile 0,1 % TFA

Table 4 (continuation): Summary of buffers and solutions.

4.4. Solid-phase peptide synthesis (SPPS)

Resin Loading: the loading of resins used for the preparation of donor probes was reduced to 0.2 mmol g^{-1} to increase the yield and reduce truncations. For that purpose, 250 mg of MBHA resin 100-200 mesh from *Novabiochem* with linker loading of 1.2 mmol g^{-1} were swollen for 1 hour in DMF. Afterwards, the resin was washed 3 times with DMF, 3 times with DMF:DIPEA (19:1 *v:v*) and then left in DMF:DIPEA (19:1 *v:v*) twice for 10 minutes. Consecutively, the resin was washed 10 times with DMF, and it was left overnight with 0,4 eq. PyBOP®, 1,2 eq. NMM in 1,5 mL DMF, and either 0,4 eq. Fmoc-Gly-OH or 0,4 eq. Boc-Cys(Fm)-OH for the ligation and transfer donor prove respectively. The resin was washed 10 times with DMF and capped twice for 5 minutes with the capping solution (Table 4). After washing 10 times with DMF and 10 times with DCM, the resin was dried in high vacuum. Resin loading was evaluated by either Fmoc or Fm monitoring: absorption at λ= 300 nm of 4 mL deprotection solution (either Fmoc or Fm) applied to 1,000 mg of resin in 1 mL series of twice 5 minutes and 2 wash steps was measured.

MPA Coupling: MPA was coupled to the preloaded Fmoc-Gly-MBHA resin described before. The N-terminal Fmoc-group was deprotected with Fmoc deprotection solution (Table 4) twice for 5 minutes and then washed 10 times with DMF. 10 eq. of 3-(tritylthio)propionic acid, (Trt)MPA, were dissolved together with 10 eq. PyBOP, 20 eq. DIPEA, and 10 eq. oxima in 400 µL DMF. The coupling was performed twice for 30 minutes. Afterwards, the resin was washed 10 times with DMF and capped with capping solution (Table 4).

Manual SPPS Fmoc protocol: Fmoc SPPS was used to synthesize acceptor probes. TentaGel® Rink Amide resin with loading of 0,18 mmol g^{-1} used as starting material for Fmoc synthesis was swollen for 30 minutes in DMF. Sequences smaller than 7 building blocks were synthesized with single couplings, with the exception of amino acids and first PNA monomers, which were always double coupled. Longer sequences were always double coupled, and N-terminal amino acids were triple coupled. As in common SPPS procedures, the N-terminal Fmoc group was deprotected with Fmoc deprotection solution (Table 4) and then washed 10 times with DMF. Coupling was performed with the coupling solution specified in Table 4 for 30 minutes. The resin was washed 3 times between couplings and 5 times as final wash with DMF. In order to avoid truncations, free terminal amino groups were capped with the capping solution (Table 4) before repeating the cycle.

Once the final product was synthesized the resin was washed 10 times with DCM and then incubated for 90 minutes in the *TentaGel®* Cleavage Solution (Table 4). The cleavage solution was collected, and the resin was washed 3 times with 200 µL TFA. Fractions were combined and the excess of TFA was evaporated in the rotavapor. Ice cold diethyl ether was used to precipitate the product. The precipitate was centrifuged for 5 minutes, dried under argon flow, and re-dissolved in re-dissolution solution (Table 4) for purification in the semi-preparative HPLC system. Spectrometric data by UPLC-MS was used to combine fractions containing the desired product. Fractions were combined, frozen, and lyophilized. The product was re-dissolved in a dissolution of CHAPS 0,1 %.

Automated Fmoc protocol: automated synthesis was carried out in a *ResPep-Parallel-Synthesizer*. Swollen Rink-Amide resins preloaded with the corresponding amino acid sequence were loaded in 1-cm-diameter columns. The procedure was similar to the manual synthesis following the deprotection, coupling, and capping cycles. The resin was washed 6 times with 200 µL DMF. The N-terminal Fmoc protecting group was cleaved with a double incubation for 2 minutes in the Fmoc cleavage solution (Table 4). After washing the resin 8 times with 200 µL of

DMF the next monomer was coupled. Double couplings each for 30 minutes were performed. The coupling solution was prepared by mixing of 4 eq. of the monomer dissolved in 100 µL of NMP, 3,6 eq. of HCTU in 30 µL DMF, and 8,0 eq. of NMM. The resin was washed 3 times with 200 µL DMF between double couplings and after the coupling. Capping of non-reacted chains was performed with a double incubation with 200 µL of the capping solution (Table 4) for 2 minutes. The resin was washed 10 times with DMF before restarting the cycle with the deprotection step.

Manual Boc protocol: The Boc protocol was used to synthesize all donor probes. After swelling of the preloaded (Trt)MPA-Gly-MBHA 30 minutes in DCM, the trityl group was removed with the Trt-deprotection solution (Table 4) twice for 15 minutes, and then the resin was washed 10 times with DCM and 10 times with DMF. Couplings were always double and were performed with the corresponding monomer dissolved in the coupling solution (Table 4) for 30 minutes, three DMF washes in between coupling, and 5 DMF washes after the second coupling. The free terminal amino groups were capped with the coupling solution and then the resin was washed 10 times with DMF and 10 times with DCM. The Boc group was removed with the Boc-deprotection solution (Table 4) twice for 5 minutes and then the cycle was repeated until completion of the sequence. Donor probes had the DOTA-moiety attached which was coupled and metalated as specified below.

Cleavage from the MBHA resin was carried out with the MBHA cleavage solution (Table 4) for 90 minutes. The cleavage solution was collected, and the resin was washed 3 times with 200 µL TFA. Fractions were combined, and the excess of TFA was evaporated in the rotavapor. Ice cold diethyl ether was used to precipitate the product, which was then centrifuged for 5 minutes, dried under argon flow and re-dissolved in re-dissolution solution (Table 4) for purification in the semi-preparative HPLC system. Spectrometric data by UPLC-MS was used to combine fractions containing the desired product. Fractions were combined, frozen, and lyophilized. The remaining product was dissolved in a dissolution of CHAPS 0,1 %.

DOTA Coupling: The metal tag was coupled on solid phase with a double coupling. The coupling solutions consisted of 4 eq. of DOTA-NHS together with 4 eq. of oxima and 54 eq. of NMM dissolved in 300 µL DMF. The resin was left to stir into the solution for 1 hour in probes shorter than 9 bases, and 3 hours in longer probes. Success of the coupling was always evaluated with a test cleavage were a small fraction was subjected to cleavage and ESI analysis. When needed, a third coupling was performed. After coupling, the resin was washed 5 times with DMF and then the ion metals were chelated.

Metalation: 10 eq. of the lanthanide chloride were dissolved in 400 µL DMF:water (9:1 *v:v*) and 6 eq. NMM were added. The suspension was left to stir overnight twice and then washed 10 times with DMF:water (9:1 *v:v*). An extra test cleavage was performed after the metalation step to ensure that all product had the metal chelated.

The source of Praseodymium, Gadolinium, Terbium, Holmium, Thulium, and Lutetium ions were the respective chlorides, whereas dysprosium ions were obtained from the corresponding oxide. Dysprosium chloride was isolated from the oxide by dissolving dysprosium oxide concentrated hydrochloric acid. The dissolution was neutralized with 4 M sodium hydroxide, lyophilized, and re-dissolved in DMF:water (9:1 *v:v*). After metalation, the product was cleaved from the resin and HPLC purified as described before.

PNA-MESNA Synthesis: MESNA-donor probes were synthesized in situ via transthioesterification in solution by incubation of the donor probe at room temperature for one hour in MESNA buffer (**Table 4**). After monitoring via UPLC-MS, the probe was directly used for the ligation reaction without further clean-up.

4.5. PNA-probes synthesized

4.5.1. Aceptor Probes

A1 H_2N -Gly gac atc c Cys- NH_2

Yield= 289 nmol (14 %); $C_{79}H_{103}N_{43}O_{22}S$; ε_{260}= 66.900 L mol^{-1} cm^{-1}; MW = 2167,18 g mol^{-1}

UPLC: t_R= 0,98 min (Gradient 3); MALDI-MS: $[M+H]^+$= 2167,1 (exp. 2167,1).

A2 H_2N - Gly Lys(Biotin) gac atc c Cys - NH_2

Yield= 1436 nmol (28 %); $C_{95}H_{129}N_{47}O_{25}S_2$; ε_{260}= 66.900 L mol^{-1} cm^{-1}; MW = 2393,49 g mol^{-1}

UPLC: t_R= 0,98 min (Gradient 3); MALDI-MS: $[M+H]^+$= 2394,49 (exp. 2393,5).

A3 H_2N - Gly Lys(Biotin) cc gcg aca tcc Cys- NH_2

Yield= 540 nmol (27 %); $C_{136}H_{181}N_{69}O_{37}S_2$; ε_{260}= 97.300 L mol^{-1} cm^{-1}; MW = 3438,46 g mol^{-1}

UPLC: t_R= 1,86 min (Gradient 3); ESI-MS: $[M+6H]^{6+}$= 574,08 (exp. 574,4), $[M+5H]^{5+}$= 688,70 (exp. 688,9), $[M+4H]^{4+}$= 959,2 (exp. 959,2).

A4 H_2N - Gly Lys(Biotin) Lys cc gcg aca t*cc Cys - NH_2

Yield= 1244 nmol (25 %); $C_{147}H_{205}N_{72}O_{38}S_2$; ε_{260}= 97.300 L mol^{-1} cm^{-1}; MW = 3638,71 g mol^{-1}

UPLC: t_R= 1,38 min (Gradient 3); MALDI-MS: $[M+H]^+$= 3639,71 (exp. 3640,3).

A5 H_2N - Gly Lys(Biotin) Lys ccg cga cat cc Cys - NH_2

Yield= 643 nmol (13 %); $C_{146}H_{193}N_{73}O_{40}S_2$; ε_{260}= 97.300 L mol^{-1} cm^{-1}; MW = 3566,63 g mol^{-1}

UPLC: t_R= 1,33 min (Gradient 3); MALDI-MS: $[M+H]^+$= 3567.63 (exp. 3566,0).

A6 H_2N - Gly Lys(Biotin) Lys ctg gta ggt cg Cys - NH_2

Yield= 1846 nmol (36 %); $C_{143}H_{192}N_{70}O_{36}S_2$; ε_{260}= 105.420 L mol^{-1} cm^{-1}; MW = 3692,70 g mol^{-1}

UPLC: t_R= 1,99 min (Gradient 3); ESI-MS: $[M+6H]^{6+}$= 616,46 (exp. 616,4), $[M+5H]^{5+}$= 739,56 (exp. 739,2), $[M+4H]^{4+}$= 924,18 (exp. 923,9).

A7 H_2N - Gly Lys(Biotin) Lys aac acc tac tc Cys - NH_2

Yield= 1436 nmol (29 %); $C_{143}H_{192}N_{70}O_{36}S_2$; ε_{260}= 103.600 L mol^{-1} cm^{-1}; MW = 3549,65 g mol^{-1}

UPLC: t_R= 1,89 min (Gradient 3); ESI-MS: $[M+6H]^{6+}$= 592,62 (exp. 592,9), $[M+5H]^{5+}$= 710,94 (exp. 711,6), $[M+4H]^{4+}$= 888,42 (exp. 888,1), $[M+3H]^{3+}$= 1184,22 (exp. 1183,6).

A8 H_2N - Gly Lys(Biotin) Lys tct cct gag ga Cys - NH_2

Yield= 526 nmol (11 %); $C_{145}H_{195}N_{71}O_{40}S_2$; ε_{260}= 103.900 L mol^{-1} cm^{-1}; MW = 3636,68 g mol^{-1}

UPLC: t_R= 1,97 min (Gradient 3); ESI-MS: $[M+5H]^{5+}$= 728,34 (exp. 728,3), $[M+4H]^{4+}$= 910,18 (exp. 909,6), $[M+3H]^{3+}$= 1213,23 (exp. 1214,1).

A9 NH_2 – Gly Lys(Biotin) Lys cga cgt gaa ga Cys-NH_2

Yield= 696 nmol (14 %); $C_{146}H_{193}N_{79}O_{36}S_2$; ε_{260}= 119.000 L mol^{-1} cm^{-1}; MW = 3694,73 g mol^{-1}

UPLC: t_R= 1,44 min (Gradient 3); ESI-MS: $[M+4H]^{4+}$= 924,69 (exp. 924,6).

A10 NH_2 – Gly Lys(Biotin) Lys gga act acc cct Cys-NH_2

Yield= 323 nmol (6 %); $C_{154}H_{207}N_{77}O_{41}S_2$; ε_{260}= 127.300 L mol^{-1} cm^{-1}; MW = 4374,41 g mol^{-1}

UPLC: t_R= 1,54 min (Gradient 3); ESI-MS: $[M+6H]^{6+}$= 730,08 (exp. 730,1), $[M+5H]^{5+}$= 875,89 (exp. 875,9), $[M+4H]^{4+}$= 1094,61 (exp. 1094,4)

A11 NH_2 – Gly Lys(Biotin) Lys cta cca cga ctt Cys-NH_2

Yield= 1061 nmol (21 %); $C_{154}H_{208}N_{74}O_{42}S_2$; ε_{260}= 109.300 L mol^{-1} cm^{-1}; MW = 3831,90 g mol^{-1}

UPLC: t_R= 1,52 min (Gradient 3); ESI-MS: $[M+6H]^{6+}$= 639,66 (exp. 639,9), $[M+5H]^{5+}$= 767,39 (exp. 767,6), $[M+4H]^{4+}$= 958,98 (exp. 958,8).

A12 NH_2 – Gly Lys(Biotin) Lys aga tag tac tgt ga Cys-NH_2

Yield= 315 nmol (6 %); $C_{180}H_{235}N_{93}O_{47}S_2$; ε_{260}= 150.400 L mol^{-1} cm^{-1}; MW = 4517,52 g mol^{-1}

UPLC: t_R= 1,49 min (Gradient 3); ESI-MS: $[M+5H]^{5+}$= 904,51 (exp. 904,6), $[M+4H]^{4+}$= 1130,39 (exp. 1130,2).

A13 NH_2 – Gly Lys(Biotin) Lys tta tat ctc ttt tc Cys-NH_2

Yield= 1171 nmol (23 %); $C_{178}H_{240}N_{74}O_{55}S_2$; ε_{260}= 122.400 L mol^{-1} cm^{-1}; MW = 4360,40 g mol^{-1}

UPLC: t_R= 1,52 min (Gradient 3); ESI-MS: $[M+5H]^{5+}$= 897,08 (exp. 897,8), $[M+4H]^{4+}$= 1091,1 (exp. 1090,8).

A14 NH_2 – Gly Lys(Biotin) Lys ctt tgg tta tct ga Cys-NH_2

Yield= 643 nmol (13 %); $C_{179}H_{238}N_{82}O_{53}S_2$; ε_{260}= 131.600 L mol^{-1} cm^{-1}; MW = 4450,45 g mol^{-1}

UPLC: t_R= 1,51 min (Gradient 3); ESI-MS: $[M+6H]^{6+}$= 742,75 (exp. 742,8), $[M+5H]^{5+}$= 891,10 (exp. 890,3), $[M+4H]^{4+}$= 1113,62 (exp. 1113,3).

4.5.2. Donor probes

D1 H_2N-Gly $OC(CH_2)_2$ S Gly cac ccc tt DOTA(Ho^{3+})

Yield= 1209 nmol (24 %); $C_{108}H_{143}N_{47}O_{37}SHo$; ε_{260}= 64.500 L mol^{-1} cm^{-1}; MW = 3352,07 g mol^{-1}

UPLC: t_R= 1,50 min (Gradient 3); ESI-MS: $[M+6H]^{6+}$= 559,82 (exp. 559,2), $[M+5H]^{5+}$= 671,58 (exp. 670,8), $[M+4H]^{4+}$= 839,23 (exp. 838,2), $[M+3H]^{3+}$= 1118,6 (exp. 1117,2).

D2 H_2N - Cys[Gly DOTA(Ho^{3+})] cac ccc tt - Ac

Yield= µmol (%); $C_{106}H_{141}N_{47}O_{35}SHo$; ε_{260}= 64.500 L mol^{-1} cm^{-1}; MW = 3349,05 g mol^{-1}

UPLC: t_R= 1,35 min (Gradient 3); ESI-MS: $[M+6H]^{6+}$= 559,18 (exp. 559,2), $[M+5H]^{5+}$= 670,82 (exp. 670,8), $[M+4H]^{4+}$= 838,27 (exp. 838,2), $[M+3H]^{3+}$= 1117,36 (exp. 1117,2)

D3 H_2N-Gly $OC(CH_2)_2$ S Gly cac ccc ttc tca DOTA(Ho^{3+})

Yield= 2623 nmol (35 %); $C_{146}H_{192}N_{67}O_{47}SHo$; ε_{260}= 101.100 L mol^{-1} cm^{-1}; MW = 3879,58 g mol^{-1}

UPLC: t_R= 1,50 min (Gradient 3); ESI-MS: $[M+5H]^{5+}$= 555,23 (exp. 554,7), $[M+6H]^{6+}$= 647,61 (exp. 647,2), $[M+5H]^{5+}$= 776,92 (exp. 775,9), $[M+4H]^{4+}$= 970,90 (exp. 969,8).

D4 H_2N-Gly $OC(CH_2)_2$ S Gly cac ccc ttc* tc*a Lys DOTA(Ho^{3+})

Yield= 3799 nmol (25 %); $C_{164}H_{230}N_{72}O_{49}SHo$; ε_{260}= 101.100 L mol^{-1} cm^{-1}; MW = 4145,90 g mol^{-1}

UPLC: t_R= 1,21 min (Gradient 3); ESI-MS: $[M+6H]^{6+}$= 691,99 (exp. 692,0), $[M+5H]^{5+}$= 830,19 (exp. 829,6), $[M+4H]^{4+}$= 1037,48 (exp. 1036,9).

D5 H_2N-Gly $OC(CH_2)_2$ S Gly cac ccc ttc tca Lys DOTA(Ho^{3+})

Yield= 3877 nmol (45 %); $C_{164}H_{230}N_{72}O_{49}SHo$; ε_{260}= 101.100 L mol^{-1} cm^{-1}; MW = 4003,65 g mol^{-1}

UPLC: t_R= 1,31 min (Gradient 3); ESI-MS: $[M+6H]^{6+}$= 668,28 (exp. 668,6), $[M+5H]^{5+}$= 801,73 (exp. 801,9), $[M+4H]^{4+}$= 1101,92 (exp. 1001.4).

D6 H_2N - Gly $OC(CH_2)_2$ S Gly ata ggt ctt ggt Lys DOTA(Tb^{3+})

Yield= 2985 nmol (28 %); $C_{158}H_{205}N_{75}O_{50}STb$; ε_{260}= 118.000 L mol^{-1} cm^{-1}; MW = 4190,87 g mol^{-1}

UPLC: t_R= 1,87 min (Gradient 3); ESI-MS: $[M+5H]^{5+}$= 839,18 (exp. 838,5), $[M+4H]^{4+}$= 1048,73 (exp. 1047,4).

D7 H_2N - Gly $OC(CH_2)_2$ S Gly tgc tgg ggt gg Lys DOTA(Tm^{3+})

Yield= 1857 nmol (35 %); $C_{149}H_{193}N_{75}O_{48}STm$; ε_{260}= 102.400 L mol^{-1} cm^{-1}; MW = 3991,64 g mol^{-1}

UPLC: t_R= 1,72 min (Gradient 3); ESI-MS: $[M+5H]^{5+}$= 799,34 (exp. 798,8), $[M+4H]^{4+}$= 998,92 (exp. 997,5).

D8 H_2N - Gly $OC(CH_2)_2$ S Gly ggc ctt cgt tc Lys DOTA(Lu^{3+})

Yield= 3787 nmol (30 %); $C_{146}H_{194}N_{66}O_{49}SLu$; ε_{260}= 93.000 L mol^{-1} cm^{-1}; MW = 3852,58 g mol^{-1}

UPLC: t_R= 1,71 min (Gradient 3); ESI-MS: $[M+5H]^{5+}$= 771,52 (exp. 771,5), $[M+4H]^{4+}$= 964,15 (exp. 963,8).

D9 NH_2 – Gly $OC(CH_2)_2$S Gly agt gtg gac acc Lys DOTA (Tb^{3+})

Yield= 166 nmol (3 %); $C_{148}H_{205}N_{81}O_{47}STb$; ε_{260}= 119.000 L mol^{-1} cm^{-1}; MW = 4169,86 g mol^{-1}

UPLC: t_R= 1,37 min (Gradient 3); ESI-MS: $[M+4H]^{4+}$= 1043,47 (exp. 1042,6).

D10 NH_2 – Gly $OC(CH_2)_2$S Gly ccc cgg gat ca Lys DOTA (Ho^{3+})

Yield= 371 nmol (7 %); $C_{145}H_{182}N_{73}O_{44}SHo$; ε_{260}= 101.200 L mol^{-1} cm^{-1}; MW = 3845,56 g mol^{-1}

UPLC: t_R= 1,38 min (Gradient 3); ESI-MS: $[M+4H]^{4+}$= 962,40 (exp. 961,6).

D11 NH_2 – Gly $OC(CH_2)_2$S Gly gat agt gaa tca ga Lys DOTA (Tm^{3+})

Yield= 379 nmol (8 %); $C_{182}H_{132}N_{96}O_{51}STm$; ε_{260}= 152.800 L mol^{-1} cm^{-1}; MW = 4769.44 g mol^{-1}

UPLC: t_R= 1,39 min (Gradient 3); ESI-MS: $[M+6H]^{6+}$= 795,91 (exp. 795,4), $[M+5H]^{5+}$= 954,90 (exp. 954,2), $[M+4H]^{4+}$= 1193,37 (exp. 1192,3).

D12 NH_2 – Gly $OC(CH_2)_2$S Gly tta gat ggc agg Lys DOTA (Pr^{3+})

Yield= 518 nmol (10 %); $C_{160}H_{206}N_{82}O_{48}SPr$; ε_{260}= 123.800 L mol^{-1} cm^{-1}; MW = 4206,88 g mol^{-1}

UPLC: t_R= 1,39 min (Gradient 3); ESI-MS: $[M+5H]^{5+}$= 842,38 (exp. 842,0), $[M+4H]^{4+}$= 1052,73 (exp. 1051,8).

D13 NH_2 – Gly $OC(CH_2)_2$S Gly gtc aat gta atg tc Lys DOTA (Gd^{3+})

Yield= 512 nmol (10 %); $C_{181}H_{234}N_{92}O_{55}SGd$; ε_{260}= 119.400 L mol^{-1} cm^{-1}; MW = 4699,70 g mol^{-1}

UPLC: t_R= 1,38 min (Gradient 3); ESI-MS: $[M+5H]^{5+}$= 940,95 (exp. 940,3), $[M+4H]^{4+}$= 1175,93 (exp. 1174,9).

D14 NH_2 – Gly $OC(CH_2)_2S$ Gly acc gaa aac ga Lys DOTA (Dy^{3+})

Yield= 634 nmol (13 %); $C_{147}H_{190}N_{80}O_{39}SDy$; ε_{260}= 117.600 L mol^{-1} cm^{-1}; MW = 3884,20 g mol^{-1}

UPLC: t_R= 1,29 min (Gradient 3); ESI-MS: $[M+5H]^{5+}$= 777,84 (exp. 777,2), $[M+4H]^{4+}$= 972,06 (exp. 971,1).

D15 H_2N - Cys[Gly DOTA(Ho^{3+})] cac ccc ttc tca Lys - Ac

Yield= 2983 nmol (30 %); $C_{152}H_{204}N_{70}O_{47}SHo$; ε_{260}= 101.100 L mol^{-1} cm^{-1}; MW = 4003,72 g mol^{-1}

UPLC: t_R= 1,21 min (Gradient 3); ESI-MS: $[M+6H]^{6+}$= 668,29 (exp. 669,2), $[M+5H]^{5+}$= 801,75 (exp. 801,7), $[M+4H]^{4+}$= 1001,94 (exp. 1002,0).

D16 H_2N-Gly $OC(CH_2)_2$ S Gly cac ccc ttc tca Lys-NH_2

Yield= 2581 nmol (25 %); $C_{136}H_{179}N_{65}O_{40}S$; ε_{260}= 101.100 L mol^{-1} cm^{-1}; MW = 3455,42 g mol^{-1}

UPLC: t_R= 1,26 min (Gradient 3); ESI-MS: $[M+6H]^{6+}$= 576,91 (exp. 577,3), $[M+5H]^{5+}$= 692,09 (exp. 692,1), $[M+4H]^{4+}$= 864,86 (exp. 864,4), $[M+3H]^{3+}$= 1152,81 (exp. 1153,1).

4.5.3. Ligation product

P01 H_2N - Gly Lys(Biotin) gac ctc c Cys Gly cac ccc ttc t DOTA(Ho^{3+})

Yield= 235 nmol (12 %); $C_{219}H_{281}N_{99}O_{68}S_3Ho$; ε_{260}= 140.300 L mol^{-1} cm^{-1}; MW = 5577,57 g mol^{-1}

UPLC: t_R= 1,65 min (Gradient 3); ESI-MS: $[M+7H]^{7+}$= 797,80 (exp. 797,8), $[M+6H]^{6+}$= 930,60 (exp. 930,6), $[M+5H]^{5+}$= 1116,52 (exp. 1116,4); MALDI: $[M]^+$ = 5570.

4.6. Synthesis of γ-PNA

The synthetic route for ᴸKγ-c-PNA was based on the work of D. H. Appella *et al.*[106] Modifications on the procedure are described on each step.

4.6.1. Nᵋ-(Benzyloxycarbonyl)-L-Lysine Hydrochloride[151]

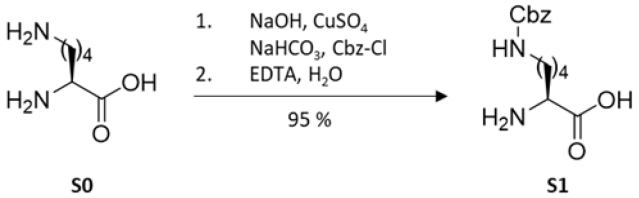

The procedure followed for the protection of the side chain of L-Lys was first described by Z. Balajthy.[151] L-Lys (S0) and 2 eq. sodium hydroxide (NaOH) were dissolved in 20 mL water. A solution of 0.5 eq. copper sulfate in 40 mL water was added. After the addition of 1,2 eq. sodium hydrogen carbonate ($NaHCO_4$), the mixture was placed in an ice bath, and 1,2 eq. of benzyl chloroformate were added dropwise. The reaction mixture was left stirring overnight at room temperature. Afterwards, the reaction mixture was filtered, and after washing with 50 mL water and 25 mL acetone, it was resuspended in 50 mL of a solution 1,1 eq. 2,2',2'',2'''-(ethane-1,2-diyldinitrilo)tetraacetic acid (EDTA) and 4,4 eq. NaOH. The pH was adjusted to 7,0 with concentrated hydrochloric acid (HCl) and the mixture was left to stir overnight. The white precipitate was filtrated and dried in a heating chamber at 40°C.

Yield: 4,750 g (16,94 mmol, 95%) $C_7H_{13}NO_3$ (280,32 g/mol)

HR-MS: m/z = 281.14 ([M^+]: 281.30).

^{1}H-NMR (300 MHz, [D_1]TFA, 25°C): δ [ppm] = 7,24–7,21 (m, 5H, CH-Cbz), 5,29 (s, 2H, OCH_2-Cbz), 4,28–4,19 (m, 1H, CH), 3,20–3,16 (m, 2H, NCH_2), 2,14–2,08 (m, 2H, CH_2), 1,82–1,81 (m, 2H, CH_2), 1,68–1,55 (m, 2H, CH_2) ppm.

^{13}C-NMR (75 MHz, [D_1]TFA, 25°C): δ [ppm] = 174,56 (COOH), 134,33 (CO), 130,99 (C_q-Cbz), 130,31 (CH-Cbz), 130,07 (CH-Cbz), 129,35 (CH-Cbz), 126,79 (CH-Cbz), 72,74 (OCH_2-Cbz), 55,65 (CH), 42,35 (NCH_2), 30,92 (CH_2), 27,94 (CH_2), 22,26(CH_2).

4.6.2. Nᵅ-(*tert*-Butyloxycarbonyl,Nᵋ-(benzyloxycarbonyl)-lysin[152]

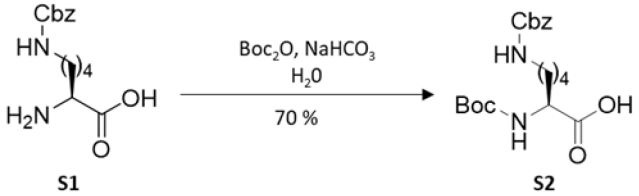

Product S1 together with 1 eq. $NaHCO_4$ was suspended in 70 mL water:2-methyl-2-propanol (4:3) and 1 eq. Di-*tert*-butyldicarbonat dissolved in 10 mL 2-methyl-2-propanol was added dropwise. The mixture was heated to 90°C until it was clear and then left at room temperature for 4 hours. The mixture was filtrated, and the filtrate was extracted once with 30 mL pentane, and after acidification with 1,2 M HCl it was further extracted 3 times with ethyl acetate. The organic phase was dried over magnesium sulfate ($MgSO_4$), and the solvent was eliminated under reduced pressure to achieve a yellow oil. The procedure was described on Keller *et al.*[152]

Yield: 3,335 g (8,74 mmol, 70 %) $C_{19}H_{28}N_2O_6$ (380,44 g/mol)

HR-MS: *m/z* = 379,1870 ([M⁻]: 379,1869).

^{1}H-NMR (500MHz, [D4]MeOD, 25°C): δ [ppm] = 7,33–7,27 (m, 5H, C*H*-Cbz), 5,05 (s, 2H, OC*H*2), 4,10–4,04 (m, 1H, C$^{\gamma}$*H*), 3,12–3,09 (m, 2H, CH_2), 1,66–1,46 (m, 6H, 3×CH_3), 1,43 (s, 9H, C(CH_3)$_3$).

^{13}C-NMR (125MHz, [D4]MeOD, 25°C): δ [ppm] = 159,15 (*C*O-Cbz), 158,37 (*C*O- Boc); 129,63 (*C*H-Cbz), 129,11 (*C*H-Cbz), 128,93 (*C*H-Cbz), 80,66 (C_q-Boc), 67,51 (OCH_2), 54,99 (*C*$^{\gamma}$H), 41,62 (NH*C*H2), 32,58 (*C*H_2), 30,59 (*C*H_2CH), 28,89 (*C*H_3), 24,27 (*C*H_2).

4.6.3. N$^{\alpha}$-(tert-Butyloxycarbonyl,N$^{\varepsilon}$-(benzyloxycarbonyl)-lysin-Weinrebamide[153]

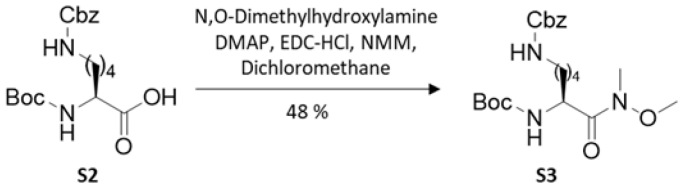

The procedure was adapted from the patent of Wang *et al.*[153] Product S2 was suspended in 40 mL dichloromethane and 1,1 eq. N-methylmorpholine, 1,2 eq. N-O-dimethylamine, and 0,05 eq. 4-dimethylaminopyridine were added. After placing the reaction mixture in an ice bad, 1,2 eq. 1-ethyl-3-(3-dimethylaminopropyl)carbodiimide) (EDCI) were added, and the reaction was left overnight at room temperature. After volatiles were removed at reduced pressure, the residue was dissolved in saturated aqueous $NaHCO_4$ and ethyl acetate. The layers were separated, and the organic was washed with brine, dried over $MgSO_4$, filtered, and evaporated to dryness. Product S3 was chromatographically purified.

Yield: 1,596 g (3,77 mmol, 48 %) $C_{21}H_{33}N_3O_6$ (423,50 g mol^{-1})

HR-MS: m/z = 446,2260 ([M+Na^{+}]: 446,2266)

^{1}H-NMR (500MHz, [D_1]$CDCl_3$, 25°C): δ [ppm] = 7,35–7,29 (m, 5H, CH-Cbz), 5,24–5,22 (NH), 5,08 (s, 2H, OCH_2Ph), 4,92 (brs, 1H, NH), 4,65 (Brs, 1H, C$^{\gamma}$H), 3,75 (s, 3H, OCH_3), 3,19 (s, 3H, NCH_3), 3,16–3,14 (m, 2H, NCH_2), 1,73–1,49 (m, 4H, CH_2), 1,41 (s, 9H, C(CH_3)$_3$), 1,39–1,35 (m, 2H, CH_2).

^{13}C-NMR (125MHz, [D_1]CDCl3, 25°C): δ [ppm] = 172,70 (CO), 156,45 (CO-Cbz), 155,72 (CO-Boc), 136,53 (Cq-Cbz), 128,51 (CH-Cbz), 128,15 (CH-Cbz), 128,07 (CH-Cbz), 79,65 (Cq-Boc), 66,58 (OCH_2), 61,65 (OCH_3), 50,02 (C$^{\gamma}$H), 40,78 ($NHCH_2$), 32,61 (CH_2), 32,08 (NCH_3), 29,22 (CH_2), 28,36 (C(CH_3)$_3$), 22,45 (CH_2).

4.6.4. N$^{\alpha}$-(*tert*-Butyloxycarbonyl)aminoethyl-N$^{\varepsilon}$-benzyloxycarbonyl)glycinmethylester[106]

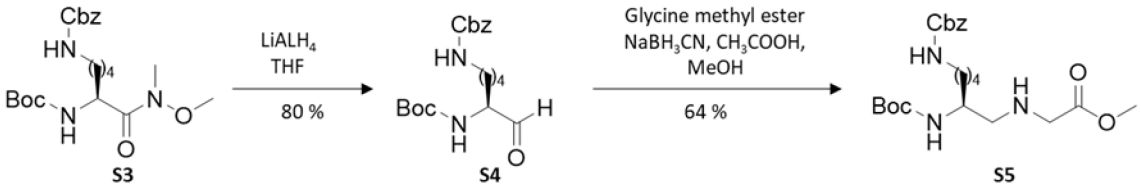

The dissolution of product S3 in 30 mL of dry tetrahydrofuran (THF) was placed in a dry ice acetone bath (-80°C). 3,5 mL of a dissolution 3,5 M lithium aluminum hydride ($LiAlH_4$) was slowly added to the dissolution. The reaction was left for 1 hour at room temperature and stopped with the slow addition of a dissolution 10 % sodium hydrogen sulfate (m/m) until no further precipitate was formed. The mixture was filtered, and the filtrate was extracted with ethyl acetate. The organic phase was extracted with brine, dried over $MgSO_4$, and it was taken to dryness under reduced pressure.

The yellow oil containing product S4 was dissolved in 90 mL THF:methanol (1:3, *v:v* ratio) and added to a 30 mL methanol solution placed in an ice bath with 3 eq. glycine methyl ester. After 1,1 eq. sodium cyanoborohydride and 0,5 mL acetic acid was added, the mixture was left overnight at room temperature. An extraction with ethyl acetate was carried out and the organic phase was further extracted with brine, dried over $MgSO_4$, and evaporated to dryness under reduced pressure. The product was cleaned-up in a column with ethyl acetate.

Yield: 0,817 g (1,87 mmol, 51 %) $C_{22}H_{35}N_3O_6$ (437,53 g/mol).

HRMS: m/z = 438,2631 ([M^+]: 438,2604).

^{1}H-NMR (500MHz, [D1]$CDCl_3$, 25 °C): δ [ppm] = 7,36–7,30 (m, 5H, CH-Cbz), 5,08 (s, 2H, OCH_2Ph), 4,90 (m, 1H, NH-Boc), 4,75 (m, 1H, NH-Cbz), 3,72 (s, 3H, OCH_3), 3,63 (brs, 1H, CH), 3,48–3,35 (m, 2H, CH_2OOMe), 3,21–3,17 (m, 2H, $NHCH_2$), 2,66–2,61 (m, 2H, $NHCH_2$), 1,55–1,45 (m, 4H, 2 × CH_2), 1,42 (s, 9H, $C(CH_3)_3$), 1,40–1,25 (m, 2H, CH_2).

^{13}C-NMR (125MHz, [D1]$CDCl_3$, 25 °C): δ [ppm] = 128,51 (CH-Cbz), 128,07 (CH-Cbz), 66,60 OCH_2-Cbz), 51,84 (OCH_3), 50,68 (CHNH), 40,72 (CH_2COOMe), 28,40 (CH_3), 22,90 (CH_2).

4.6.5. N^{α}-((N^4-benzyloxycarbonyl)cytosin-1-yl)acetyl)-N-(2-*tert*-butyloxycarbonyl)-aminoethyl)-Nε-benzyloxycarbonyl)-glycinmethylester[106]

2 eq. of Product S5 were dissolved in 17 mL acetonitryle:N,N-dimethylformamide (DMF) (1:1) and 4 eq. of N-methylmorpholine were added. The sample was placed in a methanol ice bath (-15 °C) and 3 eq. of pivaloyl chloride were added. After the reaction was left to stir for 15 minutes, a dissolution of 1 eq. product S9 in 5 mL acetonitrile:DMF (1:1) was added. The reaction was left overnight at room temperature. 100 mL ethyl acetate were added to the mixture and it was extracted with HCl 0,1 M. The organic phase was further extracted with brine, dried over magnesium sulfate, filtered, and evaporated to dryness. The product was cleaned-up in a column conditioned with ethyl acetate:methanol (9:1 v:v).

Yield: 0,735 g (1,02 mmol, 90 %) $C_{36}H_{46}N_6O_{10}$ (722,78 g/mol).

Rf-Value: (Ethylacetat/ MeOH: 9:1, v:v): 0,72.

HRMS: m/z = 723,3257 ([M^+]: 723,3353).

^{1}H-NMR (500MHz, [D1]$CDCl_3$, 25°C): δ [ppm] = 7,65–7,64 (d, 3J(H,H) = 5.0 Hz, 1H, CH), 7,53–7,52 (d, 3J(H,H) = 5,0 Hz, 1H, CH), 7,40–7,35 (m, 10H, CH-Cbz), 5,23–5,09 (m, 4H, 2 × CH_2Ph), 4,61–4,52 (m, 2H, CH_2N), 4,34–4,30 (m, 1H, xx), 3,98–3,94 (m, 1H, C$^\gamma$H), 3,80–3,72 (m, 3H, OCH_3), 3,61–3,39 (m, 2H, CH_2COOMe), 3,20 (m, 2H, CH_2CH), 1,68–1,56 (m, 4H, 2 × CH_2), 1,45–1,36 (m, 9H, $C(CH_3)_3$).

13C-NMR (125MHz, [D1]$CDCl_3$, 25°C): δ [ppm] = 183,72 (), 128,97 (CH-Cbz), 128,82 (CH-Cbz), 128,42 (CH-Cbz), 68,11 (OCH_2), 66,91 (CH), 66,84 (CH), 53,25 (CH_2COOMe), 52,62 (OCH_3), 40,64 (CH_2), 38,77 (CH_2), 36,83 (CH_3), 28,68 (CH), 28,64 (CH), 27,39 ($CCH_3)_3$), 26,83 (CH).

4.6.6. N^{α}-((N^4-benzyloxycarbonyl)cytosin-1-yl)acetyl)-N-(2-tert-butyloxycarbonyl)-aminoethyl)-Nε-benzyloxycarbonyl)-glycin[106]

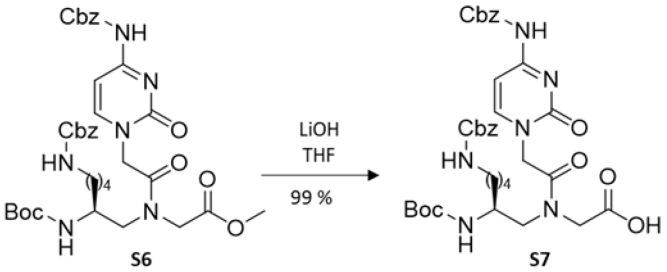

Product S6 was dissolved in 28 mL dry THF and placed into an ice bath. After 5 eq. lithium hydroxide were slowly added to the dissolution, the reaction was left at room temperature for 1,5 h. The pH was adjusted to 2 with HCl 1M and the reaction mixture was extracted with ethyl acetate. The organic phase was further extracted with brine, dried over $MgSO_4$, filtered, and evaporated to dryness under reduced pressure.

Yield: 0,728 g (1,03 mmol, 99 %) $C_{35}H_{44}N_6O_{10}$ (708,76 g/mol).

HRMS: m/z = 731,3018 ([M+Na^+]: 731,3016).

^{1}H-NMR (500MHz, [D1]$CDCl_3$, 25°C): δ [ppm] = 10,83 (brs, 1H, COOH), 7,86–7,81 (m, 1H, CH-Cyt), 7,43–7,32 (m, 10H, 2×CH-Cbz), 7,25–7,22 (m, 1H, CH-Cyt), 5,20 (s, 2H, OCH_2Ph), 5,00 (s, 2H, OCH_2Ph), 4,89 (m, 1H, $C^{\gamma}H$), 4,80–4,58 (m, 1H, CH_2N), 4,53–4,50 (m, 1H, CH_2N), 4,29–4,19 (m, 1H, CH_2), 4,06–3,87 (CH_2), 3,75–3,51 (m, 1H, NH-Boc), 3,00–2,95 (m, 2H, CH_2NH), 1,47 (m, 2H, CH_2CH), 1,39–1,36 (m, 9H, $C(CH_3)_3$), 1,30–0,84 (m, 4H, 2×CH_2).

^{13}C-NMR (75MHz, [D6]DMSO, 25°C): δ [ppm] = 169,97 (COOH), 169,02 (CO), 163,01 (CONH), 162,74 (CONH), 155,75 (CO-tBu), 150,07 (CH), 128,15 (Cq-Cbz), 128,01 (CqCbz), 127,625 (CH-Cbz), 127,59 (CH-Cbz), 127,40 (CH-Cbz), 93,67 (CH), 77,60 (Cq-tBu), 66,18 (OCH_2-Cbz), 66,16 (OCH_2-Cbz), 64,77 (CH), 62,55 (CH_2CH), 55,46 (CH_2N-tBu), 30,67 (CH2N-Cbz), 30,09 (CH_2N), 27,93 (CH_2), 27,85 (($CH_3)_3$), 22,45 (CH_2).

4.6.7. N^4-(Benzyloxycarbonyl)cytosine[106]

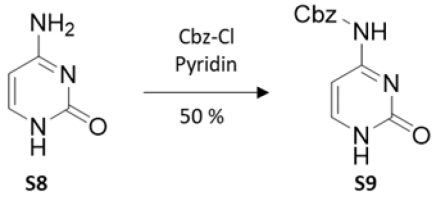

S8 S9

Cytosin (S8) was suspended in 200 mL dry pyridine. After 1.2 eq. benthyl chloroformate were slowly added, the reaction was left overnight at room temperature. The solvent was evaporated under reduced pressure and the product was re-dissolved in 50 mL water. A precipitate was formed when the pH was adjusted to 3 with concentrated HCl that was isolated by filtration. The residue was recrystallized from ethanol to achieve product S9 as a white powder.

Yield: 5 g (20,39 mmol, 50 %) $C_{12}H_{11}N_3O_3$ (245,23 g/mol)

HR-MS: m/z = 246,0871 ([M+]: 246,0873).

^{1}H-NMR (300 MHz, [D6]DMSO, 25°C): δ [ppm] = 7,81–7,79 (d, 3J(H,H) = 5,0 Hz, 1H, CH), 7,41–7,35 (m, 5H, CH-Cbz), 6,93–6,92 (d, 3J(H,H) = 5,0 Hz, 1H, CH), 5,18 (s, 2H, OCH2-Cbz).

^{13}C-NMR (75 MHz, [D6]DMSO, 25°C): δ [ppm] = 163,61 (CO), 146,69 (CH), 136,00 (CO), 128,44 (CH-Cbz), 128,09 (CH-Cbz), 127,87 (CH-Cbz), 93,47 (CH), 66,36 (OCH_2).

4.6.8. ((N^4-Benzyloxycarbonyl)cytosine-1-yl) acetic acid[106]

Experimental

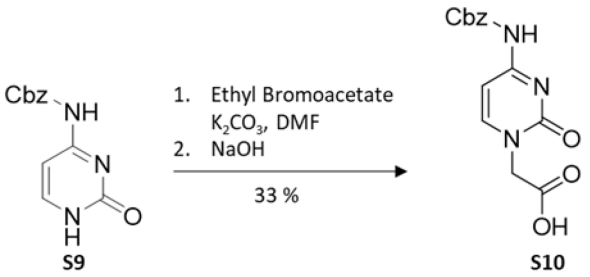

Product **S11** was suspended in 80 mL DMF with 1 eq. potassium carbonate. After 1 eq. ethyl bromoacetate was slowly added, the mixture was left stirring overnight at room temperature. The mixture was filtrated, and the filtrate was evaporated to dryness. The remaining solid was dissolved in 40 mL water and acidified with HCl 4 M to observe the formation of a precipitate. The mixture was filtered, and the residue was dissolved in 50 mL NaOH 1 M and left at room temperature with continuous stirring for 30 minutes. The reaction was cooled in an ice bath and filtered. The filtrate was acidified with HCl 4 M until a precipitate appeared. The mixture was filtered again, and the remaining residue was dried at 40°C and characterized as product S10.

Yield: 1,650 g (5,44 mmol, 33 %) $C_{14}H_{13}N_3O_5$ (303,27 g/mol)

HRMS: m/z = 304,0927 ([M+]: 304,0928).

^{1}H-NMR (500 MHz, [D6]DMSO, 25°C): δ [ppm] = 10,38 (brs, 1H, C^4NH), 7,81–7,79 (d, 3J(H,H) = 5,0 Hz, 1H, CH), 7,43–7,35 (m, 5H, CH-Cbz), 7,03–7,02 (d, 3J(H,H) = 5,0 Hz, 1H, CH), 5,19 (s, 2H, OCH-Cbz), 4,53 (s, 2H, CH_2COOH).

^{13}C–NMR (75 MHz, [D6]DMSO, 25°C): δ [ppm] = 169,36 (CO), 163,30 (C^2O), 146,62 (C^6H), 136,95 (CO), 128,49 (CH), 128,16 (CH), 127,94 (CH), 94,00 (C^5H), 66,51 (OCH_2), 50,52 (CH_2COOH).

4.7. PNA/DNA hybridization calculations

The nearest-neighbor model was used to calculate the thermodynamic data of DNA/PNA duplexes.[154-155] It was assumed that the formation of the probe/template duplex followed the equilibrium described by equation 1.

(1) $$\text{Probe} + \text{Template} \underset{\mathrm{k_{dissociation}}}{\overset{\mathrm{k_{association}}}{\longleftrightarrow}} \text{Duplex} \qquad K_a = \frac{[\text{Duplex}]}{[\text{Probe}]\cdot[\text{Template}]}$$

The values of Gibbs's free energy (ΔG) were used from DNA. The association constant K_a, was calculated with the value of the Gibb's free energy according to equation 2.

(2) $$\Delta G° = -RTlnK_a$$

where R is the ideal gas constant and T the temperature.

4.8. Native chemical ligation and transfer reaction

The acceptor probe was diluted into the degassed TCEP buffer in double the concentration required for the experiment and incubated for 20 minutes. The donor probe was dissolved at double concentration in degassed Reaction Buffer for the transfer reaction, and in the degassed MESNa buffer for the ligation and then incubated for 1 hour. The same volume of each probe was combined into the same vial and separated in aliquots of the same volume. The template was spiked into the different aliquots while one was used as non-template control (NTC). Samples were incubated for the required time with temperature control. The reaction was quenched with 1 % TFA or concentrated sodium hydroxide.

4.9. Purification method

Quenched samples were neutralized: basic quenching was neutralized with TFA and acidic quenching was neutralized with NaOH (final pH = 7.0). The volume was doubled with the incubation buffer (Table 4). The streptavidin-coated magnetic particles were incubated twice for 15 minutes in a total volume of 1 mL in the incubation buffer (Table 4). A minimum of 5 µL or 1,5 eq. of streptavidin (based on the binding capacity) were added to each sample. Samples were then incubated at room temperature for 15 minutes. Passed that time, the vials were vortexed and the beads were immobilized with a magnet. The supernatant was collected and discharged with a micropipette, and the magnetic beads were washed 3 times with the washing buffer (Table 4) and once with a dissolution of CHAPS 0,1 %. Several elution solutions were used, but the standard consisted on a dissolution of Gly-HCl 0,1 M and CHAPS 0,1 % spiked with 500 ppt internal standard which was added to the washed beads and incubated at 90 °C for 30 minutes. The supernatant was then transferred into another vial and directly injected into the ICP system.

5 Results and Discussion

5.1. NCL with ICP detection

5.1.1 Methodology

For detection with ICP-MS of template-directed NCL with PNA probes, it is necessary to attach the MeCAT chelating the lanthanoid to one of the reporter probes. After performing the reaction, measuring the lanthanoid signal is indicative of the presence of the metal tag, with disregard of the species that it is attached to. Since the plasma eliminates all short of molecular information and yield signals based on the elemental composition, it is necessary to separate the different species before injection. As indicated in the workflow of Figure 15, after the template-directed NCL reaction, purification is needed before measurement into the ICP-MS. The unambiguous assignation of the lanthanoid signal to the product of the reaction, depends on the proper elimination of the reactant containing the MeCAT. Separation was attempted via hyphenation of an HPLC to the ICP-MS and with a purification method based on the biotin-streptavidin interaction.

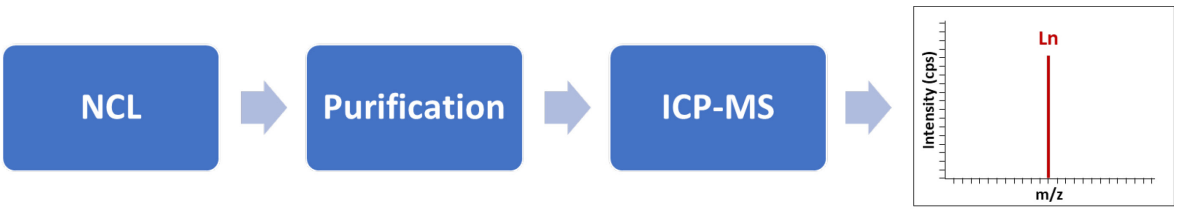

Figure 15: Workflow of the template-directed NCL of PNA probes with ICP-MS detection

5.1.2 Probe design

When designing probes for template-directed reactions (independently of the use of PNA or DNA), it is necessary to bear in mind three major considerations: G-C content, self-complementarity of the sequence, and probe length.[156] First, base composition should be between 40 and 60 % G-C, since non-specific hybridization may increase outside of this range. Additionally, in the case of PNA, the increase of G-C percentage also increases hydrophobicity of the probes. Second, self-complementary sequences within the probe may result in the formation of hairpin structures that will inhibit hybridization to the target. Finally, probes longer than 16 base pairs are required to provide a unique sequence. Statistically assuming random base distribution, a unique 16-mer sequence will only occur once every 4,3 billion nucleotides, roughly the size of the human genome.[157] However, probes of this length are relatively unselective DNA binders, since sequence specificity is inversely proportional to probe length.[158] One way to overcome such limitation is to ligate two short oligomers. In this way, the product has uniqueness that its length confers while the short probes offer the high selectivity. Once

these prerequisites have been fulfilled, templated reactions can be applied to any sequence. In this case, attention was focused on the proto-oncogene H-Ras. A proto-oncogene is a normal gene that has the potential to cause cancer due to their involvement in signal transduction and execution of mitogenic signals. Mutations of the Ras gene are found in 20 to 30 % of all human tumors,[159] and several SNPs on this gene have been associated with cancer.[160]

Probes necessary to perform a templated ligation and transfer reaction targeting a H-Ras gene as specified in Table 5 were synthesized. The target, T1, is a 23-mer from which 17 bases are complementary to the probes. One base of the 17-mer located at the ligation site is left unpaired, since it has been shown that an unselective ligation reaction can be rendered selective with such arrangement.[141] The metal tag needed for the analysis with ICP-MS was attached to the thioester probe, and therefore they were termed donor probes, while the probe with the N-terminal cysteine was the acceptor probe.

H-Ras Probe System	
3' – GTG AGA AGG GGT GTG GAT GTC GC – 5'	**T1**
^{H_2N}Cys cct aca g Gly ^{CONH_2}	**A1**
(Ho^{3+}) DOTA tct tcc cca c Gly S $(CH_2)_2CO$ Gly^{CONH_2}	**D1**
^{Ac}tct tcc cca c Cys[DOTA(Ho^{3+})]^{NH_2}	**D2**

Table 5: H-Ras target and probes for the templated ligation and transfer reaction.

PNA oligomers where synthesized via solid-phase peptide synthesis: the Boc-strategy was used for donor probes, while the Fmoc-strategy was used for acceptor probes (Figure 16). The metal tag was attached to the donor probes on solid support with oxima™ as coupling agent. Holmium was the lanthanidoid selected for the metal tag. As a monoisotopic species, it is monitored with the m/z = 165, thus sensitivity is not challenged due to the split of the signal in different isotopes. $^{149}Sm^{16}O$ is the single interference at low resolution of holmium. With an abundance of 13.82 % and low availability, ^{149}Sm oxides do not pose any background risk. Two overnight incubations of holmium chloride in DMF:water 9:1 were necessary for the metal to chelated in the DOTA ring. Shorter incubation times yielded incomplete metalation challenging to separate via liquid chromatography. Complexation of the metal in the DOTA ring was resistant towards the harsh conditions of the resin cleavage with TFMS. The desired probes were isolated as exemplified by D1 in Figure 17 with the UPLC chromatogram (A) and the ESI-MS spectrum (B). It was observed that ion intensities in the MS spectrum of donor probes with the chelated metal were lower than those of donor probes without the metal. Ion suppression is a well-known and studied effect in ESI-MS.[161] Specially, when working with lanthanoids, direct correlation between ions observed in the gas phase and species expected in solution must be made with caution.[162] Gas phase speciation is dependent on the operating condition of the ESI-MS, thus quantification of species by direct interpolation of their ion intensities should be performed with extra care.

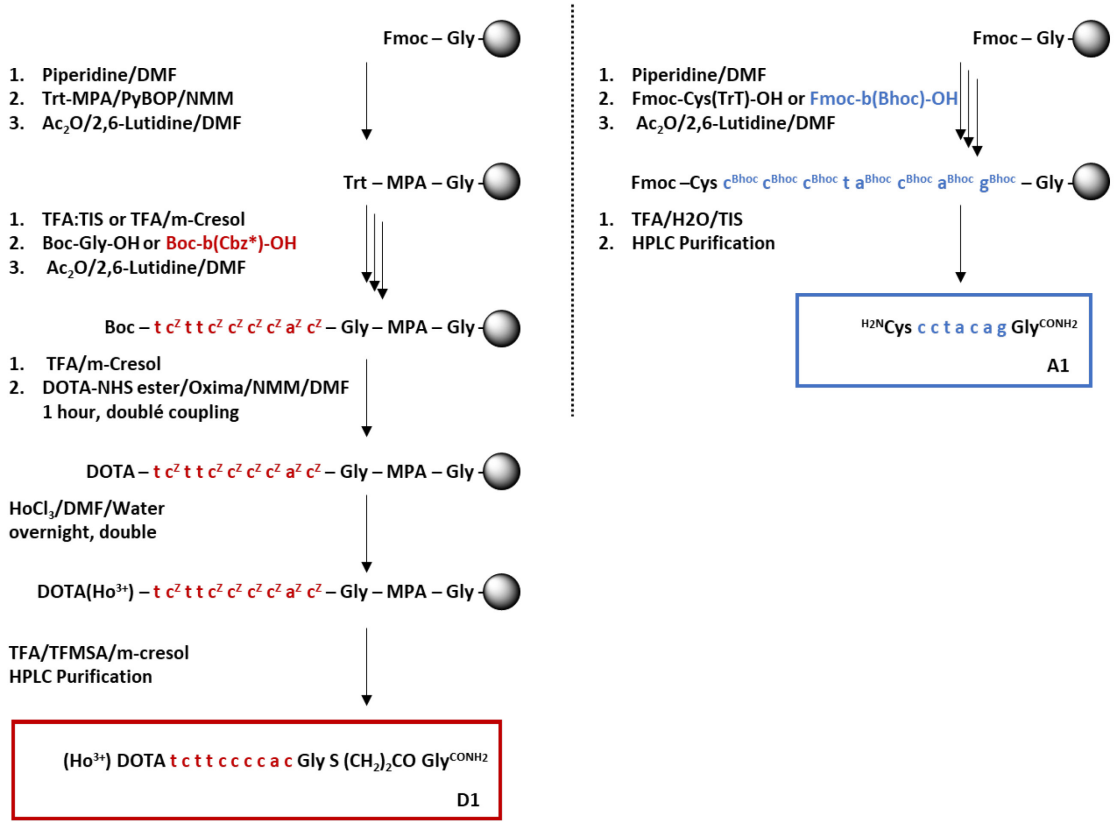

Figure 16: Synthesis of donor and acceptor probes. The amino groups in the base with Z bear a carboxybenzyl protecting group, while the bases with Bhoc bear a benzhydryloxycarbonyl protecting group.

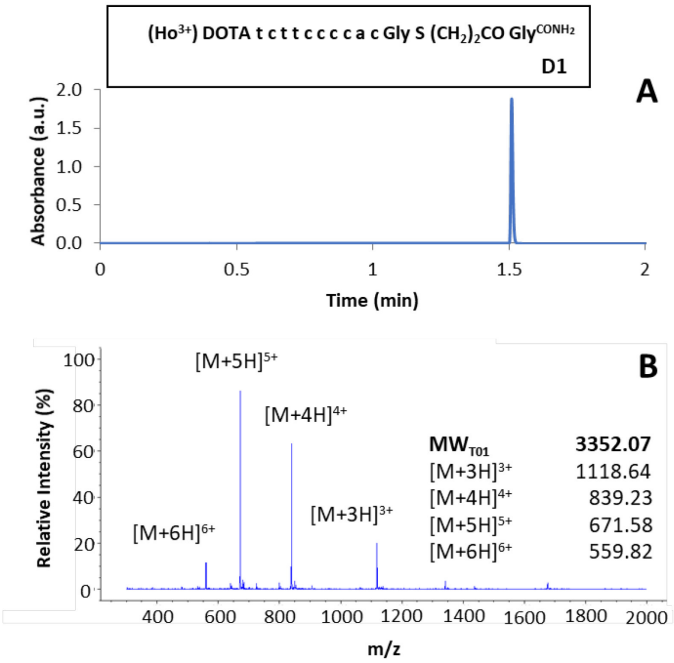

Figure 17: Characterization of donor probe T1. **A**, UPLC trace of the donor probe T1. UPLC: gradient 3 and λ= 260 nm. **B**, ESI-MS spectrum of the donor probe D1.

5.1.3 Ligation and transfer reaction

As shown in Figure 18, the reaction of donor probe D1 and acceptor probe A1 was carried in buffer at pH adjusted to 7 and room temperature. The ligation product P1 is expected to have the addition of both sequences. The transfer reaction of donor D2 and acceptor A1 was also performed in buffer at pH = 7 and room temperature. In this case, there are two expected products: P2 which carries the metal tag and the sequence of probe A1, and P2 which has the sequence of the donor probe D2.

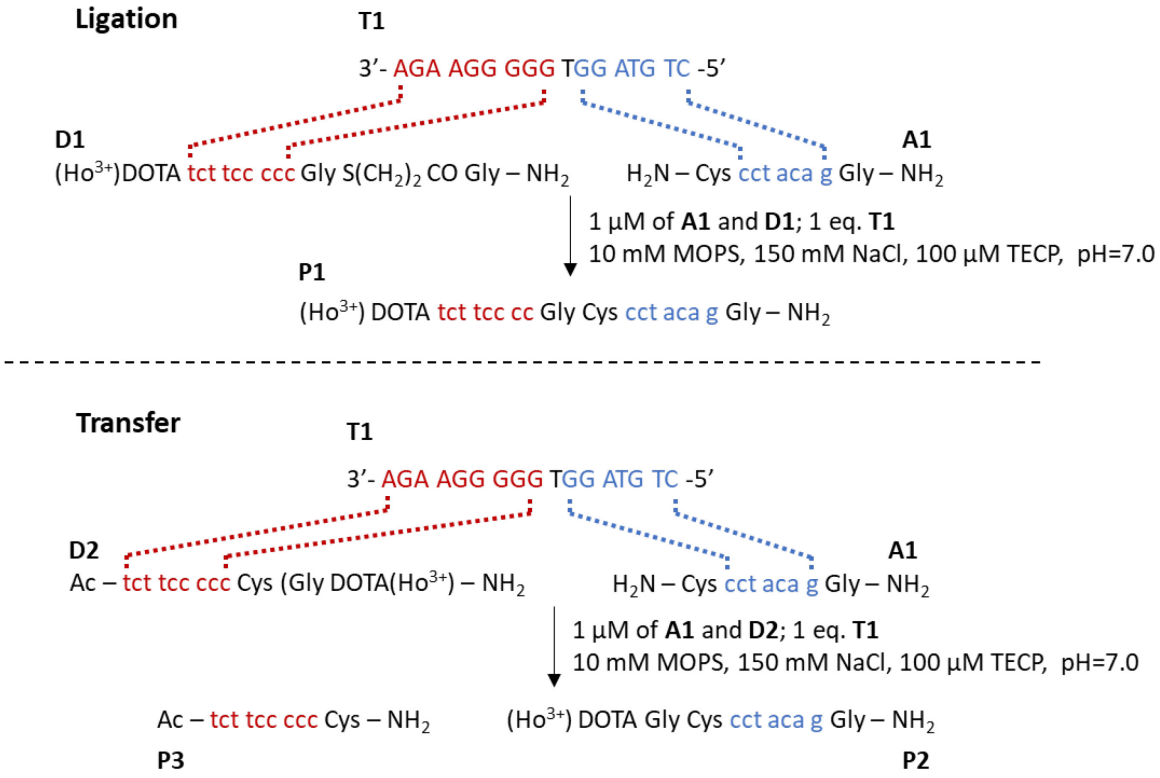

Figure 18: Ligation and transfer reactions with the metal tag.

The HPLC-UV traces of the ligation (A to C) and transfer (D to F) reactions carried out at 25 °C in 1 µM probes concentration and 1 eq. of complementary template T1 are shown in Figure 19. Aliquots quenched with 1% TFA were analyzed by MALDI-MS. At time zero, only the donor and acceptor probes are present (Figure 19 A and D). The 3-monomer shorter sequence of the acceptor probe results in a faster elution from the column than the donor probe. In the absence of DNA template, no product was formed after 30 minutes, which indicated that a template independent background reaction was slow in both, the ligation and transfer reaction (Figure 19 B and E). Incubation of the probes in the presence of the complementary target T1 resulted in the formation of: product P1 in the ligation reaction, and products P2 and P3 in the transfer case (Figure 19 C and F, respectively). The ligation product P1 was more hydrophobic than the reactants and it eluted at a higher acetonitrile percentage. On the other hand, in the transfer reaction, the retention time of both probes is increased when donating or accepting the metal tag to yield P2 and P3.

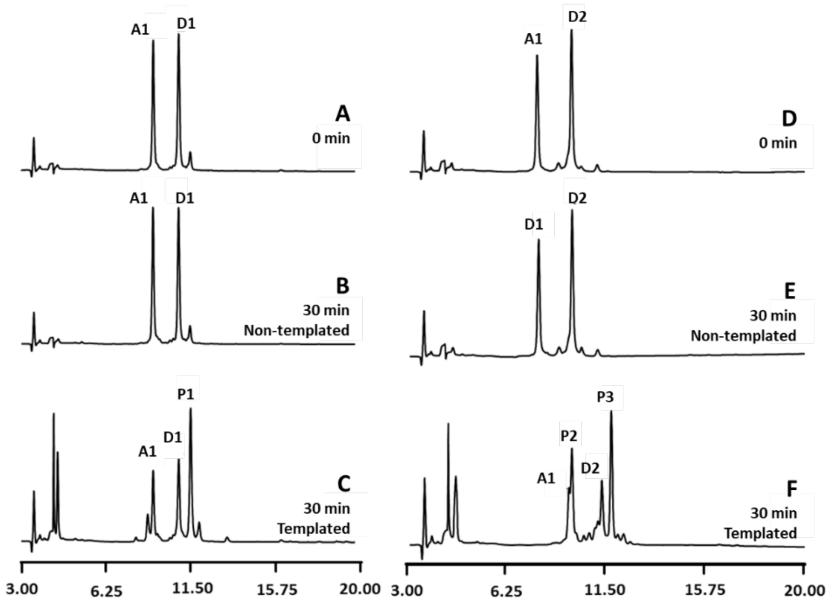

Figure 19: HPLC-UV traces of the ligation and transfer reaction. **A**, time zero for the ligation reaction. **B**, non-templated control after 30-minutes incubation of the ligation probes. **C**, templated ligation reaction after 30-minute incubation. **D**, time zero for the transfer reaction. **E**, non-templated transfer reaction after incubation of 30 minutes. **F**, templated transfer reaction after incubation of 30 minutes. All chromatograms were measured at λ= 260 nm and performed with gradient 4.

In conclusion coupling of the metal tag on the PNA probes does not interfere with the template-directed NCL and the desired products were formed. The ligation product is only formed when the template was present, and hydrolysis of the thioester was not observed in the measured time.

5.1.4 ICP-MS Monitoring: purification via HPLC

The reaction is monitored in ICP-MS via measurement of the holmium ion with m/z = 165. Since the plasma in ICP-MS eliminates all sort of molecular information it is imperative to separate the donor probe D1 from the ligation product P1, and in the transfer reaction, the signal of the donor probe D2 must be isolated from the signal of the transfer product P2. One way of achieving such separation is via hyphenation of an HPLC to the ICP-MS. The HPLC was connected to the ICP-MS through an MCN-6000. In this unit the sample is sprayed into a spray chamber using a microconcentric nebulizer operated at 60 µL min^{-1}. The nebulizer gas flow transports the aerosol through a membrane desolvator which preservers the sample while greatly reduces the solvent loading. Solvent vapor is removed through a micro-porous PTFE tubular membrane while the analyte continues through the tube into the ICP-MS.

Results of the ligation and transfer reaction measured with hyphenated nanoHPLC-ICP-MS through the MCN-6000 desolvator are shown in Figure 20. Elution of the donor probe, D1, is faster than elution of the longer ligation product, P1, (Figure 20 A). On the contrary, in the transfer reaction (Figure 20 B), the transfer product, P2, has a lower retention time than the donor probe, D2 due to its shorter PNA sequence. The MCN-6000 desolvator is optimized for methanol, and the use of other solvent can affect its performance. Separation with methanol was not possible despite the use of several columns and solvent gradients; therefore,

acetonitrile had to be considered. As it can be seen in Figure 20 where both experiments were performed at 1 µM concentration, the counts per second of holmium for the transfer reaction were one order of magnitude lower than for the ligation reaction. Incomplete elimination of the organic mobile phase resulted in signal suppression and clogging of the skimmer cone in the ICP-MS. In any case, the ligation and transfer reaction were followed by ICP-MS for the first time, although the existing instrumentation was not optimal.

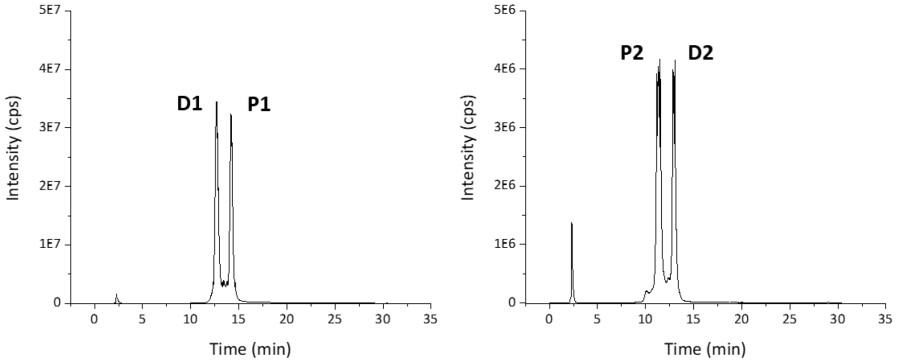

Figure 20: Ligation and transfer reaction monitored via ICP-MS. Holmium intensity of the nanoHPLC-ICP-MS trace of the ligation (A) and transfer (B) reaction after incubation of 10 minutes in presence of complementary template. Chromatograms were performed with gradient 7 and monitoring the m/z correspondent to holmium.

The ICP system is limited in the maximum flow that can directly hyphenate without bypass. This limitation comes from the efficiency of the desolvator unit eliminating the organic phase, and ultimately from the maximum amount of aerosol that can be directed towards the plasma without destabilizing it. This flow limitation, influences instrumentation, column, and injected amount, which are all factors that affect the limit of detection. Since sensitivity of the method was one of the main goals of the project and having in mind that the instrumental flow limitation and the separation problems, hyphenation of the nanoHPLC and ICP-MS was dismissed. Instead, development of a purifying method was considered. This purification step would separate the donor probe from the reaction product before measurement, thus samples could be analyzed with direct aspiration into the ICP-MS, solving then the sensitivity problem.

5.1.5 ICP-MS Monitoring: purification via biotin-streptavidin interaction

The sample obtained after the ligation reaction is a mixture of non-reactive reactants and products. Since the only visible species in ICP are the donor probe and product (in the transfer case just one of the products), the purification method should either fish out any remaining donor probe or capture the ligation product. Removing the donor probe would be effective in the ligation reaction. On the contrary, the transfer reaction would not be suitable for such approach. Both, the ligation and transfer donor probes are susceptible to hydrolysis of the thioester, but in the transfer case, hydrolysis leads to the release of metal tag. Measuring with direct aspiration into the ICP-MS would not allow the differentiation between free metal tag and reaction product; therefore, the methodology would lead to an artifact in the form of an overestimation of the product concentration in the form of hydrolyzed metal tag. Even if in the measure reaction no hydrolysis product was detected, hydrolysis is possible; therefore, it is necessary to focus on the product of the reaction. The alternative is to focus on the acceptor probe. In this case, the detectable species that would enter the ICP-MS would be necessarily products of the ligation or transfer reaction. The acceptor probe is not visible while monitoring

the metal in ICP-MS before the reaction, and its structure is integrated into species that are visible after the reaction.

Scheme 1: template-directed NCL of PNA reporter probes with ICP-MS detection and biotin-streptavidin purification.

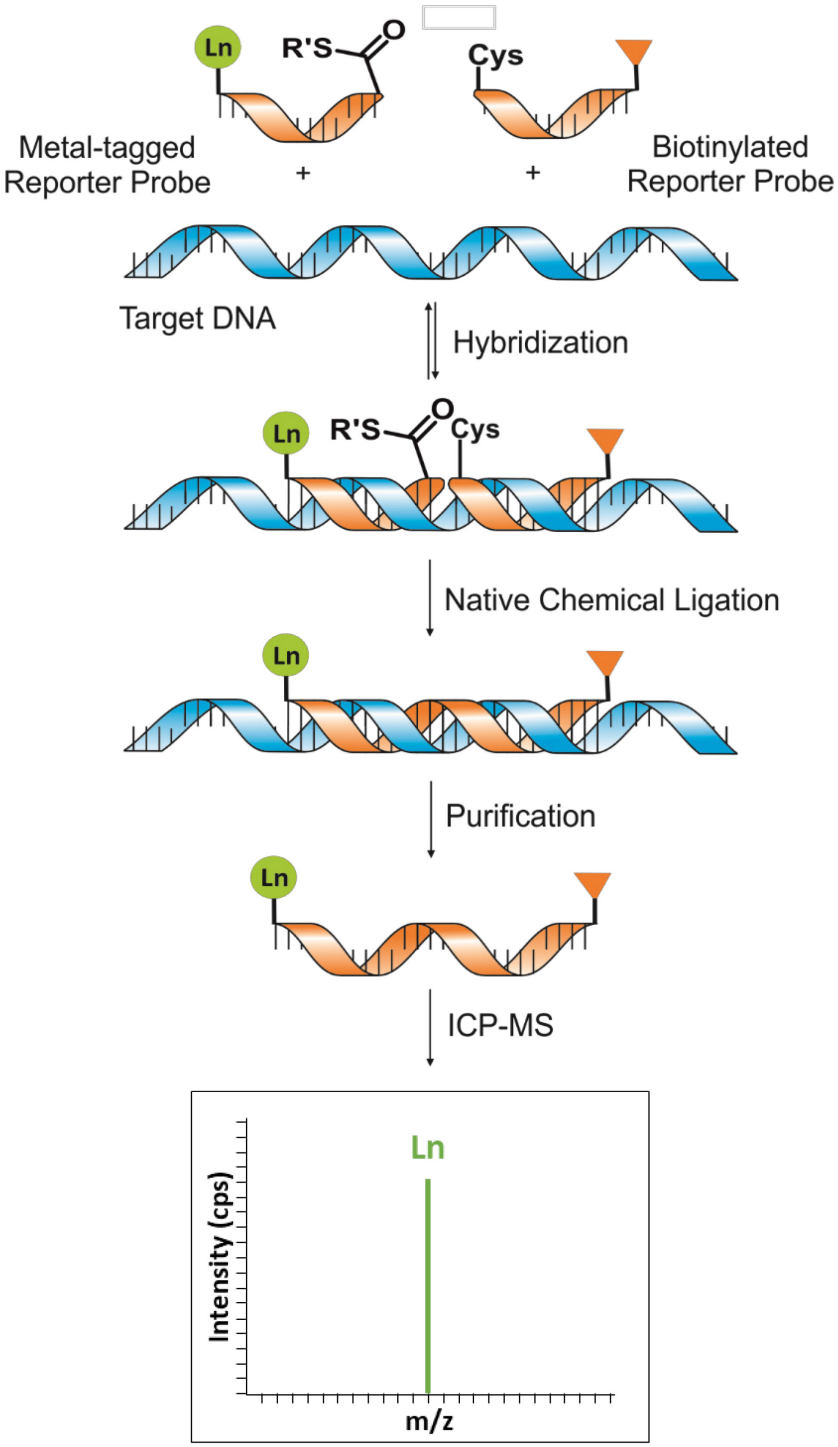

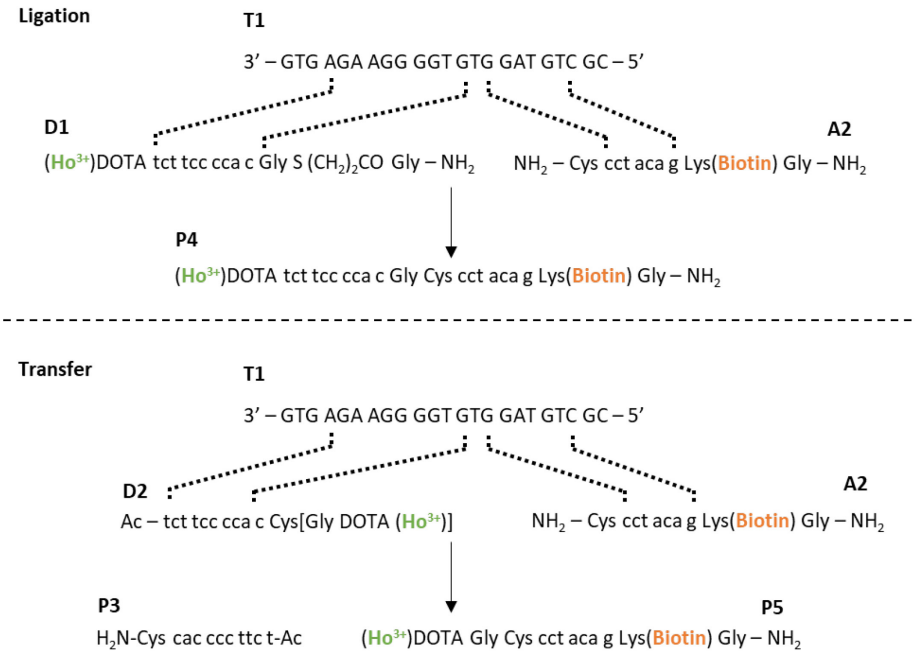

Figure 21: Probe design for the purification method. In green is marked the ion that was monitored with the ICP-MS system; therefore, the molecule that can be seen. In orange is the part that will be selectively captured in the purifying method; therefore, carried into the ICP-MS system.

By introducing a biotin on the side chain of a lysine residue on the acceptor probe, A2, as seen in Figure 21, it is possible to fish out the product and acceptor probe from the reaction mixture. With its reduced size, the biotin-streptavidin pair offers a stronger binding constant (k_D= 10^{-14} mol L^{-1}) than other common affinity tags such as the His tag (k_D= 10^{-6} mol L^{-1}) or GST-fusion protein (k_D= 10^{-9} mol L^{-1}) allowing for a harsher wash step which should translate in a lower background. The use of a covalent pair such as click reactions[163] or hydrazine ligations[164] for the purifying step would allow a more stringent wash, thus it would theoretically produce a lower background. However, a covalent pair would require the digestion of the beads before injection into the IC-MS, adding an additional step to the work up procedure, and increasing the number of species in the sample. Moreover, there are multiple paramagnetic streptavidin-coated beads commercially available which facilitates the implementation of the method.

Since the purification step is the direct link between the ligation or transfer reaction and measurement, optimization and evaluation of the step was needed for the method to be as reliable as possible. The optimized parameters were the beads coating, incubation time, incubation and wash buffer composition, and elution solution/conditions. The results of selected optimized parameters are summarized from Figure 22 to 24.

Several magnetic beads coated with streptavidin were tested: Dynabeads MyOne, Dynabeads M-270, and Roche SA (see experimental section for details). The structure of all particles was very similar. They were all superparamagnetic particles encapsulated into a polymer shell onto which the streptavidin was coated. The polymer was usually hydrophobic, and its composition was the main difference among commercially available products. PNA is known to attach to hydrophobic surfaces, thus non-specific carry over had to be evaluated. For that purpose, the ligation product P4**,** which had holmium as metal tag, was incubated with the different beads in the presence of an acceptor probe loaded with terbium D1(Tb) (Figure 22 A). With such experimental configuration, not only the bead carryover, but also the possible PNA-PNA

agglutination can be monitored by measuring the terbium concentration. Both Dynabeads have the same hydrophilic bead coating based on carboxylic acid groups, the MyOne beads have a higher streptavidin loading than the M-270. With background signal in the same order of magnitude, the standard deviation in the beads with higher streptavidin loading is higher. This effect was most likely due to the steric hindering of streptavidin active centers. On the other hand, the Roche beads had a hydrophobic coating which resulted in a higher background. The low background and higher binding capacity, thus lower cost, resulted in the selection of the Dynabeads M-270.

The kinetics of the binding of the biotinylated ligation product to the streptavidin beads was also studied. The ligation product P4 was incubated in the presented of Dynabeads M-270 and aliquots of the supernatant were taken at different incubation times to measure the holmium content. As it can be seen in Figure 22 B, the concentration of holmium in solution steadily drops after one minute incubation, indicating that the ligation product was captured by the streptavidin beads.

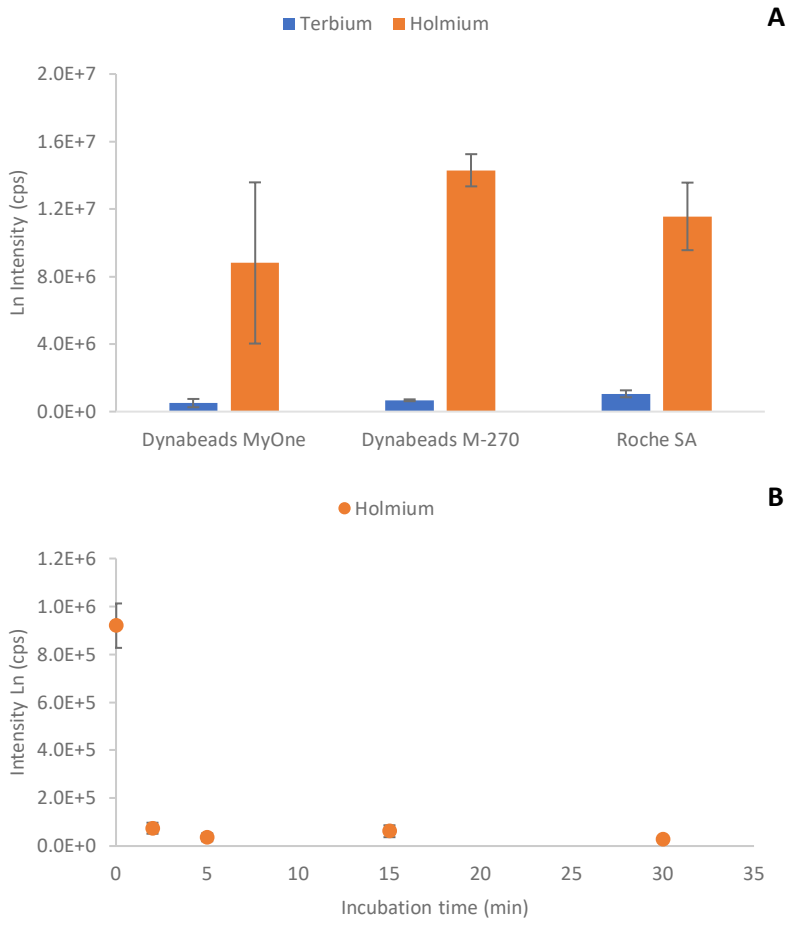

Figure 22: Purification method optimization. **A**, Background dependence on the bead coating. **B**, Incubation time dependence on the background. Error bars represent the standard deviation of triplicates and reflect variations in sample preparation and measurement.

On the condition that the washing was efficient, the next critical step was the elution of the product from the beads. The biotin-streptavidin interaction could be broken with several elution solutions. The beads manufacturer recommended the use of Guanidine-HCl 6M or Gly-HCl 0.1 M pH = 2 and mild heating. Rybak *et al.*[165] recommend elution with a solution 6 M Urea, 2 M

thiourea, 2 % SDS, 50 mM Na_2HPO_4, 100 mM NaCl, 30 mM biotin and pH = 12 at 94 °C. Moreover, 5 % TFA was used as a control for total denaturation of the streptavidin. All elution solutions gave recoveries around 50 % as shown in Figure 23 A when performed at 40 °C. Although different alternatives were possible from an experimental point of view, the ICP-MS had some limitations regarding the matrix input. The use of the urea solution yielded accumulation of solids on the torch and cones of the ICP-MS system that resulted in a decrease of sensitivity over time. Therefore, only elution with 5 % TFA and Glycine-HCL 0.1 M was further studied. Recovery with Glycine-HCl 0.1 M was more effective at higher temperatures as shown in Figure 23 B, approaching 89 % efficiency. On the other hand, TFA did not show any improvement neither with heat nor concentration. Therefore, the elution solution was chosen to be Gly-HCl 0.1 M pH= 2.0.

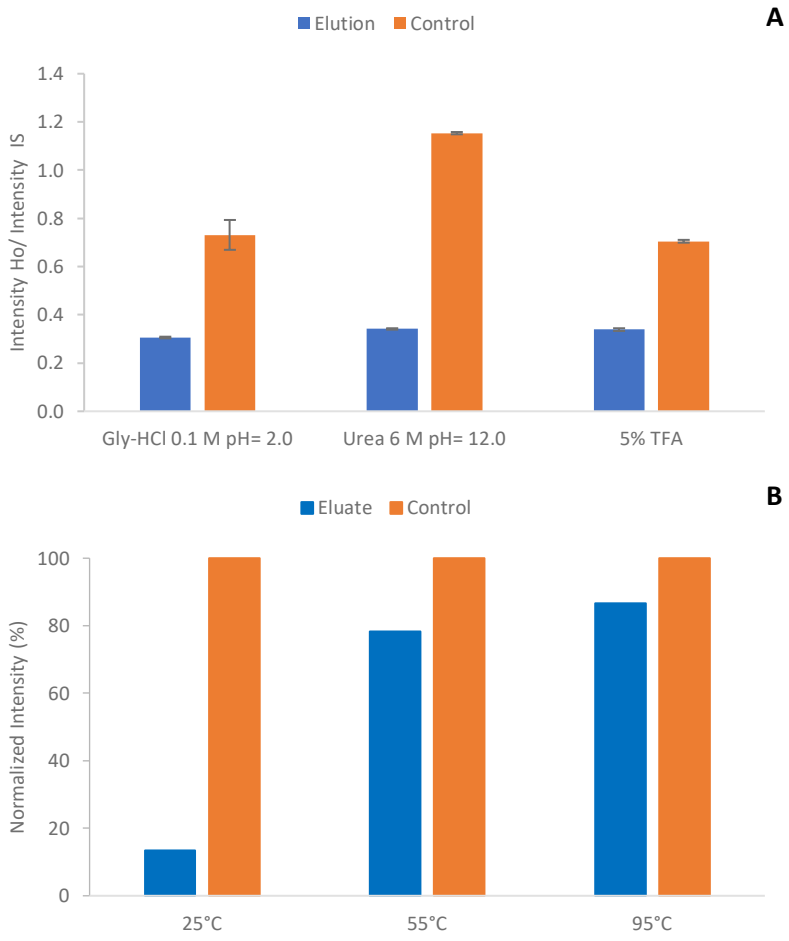

Figure 23: Elution optimization. **A**, Effect of the elution solution composition on recovery. **B**, Temperature effect on elution with the elution solution of Gly-HCl 0.1M pH = 2. Error bars represent the standard deviation of triplicates and reflect variations in sample preparation and measurement.

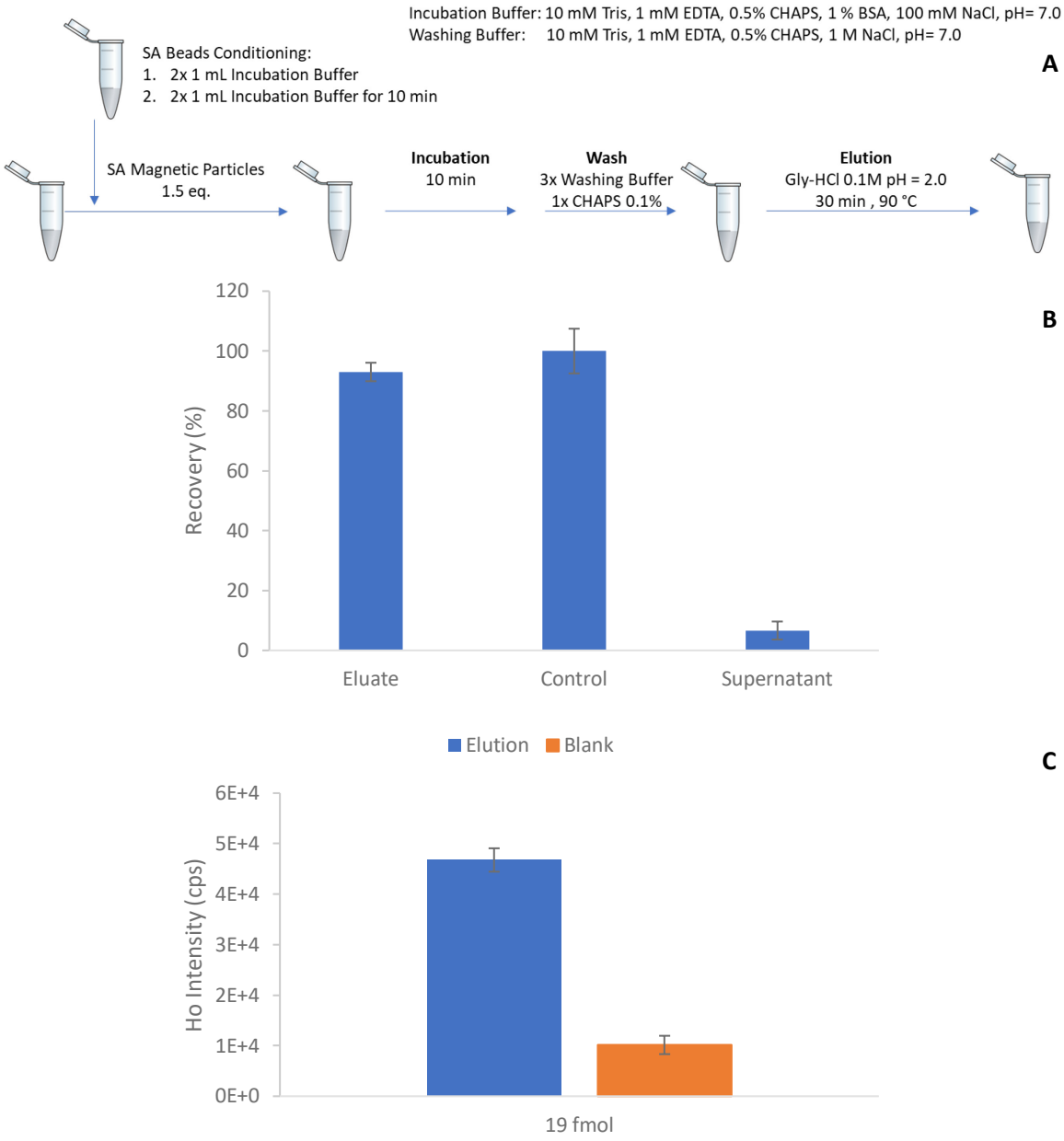

Figure 24: Purification step. **A**, Performance of the purifying step with a 100-pM solution of the ligation product. **B**, Summary on the performance of the purifying method. **C**, Purification of 200 µL of a dissolution 100 pM of ligation product P4.

The purification method was changed and improved along the project to correct or enhance its performance. Modifications will be discussed in the corresponding section, but the final version used can be seen in Figure 24 A. Recovery of the purification method was of 93 % with 3.1 % standard deviation. The method was successfully applied to triplicates of 19 fmol ligation product P4 solutions (200 µL 100 pM) to assess the suitability of the procedure for the sensitivity requirements of the project (Figure 24 C).

In conclusion, ICP-MS was successfully used to monitor the templated ligation and transfer reaction. Additionally, and to avoid hyphenation of the ICP-MS to a nanoHPLC, thus reach the higher level of sensitivity, a purifying step to only introduce metal ion contained in the product

was developed. An overview of the first optimization was presented, and its suitability to reliably measure samples of low concentrations was demonstrated.

5.2. Bridging the gap: from µM to pM

The limit of detection of Holmium on the ICP-MS system was determined. The calculation was performed with the standard deviation of a calibration curve with an elemental standard of holmium. The lowest limit of detection achieved under operated conditions was of 10 pM, thus the aim was to approximate as much as possible that limit with the templated reaction. For the reaction to yield product in such concentration range, it is necessary that the triplex between the donor probe, acceptor probe, and template forms in significant amounts. In other words, the affinity of each probe for the template must be strong enough to keep them together for the product to form in the sensitivity range. Since sequence length has a direct influence on duplex binding strength, probe size had to be optimized.

$$\text{(1)} \qquad \text{Probe} + \text{Template} \underset{\mathrm{k_{dissociation}}}{\overset{\mathrm{k_{association}}}{\longleftrightarrow}} \text{Duplex} \qquad K_a = \frac{[\text{Duplex}]}{[\text{Probe}]\cdot[\text{Template}]}$$

As it was described along the fundamentals chapter, the nearest-neighbour model can be used to predict the stability of a DNA duplex under a given set of solution conditions. With the thermodynamic data of the different possible base pair, it is possible to calculate the stability and melting behaviour of any DNA duplex. Free Gibbs' energy data calculated with the nearest neighbour model[154-155] using thermodynamic data of DNA was used to calculate the association constant, K_a, of probes A2 ($1.7\cdot10^4$ M^{-1}) and D1 ($2.8\cdot10^6$ M^{-1}). Since PNA has a higher affinity than DNA at low ionic strength, this values are considered to be a minimum K_a value. The shorter acceptor probe A2 has the lower K_a; therefore, it is the limiting factor of the reaction. Assuming the duplex formation as described in equation 1, and that all duplex would yield ligation product independently of the donor probe, a template concentration of 5.6 nM would be needed for final ligation product concentration of 10 pM with concentration of A2 of 100 nM. Since the function of the reaction product is to indicate the concentration of template, there would be a loss on sensitivity of three orders of magnitude due to the wrong probe design (10 pM product to 5.6 nM template).

Several theoretical assumptions were made for the calculations that differ from reality and that would make the sensitivity loss even greater. First, a 100 % reaction yield was assumed. Second, the model was set with only one duplex involved in the reaction when there are two different probes binding the target. Last, there is an experimental contribution with the purifying method having a 94% recovery. The bias resulting from such assumptions was experimentally verified when performing the ligation reaction at different probe concentration (Figure 25). The signal of the templated ligation of A2 and D1 was successfully differentiated from the signal of the non-templated reaction (NTC) at 10 nM template concentration; however, the templated reaction was indistinguishable from the non-templated control at 1 nM template concentration. In addition to the low performance of the probes, the background was exceptionally high in both samples. With the lack of any Holmium source rather than the donor probes, the background had to be a result of carryover during purification. This effect will be later discussed in greater detail (section 5.3).

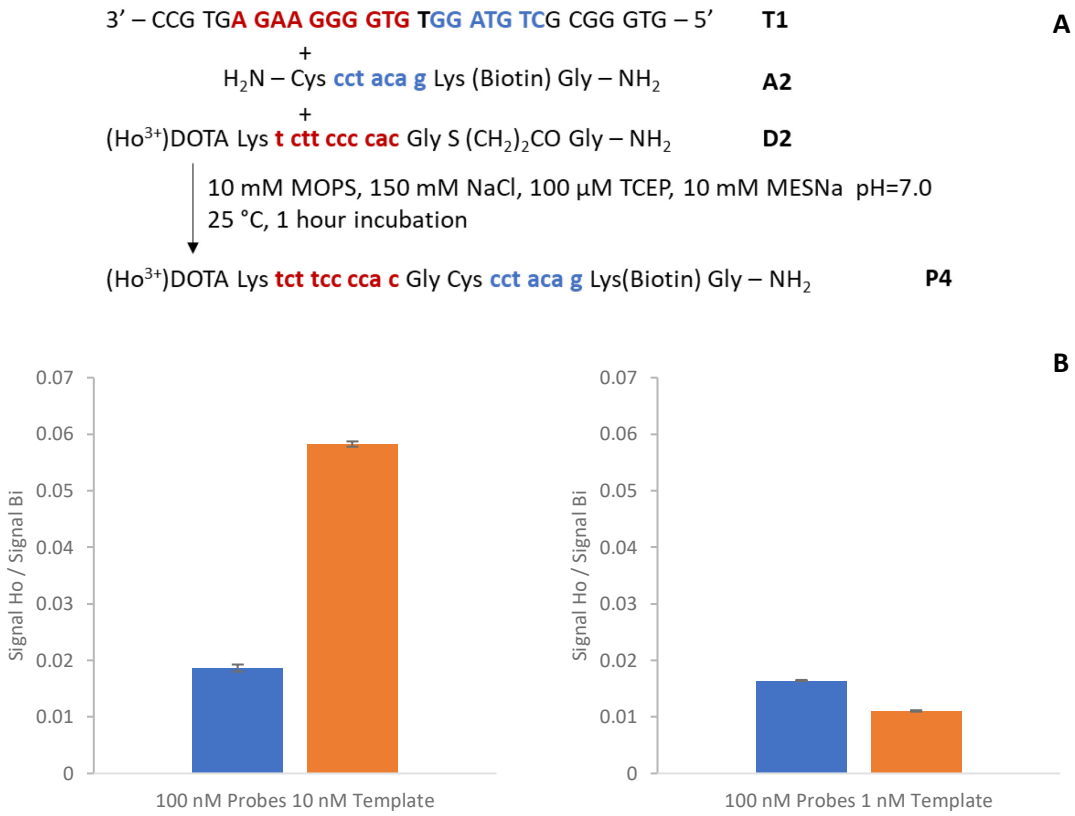

Figure 25: Ligation of C2 and T1 with template R1 at different concentrations. **A**, Reaction system. **B**, ICP-MS measurements of samples quenched with 1% TFA after one hour and purified. Error bars represent the standard deviation of triplicates and reflect variations in reaction and clean-up procedure.

As it was discussed, longer probes with higher association constants were needed. A higher association constant involves higher affinity between probe and template. The stronger affinity implicates that at equal initial probes concentration, the equilibrium is more displaced towards the formation of the duplex. The greater relative duplex abundancy was expected to yield ligation product in concentrations above the limit of detection of the ICP-MS system. With such thought in mind, probes could be elongated to confer affinity for the target well beyond the limit of detection; however, increasing the length of the PNA sequence not only elevates the affinity, but it also enhances the hydrophobicity of the probes. Higher hydrophobicity can cause non-specific interactions during the purification step and it decreases solubility of the reactants. Since both of them have an effect on the limit of detection, the length of the sequence should confer enough affinity, but it should be as short as possible. Table 6 summarizes the values of free Gibbs' energy, ΔG°, of the DNA/DNA duplex formation for donor and acceptor sequences of different length. The association constant, K_a, was calculated with the value of the Gibbs's free energy according to equation 2:

(2) $$\Delta G° = -RTlnK_a$$

where R is the ideal gas constant and T the temperature. Additionally, Equation 2 was used to calculate the concentration of free template when 10 pM duplex is formed with 1 nM probe concentration.

Table 6: Calculated thermodynamic data of different size fragments of the acceptor and donor probes.

Length	Sequence	ΔG° (Kcal mol^{-1})	K_a (M^{-1})	Template concentration at equilibrium (pM)
		Acceptor Probe		
7	CTGTAGG	-5.8	$1.7 \cdot 10^{4}$	$5.5 \cdot 10^{5}$
9	CGCTGTAGG	-10.9	$9.9 \cdot 10^{7}$	$1.0 \cdot 10^{2}$
11	GGCGCTGTAGG	-15.3	$1.6 \cdot 10^{11}$	$6.0 \cdot 10^{-2}$
13	TGGGCGCTGTAGG	-19.1	$1.0 \cdot 10^{14}$	$9.8 \cdot 10^{-5}$
		Donor Probe		
8	GTGGGGAA	-8.8	$2.8 \cdot 10^{6}$	$3.5 \cdot 10^{3}$
10	GTGGGGAAGA	-11.8	$4.5 \cdot 10^{8}$	$2.2 \cdot 10^{1}$
12	GTGGGGAAGAGT	-14.8	$7.2 \cdot 10^{10}$	$1.4 \cdot 10^{-1}$
14	GTGGGGAAGAGTGC	-18.8	$1.7 \cdot 10^{13}$	$1.6 \cdot 10^{-4}$

At equilibrium, with the 9-mer acceptor probe, the formation of 10 pM duplex would require the presence of 100 pM of free template. Adding one base, greatly displaces the equilibrium leaving only $6.0 \cdot 10^{-2}$ pM (60 fM) of free template. The donor probe with 10 bases would require 22 pM of free template for the duplex to form at 10 pM concentration. With 12 bases, such concentration is reduced to 140 fM. The extra base in the donor probes is needed to compensate for the lower guanine-cytosine content. It should be noted that calculations were performed with thermodynamic data from DNA/DNA duplex although in this case the duplex is PNA/DNA. PNA binds to complementary DNA stronger than the analogous DNA, so the displacement is supposed to be of greater extent. The extra affinity of PNA would be used as approximation to compensate for the several assumptions numbered before; therefore, an acceptor probe with 11 bases and a donor probe with 12 bases were synthesized.

The ligation reaction with longer probes was carried out at 15 and 1.5 nM probe concentration (Figure 26). Not only the reaction at 10 nM template concentration could be monitored, but also the reaction with 1 nM template concentration. In previous experiments, the limiting factor was the affinity of the probes for the template when no product formation was observed, or formation was in the range of the limit of detection. However, with longer probes, the background signal becomes the issue. The lack of background reaction at higher concentrations, together with the fact that harsher washing steps have, although limited, an effect on the background, indicate that the problem relies in non-specific interactions. Several modifications were attempted in the purification procedure following the same procedure as reviewed in chapter 5.1, but the improvement on clean-up performance was limited and dependent on the initial concentrations of probes as it can be seen in Figure 26 B. Background with an initial concentration of probes of 15 nM is 40 % higher than with an initial probe concentration of 1.5 nM. This effect limits the application of the high linear range of the ICP-MS and makes the LOD dependent on the initial probe concentration used.

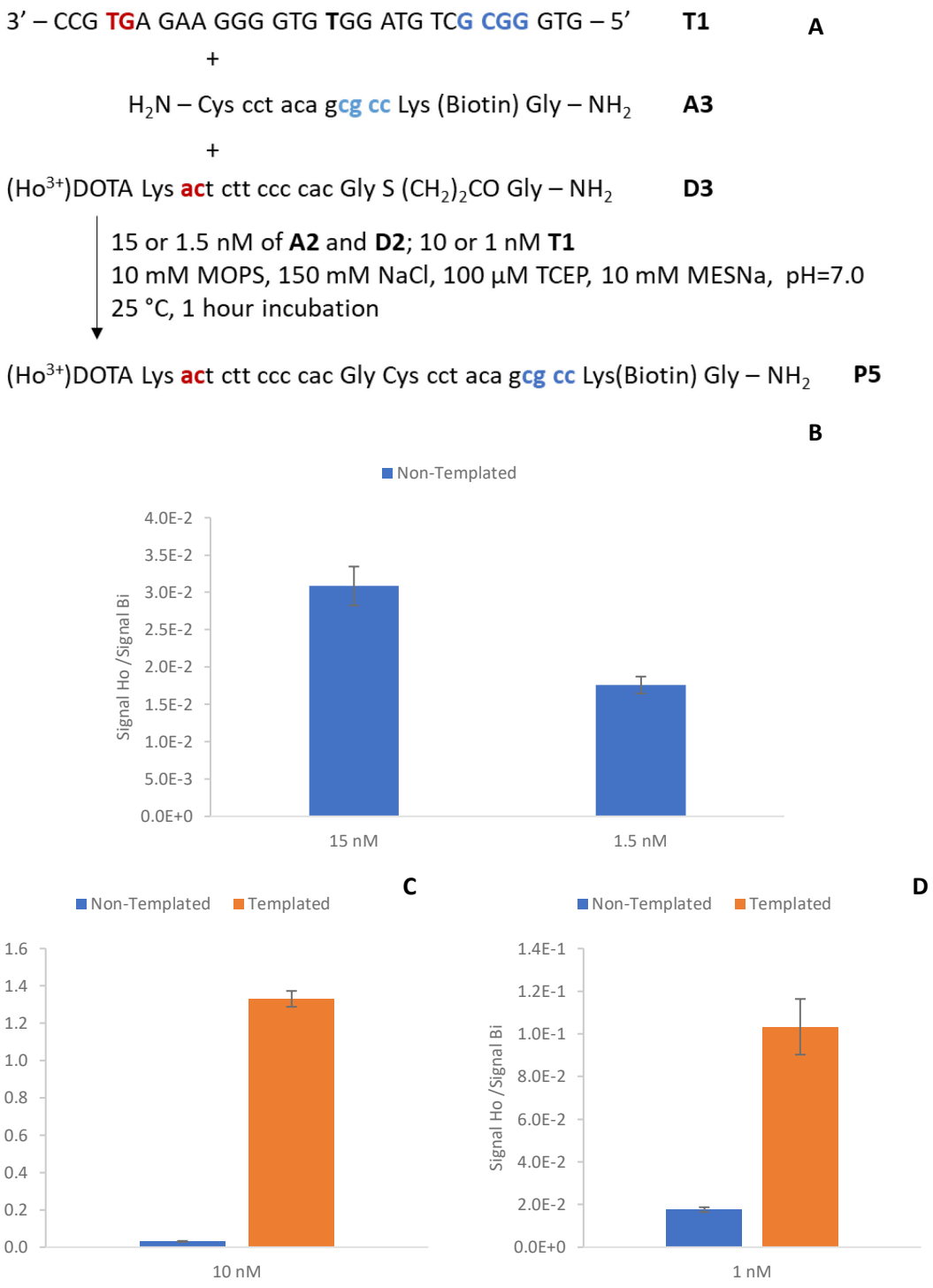

Figure 26: Ligation reaction at lower concentrations and background noise. **A**, reaction system with longer probes. **B**, Background at different initial probe concentration. **C**, Reaction at 15 nM probe concentration and 10 nM template. **D**, Reaction at 1.5 nM probe concentration and 1.0 nM template concentration. All samples were quenched with 1 % TFA and neutralized before purification. Error bars represent the standard deviation of triplicates and reflect variations in reaction and sample preparation.

Product inhibition is one of the main limitations of most nucleic acid templated reactions. It is particularly critical on ligation reactions, since the product binds stronger to the target template.

Such effect was exploited as it can be seen in Figure 27 A to perform a calibration curve on the concentration of template. The concentration of probes A3 and D3 was kept constant at 15 nM, while the concentration of template T1 ranged from 0.5 to 13 nM. After one hour, the reaction was quenched and purified before measurement into the ICP-MS. The high affinity of the ligation product for the template can be translated into a 1:1 product to target stoichiometry, which allows for direct interpolation between ligation product and holmium content. Although the correlation coefficient for the calibration with the template, R^2, was low (0.9878), as it can be seen in Figure 27 B, it was similar to the one achieved with a standard elemental solution of holmium (0.9793). The low coefficient was therefore, not the result of the method per se, but of the instrumental conditions. The ICP-MS equipment underwent several cycles of repairs during this work due to the low intensity and instability of the signal.

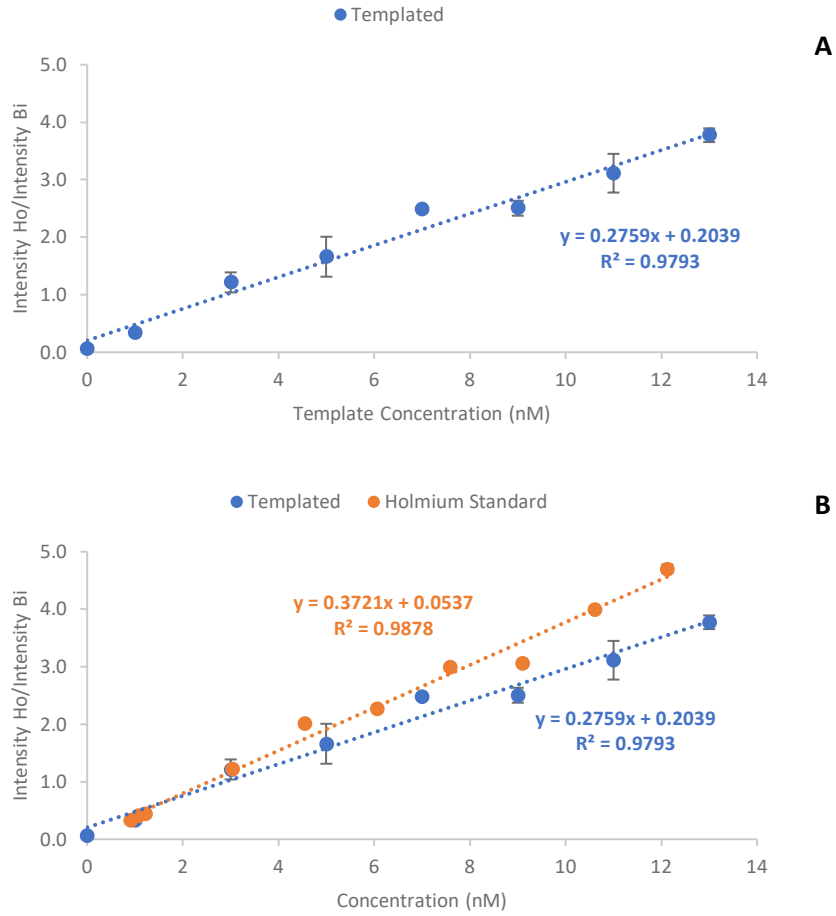

Figure 27: Calibration with templated reaction. **A**, Holmium response to templated reactions with concentrations of acceptor and donor probe of 15 nM and concentration of template ranging from 0.5 to 13 nM. **B**, Comparison of the ICP-MS response to elemental holmium standard and templated reaction. Error bars represent the standard deviation of triplicates of the reaction (A) and of standard solutions of holmium (B) and reflect variations in method application (A) and instrumental performance (B).

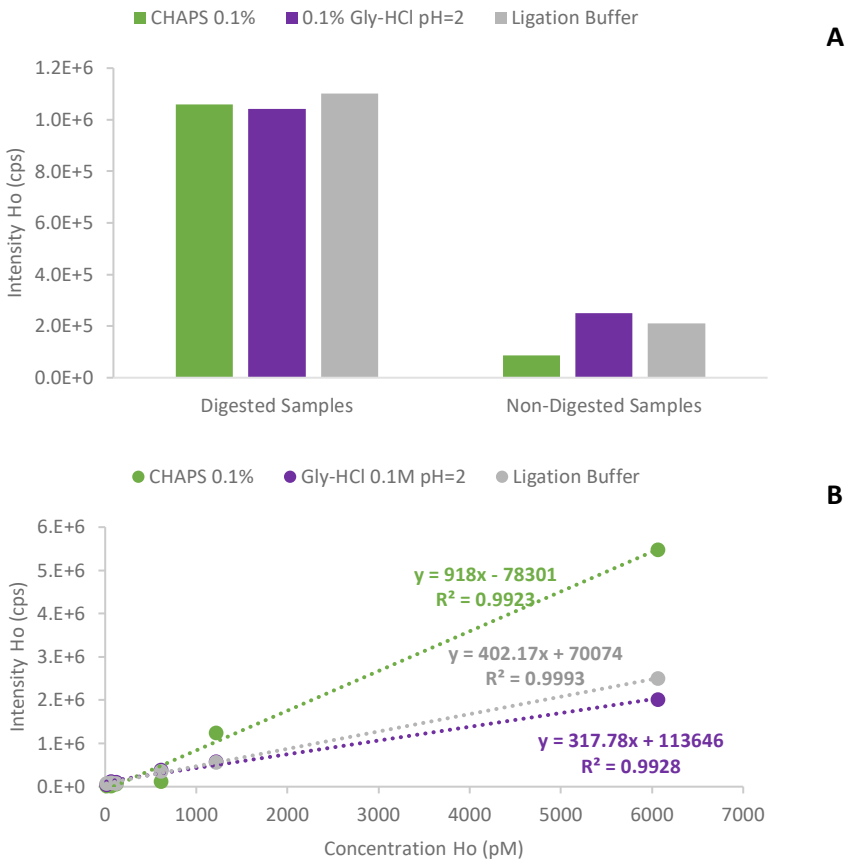

Figure 28: Signal intensity dependency of the matrix in ICP-MS. **A**, Signal of the donor probe T4 before and after an overnight digestion with H_2SO_4:H_2O_2 3:1 at 95 °C. **D**, Calibration of the ICP-MS system with elemental holmium dissolved in different matrices

The signal of the ligation product diverges from the one achieved with elemental holmium. Although ICP-MS is considered to have low matrix dependence, it was found that there were small variances in the signal of free holmium and holmium chelated in the metal tag linked to PNA oligomers. Such deviance becomes more intense at higher concentration. It was hypothesized that intensity differences were not due to a difference in holmium content, but due to differences in the ionization process. To verify such hypothesis, several aliquots of thioester in different matrices were split in two fractions; one was directly measured, and the second one was digested overnight with a mixture of H_2SO_4:H_2O_2 3:1 (v:v) at 95 °C, and re-dissolved in HNO_3 3.5%. The signal of all the digested samples were similar and higher than the signal of the non-digested samples (Figure 28 A). Moreover, there was also a divergence on the calibration curves of elemental holmium in the different matrices (Figure 28 B). The different environment of the holmium ion when entering the ICP-MS system can result in ionization at a different position along the plasma. By altering the plasma position (X, Y, and Z relative position) it was possible to increase the ligation product signal and decrease the one of elemental holmium, but it was not possible to make both values converge. The most straight forward approach was to simply calibrate the instrument using the donor probe instead of the elemental holmium standard and comparing only measurements performed in the same matrix.

The reaction system demonstrated that it is feasible to use a lanthanoide concentration as an indicator of the target template concentration. The formation of product was quantitative with the target (Figure 29).

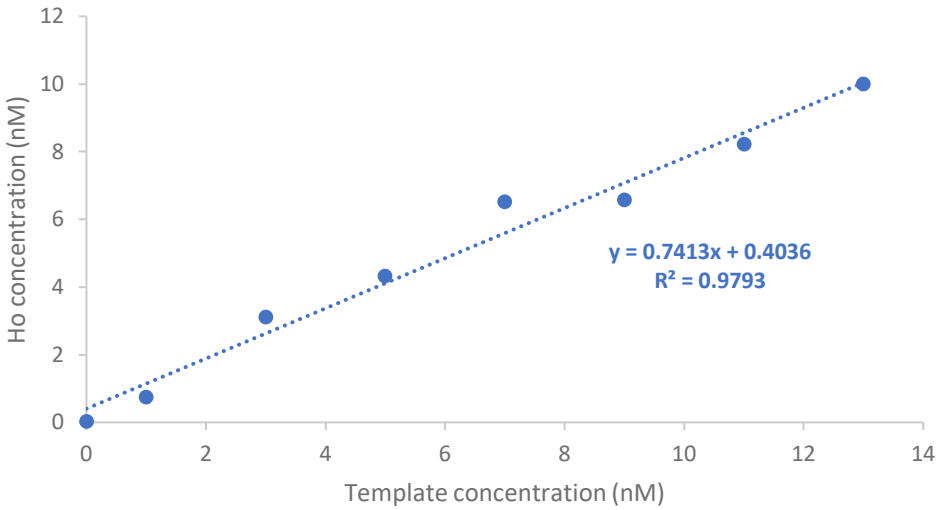

Figure 29: Calculated concentration of Ho as a fraction of target DNA concentration. Reaction conditions: 15 nM probe D3 and A3, 1 to 13 nM target template T1, 5 mM MESNa, 10 mM MOPS, 150 mM NaCl, 100 µM TCEP, 0.1 % CHAPS and pH 7.0. Samples were quenched with TFA 1% and neutralized to pH 7 with NaOH 0.5 M before purification.

The LOD calculated with the standard deviation of the slope was of 1 nM. On the other hand, if the LOD is calculated with the standard deviation of the blank, this represented as the non-templated reaction (3.3x SD of blank/slope of calibration curve), the LOD was 360 pM. These values were calculated for the calibration presented in Figure 30 A, which was performed with initial probe concentration of 15 nM. The lower value while using the standard deviation of the blank is supported by the fact that with lower initial probes concentration, the background is lower; thus, lower concentrations can be measured. For example, the reaction was monitored well below the 1 nM LOD when the initial probe concentration was 1700 pM as shown in Figure 30 B. In this case, a 500 pM template sample was well above the non-templated control, since the initial lower probe concentration generated less background.

A

3' – CCG TGA GAA GGG GTG **T**GG ATG TCG CGG GTG – 5' **T1**

+

H_2N – Cys cct aca gcg cc Lys (Biotin) Gly – NH_2 **A3**

+

(Ho^{3+})DOTA Lys act ctt ccc cac Gly S $(CH_2)_2CO$ Gly – NH_2 **D3**

1.7 nM of **A3** and **D3**; 10 or 1 nM **T1**
10 mM MOPS, 150 mM NaCl, 100 µM TCEP, 10 mM MESNa, pH=7.0
25 °C, 1 hour incubation

(Ho^{3+})DOTA Lys act ctt ccc cac Gly Cys cct aca gcg cc Lys(Biotin) Gly – NH_2 **P5**

B

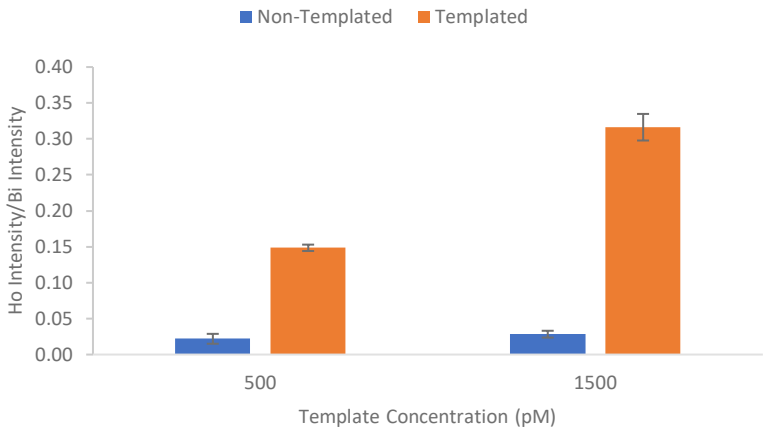

Figure 30: Ligation reaction for A4 and D4 in the pM range. **A**, Reaction system. **B**, ICP-MS measurement of the experiment performed at 1.7 nM probe concentration and 0.5 or 1.5 nM template T1 concentration. Error bars represent the standard deviation of triplicates of the reaction and reflect variations in method application and instrumental performance.

In a second attempt, the concentration of probes C3 and T3 was kept constant at 1.5 nM, while the template T1 concentration ranged from 100 to 1000 pM (Figure 31). The lower background enabled the detection of concentrations one order of magnitude above LOD of holmium on ICP-MS (6 pM). The LOD calculated with the blank was of 46 pM. This value was more in agreement with the methodological limit of detection of 29 pM, which was calculated as 3.14 times the standard deviation of 7 samples near the expected limit of detection (150 pM concentration of probes and 100 pM of template). The RSD calculated with 5 samples measured at 50 pM concentration was 6.7 %.

A

3' – CCG TGA GAA GGG GTG **T**GG ATG TCG CGG GTG – 5' **T1**

+

H_2N – Cys cct aca gcg cc Lys (Biotin) Gly – NH_2 **A3**

+

(Ho^{3+})DOTA Lys act ctt ccc cac Gly S $(CH_2)_2CO$ Gly – NH_2 **D3**

1.5 nM of **A3** and **D3**; 10 or 1 nM **T1**
10 mM MOPS, 150 mM NaCl, 100 µM TCEP, 10 mM MESNa, pH=7.0
25 °C, 1 hour incubation

(Ho^{3+})DOTA Lys act ctt ccc cac Gly Cys cct aca gcg cc Lys(Biotin) Gly – NH_2 **P5**

B

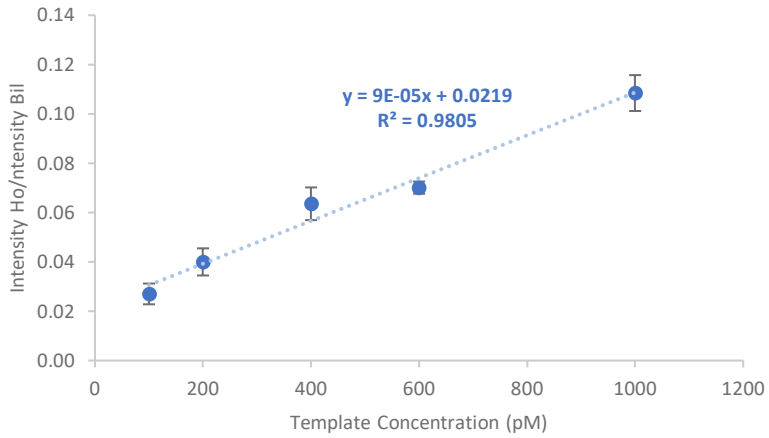

Figure 31: Calibration with templated reaction of A3 and D3 in the pM range. **A**, Reaction system. **B**, ICP-MS response to templated reactions with concentrations of acceptor and donor probe of 1.5 nM and concentration of template ranging from 100 to 1000 pM. Error bars represent the standard deviation of triplicates of the reaction and reflect variations in method application and instrumental performance.

ICP-MS has been used for DNA quantification in two different approaches: quantification of its phosphorous content or through a metal tag. First methodologies took advantage of the phosphorous content of DNA to draw a direct connection between phosphorous and DNA concentration. Such approaches usually present LODs in the low nM range.[166-168] Hyphenation is usually required to differentiate from other phosphorous-containing species, and in most cases, a mass balance between digested and speciated DNA is needed. Moreover, ^{31}P detection must be performed with resolution enough to discriminate from $^{15}N^{16}O+$ and $^{14}N^{16}OH^+$ or with the use of a reaction cell.[169]

Methods based on metal tags further enhance sensitivity to the low pM range.[86-88] Attempts to increase sensitivity are based on the use of RCA and enzymes such as in the works of K. Bruckner *et al.*[88], where the target was a 50mer ssDNA. Shorter DNA targets (between 20-24 nucleotides) were measured on Northern blot membranes using complementary lanthanoid-label DNA probes by LA-ICP-MS achieving limits of detection between 18 and 1.5 fmol;[170] however, breaking the pM limit is mainly achieved with the use of enzymes.[171-172]

Nanoparticles have been seen as a way to increase the amount of metal ions per reporter tag promising a significant sensitivity enhancement. However, no approach has been successfully

combined with ICP-MS to harvest the theoretical performance improvement. Merkoci et al. used a gold nanoparticle modified with immunoglobulin G to trace oligonucleotides carrying a peptide antigen to achieve limits of detection for peptide-modified DNA of 0.2 pmol.[83] This approach has been further developed into a DNA hybridization assay by coupling the capture probe to different gold nanoparticles which bind and cross link in the presence of the target template, altering the frequency and peak distribution when measuring in single particle ICP-MS.[173] The convoluted approach could hardly justify the 1 pM limit of detection. Although sensitive, methods based on nanoparticle have the drawback of the tedious coupling and working procedures of nanoparticles use, and the necessity to know the loading of capture/reporter probe for most quantifications.

In conclusion, the presented approach was used for the detection of a 30 bases long target in the low pM range. Linearity was comparable to a calibration with standards of elemental holmium. Results are strongly dependent on the measured matrix; therefore, procedures and matrices have to be taken into account on the planning of further experiments. The LOD is dependent on the initial probe concentration, due to non-specific carry over during the purification process, but they are in the same range as values found in literature. In any case, it is critical to study in detail the background and propose alternatives or/and improvements to correct such deviation.

5.3. Reducing the background

As described in chapter 5.1, background was higher with the use of hydrophobic polystyrene beads than with more hydrophilic carboxylic acid coated beads. Streptavidin is well known for yielding non-specific hydrophobic interactions;[174] moreover, the hydrophobicity of PNA is a factor that is enhanced with aggregation with the use of biotin.[175] An increase on probe solubility would, not only avoid such non-specific interactions, but also enhance efficiency of the washing steps, and therefore, reduce the background. Much work on PNA has been on chemically modifying its structure to modulate solubility, improve hybridization and conjugation chemistry, and enhance membrane permeability. As it was discussed in Chapter 2.3, there are three main approaches to enhance solubility of PNA: conjugation with a charged moiety, modification of the nucleobases, or modification of the PNA backbone.

One solution to increase solubility along the PNA sequence is to use building blocks that are charged. The introduction of cationic groups on either α- or γ-position (Figure 32) has proven to enhance binding to complementary DNA due to interactions with the negatively charged phosphate backbone.[100] The modification in this case would not search the extra affinity, but to add an extra charge to increase hydrophilicity. Modifications usually involve the synthesis of the PNA building block from a different amino acid than glycine. Such amino acid should bear a positively charged side chain such as lysine,[106] or a group onto which other functional groups that enhances PNA properties could be added.[176]

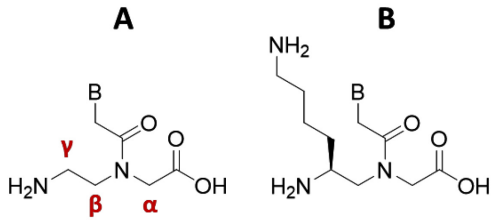

Figure 32: backbone modification of PNA. **A**, General PNA molecule with the α, β, and γ position marked. **B**, ^{L}Kγ-PNA synthesized by E. A. Englund and D. H. Appella with the amino group of the starting L-Lys in the γ-position.

In this case, the high versatility of the ^{L}Kγ-PNA was the determining factor. Background is a direct consequence of non-specific binding of the donor probe, since it is the one bearing the lanthanoid metal visible in ICP-MS. The use of γ-modified PNA responds to the immediate necessity to increase hydrophilicity of the donor probe and non-specific hydrophobic interactions. However, γ-modified PNA has shown enhanced duplex stability[105] as well as enhanced cell permeability[177] which are both properties useful for future applications.

The synthesis of the ^{L}Kγ-PNA building blocks was performed following the work of E. A. Englund and D. H. Appella[106] with L-Lys used as starting material (Scheme 1). The amino group on the side chain of L-lysine was selectively protected with a carboxybenzyl protecting group in the presence of copper (II) ions. The N-terminal amino group was then protected with a tert-butyloxycarbonyl group. Afterwards, a Weinrebamide was formed with N-O-dimethylamine, 1-ethyl-3-(3-dimethylamonipropyl)carbodiimide (EDCI), and 4-Dimethylaminopyridine (DMAP), and then reduced to the aldehyde with lithium aluminum hydride in THF. Instead of the glycineethylester prepared by Appella et al., the glycinemethylester synthesized with glycine and thionyl chloride in methanol was then added in a reductive amination to form the rest of the PNA backbone in methanol. Either the carboxybenzyl protected cytosine or thymidine were

alkylated by using ethyl bromoacetate in DMF, and then coupled to the PNA backbone with pivanolyl chloride also in DMF. Finally, the methyl ester was hydrolyzed with lithium hydroxide to yield the correspondent Boc-protected ^{L}Kγ-PNA building block that was chromatographically purified.

Scheme 2: Synthesis of Boc-^{L}Kγ-c(CbZ)-PNA-OH. [106]

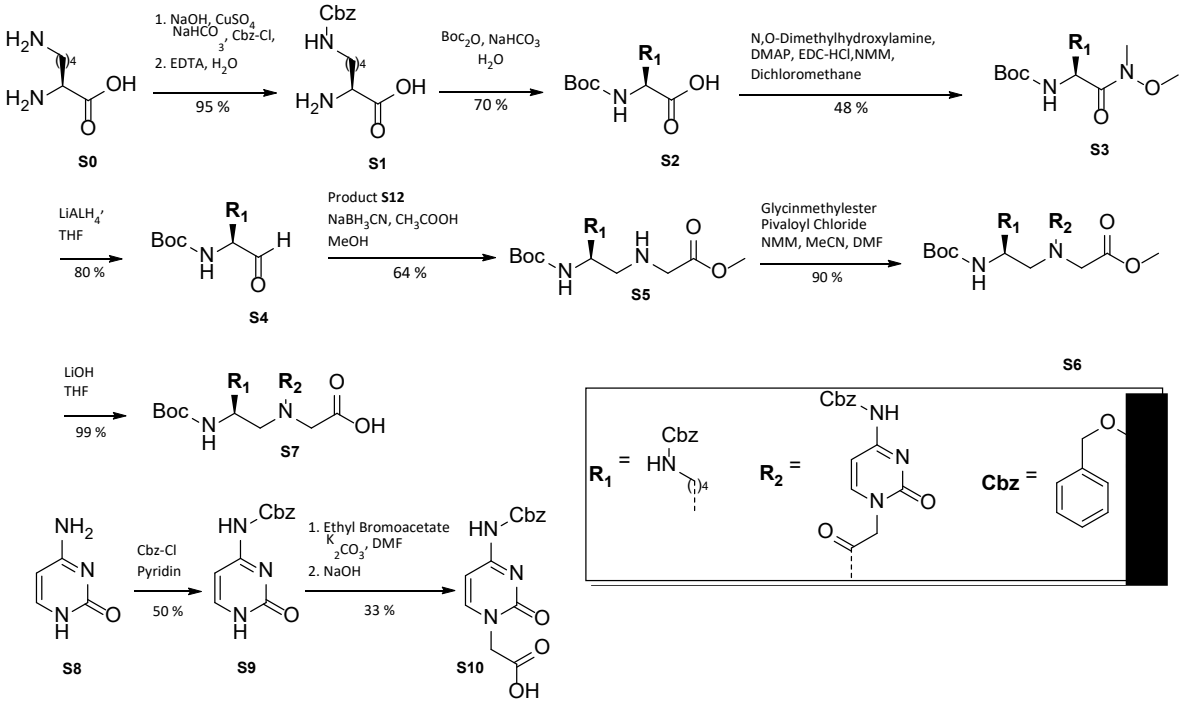

Following the synthesis and purification of the γ-modified monomers, a new set of acceptor and donor probes (A4 and D4 respectively) was synthesized containing the γ-modified PNA building blocks (Scheme 2). Since background is dependent on the donor probe, the stronger hydrophilicity enhancement was performed on the donor side; therefore, two γ-modified monomers were introduced on D4. γ-Modified bases were placed with alternate spacing since it has been shown that this configuration yields a higher binding affinity.[113] Moreover, γ-modified bases were located away from the reactive site of the probes, in order to avoid an effect on reactivity. Additionally, one γ-modified monomer was included into the acceptor probe. The modified monomer on A4 was located near the studied SNP. The acceptor probe is the one in charge of recognition of the SNP, thus its location was determined in order to assess whether the enhancement in affinity can influence sensitivity on SNP detection.

The introduction of γ-modified bases successfully resulted in an increase in hydrophilicity and affinity for the target as shown in Figure 33. The acceptor probe with γ-modified base A4 has a shorter retention time in a reversed-phase column than the non-modified counterpart A3 (Figure 33 B). In agreement, the donor probe with two γ-modified monomers experienced an even greater decrease on retention time when compared to D3. On the affinity side, the probe/target duplex had a 3.3 °C higher melting temperature when γ-modified bases were present on the donor probe sequence (Figure 33 C). The mismatch effect was also evaluated. The difference between matched and mismatched was similar among probe systems. However, probes with γ-modified bases had a higher melting temperature than non-modified probes. Sensitivity towards SNP recognition depends on the affinity difference between the probe and the matched or mismatched target. The introduction of a γ-modified base near the SNP did not

have an effect on the melting temperature difference in this case; However, more data on sequence dependency is needed to draw any conclusion.

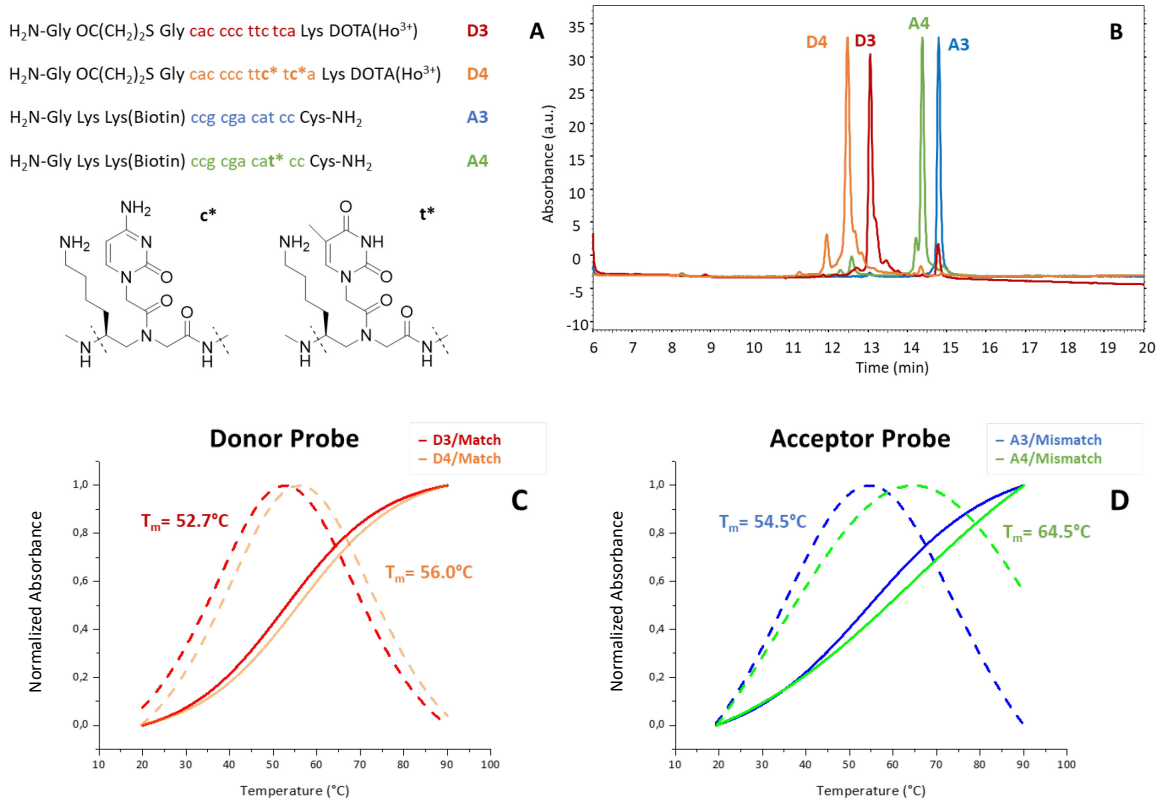

Figure 33: Comparison of probes with γ-PNA and with standard PNA. **A**, Schematics of the non-modified probes, γ-modified probes, and γ-modified bases. **B**, Elution trace of different probes in a reversed-phase column operated with Gradient 5. **C**, melting curves of the donor probes D3 and D4 with the matched template. **D**, Melting curves of the acceptor probes A3 and A4 with the mismatched template.

The incorporation of γ-modified monomers on the sequence also has an effect on the yield of the reaction (Figure 34). In the templated reaction performed at 1 µM concentration of probes and 1 eq. of template at 25°C, neither templated system presents any background reaction in the absence of template. Differences arise in the templated reaction with the non-modified probes giving a yield of 80% while the probes with γ-PNA have a maximum yield of 50%. It was hypothesized that the difference in reactivity is likely due to the increase in affinity of the probe to the template. This enhanced affinity results in a more rigid structure that does not allow the templated reaction to proceed. Moreover, the greater affinity can also decrease the exchange once the duplex is formed under the chosen reaction conditions.

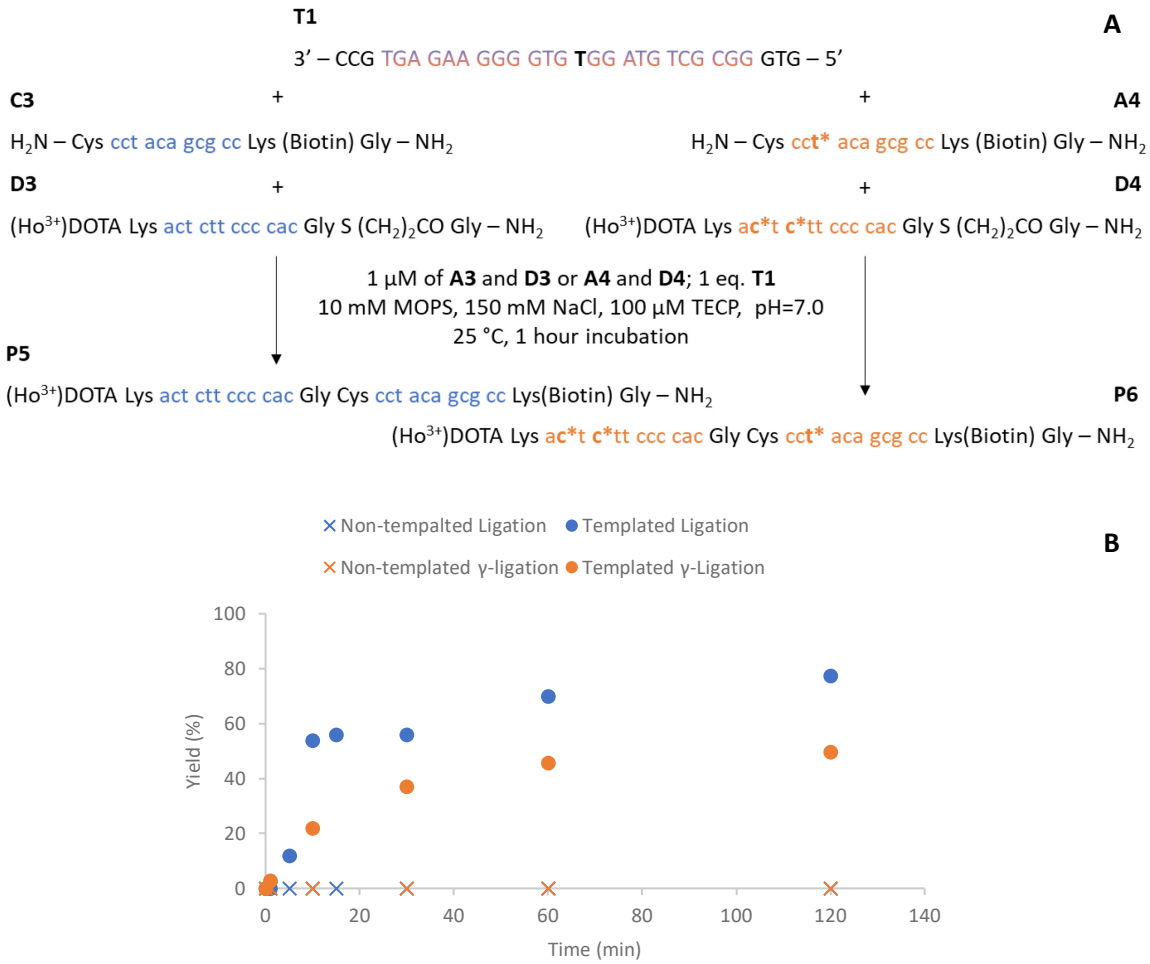

Figure 34: Comparison of the ligation reaction of probes with and without γ-modified PNA. **A**, Reaction scheme for both systems. **B**, Time course of the template-controlled reaction performed at 1 µM probes and template concentration, quenched with 1% TFA, and monitored via HPLC-UV.

Figure 35 shows the results of the ligation reaction between the probes containing the γ-modified PNA and standard PNA at 10 nM probe concentration and 1 eq. of template and measured via ICP-MS. The kinetics of the reaction are equal for the modified and non-modified probes, and they are in agreement with rate constants previously reported values.[144] However, the ratio of the non-templated reaction to the templated reaction is greater for standard PNA, with four times more background in the case of γ-modified PNA probes. This indicates that, in addition to the lower yield of the γ-probes, the introduction of charges along the sequence fail to reduce the background. It is unknown whether the non-specific interactions were not disrupted, or whether there are new interactions that jeopardize the performance of the purification step. The purification method was performed with the carboxylic acid hydrophilic coated beads and with the more hydrophobic polystyrene beads with similar results. The control sample, which sets the 100% reaction yield and recovery of the purification method, is greater for the modified probes. Since solubility of this probes is higher, the effect is more likely to be due to aggregation of the standard probes.

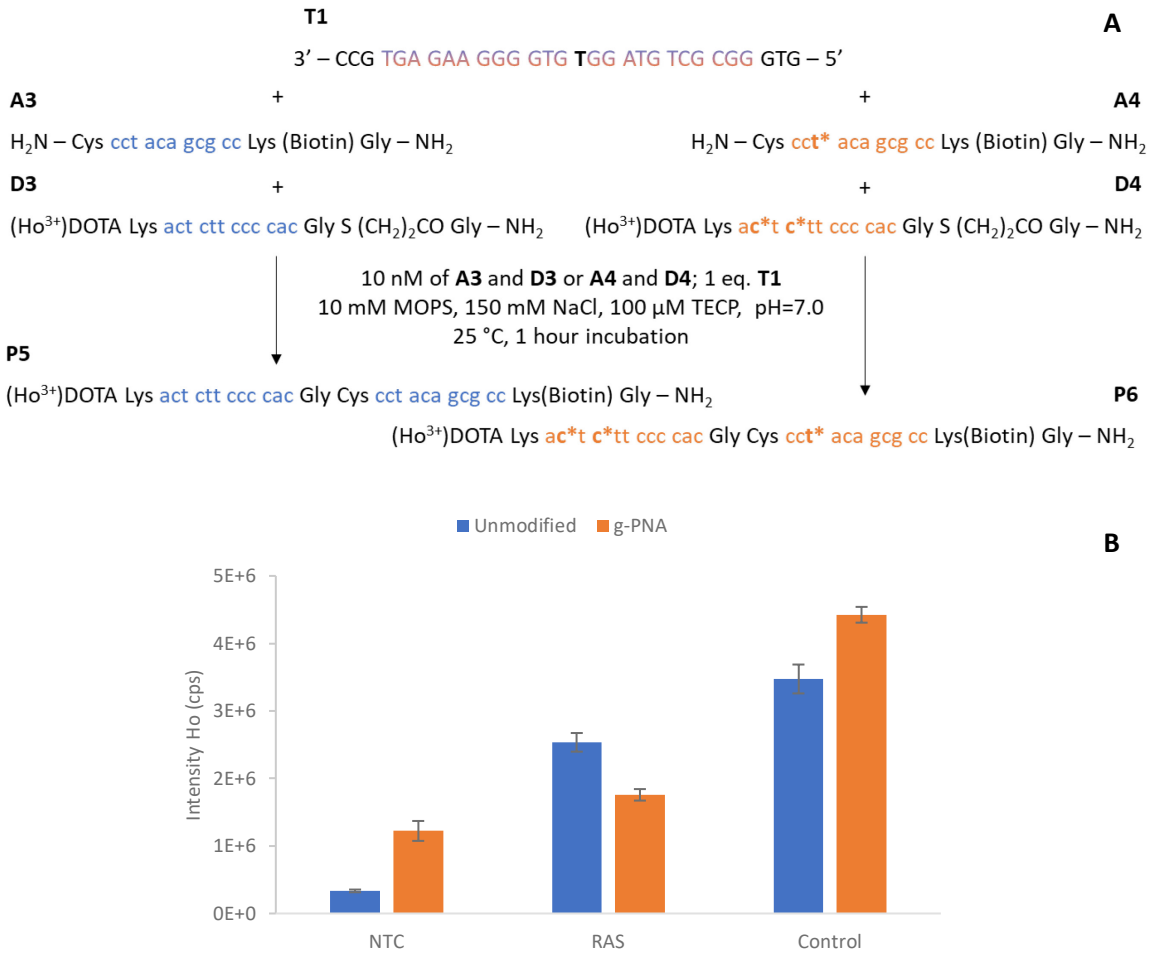

Figure 35: Comparison of the ligation reaction of probes with and without γ-modified PNA. **A**, Reaction scheme for both systems. **B**, Ligation of standard and γ-modified probes performed at 10 nM probes and template concentration, quenched with 1% TFA, and monitored via ICP-MS after purification with streptavidin magnetic beads.

In conclusion, background is the main factor that hampers the limit of detection of the method. It is most likely caused by non-specific interactions between the donor probe and the beads used on the purification method, and it could not be corrected with this modification of the PNA backbone. Moreover, modifications can induce reactivity changes as seen in this case, that would cancel the background improvements. Since an increase in hydrophilicity of the probes did not solve the non-specific carry over, improvements on the current purification method, or alternative steps should be considered. The purification method is the direct linker between the chemistry and instrumental measurement. Therefore, it has critical importance. Improvements in the purification method have greater influence than any yield or sensitivity improvement.

Without a suitable solution to the background problem, the benefits of the transfer reaction are neutralized. The transfer reaction allows to translate an excess of probe concentration, into a high target to product ratio, due to its high turnover. In other words, product formation is dependent on an excess of probes in regard to target concentration. The higher turnover ratios, thus greater amplification, have been achieved when the difference between probe concentration and target have been the greatest.[146] However, the method has proven to lack sensitivity when the initial probe concentration is too high. For such reason, the transfer reaction

was not attempted any further, and the spotlight turned on the benefits that the ICP-MS detection could bring to the methodology.

5.4. Multiplexing

After quantification of a ssDNA target based on the metal ion concentration of a reporter donor probe was achieved, the next natural step was to attempt the simultaneous detection of several targets. Chelating different metals on donor probes complementary to different templates would allow for simultaneous determination of target sequences: in other words, multiplexing. Three additional sequences neighboring the G→T (wt→mt) H-ras SNP from *Sus scrofa* (AF116346.1) where chosen, and ligation probe sets were synthesized. Each complementary donor probe set was labeled with a different lanthanoid (Table 7), so each system can be independently visualized with different isotopes.

H-Ras Probes		
3' – CCG TGA GAA GGG GTG TGG A(T/G)G TCG CGG GTG – 5'	**T1 m/w**	
^{H_2N} Cys cct aca gcg cc Lys Lys(Biotin) Gly ^{CONH_2}	**A5**	**Probe System 1**
(**Ho^{3+}**)DOTA Lys act ctt ccc cac Gly S $(CH_2)_2CO$ Gly ^{CONH_2}	**D5**	
3' – TTC ACC AAG ACC TAT TCG ACC TAC CAG TCC – 5'	**T2**	
^{H_2N} Cys gct gga tgg tc Lys Lys(Biotin) Gly ^{CONH_2}	**A6**	**Probe System 2**
(**Tb^{3+}**)DOTA Lys tgg ttc tgg ata Gly S $(CH_2)_2CO$ Gly ^{CONH_2}	**D6**	
3' – AGA TAC CCA CCC CAG CAT GAG TAG GTG TTT C – 5'	**T3**	
^{H_2N} Cys ctc atc cac aa Lys Lys(Biotin) Gly ^{CONH_2}	**A7**	**Probe System 3**
(**Tm^{3+}**)DOTA Lys ggt ggg gtc gt Gly S $(CH_2)_2CO$ Gly ^{CONH_2}	**D7**	
3' – GTG TGA ACG AAG GCC ATC CTC AGG AGA TAG – 5'	**T4**	
^{H_2N} Cys agg agt cct ct Lys Lys(Biotin) Gly ^{CONH_2}	**A8**	**Probe System 4**
(**Lu^{3+}**)DOTA Lys ctt gct tcc gg Gly S $(CH_2)_2CO$ Gly ^{CONH_2}	**D8**	

Table 7: H-RAS reporter probes for multiplexing. T1 contains the SNP 11 G→T (wt→mt). T2, T3, and T4 are neighboring sequences to the described SNP.

NCL with PNA probes is a technique with high sequence specificity; such characteristic was verified for this system. The set of probes A5/D5 in 10 nM concentration was independently incubated with the target templates T1 m, T2, T3, and T4 (Figure 36). The ligation product was only formed once the complementary template, T1 m, was added. The remaining non-complementary templates, T2, T3 and T4, yielded signals indistinct of the non-templated reaction which served as control.

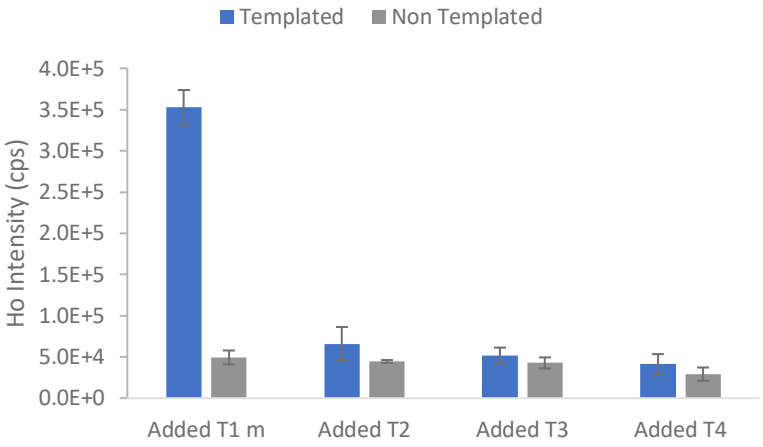

Figure 36: Template specificity in multiplexing experiments. Each sample contained the A5/D5 reporter probes in 10 nM concentration, and they were all spiked with 1 eq. of the corresponding template. Samples were taken after 1-hour incubation at room temperature and quenched with sodium hydroxide (4 M) before purification. Error bars represent the standard deviation of triplicates.

Increasing the number of systems monitored, increases the number of species presented in the sample. Once the template specificity was demonstrated, the next step was to assess the influence that an increase on the number of species has on the method. For that purpose, an attempt to monitor each of the ligation reactions in the presence of all the reporter probes was carried out. Five different samples were prepared as summarized in Table 8. Each of the samples contained 10 nM of all the reporter probes (A5/D5, A6/D6, A7/D7, and A8/D8); moreover, each sample was spiked with 1 eq. of the target template with the same name. After purification, the ion intensities were measured and plotted as shown in Figure 37 A. The addition of each template increases the signal of the reporter ion with respect to the non-templated reaction. However, results disagree with the hypothesized situation. First, the magnitude of the enhancement is dependent on the system. For example, the signal of terbium is 10 times higher in the sample spiked with T2 that in the control, but the difference on the reporter of T3 over the non-templated sample is of only 2,33. The difference comes from an abnormally high background intensity, with signals that correspond with nM concentrations of lanthanoids. Second, in addition to different enhancement, the background of each ion is divergent and not characteristic: For example, the signal of Holmium varies from sample to sample, although only one of them contains the complementary sequence.

Sample	Spiked Target	Spiked Probes
NTC	-	
T1 m	**T1 m**	
T2	**T2**	**A5 D5 A6 D6 A7 D7 A8 D8**
T3	**T3**	
T4	**T4**	

Table 8: Samples composition of **Figure 37**. All samples contain all the probe sets designed for the H-ras of *Sus scrofa*. The NTC was not spiked with any target sequence. All the other samples were spiked with the target with the same name.

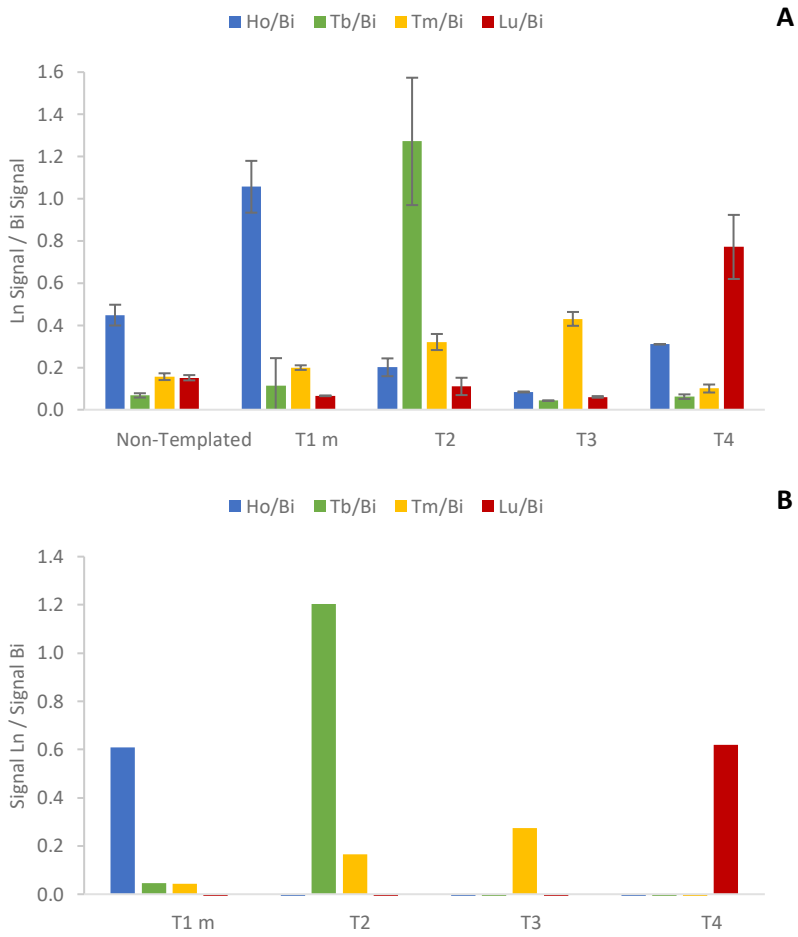

Figure 37: Templated ligation reaction of sets of probes A5-8 and D5-8. The donor/acceptor set of probes was present at 10 nM concentration in all samples, while only one template was added to each of them (from R1-mt to R4). Samples were incubated for 1 hour at 25 °C and quenched with sodium hydroxide (4 M) before purification: **A**, All isotopic traces. **B**, blank correction as subtraction of the non-templated reaction signal. Error bars represent the standard deviation of triplicates.

In conclusion, the different systems behave independently, but the observed background problem is exacerbated with a greater number of species present. The templated reaction is however present and more evident when the background is subtracted (Figure 37 B), centering the attention on non-specific interactions that can arise.

The aim of the project was to detect several reaction systems simultaneously, and to assess the suitability for SNP detection. When several probe systems coexist in solution and different ligation products are formed, non-specific interactions are the result of a complex combination between probes and products. Thus, the non-specific carry-over of the purification method is not the result of one donor probe with the streptavidin beads and ligation product, but the result of several donor probes with several products and the streptavidin beads. The extent of the effect that background has on specificity cannot be studied with an isolated reaction system, but with parallel and simultaneous reactions. To study the influence on the formation of other products on the reaction specificity and the specificity towards SNP detection the H-Ras reporter probes were subjected to combinations in the target availability. The reaction system consisted in three different samples containing the H-Ras probes at 10 nM concentration and 1 eq. of selected target templates. Experiment A was spiked with all complementary sequences.

Experiment B was spiked with the mismatched template T1 w instead of the matched T1 m, and no complementary template to the set of probes A7/D7 was added. Last, the non-templated reaction which serves as background control was left template free. A summary of the species present in each sample can be seen in Table 9, and the results of the ICP-MS measurement of the reaction performed at 25 °C after purification are shown in Figure 38 A.

Sample	Spiked Target	Spiked Probes			
NTC	-				
Experiment A	T1 m T2 T3 T4	A5 D5 (Ho)	A6 D6 (Tb)	A7 D7 (Tm)	A8 D8 (Lu)
Experiment B	T1 w T2 - T4				

Table 9: Samples composition of **Figure 38**. Sample triplicates contain all the probe sets designed for the H-ras of *Sus scrofa*. The NTC was not spiked with any target sequence. All the other samples were spiked with 1 eq. of the target sequences shown.

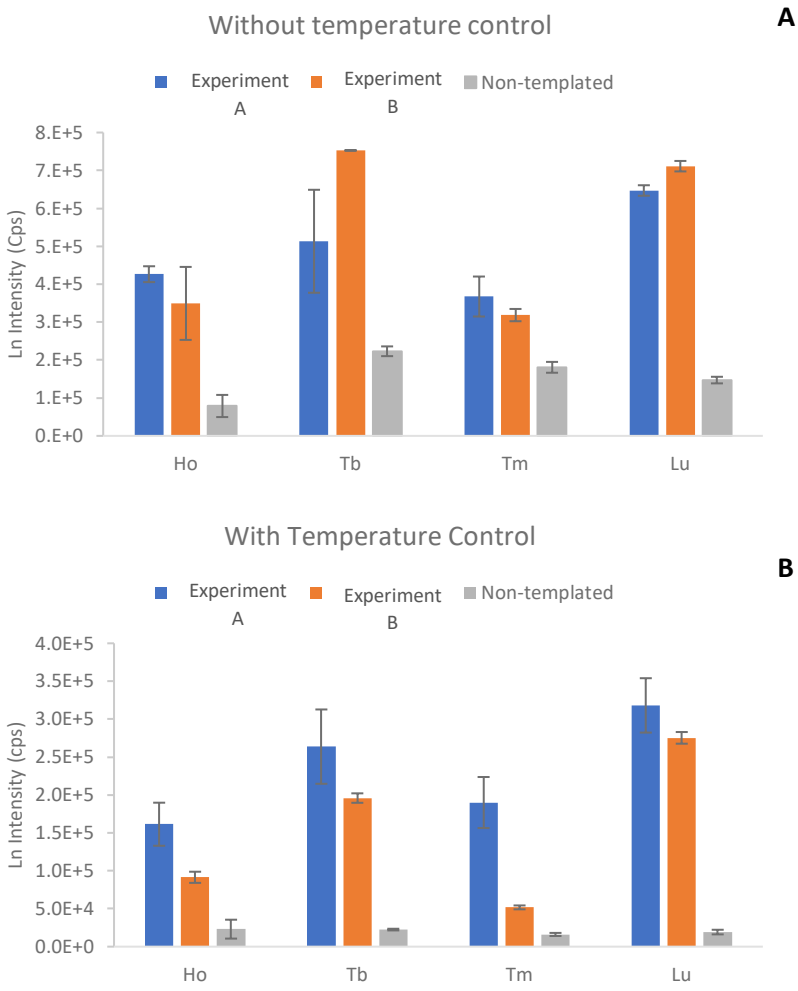

Figure 38: Multiplex specificity temperature dependency. **A**, ICP-MS measurements of the ligation reaction performed at 25°C, quenched with 1 % TFA, and purified. **B**, ICP-MS measurements of the ligation reaction performed with a temperature gradient, quenched with 1 % TFA, and purified. Error bars represent the standard deviation of triplicates.

The set of probes A5/D5, which was monitored with Ho, was used to assess the influence of an SNP. Both templated reactions have signals significantly larger than the control, but the signal with the matched template (Experiment A) could not be differentiated from the mismatched template (Experiment B). The effect on template presence was evaluated with probe systems

A6/D6, A7/D7, and A8/D8 which are monitored with Tb, Tm, and Lu respectively. The systems with Tb and Lu present the complimentary template on both Experiment A and B. Signals can be differentiated from the control, and they showed to be reproducible in the case of A8/D8 (Lu), but not in the case of A6/D6 (Tb). The complementary template for A7/D7 was not present in Experiment B, but the signal is comparable to the templated reaction. In conclusion, neither template specificity nor SNP sensitivity were fulfilled. In previous experiments of lower complexity, probe sets were independent of the other components of the sample; however, specificity and performance are challenged with the increase in the number of species present.

PNA probes are of hydrophobic nature, which makes them likely to aggregate in aqueous solution. The greater the number of probes, the more likely it is for non-specific reactions to happen. That effect can be seen from the progression of non-specific interactions from Figure 36 where template specificity was shown, along Figure 37 with an increased background when more probes where present, until Figure 38 A where all short of template specificity and reproducibility was lost. The more complex the system gets, the higher the background and the lower the specificity. Since aggregates are held together by weak intramolecular forces, it was considered that the process could be controlled with temperature. Having such factor in mind, the experiment previously described in Figure 38 A was repeated with the application of a temperature gradients during the ligation. The reaction mixture was heated to 50 °C and held for 5 minutes. The temperature was then decrease at 5 °C min^{-1} until 25 °C. The reaction was then left at 25°C for 50 minutes. It was hypothesized that in the first stage at high temperature, only the more thermodynamically favorable duplexes would form. Once temperature was progressively decreased, duplexes from more to less thermodynamically favorable would assembled. Finally, in the last stage at room temperature, the reaction would proceed as usual. Hydrolysis of the thioester is enhanced at higher temperatures; however, noticeable changes did only occur after 20 minutes and an excess of thioester was used.

Results of the ligation of H-Ras probes with the application of the temperature gradient are shown in Figure 38 B. In this case, the SNP presence shows a decrease in product yield of approximately 50%. Moreover, the absence of template on experiment B (monitored with thulium) is greatly reduced in comparison to the same sample from the experiment without a temperature gradient. The reaction system still lacks reproducibility to the extent that the set of probes whose condition do not change from experiment A and B (A6/D6 measured with terbium and A8/D8 measured with lutetium) yield different signals. However, a selectivity improvement over the reaction at room temperature was achieved. In agreement with previous experiments, it was observed that different probe systems give different maximum signals when the complementary template is present. For example, the maximum of holmium is much lower than the one of lutetium. No systematic explanation could be given to such effect. There is no direct relationship between affinity of the product for the template and product formation. The melting temperature of the ligation product with lutetium (65.4 °C) is lower than the one of holmium (68 °C), but so it is the one of terbium (61.7 °C) and thulium (64.2 °C) and both have lower signals than lutetium. It was also speculated that flexibility or binding strength of the probes near the reaction site could influence the yield of the reaction. The system with lutetium has an adenine base while the other three have a thymine and the tendency on GC content of the immediate adjacent sequences does not follow the observed reactivity (Table 10).

Probe System	T_m Product (°C)	Abasic Site	Sequence near Reaction Site	G/C content (%)
D8/A8 (Lu)	65.4	A	GGA GGC	83.3
D6/A6 (Tb)	61.7	T	CTC ATA	33.3
D7/A7 (Tm)	64.2	T	CTC TGG	66.7
D5/A5 (Ho)	68.3	T	TCC CAC	66.7

Table 10: Melting temperature of ligation product, abasic site, sequence near reaction site and G/C content of the sequence near the reaction site for the different system ordered from higher to lower ligation product detected on ICP-MS.

Instrumentally there was one more observation to keep in mind. Experiments with and without the gradient were measured with a temporal separation of one week, but the second experiment has an order of magnitude less of counts per second than the first one. As it was already mentioned, the ICP-MS system used had many performance issues that were addressed along the project, but in many cases, they hampered the limits of the technique. It is necessary to point out that standard variation along samples, even when using internal standards, have a great variance from experiment to experiment. In any case, the independence among systems was achieved and the background was controlled with the use of a temperature gradient.

		Concentration (nM)
3' – CCG TGA GAA GGG GTG TGG ATG TCG CGG GTG – 5'	**T1 m**	0.5, 1, 4, 7, 10, 13
^{H_2N} Cys cct aca gcg cc Lys Lys(Biotin) Gly ^{NH_2}	**A5**	15
(Ho^{3+})DOTA Lys act ctt ccc cac Gly S $(CH_2)_2CO$ Gly ^{CONH_2}	**D5**	15
3' – TTC ACC AAG ACC TAT TCG ACC TAC CAG TCC – 5'	**T2**	13
^{H_2N} Cys gct gga tgg tc Lys Lys(Biotin) Gly ^{CONH_2}	**A6**	15
(Tb^{3+})DOTA Lys tgg ttc tgg ata Gly S $(CH_2)_2CO$ Gly ^{CONH_2}	**D6**	15

Table 11: Samples composition of the experiment shown in **Figure 39**. All samples contain the probe sets A5/D5 and A6/D6 in 15 nM concentration. The template T2 was spiked at 15 nM while the concentration of T1 m varied from 0,5 to 13 nM.

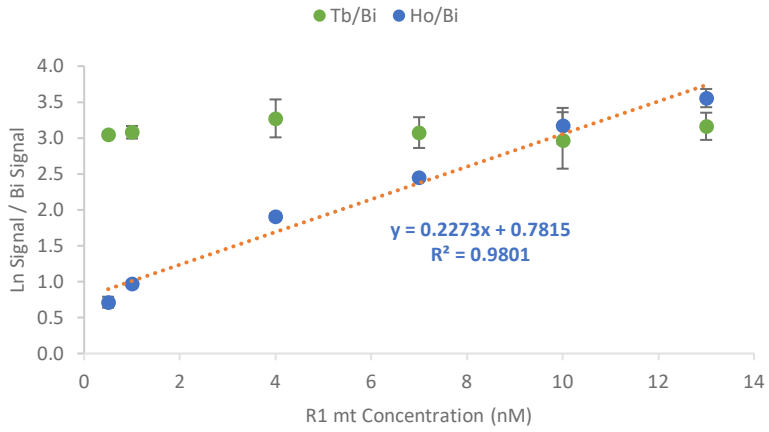

Figure 39: Calibration curve of template T1 m with constant T2 concentration. Both sets of probes A5/D5 and A6/D6 were present, the concentration of T2 was the same in all samples, and the concentration of T1 m was changed. Error bars represent the standard deviation of triplicates and reflect variations in sample preparation.

The extent of system independence was tested with the quantification of template T1 m at constant T2 concentration. A calibration was prepared with probes A5/D5 and A6/D6 at 15 nM concentration, 13 nM concentration of T2, and concentration of T1 m ranging from 0.5 to 13 nM (Figure 39). The steady T2 concentration was in agreement with the constant terbium concentration. Moreover, quantification of T1 mt was possible with the determination of holmium. The coefficient R^2 0.9801 was similar to the one achieved with the ICP-MS system for elemental holmium at the time.

The use of ICP-MS for multiplexing detection of DNA templates was previously reported. Han *et al.* had already used a sandwich assay based on DNA-based capture probe bound to a magnetic particle and a DNA-based reporter tag with a coupled lanthanoid, both complementary to a DNA template.[86] Their assay could detect 15 different DNA targets with individual limit of detection between 5 and 20 nM. This approach was further improved by Luo *et al.*[87] with DNA capture and reporter probes used to detect three different DNA templates with method detection limits in the amol range or zmol range once a bridge DNA containing a primer for the reporter probe and polymerase-based rolling cycle amplification was used. With the aim of improving the limit of detection with multiplex detection of three different targets by increasing the amount of metal correspondent to each unit of template, Zhang *et al.*[90] coupled nanoparticles of gold, silver, and platinum to the reporter probe. The limit of detection in this case were around 1 pM of template concentration, and they were also able to see the effect of a SNP on the sample. In all cases ICP-MS provides a unique tool for simultaneous measurement of different targets, but as in this case their signal is template dependent. G. Han *et al.* justified them as an isotope abundance effect although differences were present also in monoisotopic species, making sequence dependency a common problem. In all mentioned cases, reporter probes and capture probes are based on a weaker DNA/DNA interaction instead of the PNA-DNA used in this work. Multiplexing detection of SNPs based on PNA probes was first shown by Mattes and Seitz.[178] Detection in that case was based on MALDI measurements with template concentrations of 10 µM.

It can be concluded that multiplexing with template-directed NCL and ICP-MS monitoring is possible. Increasing the number of probes, thus complexity of the system, also increases the background and reduces specificity, but it is a process that can be controlled by modulating temperature. Quantification of a template was performed in the presence of another reaction system without major interference, and sensitivity of the method towards SNP presence was demonstrated.

5.5. SNP detection and quantification

Two major modification were added to the methodology in order to tackle the background problem. First, the fraction of BSA in the incubation- and wash-buffers was increased to 1% to reduce non-specific interactions responsible for the background. Second, the reaction quenching was altered. Instead of the 1% TFA solution, which hydrolyzes the phosphodiester bond of the target DNA, a quenching solution based on concentrated sodium hydroxide was used. At high pH, not only the phosphodiester bond of DNA is hydrolyzed, but also the thioester of the donor probe. It was speculated, that hydrolysis of the thioester before the purification method would avoid any side reaction derived from the combination of mutivalency effects and non-specific interactions: the non-specific binding to the beads of the donor probes would result in an enhancement on the effective concentration that would result in an increase of the non-templated reaction. Removing the functionality before purification, would leave the donor probe unable to react.

To verify the reach of the described method enhancements on the sensitivity and background, a ligation experiment with probes A5/D5, A6/D6, and A8/D8 was performed. Triplicates of three samples with probes in 1 nM concentration were prepared. The control, NTC, was not further spiked. The sample called Experiment A was spiked with 1 eq. of the three complimentary templates (T1 m, T2, and T4). The sample called Experiment B was spiked with 1 eq. of the mismatched T1 w and 1 eq. of the complimentary template T4. Upon mixing of the probes, the temperature gradient described before was applied (50 °C for 5 minutes, cold down 5 °C min^{-1} rate until 25°C and a final incubation at 25 °C for additional 50 minutes). Results of the experiment can be seen in Figure 40, and a summary of the probes and templates contained in each sample is presented in Table 12.

Sample	Spiked Targets			Spiked Probes		
No Template Control	-			A5 D5 (Ho)	A6 D6 (Tb)	A8 D8 (Lu)
Experiment A	T1 m	T2	T4			
Experiment B	T1 w	-	T4			

Table 12: Samples composition of the experiment shown in **Figure 40**. All samples contain the probe sets A5/D5, A6/D6, and A8/D8 in 1 nM concentration. The NTC was not spiked with any target sequence. The Templated A and Template B samples were spiked with 1 eq. of the target sequences shown.

Each system of probes was intended to show a different effect in a multiplex experiment. First, probes A5/D5 were set to show the sensitivity towards the presence of an SNP in the complementary sequence. From the templated reaction with T1 m (Experiment A) to the reaction with the SNP G→T containing T1 w (Experiment B), there was a signal intensity decrease of 50%. Second, the pair of probes A6/D6 was set to assess the template specificity of the system when more templated reactions happen simultaneously. In the absence of complementary templates (NTC) the background was in the same order of magnitude as when other two non-complementary templates were present (Experiment B), while the presence of the complementary template (Experiment A) showed an enhance in lanthanoid signal. Last, the pair of probes A8/D8 intended to show the reproducibility of the assay. Independently from the existence of other templates, the template-directed ligation yielded signals of the same magnitude; in the Experiment A, there are two additional templates, while in the Experiment B there is just one additional template. In conclusion, methodological improvements allowed the independent monitoring of the different systems, to the point that the assay showed sensitivity towards SNP detection in multiplexing conditions.

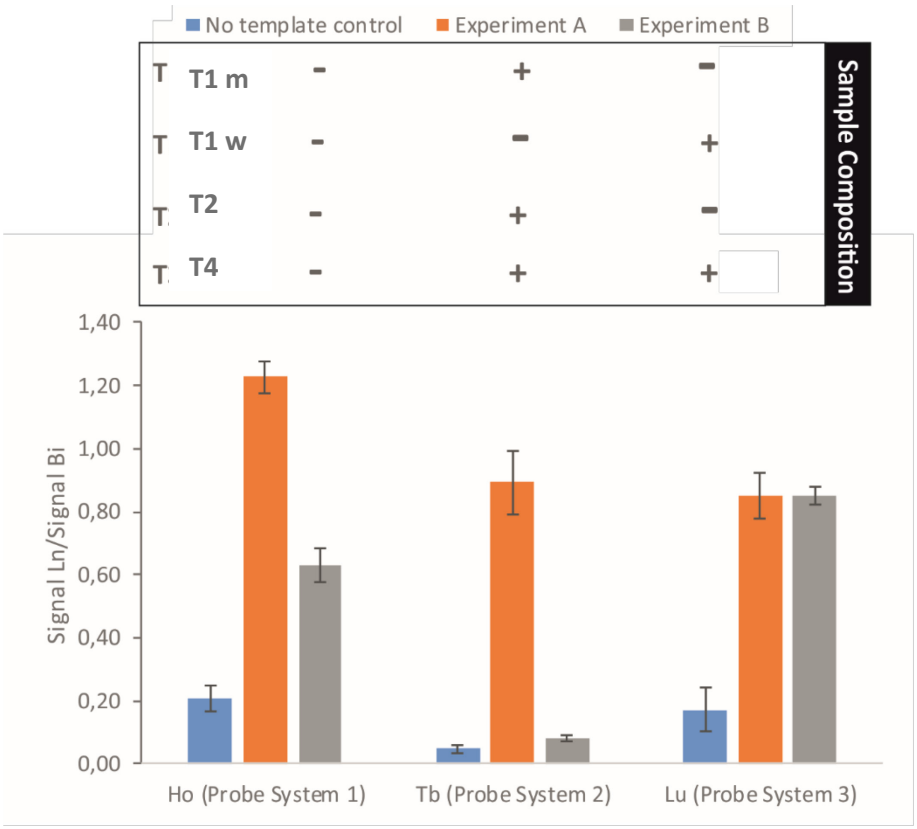

Figure 40: Multiplex experiment with H-Ras probes. Three different set of probes complementary each to a different template were added in three different vials. In the NTC sample no template was added, in the Templated A sample all three templates were added. In the Template B sample, no template is added for the first set of probes, a complementary template with a SNP is added for the second set of probes, and a complementary template is added to the third system (first, second, and third from left to right).

Probe systems behaved independently and were measured simultaneously; therefore, it was assumed that one of the systems could be used to detect a SNP while another probe system served as control (Scheme2). The approach would be based on the use of one pair of probes complementary to the region where the target SNP is present, and a second pair of probes designed to hybridize a neighboring region. The first pair acts as reporter, thus they were named reporter probes, while the second pair worked in a similar fashion to an internal standard, and thus they were termed control probes. In the presence of either target, matched or mismatched, the control probe system would react in the same manner, and yield a signal whose intensity would only be dependent on the target concentration. The reporter probe system on the other hand, would depend on the ratio of matched and mismatched target, being unfavorable for the reaction when more mismatched target is present. The signal decrease consequence of the presence of mismatch would not be discernible from a concentration change when measured independently; however, in combination with the control probe system, a ratio could be stablished.

Scheme 3: Sister probe approach. Two set of probes are designed so the first one (Reporter Probes) is complementary to the SNP region while the second one is complementary to an adjacent region. The differences in reactivity of the Reporter Probes due to the presence of either the matched or mismatched target are monitored based on the ratio with the signal of the control probe system.

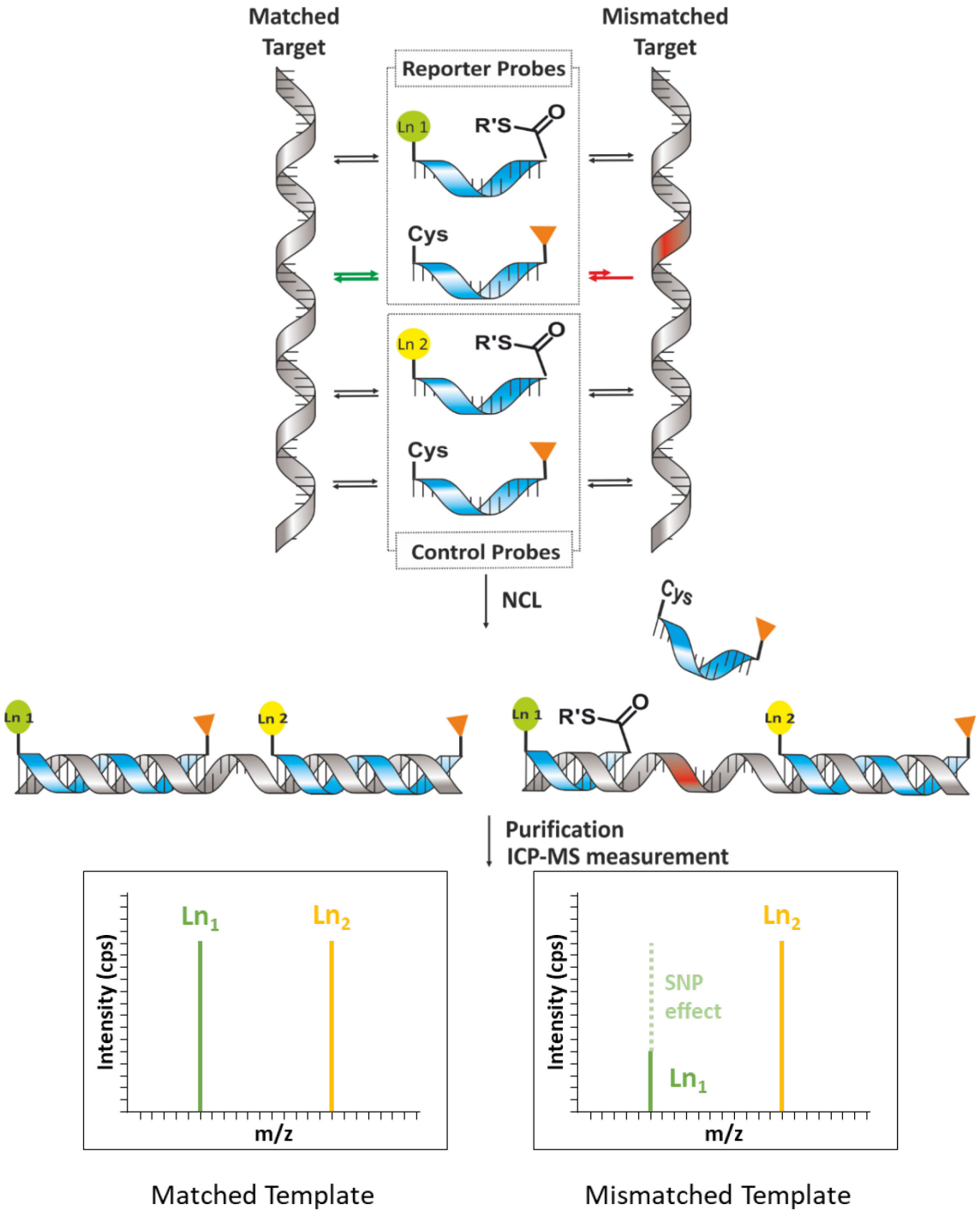

The highest value of the ratio between reporter and control probes would be consequence of the higher yield of the template-directed NCL of reporter probes; therefore, when the target is the matched allele. On the contrary, the smallest value of the ratio would arise when the reporter probes yield the lowest intensity, thus when the template presents a mismatch. Once the maximum and minimum values would be calculated, mixtures of matched and mismatched

targets could be measured. When the ratio is greater than the uncertainty of the method, the reporter and control probes would allow for the quantification of the SNP based on the ration between their signals. The greater the decrease in signal due to the SNP presence, the greater the sensitivity of the method to quantify SNPs.

The suitability of the approach was tested with A5/D5 as reporter probes and A6/D6 as control (Figure 41). Probes were in 5 nM concentration, while the target concentration was as specified in Table 13. The concentration of T2 which was complementary to the control probes was kept constant in all experiments. On the other hand, ratios from 100 % matched to 100 % mismatched template to the reporter probes A5/D5 were used.

		Concentration (nM)
3' – CCG TGA GAA GGG GTG TGG ATG TCG CGG GTG – 5'	**T1 m**	4 2 0
3' – CCG TGA GAA GGG GTG TGG AGG TCG CGG GTG – 5'	**T1 w**	0 2 4
^{H_2N} Cys cct aca gcg cc Lys Lys(Biotin) Gly ^{NH_2}	**A5**	15
(Ho^{3+})DOTA Lys act ctt ccc cac Gly S $(CH_2)_2CO$ Gly ^{CONH_2}	**D5**	15
3' – TTC ACC AAG ACC TAT TCG ACC TAC CAG TCC – 5'	**T2**	13
^{H_2N} Cys gct gga tgg tc Lys Lys(Biotin) Gly ^{CONH_2}	**A6**	15
(Tb^{3+})DOTA Lys tgg ttc tgg ata Gly S $(CH_2)_2CO$ Gly ^{CONH_2}	**D6**	15

Table 13: Concentrations of the different target templates in the samples. The target of the control, T2, was kept constant, while different ratios of the matched mismatched (T1 m/w) template were used for the reporter system.

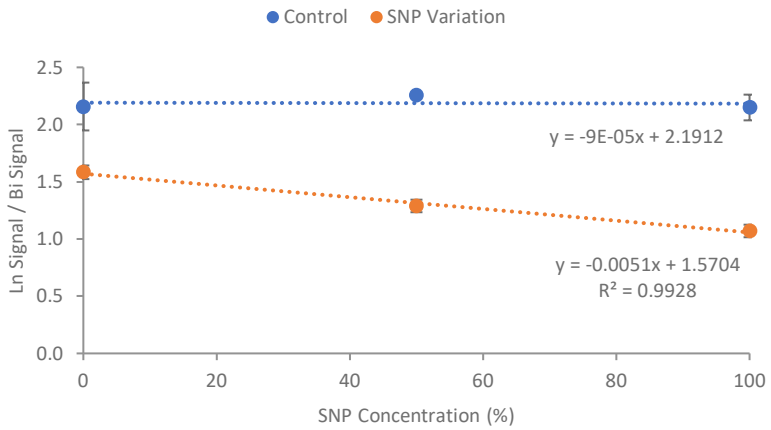

Figure 41: Sister probes approach application. Probes present at 5 nM were incubated with templates in ratios specified in **Table 13**. The Reporter probes had mixtures of matched and mismatched template, while the control had a constant template concentration.

As it can be seen in Figure 41, the assay successfully detected the differences between matched and mismatched templates. The control system consistently yields product in the same range, while the reporter probes show the trend in SNP concentration. The signal decrease from the 100% matched to 100% mismatched template was 27%, and changes of the ratio of 50 % were successfully differentiated. Sensitivity towards SNPs depends on the different of affinity between the matched and mismatched template. The identity of the SNP (which base is changed) and the remaining pair (which bases are opposed to each other) are expected to have

an influence on the affinity difference. Duplex destabilization by an SNP is a problem that has been extensively studied.[179-182] Although there is no consensus on which exact base pair has a greater effect, it is widely accepted that G-T and G-A mismatches slightly destabilize a duplex, while the pairs of A-A, T-T, C-T, and C-A have a stronger effect. In this particular case, the mutation is a T→G change, which leaves a G-A base pair, that is one of the weakest destabilizing pairs.

The assay could differentiate wild from mutagenic species, and a mixture of both alleles with the less sensitive mutation. The experiment was performed with two sets of probes and two lanthanoids, despite the fact that ICP-MS offers a higher degree of multiplexing. In order to test for the limits of the technique, three new SNPs, associated with pancreatic cancer with an OR>1,[184] were selected. In order to facilitate the interpretation, the standard codes rs9543325, rs9564966, and rs4465241 were changed by SNP 1, SNP 2, and SNP 3. The first and third SNP presented a T→C mutation, while the second SNP had a G→A mutation, but all of them left a A-C base pair, which is one of the most destabilizing mutation. Reporter probes complementary to the three SNPs and controls complementary to neighboring sequences were synthesized. A9/D9, A10/D10, and A11/D11 are reporter probes set to detect a different SNP, and A12/D12, A13/D13, and A14/D14 are controls of the former. Each donor probe chelates a different lanthanoid for simultaneous detection. Since sensitivity towards the detection of the probes depends on ion transmission, lanthanoids were chosen in order to avoid interferences at low resolution. To maximize the analytical performance, reporter probes were labeled with monoisotopic species, while control probes, were detection is not the ultimate challenge, were labeled with less abundant species. A summary of target sequences, reporter and control probes for the SNPs associated to pancreatic cancer can be seen in Table 14.

H-Ras Probes		
3' – TCG GTG TCC ACA CTA TCT **(T/C)**CA CGT CGT TC – 5'	**T5 m/w**	**Reporter Probe System SNP 1**
^{H_2N} Cys aga agt gca gc Lys Lys(Biotin) Gly ^{CONH_2}	**A9**	
DOTA(**Tb^{3+}**) Lys cca cag gtg tga Gly S $(CH_2)_2CO$ Gly ^{CONH_2}	**D9**	
3' – TAG TGA TCC CGG GGA AGG **(G/A)**GT AGT TCC TT – 5'	**T6 m/w**	**Reporter Probe System SNP 2**
^{H_2N} Cys tcc cca tca agg Lys Lys(Biotin) Gly ^{CONH_2}	**A10**	
DOTA(**Ho^{3+}**) Lys act agg gcc cc Gly $S(CH_2)_2CO$ Gly ^{CONH_2}	**D10**	
3' – TCT GAT TCA CTA TCC AAG **(T/C)**CG TGG TAG AT – 5'	**T7 m/w**	**Reporter Probe System SNP 3**
^{H_2N} Cys ttc agc acc atc Lys Lys(Biotin) Gly ^{CONH_2}	**A11**	
DOTA(**Tm^{3+}**) Lys aga cta agt gat ag Gly $S(CH_2)_2CO$ Gly ^{CONH_2}	**D11**	
3' – TGT CCT GCC ATC TAA TTC ACA GTA CTA TCT – 5'	**T8**	**Control Probe System SNP 1**
^{H_2N} Cys agt gtc atg ata ga Lys Lys(Biotin) Gly ^{CONH_2}	**A12**	
DOTA(**Pr^{3+}**) Lys gga cgg tag tta Gly $S(CH_2)_2CO$ Gly ^{CONH_2}	**D12**	

Table 14: Multiplex probes for pancreatic cancer SNPs. Probes set to detect the SNP were labeled with monoisotopic lanthanoids, while control sequences were monitored with less abundant species.

3' – AGA CAT TAC ATT GAC CGA AAA GAG ATA TAA – 5'	**T9**	
^{H_2N} Cys ctt ttc tct ata tt Lys Lys(Biotin) Gly ^{CONH_2}	**A13**	**Control Probe System SNP 2**
DOTA(**Gd^{3+}**) Lys tcg taa tgt aa ctg Gly $S(CH_2)_2CO$ Gly ^{CONH_2}	**D13**	
3' – TCA ATC GTT TTC GGT GTC AGA TAA CCA AAG – 5'	**T10**	
^{H_2N}Cys agt cta ttg gtt tc Lys Lys(Biotin) Gly ^{CONH_2}	**A14**	**Control Probe System SNP 3**
DOTA(**Dy^{3+}**) Lys agc aaa agc ca Gly $S(CH_2)_2CO$ Gly ^{CONH_2}	**D14**	

Table 14 (continuation): Multiplex probes for pancreatic cancer SNPs. Probes set to detect the SNP were labeled with monoisotopic lanthanoids, while control sequences were monitored with less abundant species.

In order to test the system, triplicates of two different samples, matched and mismatched, were prepared. Samples contained all sets of probes for pancreatic cancer at 7,5 nM. The template concentration complementary to the controls was kept constant in all samples at 5 nM. On the other hand, different ratios were used on the concentration of the targets of the reporter probes. In the Matched sample, only the complementary templates were present at 5 nM concentration. In the Mismatched sample, only the SNP-containing templates T5 m, T6 m, and T7 m were spiked at 5 nM concentration. A summary of the probe and target species in the different samples is summarized in Table 15 and results are shown in Figure 45.

Sample	Spiked Targets	Spiked Probes		
Matched	T5 **m**, T6 **m**, T7 **m**, T8, T9, T10	A9 D9 (Tb)	A10 D10 (Ho)	A11 D11 (Tm)
Mismatched	T5 **w**, T6 **w**, T7 **w**, T8, T9, T10	A12 D12 (Pr)	A13 D13 (Gd)	A14 D14 (Dy)

Table 15: Sample composition in the multiplex experiment with pancreatic cancer targets.

All probe systems were measured simultaneously in the same sample, but the results are shown relatively to each SNP in Figure 42 A SNP 1, 2, and 3. As it can be seen, intensities of all the mismatched samples were lower than the matched sample. However, the decrease in intensity varies for the different probe systems. For SNP 1 probe system monitored with Tb, the presence of the mismatched template yielded a signal that was 28 % lower than the one produced by the matched template. On the other hand, the signal contractions for SNP 2 and 3 measured with probe system 2 (Ho) and 3 (Tm) were of 58 and 34 % respectively. Although the mutation leads to the same remaining mismatch base pair, the yield of the reaction differs greatly, suggesting that not only the involved base pair is important, but also the whole sequence. This statement is in agreement with previous experiments,[86-89] highlighting the importance of sequence dependence in templated reactions.

Regarding the controls, their performance was consistent with all SNPs, yielding signals with the same magnitude in all samples. Since the method is based on the combination of systems, the signals of the reporter probes were divided by the signal of the correspondent internal standard (Figure 42 B). The intensity decrease due to the mismatch presence in this case is of 24, 52, and 29 % for SNP 1, 2, and 3 respectively, which means that there is an underestimation of 10,3 to 15,8 %. It is worth to point out that in each of the reaction vials were 6 different sets of PNA probes that were template-directed ligated. Each of the reactions responded to its template

concentration and fidelity regardless of the other probe systems, and they were simultaneously detected.

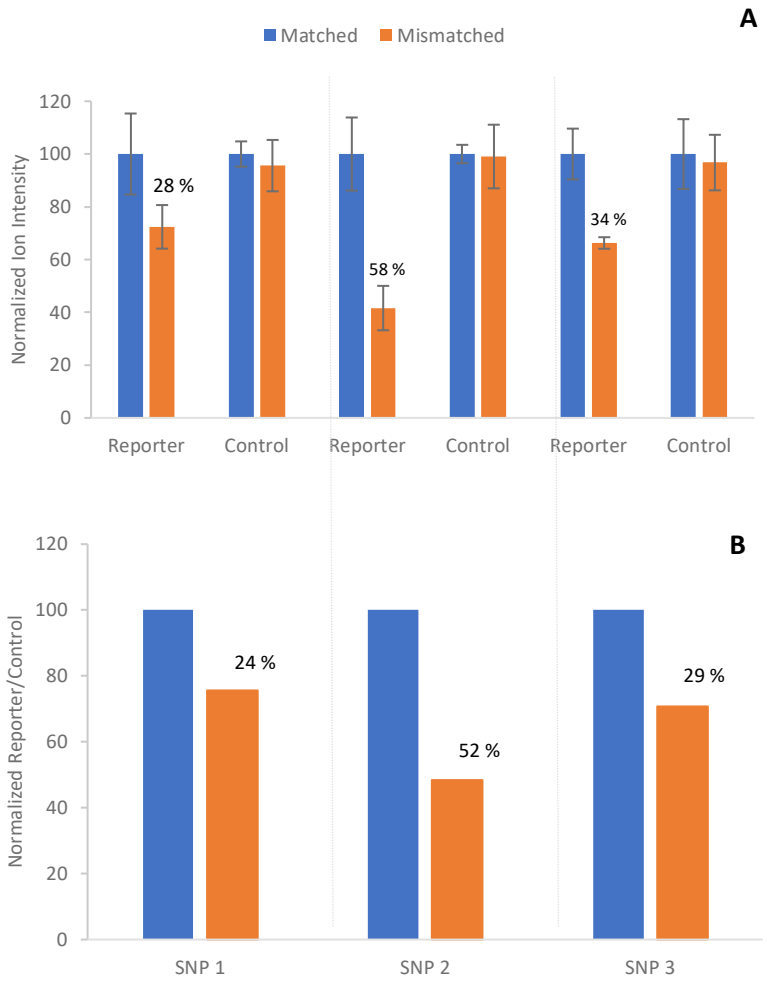

Figure 42: Multiplex SNP detection. **A**, Reporter and control probes for SNP 1, 2, and 3. **B**, Application of the sister probe approach by dividing the signal of the reporter by the one of the corresponding control.

In a second demonstration of the method, the two set of probes with the highest SNP sensitivity, SNP 2 and SNP 3, were incubated with different ratios of the matched and mismatched templates. The aim was to evaluate samples with mismatched to matched ratios of 0, 25, 50, 75, and 100 %. Therefore, the concentration of control probe sets and targets were kept constant, while the reporter probes at constant concentration were incubated with mentioned ratios of the matched and mismatched templates. In an attempt to show once again the independency of the different probe systems, the concentration of the matched templates is indirectly proportional; in other words, the sample with the highest matched template for SNP 2 is the sample with the lowest amount of matched template for SNP 3. Results after combination of the signals following the sister probe approach are shown in Figure 43.

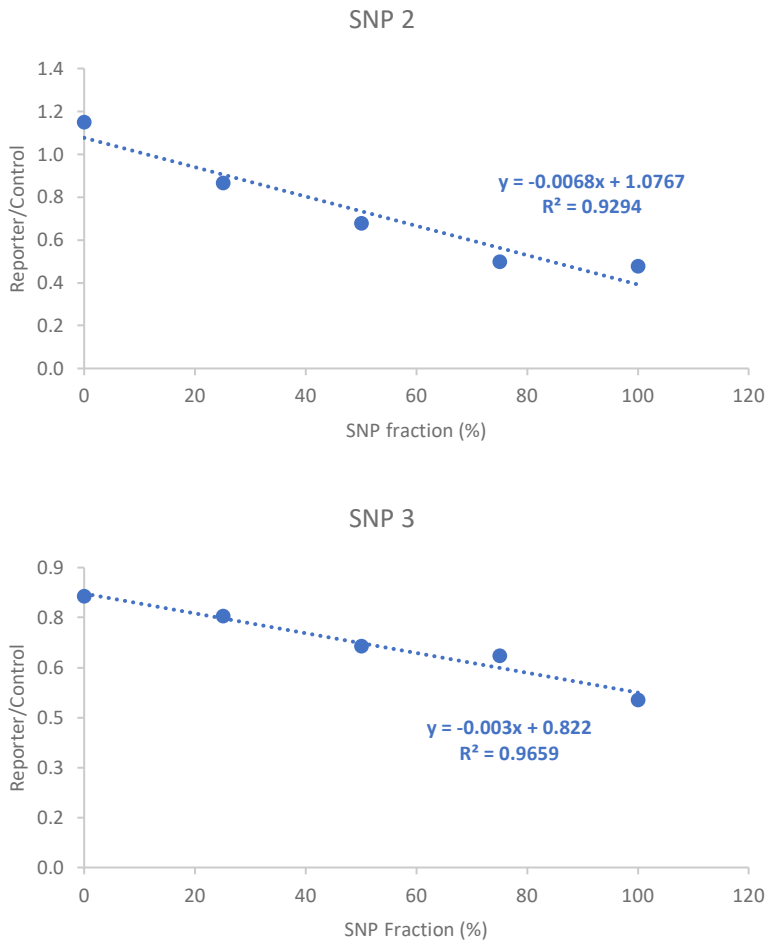

Figure 43: Multiplex SNP detection. Simultaneous determination of matched and mismatched templates for SNP 2 and 3.

The different ratios of matched and mismatched samples were successfully quantified. The intensity decrease was consistent with previous findings and the intensity trend followed the mismatched concentration. Sensitivity was still an issue, with a 59 % and 38% decrease for SNP 1 and SNP 2 respectively. In any case, the matched, mismatched and 1:1 mixture were differentiated unambiguously, highlighting the suitability for the differentiation between homozygotes heterozygotes. The sister probe approach was therefore a suitable method for the simultaneous detection of SNPs, although improvements in probe specificity and template recognition should be implemented

During this last chapter, the independence between PNA-probe systems was exploited in combination with the multiplexing capabilities of ICP-MS to develop the sister probe approach. Following the suitability to determine short fragments of nucleic acids in the low pM range, the simultaneous determination of SNPs was demonstrated. Although sensitivity remains a limiting factor, its suitability of the assay on the differentiation between heterozygotes and homozygotes was successfully tested.

6 Summary and outlook

The analysis of nucleic acids is becoming of paramount importance in the development of medicine. From quantification of micro RNA for the study of cell death, proliferation, and regulation, to the assessment of genetic variability towards disease development and treatment, methods in the field need to be not only sensitive and selective, but also provide a high degree of throughput and multiplexing capabilities. As stated in chapter 3, the aim of the project was to propose a method to detect nucleic acids which was sensitive to the wild and mutagenic alleles of an SNP. The proposed approach was based on the combination of two established techniques: template-directed NCL of PNA reporter probes and MeCAT. The goal was to harvest the possible synergies of the combination of the enhanced recognition and robustness of template-directed reactions with PNA probes and the superior sensitivity and multiplexing capabilities of ICP-MS.

The combination of both techniques required the attachment of the metal tag to one of the reporter probes which was termed donor probe. Measuring the concentration of the incorporated lanthanide was an indicator of the metal tag, and it was related to either the donor probe or reaction product. Since ICP-MS is an elemental technique that does not provide molecular information, it was necessary to separate the different species containing the same metal ion. In that respect, a purification method based on the biotin-streptavidin interaction was developed. A biotin was added on the remaining reporter probe, which was then termed acceptor probe. The biotin on the acceptor probe was used to fish out the product after ligation. Validation of the purification method was performed, and its suitability to work with samples in the low pM range was verified. Great effort was placed on the correct operation of the purification method, in order to unambiguously assign the lanthanide signal to the product and not the donor probe.

Product inhibition is one of the main limitation of most nucleic acid templated reaction. It is particularly critical on ligation reactions, since the product binds stronger to the template. This principle was used as an advantage to develop an assay for short ssDNA targets. Detection of 30-mer ssDNA near the LOD of lanthanides in ICP-MS was demonstrated, and linearity over 3 orders of magnitude was proved. The limit of detection was 29 pM with RSD 6.8% at 50 pM (n=5)

Apart from sensitivity, one of the main advantages of ICP-MS is its suitability for multiplexing analysis. In this case, simultaneous detection of several targets was performed by assigning a different lanthanide to each target. Control of the reaction temperature resulted critical in this step, but six different targets were detected in the same sample. Isolation between probe systems and the possibility to simultaneously follow each reaction product was used to develop the so-called sister probe approach for the detection of SNPs. The assay utilized one pair of probes complementary to a region where the SNP was present, and a second pair of probes in the neighboring region. The first pair acted as reporter, thus they were named reporter probes, while the second pair worked in a similar fashion to an internal standard, and thus they were called control probes. In the presence of either target, matched or mismatched, the Internal standard probe system reacts in the same manner, and yield a signal whose intensity only depends on the target concentration. On the other hand, the yield of the reaction of the Reporter Probe system depends on the ratio of matched/mismatched target, being unfavorable for the reaction when more mismatched target is present. The signal decrease consequence of the presence of mismatch would not be discernible from a concentration change when

measured independently; however, in combination with the Internal Standard probe system a ratio was established, and 3 different SNPs were successfully simultaneously detected. In a similar fashion, the capability to simultaneously quantify different targets was also demonstrated, indicating the suitability of the method for multiplex detection of short nucleic-acid targets (less than 30 base pairs).

The successful combination of technologies opens multiple applications and challenges in the short and long run. On the challenge side, the method is as strong as the link between the reaction system and detection. The reduction of non-specific interactions in the purification step could increase the linear range of the assay and allow the exploitation of the increased turnover of the transfer reaction. In this regard, there are two different ways to tackle the problem. Either further increase the hydrophobicity of the probes or change the interaction exploited in the purification method. Increasing the hydrophobicity of the probes can also benefit and potentiate the multiplexing capabilities avoiding aggregation between probes; therefore, it should be the main focus. Additionally, more work should be placed on enhancing sensitivity towards SNP presence. Although it was possible to differentiate between alleles, methods with per-thousand sensitivity are desirable in cancer studies. Both points can be theoretically tackled with the use of γ-modified PNA and some efforts were placed in this direction. So far, the level of difficulty that γ-PNA introduces in the analytical procedure is not balanced by the benefits of its use. However, an increase in either SNP sensitivity or background correction could displace such balance.

On the application side, the method is promising in two main application fields with high demand: detection of SNPs and high-throughput multiplexing detection of short RNA fragments. For the detection of short RNA fragments, I envision a system in which several acceptor probes are coated to a solid support onto which the target, donor probes, and reaction buffer are added. The advantage of having one of the reporter probes coated on solid support would be the higher multivalency of the system. This could translate into a higher effective molarity of the probes and target to form the triplex needed for the ligation or transfer reaction, thus yield ligation or transfer product at lower template concentration. After the template-directed reaction, the metal would be immobilized on the solid support, so the slide would be measured via laser ablation ICP-MS after washing. The presence of the metal would be an indication on the presence of the reaction product which could be used as indicator of the target sequence. Several reporter probe systems could be measured with different metals; thus, each laser ablation would result in the simultaneous detection of several targets. Moreover, the acceptor probes could be solid-coated to specific locations on the solid support, so multiplexing would depend on the monitored lanthanide and the location of the ablation. In other words, the same metal could be used to target different templates, if their reporter probes are coated in different parts of the solid support. The throughput and possibilities for multiplexing would exponentially increase with the number of reporter metals and probe clusters.

Detection and quantification of SNPs would require some extra considerations. First, the approach cannot be in solid support due to the difficulty to establish a ration between Reporter and Internal Standard systems. Approaches for quantification on LA-ICP-MS are not universal, and the sister probe approach relies on ration between the two probe systems. In addition, the target concentration should be present in sufficient concentration. This last point can be achieved via PCR amplification. The advantage when compared to other methodologies relies on the focus of the approach on the SNP recognition after and not during amplification. This

eliminates the necessity for the probe-hybridization optimization and it allows a higher sensitivity and increased focus on recognition due to the use of PNA.

In conclusion, the combination of template-directed NCL of PNA reporter probes and MeCAT is suitable for the analysis of nucleic acids offering a degree of multiplexing difficult to fulfill by other techniques. Challenges on sensitivity towards concentration and SNP presence lay ahead, but the technologies needed are already present, and they can be directly implemented. Recognition and sensitivity can be further increased with the introduction of modifications on the PNA backbone, and several approaches can be implemented to enhance the multiplexing capabilities and automatization possibilities of the technique. I started this work setting forth the need of analytical methods for the development of science. For example, in the study of miRNA and from an analytical point of view, the long-term goal would be the simultaneous detection and quantification of all the species over time. In a similar fashion, steps in the development of personalized medicine will require the study of association effects of several SNPs, and therefore, their simultaneous detection. It is because of this simultaneity need that mass spectrometry has to be at the heart of the nucleic acids detection field. The degree of multiplexing that can be achieved via mass spectrometry cannot be matched by any technique as of yet.

7 Appendix

7.1. Literature

[1] International Human Genome Sequencing Consortium; Finishing the euchromatic sequence of the human genome. Nature, 2004, 431, 931-945.

[2] The 1000 Genomes Project Consortium; A global reference for human genetic variation. Nature, 2015, 526, 68-74.

[3] J. L. Rukov and N. Shomron; MicroRNA pharmacogenomics: post-transcriptional regulation of drug response. Trends in Molecular Medicine, 2011, 17, 412-423.

[4] Palchaudhuri R., Hergenrother P. J.; Transcript profiling and RNA interference as tools to identify small molecule mechanism and therapeutic potential. ACS Chem Biology, 2011, 6, 21-33.

[5] K. A. Frazer, S. S. Murray, N. J. Schork, and E. J. Topol; Human genetic variation and its contribution to complex traits. Nature Reviews Genetics, 2009, 10, 241-251.

[6] D. Duggan, S. L. Zheng, M. Knowlton, D. Benitez, L. Dimitrov, F. Wiklund, et al.; Two genome-wide association studies of aggressive prostate cancer implicate putative prostate tumor suppressor gene DAB2IP. Journal of National Cancer Institute, 2007, 99 (4), 1836-1844.

[7] D. Gonzalez de Castro, P. A. Clarke, B. Al-Lazikani, P. Workman; Personalized cancer medicine: molecular diagnostics, predictive biomarkers, and drug resistance. Clinical Pharmacology and Therapeutics, 2013, 93(3) 252-259.

[8] S. T. Sherry, M. H. Ward, M. Kholodov, J. Baker, L. Phan, E. M. Smigielki, and K. Sirotkin; dbSNP: the NCBI database of genetic variation. Nucleic Acids Research, 2001, 29 (1), 308-311.

[9] G. R. Cutting, L. M. Kasch, B. J. Rosenstein, J. Zielenski, L. C. Tsui, S. E. Antonarakis, and H. H. Jr. Kazazian; A cluster of cystic fibrosis mutation in the first nucleotide-binding fold of the cystic fibrosis conductance regulator protein. Nature, 1990, 346, 366-369.

[10] J. C. Chang, and Y. W. Kan; β0 thalassemia, a nonsense mutation in man. Proc. Natl. Acad. Sci. USA, 1979, 76, 2886-2889.

[11] O. Kilpivaara, S. Mukherjee, A. M. Schram, M. Wadleigh, A. Mullally, B. L. Ebert, A. Bass, S. Marubayashi, A. Heguy, G. García-Manero, H. Kantarjian, K. Offit, R. M. Stone, D. G. Gilliland, R. J. Klein, and R. L. Levine; A germline JAK2 SNP is associated with predisposition to the development of JAK2(V617F)-positive myeloproliferative neoplasms. Nature Genetics, 2009, 41 (4), 455-459.

[12] A. Miyashita, A. Koike, G. Jun, L. Wang, S. Takahashi, E. Matsubara, T. Kawarabayashi, M. Shoji, N. Tomita, H. Arai, T. Asada, Y. Harigaya, M. Ikeda, and R. Kuwano; SORL1 is genetically associated with late-onset Alzheimer's disease in Japanese, Koreans and Caucasians. PLOS One, 2013, 8 (4), e58618.

[13] A. Goris, I. Pauwels, M. W. Gustavsen et al.; Genetic variants are major determinants of CSF antibody levels in multiple sclerosis. Brain, 2015, 138, 632-643.

[14] P. C. Cha, H. Zembutsu, A. Takahashi, M. Kubo, N. Kamatani, Y. Nakamura; A genome-wide association study identifies SNP in DCC is associated with gallbladder cancer in the Japanese population. Journal of Human Genetics, 2012, 57 (4), 235-237.

[15] H. J. Lee, H. G. Woo, T. A. Greenwood, D. F. Kripke, J. R. Kelsoe; A genome-wide association study of seasonal pattern mania identifies NF1A as a possible susceptibility gene for bipolar disorder. Journal of Affective Disorders, 2012, 145 (2), 200-207.

[16] S. Tao, Z. Wang, F. C. Hsu, et al.; A genome-wide search for loci interacting with known prostate cancer risk-associated genetic variants. Carcinogenesis, 2012, 33 (3), 598-603.

[17] H. Mbarak, Y. Milaneschi, I. O. Fedko, et al.: The genetics of alcohol dependence: Twin and SNP-based heritability, and genome-wide association study based on AUDIT scores. American Journal of Medical Genetics. Part B, Neuropsychiatric Genetics, 2015, 168 (8), 739.748.

[18] W. C. Chang, Y. Y. Fang, H. W. Chang, L. Y. Chuang, Y. D. Lin, M. F. Hou, and C. H. Yang; Identification association model for single nucleotide polymorphisms of ORAI 1 gene for breast cancer. Cancer Cell International. 2014, 14 (29).

[19] D. Sun, L. Sun, Q. Yu, Y. Gong, H. Wang, J. Yang, and Y. Yuan; SNP-SNP interaction between TLR4 and MyD88 in susceptibility to coronary artery disease in the Chinese Han population. International Jorunal of Environmental Research and Public Health, 2016, 13 (3), 278/1-278/13.

[20] S. S. Verma, J. N. Cooke, A. Lucas, Y. Bradfort, J. G. Linneman, M. A. Hauser, L. R. Pasquale, P. L. Peissig, M. H. Brilliant, and C. A. McCarthy; Epistatic gene-based interaction analysis for glaucoma in eMERGE and NEIGHBOR consortium. PLoS Genetics, 2016, 12 (9), e100618/1-e1006186/21.

[21] C. Dubertret, C. Bardel, N. Ramoz, P. M. Martin, J. C. Deybach, J. Ades, P. Gorwood, and L. Gouya; A genetic schizophrenia-susceptibility region located between the ANKK1 and DRD2 genes. Progress in Neuro-Psychopharmacology and Biological Psychiatry, 2010, 34 (3), 492-499.

[22] H. Y. Lin, E. K. Amankwah, R. S. Tseng, X. Qu, D. T. Chen, and J. Y Park; SNP-SNP interaction network in angiogenesis genes associated with prostate cancer aggressiveness. PloS One, 2013, 8 (4), e59688.

[23] F. Sanger, S. Nicklen, and A. R. Coulson; DNA sequencing with chain-terminating inhibitors. Proceedings of the National Academy of Sciences of the United States of America, 1977, 74 (12), 5463-5467.

[24] S. Anderson; Shotgun DNA sequencing using cloned DNase I-generated fragments. Nucleic Acids Research, 1981, 9 (13), 3015-3027.

[25] W. S. Bush and J. H. Moore; Genome-wide association studies. PLOS Computational Biology, 2012, 8 (12), e1002822.

[26] J. Shendure and H. Ji; Next-generation DNA sequencing. Nature Biotechnology, 2008, 26 (10), 1135-1145.

[27] M. L. Metzker; Sequencing technologies – the next generation. Nature Reviews, 2010, 11, 31-46.

[28] A. N. Desai and A. Jere; Next-generation sequencing: ready for the clinics? Clinical Genetics, 2012, 81, 503-510.

[29] T. Kanagawa; Bias and artifacts in multitemplate polymerase chain reactions. J. Biosci. Bioeng., 2003, 96 (4), 317-323.

[30] E. J. Fox, K. S. Reid-Bayliss, M. J. Emond, and L. A. Loeb; Accuracy of next generation sequencing platforms. Next Generation Sequencing Applications, 2014, 1, doi:10.4172/jngsa.1000106.

[31] P. M. Holland, R. D. Abramson, R. Watron, and D. H. Gelfand; Detection of specific PCR product by utilizing the 5'---3' exonuclease activity of *Themus aquiaticus* DNA polymerase. Proceedings of the National Academy of Sciences, 1991, 88 (16), 7276-7280.

[32] B. M. Venkatesan and R. Bashir; Nanopore sensors for nucleic acid analysis. Nature Nanotechnology, 2011, 6, 615-624.

[33] L. Liu and H. C. Wu; DNA-based nanopore sensing. Angewandte Chemie International Edition, 2016, 55, 15216-15222.

[34] O. Köhler, D. V. Jarikote, and O. Seitz; Forced intercalation probes (FIT Probes): thiazole orange as a fluorescent base in peptide nucleic acids for homogeneous single nucleotide-polymorphism detection. ChemBioChem, 2005, 6, 69-77.

[35] L. Bethge, D. V. Jarikote, and O. Seitz; New cyanine dyes as base surrogates in PNA: forced intercalation probes (FIT-probes) for homogeneous SNP detection. Bioorganic and Medicinal Chemistry, 2008, 16, 114-125.

[36] E. Socher, D. V. Jarikote, A. Knoll, L. Röglin, J. Burmeister, and O. Seitz; FIT probes: peptide nucleic acid probes with fluorescent base surrogate enable real-time DNA quantification and single nucleotide polymorphism discovery. Analytical Biochemistry, 2008, 375, 318-330.

[37] E. Socher, A. Knoll, and O. Seitz; Dual fluorophore PNA FIT-probes – extremely responsive and bright hybridization probes for the sensitive detection of DNA and RNA. Organic and Biomolecular Chemistry, 2012, 10, 7363-7371

[38] F. Hövelmann, I. Gaspar, S. Loibl, E. A. Ermilov, B. Röder, J. Wengel, A. Ephrussi, and O. Seitz; Brightness through local constraint – LNA-enhanced FIT hybridization probes for in vivo ribonucleotide particle tracking. Angewandte Chemie International Edition, 2014, 53, 11370-11375.

[39] V. Karunakaran, J. L. Pérez Lustres, L. Zhao, N. P. Ernsting, and O. Seitz; Large dynamic Stokes shift of DNA intercalation dye thiazole orange has contribution from a high-frequency mode. Journal of the American Chemistry Society, 2006, 128, 2954-2962

[40] S. Tyagi and F. R. Kramer; Molecular beacons: probes that fluoresce upon hybridization. Nature Biotechnology, 1996, 14, 303-308.

[41] A. Tsourkas, M. A. Behlke, S. D. Rose, and G. Bao; Hybridization kinetics and thermodynamics of molecular beacons. Nucleic Acids Research, 2003, 31 (4), 1319-1330.

[42] S. Tyagi, S. A. E. Marras, and F. R. Kramer; Wavelength-shift molecular beacons. Nature Biotechnology, 2000, 18, 1191-1196.

[43] V. M. Farzan, M. L. Markelov, A. Y. Skoblov, G. A. Shipulin, and T. S. Zatsepin; Specificity of SNP detection with molecular beacons is improved by stem and loop separation with spacers. Analyst, 2017, 142 (6), 945-950.

[44] P. Y. Kwok; Methods for genotyping single nucleotide polymorphisms. Annual Review of Genomics and Human Genetics, 2001, 2, 235-258.

[45] R. A. Cardullo, S. Agrawal, C. Flores, P. C. Zamecnik, and D. E. Wolf; Detection of nucleic acid hybridization by nonradiative fluorescence resonance energy transfer. Proceedings of the National Academy of Sciences of the USA. 1988, 85 (23), 8790-8794.

[46] A. A. Marti, C. A. Puckett, K. Dyer, N. Stevens, S. Jockusch, J. Ju, J. K. Barton, and N. J. Turro; Inorganic-organic hybrid luminescent binary probe for DNA detection based on spin-forbidden resonance energy transfer. Journal of the American Chemical Society, 2007, 129, 8680-8681.

[47] D. M. Kolpashchikov; A binary DNA probe for highly specific nucleic acid recognition. Journal of the American Chemical Society, 2006, 128, 10625-10628.

[48] D. M. Kolpashchikov; Split DNA enzyme for visual single nucleotide polymorphism typing. Journal of the American Chemical Society, 2008, 130, 2934-2935.

[49] A. Jiao, J. Zheng, Y. Hu, G. Zhu, J. Li, H. Li, R. Yang, and W. Tan; Hybridization-triggered isothermal signal amplification coupled with MutS for label-free and sensitive fluorescent assay of SNPs; Chem. Communications, 2012, 48, 5659-5661.

[50] H. Wang, J. Li, Y. Wang, J. Jin, R. Yang, K. Wang, and W. Tan; Combination of DNA ligase reaction and gold nanoparticle-quenched fluorescent oligonucleotides: a simple and efficient approach for fluorescent assaying of SNPs. Analytical Chemistry, 2010, 82 (18), 7684-7690.

[51] H. Ji, F. Yan, J. Lei, and G. Ju; Ultrasensitive electrochemical detection of nucleic acids by template enhanced hybridization followed with rolling circle amplification. Analytical Chemistry, 2012, 84 (16), 7166-7171.

[52] U. Landegren, R. Kaiser, J. Sanders, and L. Hood; A ligase-mediated gene detection technique. Science, 1988, 241 (4869), 1077-1080.

[53] W. Cao; Recent developments in ligase-mediated amplification and detection. Trends in Biotechnology, 2004, 22 (1), 38-44.

[54] H. Yang, J. Li, Y. Wang, J. Jin, R. Yang, K. Wang, and W. Tan; Combination of DNA ligase reaction and AU-NP-quenched fluorescent oligonucleotides. Analytical Chemistry, 2010, 82 (18), 7684-7690.

[55] S. Bi, L. Li, and S. Zhang; Triggered polycatenated DNA scaffolds for DNA sensors and aptasensors by combination of rolling circle amplification and DNAzyme amplification. Analytical Chemistry, 2010, 82 (22), 9447-9454.

[56] Y. Q. Cheng, Q. Du, L. Y. Wang, H. L. Jia, and Z. P. Li; Fluorescently cationic conjugated polymer as an indicator of ligase chain reaction for sensitive and homogeneous detection of SNP. Analytical Chemistry, 2012, 84 (8), 3739-3744.

[57] C. J. Wienken, P. Baaske, S. Duhr, and D. Braun; Thermophoretic melting curves quantify the conformation and stability of DNA and DNA. Nucleic Acids Research, 2001, 39 (8), e52.

[58] K. Knez, D. Spasic, K. P. F. Janssen, and J. Lammertyn; Emerging technologies for hybridization based single nucleotide polymorphism detection. Analyst, 2014, 139, 353-370.

[59] T. B. Reed; Induction-coupled plasma torch. J. Appl. Phys, 1961, 32, 821-824.

[60] R. S. Houk, V. A. Fassel, G. D. Fleschm H. J. Svec, A. L. Gray, and C. E. Taylor; Inductively coupled argon plasma as an ion source for mass spectrometric determination of trace elements. Analytical Chemistry, 1980, 52 (14), 2283-2289.

[61] R. Thomas; Practical guide to ICP-MS, CRC Press (Boca Ratón, USA), 2013, 3rd Ed.

[62] S. J. Jiang and R. S. Houk; ICP MS detection for phosphorous and sulfur compounds separated by liquid chromatography. Spectrochimica Acta, 1988, 43B (4/5), 405-411.

[63] P. Tothill, L. M. Matheson, and J. F. Smyth; ICP-MS for the determination of platinum in animal tissue and a comparison with atomic absorption spectrometry. Journal of Analytical Atomic Spectrometry, 1990, 5, 619-622.

[64] J. G. Morrison, D. Bissett, I. F. D. Stephens, K. McKay, R. Brown, M. A. Graham, A. M. Fichtinger-Schepman, and D. J. Kerr; Isolation and identification of cis-diamminedichloroplatinum(II)-DNA adducts by anion exchange HPLC and inductively coupled plasma mass spectrometry. International Journal of Oncology, 1993, 2 (1), 33-37.

[65] A. Bonetti, P. Apostoli, M. Zaninelli, F. Pavanel, M. Colombatti, L. Gian, T. Francheschi, L. Sperotto, and R. Leone; Clinical Cancer Research, 1996, 2 (11), 1829-1835.

[66] W. Meng, F. Weiyue, L. Wenwei, L. Bai, W. Bing, Z. Motao, W. Yun, Y. Huj, Z. Yuliang, and C. Zhifang; Quantitative analysis of proteins via sulfur determination by HPLC coupled to isotope dilution ICPMS with a hexapole collision cell. Analytical Chemistry. 2007, 79 (23), 128-134.

[67] J. Wan, R. S. Houk, D. Dreessen, and R. D. Wiederin; Identification of inorganic elements in proteins in human serum and in DNA fragments by size exclusion chromatography and inductively coupled plasma mass spectrometry with a magnetic sector MS. Journal of the American Chemical Society, 1998, 120 (23), 5793-5799.

[68] M. E. del Castillo-Busto, M. Montes-Bayón, and A. Sanz-Medel; Accurate determination of human serum transferrin isoforms: Exploring metal-specific isotope dilution analysis as a quantitative proteomic tool. Analytical Chemistry, 2006, 78 (24), 218-226.

[69] C. Zhang, F. Wu, Y. Zhang, X. Wang, and X. Zhang; A novel combination of immunoreaction and ICP-MS hypenated technique for the determination of thyroid-stimulating hormone (TSH) in human serum. J. Anal. At. Spectrom., 2001, 16, 1393-1396.

[70] X. Lou, G. Zhang, I. Herrera, R. Kinach, O. Ornatsky, V. Baranov, M. Nitz, and M. A. Winnik; Polymer-based elemental tags for sensitive bioassays. Angewandte Chemie International Edition, 2007, 46 (32), 6111-6114.

[71] S. D. Tanner, O. Ornatsky, D. R. Bandura, and V. I. Baranov; Multiplex bio-assay with inductively coupled plasma mass spectrometry: Towards a massively multivariate single-cell technology. Spectrochimica Acta Part B, 2007, 62, 188-195.

[72] K. S. Smith and H. L. O. Huyck; An overview of the abundance, relative mobility, bioavailability, and human toxicity of metals. Reviews in economic geology, 1999, 6A and 6B, 29-70.

[73] D. Parker, R. S. Dickins, H. Puschmann, C- Crossland, and J. A. K. Howard; Being excited by lanthanide coordination complexes: aqua species, chirality, excited-state chemistry, and exchange dynamics. Chem. Rev., 2002, 102, 1977-2010.

[74] J. C. G. Bünzli; Benefiting from the unique properties of lanthanide ions. Acc. Chem. Res., 2006, 39, 53-61.

[75] R. Ahrends, S. Pieper, A. Kühn, H. Weisshoff, M. Hamester, T. Lindemann, C. Scheler, K. Lehmann, K. Taubner, and M. W. Linscheid; A metal-coded affinity tag approach to quantitative proteomics. Molecular and Cellular Proteomics, 2007, 6, 1907-1916.

[76] D. E. Fernández, C. Cheler, and M. W. Linscheid; Absolute protein quantification by LC-ICP-MS using MeCAT peptide labeling. Anal. Bioanal. Chem., 2011, 401, 657-666.

[77] D. E. Fernández, F. S. Bierkandt, and M. W. Linscheid; MeCAT labeling for absolute quantification of intact proteins using label-specific isotope dilution ICP-MS. J. Anal. At. Spectrom., 2012, 27, 1701-1708.

[78] N. Jakubowski, L. Wänting, H. Hayen, A. Venkatachalam, A. con Bohlen, P. H. Roos, and A. Manz; Labelling of proteins with 2-(4-isothiocyanatobenzyl)-1,4,7,10-tetraazacyclododecane-1,4,7,10-tetraacetic acid and lanthanides and detection by ICP-MS. Journal of Analytical Atomic Spectrometry, 2008, 23 (11), 1497-1507.

[79] A. H. El-Khatib, D. E. Fernández, and M. W. Linscheid; Dual labeling of biomolecules using MeCAT and DOTA derivatives: Application to quantitative proteomics. Anal. Bioanal. Chem., 2012, 403, 2255-2267.

[80] S. Pieper, S. Beck, R. Ahrends, C. Scheler, and M. W. Linscheid; Fragmentation behavior of metal-coded affinity tag (MeCAT)-labeled peptides. Rapid Communications in Mass Spectrometry, 2009, 23, 2045-2052.

[81] G. Schwarz, S. Back, M. G. Weller, and M. W. Linscheid; MeCAT – New iodoacetamide reagents for metal labeling of proteins and peptides. Anal. Bioanal. Chem., 2011, 401, 1203-1209.

[82] M. E. Martin, S. G. Parameswarappa, M. S. O'Dorisio, F. C. Pigge, and M. K. Schultz; A DOTA-peptide conjugate by copper-free click chemistry. Bioordanic and Medicinal Chemistry Letters, 2010, 20, 4805-4870.

[83] A. Merkoci, M. Aldavert, G. Tarrason, R. Eritja, and S. Alegret; Towards an ICPMS-linked DNA assay based on gold nanoparticles immunoconnected through peptide sequences. Analytical Chemistry, 2005, 77 (19), 6500-6503.

[84] S. L. Kerr, and B. Sharp; Nano-particle labeling of nucleic acids for enhanced detection by inductively-coupled plasma mass spectrometry; Chemical Communications, 2007, 43, 4537-4539.

[85] O. I. Ornatsky, X. Lou, M. Nitz, S. Schäfer, W. S. Sheldrick, V. I. Baranov, D. R. Bandura, and S. D. Tanner; Study of cell antigens and intracellular DNA by identification of element-containing labels and metallointercalators using ICP-MS. Analytical Chemistry, 2008, 80, 2539-2547.

[86] G. Han, S. Zhang, Z. Xing, and X. Zhang; Absolute and relative quantification of multiplex DNA assay based on an elemental labeling strategy. Angewandte Chemie International Edition, 2013, 52, 1466-1471.

[87] Y. Lou, X. Yan, Y. Huang, R. Wen, Z. Li, L. Yang, J. C. Yang, and Q. Wang; ICP-MS-based multiplex and ultrasensitive assay of viruses with lanthanide-coded biospecific tagging and amplification strategies. Analytical Chemistry, 2013, 85 (20), 9428-9432.

[88] K. Brückner, K. Schwarz, S. Beck, and M. W. Linscheid; DNA quantification via ICP-MS using lanthanide-labeled probes and ligation-mediated amplification. Analytical Chemistry, 2014, 86, 585-591.

[89] K. Brükner, R. Zitterbart, O. Seitz, S. Beck, and M. W. Linscheid; Solid-phase synthesis of short peptide-based multi-metal tags for biomolecule labeling. Bioconjugate chemistry, 2014, 25 (6), 1069-1077.

[90] S. Zhang, G. Han, Z. Xing, S. Zhang, and X. Zhang; Multiplex DNA assay based on nanoparticle probes by single particle ICP-MS. Analytical Chemistry, 2014, 86, 2541-3547.

[91] P. E. Nielsen, M. Egholm, R. H. Berg, and O. Buchardt; Sequence-selective recognition of DNA by strand displacement with a thymine-substituted polyamide. Science, 1991, 254, 1497-1500.

[92] M. Eghom, O. Buchardt, L. Christensen, C. Behrens, S. M. Freier, D. A. Driver, R. M. Berg, S. K. Kim, B. Norden, and P. E. Nielsen; PNA hybridizes to complementary oligonucleotides obeying the Watson-Crick hydrogen-bonding rules. Nature, 1993, 365, 566-568.

[93] P. E. Nielsen; Structural and biological properties of peptide nucleic acid (PNA). Pure Applied Chemistry, 1998, 70, 105-110.

[94] V. V. Demidov, and M. D. F. Kamenetskii; Two sides of the coin: affinity and specificity of nucleic acid interactions. Trends in Biochemical Sciences, 2004, 29, 62-71.

[95] V. V. Demidov, V. N. Potaman, M.D. F. Kamenetskii, Egholm, O. Buchardt, S. H. Sönnichsen, and P. E. Nielsen; Stability of peptide nucleic acids in human serum and cellular extracts. Biochemical Pharmacology, 1994, 48 (6), 1310-1313.

[96] T. Shiraishi and P. E. Nielsen; Enhanced delivery of cell-penetrating peptide-peptide nucleic acid conjugates by endosomal disruption. Nature Protocols, 2006, 1 (2), 633-636.

[97] S. Hyeon, E. Moroz, B. Castagner, and J. C. Lerouc; Activatable cell penetrating peptide- peptide nucleic acid conjugate via reduction of azobenzene PEG chains. J. Am. Chem. Soc. 2014, 136, 12868-12871.

[98] C. Cordier, F. Boutimah, M. Bourdeloux, F. Dupuy, E. Met, P. Alberti, F. Loll, G. Chassaing, F. Burlina, T. W. Saison-Behmoaras; Delivering of antisense PNA to cells by conjugation with small arginine-rich cell-penetrating peptide (R/W)9. PLOS ONE, 2014, 9 (8), e104999.

[99] O. Vázquez and O. Seitz; Cytotoxic peptide-PNA conjugates obtained by RNA-programmed peptidyl transfer with turnover. Chem. Sci. 2014, 5, 2850-2854.

[100] R. Corradini, S. Sforza, T. Tedeschi, F. Totsingan, A. Manicardi, and R. Marchelli; Peptide nucleic acids with a structurally biased backbone: Updated review and emerging challenges. Current Topics in Medicinal Chemistry, 2011, 11, 1535-1554.

[101] F. Wokciechowski and R. H. E. Hudson; Nucleobase modification in PNA. Current Topics in Medicinal Chemistry, 2007, 7, 667-679.

[102] B. Hyrup, M. Egholm, P. E. Nielsen, P. Wittung, B. Norden, and O. Buchardt; Structure-activity studies of the binding of modified PNA to DNA. Journal of the American Chemical Society, 1994, 116 (18), 7964-7970.

[103] V. A. Kumar, and K. N. Ganesh; Conformationally constrained PNA analogues: Structural evolution towards DNA/RNA binding selectivity. Accounts of Chemical Research. 2005, 38 (5), 404-412.

[104] J. K. Pokorski, M. A. Witschi, B. L. Pumell, and D. H. Appella; (S,S)-trans-cyclopentane-constrained PNA: A general backbone modification that improves binding affinity and sequence specificity. Journal of the American Chemical Society, 2004, 126, 15067-15073.

[105] A. Dragulescu-Andrasi, S. Rapireddy, B. M. Frezza, C. Gayathri, R. R. Gil, and D. H. Ly; A simple gamma-backbone modification preorganizes peptide nucleic acid into a helical structure. Journal of the American Chemical Society, 2006, 128 (31), 10258-10267.

[106] E. A. Englund and D. H. Appella; γ-Substituted peptide nucleic acids constructed from L-Lysine are a versatile scaffold for multifunctional display. Angewandte Chemie International Edition, 2007, 46, 1414-1418

[107] H. Nagahara, A. M. Vocero-Akbani, E. L. Snyder, A. Ho, D. G. Latham, N. A. Lissy, M. Becker-Hapak, S. A. Ezhevsky, and S. F. Dowdy; Transduction of full-length TAT fusion proteins into mammalian cells: TAT-p27Kip1 induces cell migration. Nature Medicine, 1998, 4 (12), 1449-1452.

[108] A. M. Covero-Akbani, N. V. Heyden, N. A. Lissy, L. Ratner, and S. F. Dowdy; Killing HIV-infected cells by transduction with an HIV protease-activated caspase-3 protein. Nature Medicine, 1999, 5 (1), 29-33.

[109] M. Lewin, N. Carlesso, C. H. Tung, X. W. Tang, D. Cory, D. T. David, R. Weissleder; Tat peptide-derivatized magnetic nanoparticles allow in vivo tracking and recovery of progenitor cells. Nature Biotechnology, 2000, 18 (4), 410-414.

[110] P. A. Wender, D. J. Mitchell, K. Pattabiraman, E. T. Pelkey, L. Steinman, and J. B. Rothbard; The design, synthesis, and evaluation of molecules that enable or enhance cellular uptake: peptoid molecular transporters. Proceedings of the National Academy of Sciences of the USA. 2000, 97 (24), 13003-13008.

[111] P. Zhou, M. Wang, L. Du, G. W. Fisher, A. Waggoner, and D. H. Ly; Novel binding and efficient cellular uptake of guanidine-based PNA (GPNA). Journal of the American Chemical Society, 2003, 125, 6878-6879.

[112] B. Sahu, V. Chenna, K. L. Lathrop, S. M. Thomas, G. Zon, K. J. Livak, and D. H. Ly; Synthesis of conformationally preorganized and cell-permeable guanidine-based γ-PNA (γGPNAs). Journal of Organic Chemistry, 2009, 74, 1509-1516.

[113] S. Rapireddy, G. He, R. Subhadeep, A. A. Bruce, and D. H. Ly; Strand invasions of mixed-sequence B-DNA by acridine-linked, γ-PNA. Journal of the American Chemical Society, 2007, 129, 15596-15600.

[114] V. Chenna, S. Rapireddy, B. Sahu, C. Ausin, E. Pedroso, and D. H. Ly; A simple cytosine to G-clamp nucleobase substitution enables chiral γ-PNAs to invade mixed sequence double-helical B-form DNA. ChemBioChem, 2008, 9, 2388-2391.

[115] G. He, S. Rapireddy, R. Bahal, B. Sahu, and D. H. Ly; Strand invasion of extended, mixed-sequence B-DNA by γ-PNAs. Journal of the American Chemical Society, 2009, 131, 12088-12090.

[116] R. Bahal, B. Sahu, S. Rapireddy, C. Lee, and D. H. Ly; Sequence-unrestricted, Watson-Crick recognition of double helical B-DNA by (R)-MiniPEG-γ-PNA. ChemBioChem, 2012, 13, 56-60.

[117] J. M. Goldman, L. A. Zhang, A. Manna, B. A. Armitage, D. H. Ly, and J. W. Schneider; High affinity γ-PNA sandwich hybridization assay for rapid detection of short nucleic acid targets with single mismatch discrimination. Biomacromolecules, 2013, 14, 2253-2261.

[118] P. L. Ross, K. Lee, and P. Belgrader; Discrimination of SNPs in human DNA using PNA probes detected by MALDI-TOF-MS. Analytical Chemistry, 1997, 69, 4197-4202.

[119] B.Boontha, J. Nakkuntod, N. Hirankarn, P. Chaumplunk, and T. Vilaivan. Multiplex mass spectrometric genotyping of single nucleotide polymorphisms employing pyrrolidinyl peptide nucleic acid in combination with ion-exchange capture. Analytical chemistry, 2008, 80, 8178-8186.

[120] S. Ye, X. Liang, Y. Yamamoto, and M. Komiyama; DNA protection by PNA from enzymatic digestion for MS genotyping. Chemistry Letters, 2003, 32 (1), 10-11.

[121] B. Ren, J. M. Zhou, and M. Komiyama; Straightforward detection of SNPs in double stranded DNA by using exonuclease III/nuclease S1/PNA system. Nucleic Acids Research, 2004, 32 (4), e42.

[122] F. R. Bowler, P. A. Reid, A. C. Boyd, J. J. Diaz-Mochon, and M. Bradley; Dynamic chemistry for enzyme-free allele discrimination in genotyping by MALDI-TOF MS. Analytical Methods, 2011, 3, 1656-1663.

[123] N. Hüsken, M. Gebala, W. Schuhmann, and N. Metzler-Nolte; A single-electrode, dual-potential ferrocene-PNA biosensor for the detection of DNA. Chembiochem, 2010, 11, 1754-1761.

[124] X. Luo and I.-M. Hsing; Immobilization-free multiplex electrochemical DNA and SNP detection. Biosensors and Bioelectronics, 2009, 25, 803-808.

[125] B. S. Gaylord, M. R. Massie, S. C. Feinstein, and G. C. Bazan; SNP detection using PNA probes and conjugated polymers: Applications in neurodegenerative disease identification. PNAS, 2005, 102 (1), 34-39.

[126] S. Kummer, A. Knoll, E. Socher, L. Bethge, A. Hermann, and O. Seitz; Fluorescence imaging of influenza H1N1 mRNA in living infected cells using single-chromophore FIT-PNA. Angewandte Chemie International Edition, 2011, 50, 1931-1934.

[127] N. Kolevzon, D. Hashoul, S. Naik, A. Rubinstein, and E. Yavin; Single point mutation detection in living cancer cells by far-red emitting PNA-FIT probes. Chemistry Communications, 2016, 52, 2405-2407.

[128] H. Shi, F. Yang, W. Li, W. Zhao, K. Nie, B. Dong, and Z. Liu; Fabrication, detections and applications of PNA microarrays. Biosensors and Bioelectronics, 2015, 66, 481-489.

[129] F. Yang, B. Dong, K. Nie, H. Shi, Y. Wu, H. Wang, and Z. Liu; Light-directed synthesis of high-density PNA microarrays. ACS Combinatorial Science, 2015, 17, 608-614.

[130] Y. Wu, F. Yang, H. Wang, J. Liu, and Z. Liu; PNA patterning by an automated microarray synthesis system through photolithography. Journal of Nanoscience and Nanotechnology, 2013, 13 (3), 2061-2067.

[131] P. Rashatasakhon, K. Vongnam, W. Siripornnoppakhun, T. Vilaivan, and M. Sukwattanasinitt; FRET detection of DNA sequence via electrostatic interaction of polycationic phenyleneethynylene dendrimer with DNA/PNA hybrid. Talanta, 2012, 88, 593-598.

[132] J. Choi, C. Kim, and H. Park; PNA-based array for detecting and genotyping human papillomaviruses. Journal of Clinical Microbiology, 2009, 47 (6), 1785-1790.

[133] F. Bowler, P. Reid, C. Boyd, J. Diaz-Mochon, M. Bradley; Dynamic chemistry for enzyme-free allele discrimination in genotyping by MALDI-TOF MS. Analytical Methods, 2011, 3 (7), 1656-1663.

[134] A. Germini, S. Rossi, A. Zanetti, R. Corradini, C. Fogher, and R. Marchelli; Development of a PNA array platform for the detection of GMOs in food. Agricultural and Food Chemistry, 2005, 53, 3958-3962.

[135] T. Tedeschi, A. Calabretta, M. Bencivenni, A. Manicardi, G. Corrado, M. Caramante, R. Corradini, R. Rao, S. Sforza, R. Marchelli; A PNA microarray for tomato genotyping. Molecular BioSystems, 2011, 7, 1902-1907.

[136] J. Lee, K. Bang, J. Choi, J. Chung, J. Lee, I. Jo, A. Seo, Y. Kim, O. Kim, and S. Cha; Development of PNA microarray for identification of *Panax* species based on the nuclear ribosomal internal transcribed spacer and 5.8S rDNA regions. Genes and Genomics, 2010, 32, 463-468.

[137] C. Pilarsky, L. K. Nanduri, and J. Roy; Gene expression analysis in the age of mass sequencing: an introduction. Cancer Gene Profiling. Methods in Molecular Biology, 2016, 1381, Humana Press, New York (USA).

[138] P. E. Dawson, T. W. Muir, I. C. Lewis, S. B. H. Kent; Synthesis of proteins by native chemical ligation. Science, 1994, 244.

[139] A. Mattes and O. Seitz; Sequence fidelity of a template-directed PNA-ligation reaction. Chemical Communications, 2001, 2050-2051.

[140] S. Ficht, C. Dose, and O. Seitz; As fast and selective as enzymatic ligations: unpaired nucleobases increase the selectivity of DNA-controlled native chemical PNA ligation. ChemBioChem, 2005, 6, 2098-2103.

[141] S. Ficht, A. Mattes, and O. Seitz; Single-nucleotide-specific PNA-peptide ligation on synthetic and PCR DNA templates. Journal of the American Chemical Society, 2004, 126, 9970-9981.

[142] C. Dose, S. Ficht, and O. Seitz; Reducing product inhibition in DNA-template-controlled ligation reactions. Angewandte Chemie International Edition, 2006, 45, 5369-5373.

[143] B. Hyrup, M. Egholm, P. E. Nielsen, P. Wittung, B. Nordén, and O. Buchardt; Structure-activity studies of the binding of modified PNA to DNA. Journal of the American Chemical Society, 1994, 116, 7964-7970.

[144] T. N. Grossmann and O. Seitz; DNA-Catalyzed transfer of a reporter group. Journal of the American Chemical Society, 2006, 128, 15596-15597.

[145] J. Michaelis, A. Maruyama, and O. Seitz; Promoting strand exchange in a DNA-templated transfer reaction. Chemical Communications, 2013, 49, 618-620.

[146] T. N. Grossmann. L. Röglin, and O. Seitz; Target-catalyzed transfer reactions for the amplified detection of RNA. Angewandte Chemie International Edition, 2008, 47, 7119-7122.

[147] A. Erben, T. N. Grossmann, and O. Seitz; DNA-triggered synthesis and bioactivity of proapoptotic peptides. Angewandte Chemie International Edition, 2011, 50 (12), 2828-2832.

[148] A. Shibata, T. Uzawa, Y. Nakashima, M. Ito, Y. Nakano, S. Shuto, Y. Ito, and H. Abe; Very rapid DNA-templated reaction for efficient signal amplification and its steady-state kinetic analysis of the turnover cycle. Journal of the American Chemical Society, 2013, 135 (38), 14172-14178.

[149] X. H. Chen, A. Roloff, and O. Seitz; Consecutive signal amplification for DNA detection based on de novo fluorophore synthesis and host-guest chemistry. Angewandte Chemie International Edition, 2012, 51 (18), 4479-4483.

[150] Atdbio oligo-calculator tool website: http://www.atdbio.com/tools/oligo-calculator (active on April 26, 2017).

[151] Z. Balanthy; An improved preparation of n-benzyloxycarbonyl-L-lysine methyl ester hydrochloride. Oppi Briefs, Vol. 23, No. 3, P. 375-376, 1991.

[152] O. Keller, W. E. Keller, G. Van Look, and G. Wersin; tert-Butoxycarbonylation of amino acids in their derivates: N-tert-butoxycarbonyl-1-phenilalanine. Organic Synthesis, Vol. 63, P.160, 1990.

[153] J. Wang, M. Ledeboer, A. Pierce; US2006/18276/A1,2006, 2006.

[154] Yakovchuck, E. Protozanova, and M. D. F. Kamenetskii; Base-stacking and base-pairing contributions into thermal stability of the DNA double helix. Nucleic Acids Research, 2006, 34 (2), 564-574.

[155] K. J. Breslauer, R. Frank, H. Blöcker, and L. A. Marky; Predicting DNA duplex stability from the base sequence. Proc. Natl. Acad. Sci. USA, 1986, 83, 3746-3750.

[156] M. A. de Muro; Medical Biomethods Handbook: probe design, production, and applications. Humana Press, Totowa (USA)

[157] Q. Liu, D. J. Segal, J. B. Ghiara, and C. F. Barbas; Design of polydactyl zinc-finger proteins for unique addressing within complex genomes. PNAS, 1997, 94 (11), 5525-5530.

[158] A. P. Silverman and E. T. Kool; Detecting RNA and DNA with templated chemical reactions. Chemistry Reviews, 2006, 106 (9), 3775-3789.

[159] A. Wittinghofer and H. Waldmann; Ras-a molecular switch involved in tumor formation. Angewandte Chemie International Eddition, 200, 39 (23), 4192-4214.

[160] I. A. Prior, P. D. Lewis, and C. Mattos; A comprehensive survey of Ras mutation in cancer. Cancer research, 2012, 72 (10), 2457-2467.

[161] T. M. Annesley; Ion suppression in mass spectrometry. Clinical Chemistry, 2003, 1041-1044.

[162] L. W. McDonald, J. A. Campbell, S. B. Clark; Failure of ESI to represent metal-complex solution composition: a study of lanthanide-carboxylate complexes. Analytical chemistry, 2014, 86, 1023-1029.

[163] C. W. Tornøe, C. Christensen, and M. Meldal; Peptidotriazoles on solid phase: [1,2,3]-triazoles by regiospecific copper(I)-catalized 1,3-dipolar cycloadditions of terminal alkynes to azides. J. Org. Chem. 2002, 67, 3057-3064.

[164] A. Dirksen and P. E. Dawson; Rapid oxime and hydrazine ligations with aromatic aldehydes for biomolecular labeling. Bioconjugate Chem. 2008, 19, 2543-2548.

[165] J. N. Rybak, S. B. Scheurer, D. Neri, and G. Elia; Purification of biotinylated proteins on streptavidin resin: a protocol for quantitative elution. Proteomics, 2004, 4, 2296-2299.

[166] C. Siethoff, I. Feldmann, N. Jakubowski, and M. Linscheid; Quantitative determination of DNA adducts using liquid chromatography/electrospray ionization mass spectrometry and liquid chromatography/high-resolution inductively coupled plasma mass spectrometry. Journal of mass spectrometry. 1999, 34, 421-426.

[167] C. L. Camp, B. L. Sharp, H. J. Reid, J. Entwisle, and H. Goenaga-Infante; Analysis of mono-phosphate nucleotides as a potential method for quantification of DNA using high performance liquid chromatography-inductively coupled plasma-mass spectrometry. Anal Bioanal Chem, 2012, 402, 367-372.

[168] O. Leclerc, P. Fraisse, G. Labarraque, C. Oster, J. Pichaut, M. Baume, S. Jarraud, P. Fisicaro, S. Vaslin-Reimann; Method development for genomic *Legionella pneumophila* DNA quantification by ICP-MS. Analytical Biochemistry, 2013, 435, 153-158.

[169] S. Fujii, K. Inagaki, S. Miyashika, K. Nagasawa, K. Chiba, and A. Takatsu; A coupling system of capillary gel electrophoresis with ICP-MS for the determination of double stranded DNA fragments. Metallomics, 2013, 5, 424-428.

[170] T. C. de Bang, P. Shah, S. K. Cho, S. W. Yang, S. Husted; Multiplexed microRNA detection using lanthanide-labeled DNA probes and LA-ICP-MS. Analytical Chemistry, 2014, 86, 6823-6826.

[171] Y. He, D. Chen, M. Li, L. Fang, W. Yang, L. Xu, F. Fu; Rolling circle amplification combined with gold nanoparticles-tag for ultra-sensitive and specific quantification of DNA by inductively coupled plasma mass spectrometry. Biosensors and Bioelectronics, 2014, 58, 209-213.

[172] C. Deng, C. Zhang, H. Tang, and J. Jiang; ICP-MS DNA assay based on lanthanide labels and hybridization chain reaction amplification. Analytical Methods, 2016, 7, 5767-5771.

[173] G. Han, Z. Wing, Y. Dong, S. Zhang, and X. Zhang; One-step homogeneous DNA assay with single-nanoparticle detection. Angewandte Chemie International Edition, 2011, 50, 3462-3465.

[174] R. Norton, M. Heuzenroeder, P. A. Manning; Non-specific serum binding to streptavidin in a biotinylated peptide based enzyme immunoassay. J. Immunoassay, 1996, 17 (3), 195-204.

[175] P. E. Nielsen and M. Egholm; PNA: protocols and applications. Horizon Scientific Press, Norfolk (United Kingdom).

[176] B. Sahu, V. Chenna, K. L. Lathrop, S. M. Thomas, G. Zon, K. J. Livka, and D. H. Ly; Synthesis of conformationally preorganized and cell-permeable guanidine-based γ-PNA. Journal of Organic Chemistry, 2009, 74, 1509-1516.

[177] P. Zhou, M. Wang, L. Du, G. W. Fischer, A. Waggoner, and D. H. Ly; Novel binding and efficient cellular uptake of guanidine-based peptide nucleic acids. J. Am. Chem. Soc., 2003, 125, 6878-6879.

[178] A. Mattes and O. Seitz; Mass-spectrometric monitoring of a PNA-based ligation reaction for the multiplex detection of DNA single-nucleotide polymorphisms. Angewandte Chemie International Edition, 2001, 40 (17), 3178-3181.

[179] L. Wick, J. Rouillard, T. Whittam, E. Gulari, J. Tiedje and S. A. Hashsham; On-chip non-equilibrium dissociation curves and dissociation rate constants as methods to assess specificity of oligonucleotide probes. Nucleic Acids Research, 2006, 34 (3), e26.

[180] T. Naiser, O. Ehler, J. Kayser, T. Mai, W. Michel, and A. Ott; Impact of point-mutations on the hybriditation affinity of surface-bound DNA/DNA and RNA/DNA oligonucleotide-duplexes: Comparison of single base mismatches and base bulges. BMC Biotechnology, 2008, 8 (48).

[181] N. Payret, P. A. Seneviratne, H. T. Allawi, and J. SantaLucia; Nearest-Neighbor Thermodynamics and NMR of DNA internal A-A, C-C, G-G, and T-T mismatches; Biochemistry, 1999, 38 (12), 3468-3477.

[182] S. Ikuta, K. Takagi, R. B. Wallace, and K. Itakura; Dissociation kinetics of 19 base paired oligonucleotide-DNA duplexes containing different single mismatched base pairs. Nucleic Acids Research, 1986, 15 (2), 797-811.

[183] H. Binder, M. Fasold, and T. Glomb; Mismatch and G-Stack modulated probe signals on SNP microarrays. PLOS One, 2009, 4 (11), e7862.

[184] G. M. Petersen, L. Amundadottir, C. S. Fuchs, P. Kraft, et al.; A genome-wide association study identifies pancreatic cancer susceptibility loci on chromosomes 13q22.1, 1q32.1, and 5p13.33. Nature genetics, 2010, 42 (3), 224-228.

7.2. Additional Figures

7.2.1. Characterization of synthesized probes

A1 **H_2N -Gly gac atc c Cys- NH_2**

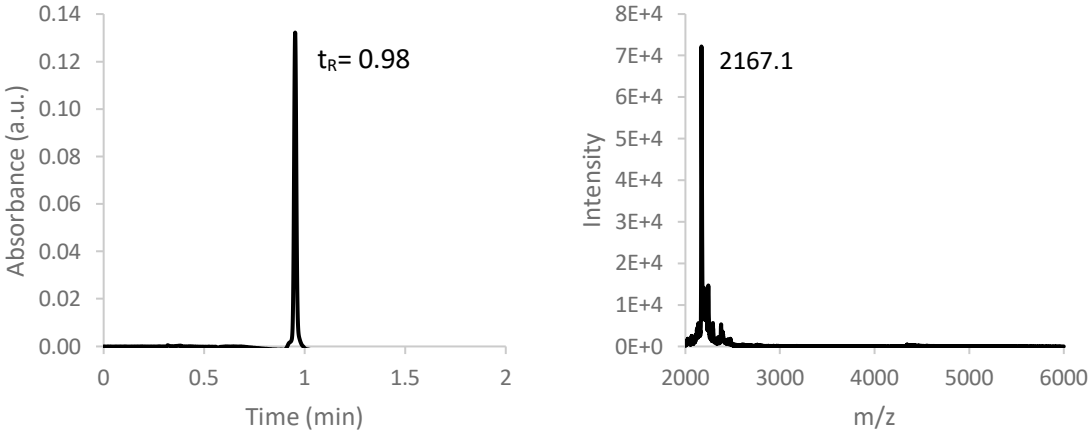

A2 **H_2N - Gly Lys(Biotin) gac atc c Cys - NH_2**

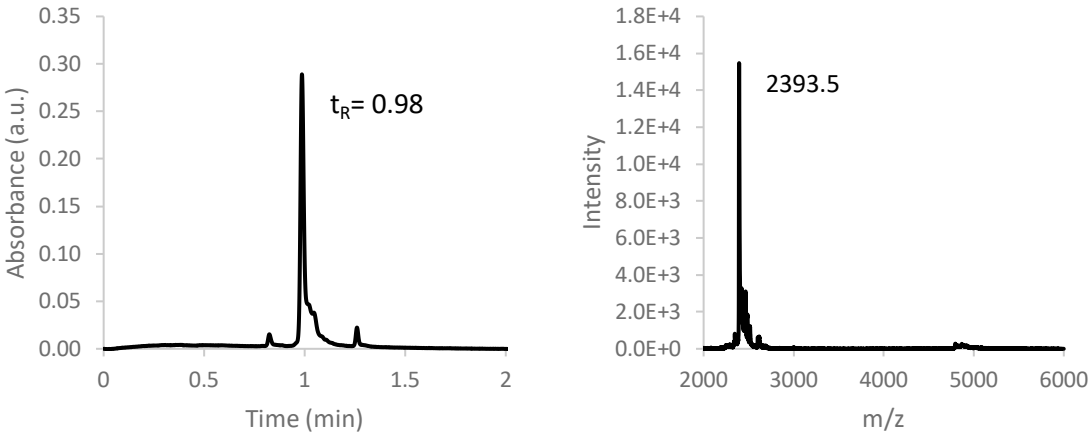

A3 **H_2N - Gly Lys(Biotin) cc gcg aca tcc Cys- NH_2**

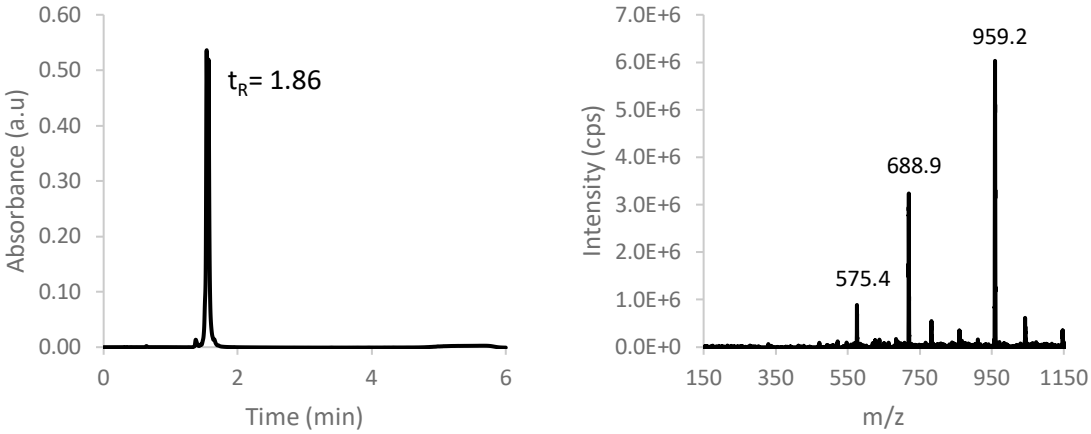

A4 **H_2N - Gly Lys(Biotin) Lys cc gcg aca t*cc Cys - NH_2**

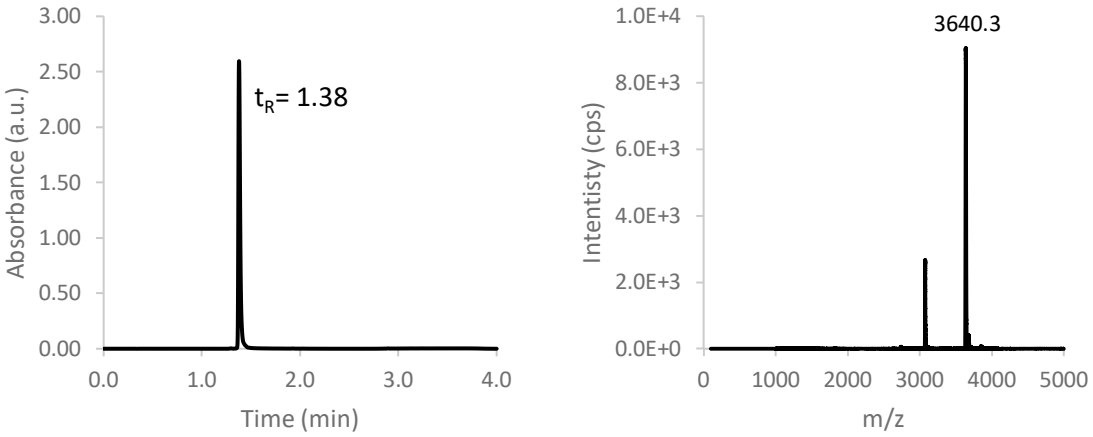

A5 **H_2N - Gly Lys(Biotin) Lys ccg cga cat cc Cys - NH_2**

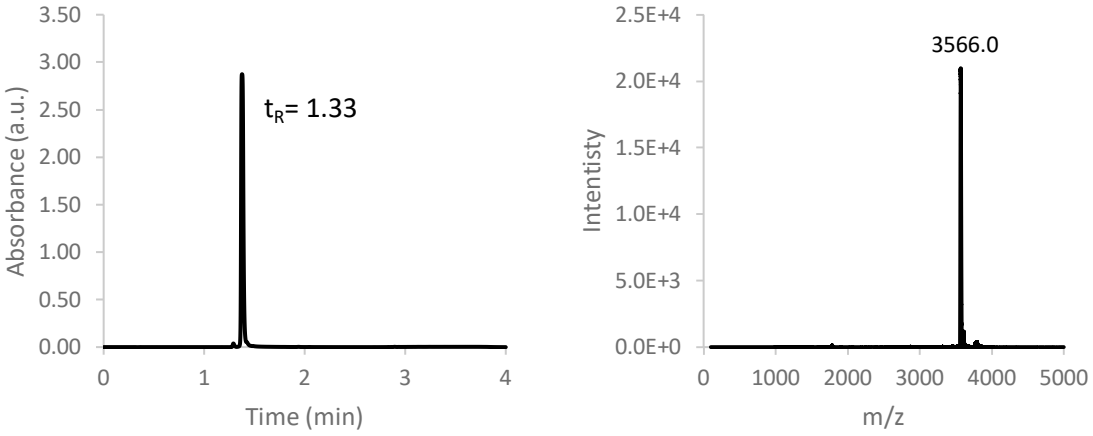

A6 **H_2N - Gly Lys(Biotin) Lys ctg gta ggt cg Cys - NH_2**

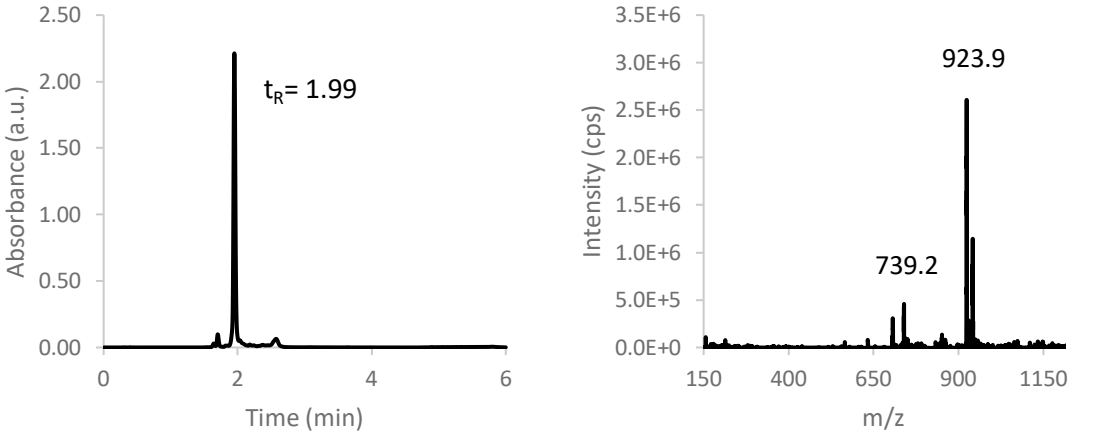

A7 **H_2N - Gly Lys(Biotin) Lys aac acc tac tc Cys - NH_2**

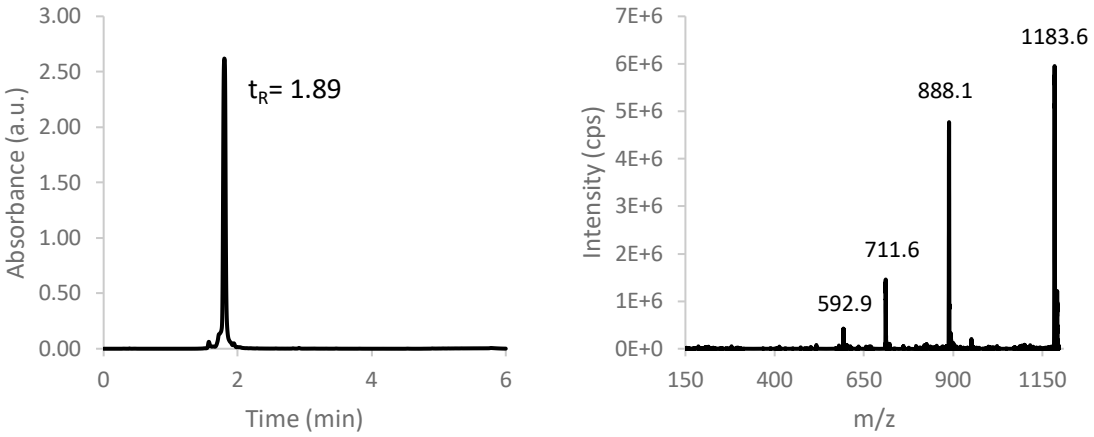

A8 **H_2N - Gly Lys(Biotin) Lys tct cct gag ga Cys - NH_2**

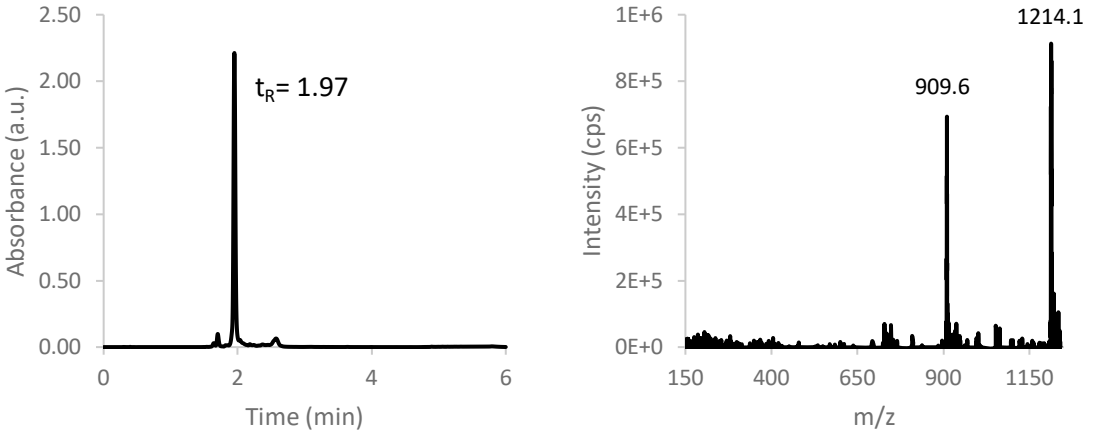

A9 **NH_2 – Gly Lys(Biotin) Lys cga cgt gaa ga Cys-NH_2**

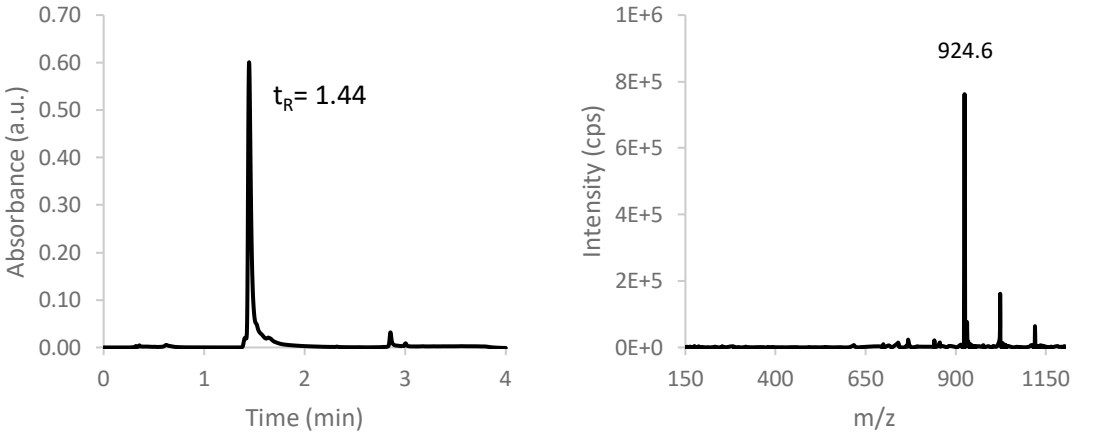

A10 **NH_2 – Gly Lys(Biotin) Lys gga act acc cct Cys-NH_2**

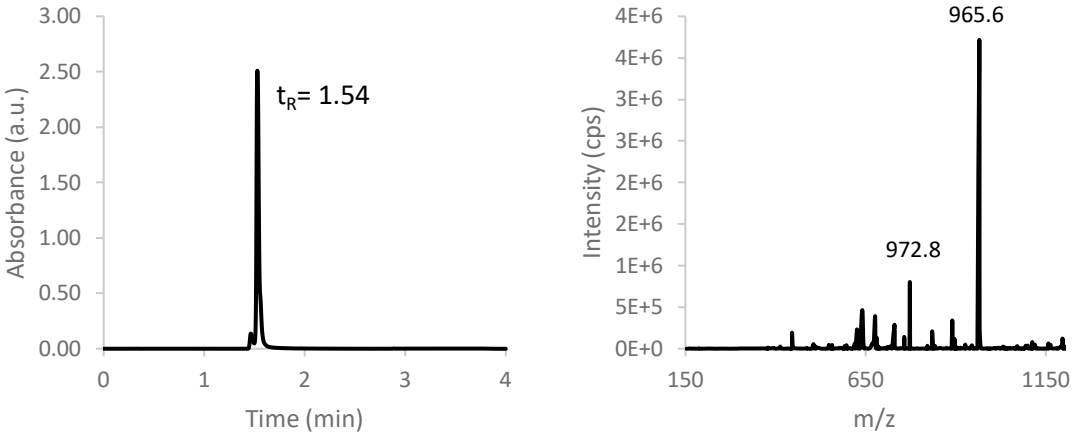

A11 **NH_2 – Gly Lys(Biotin) Lys cta cca cga ctt Cys-NH_2**

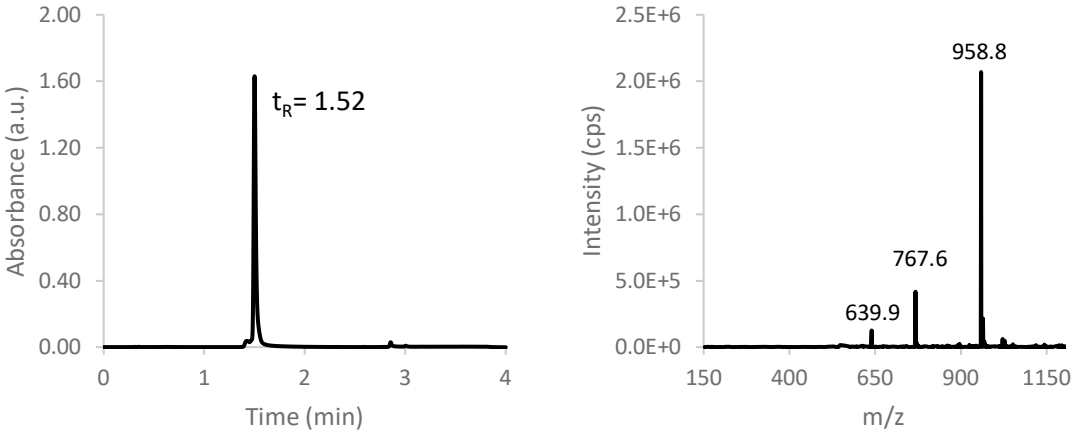

A12 **NH_2 – Gly Lys(Biotin) Lys aga tag tac tgt ga Cys-NH_2**

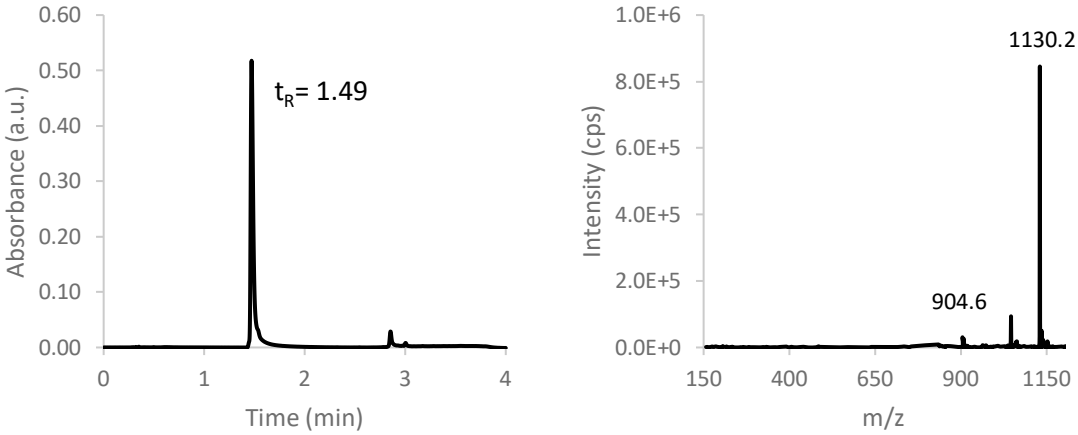

A13 **NH_2 – Gly Lys(Biotin) Lys tta tat ctc ttt tc Cys-NH_2**

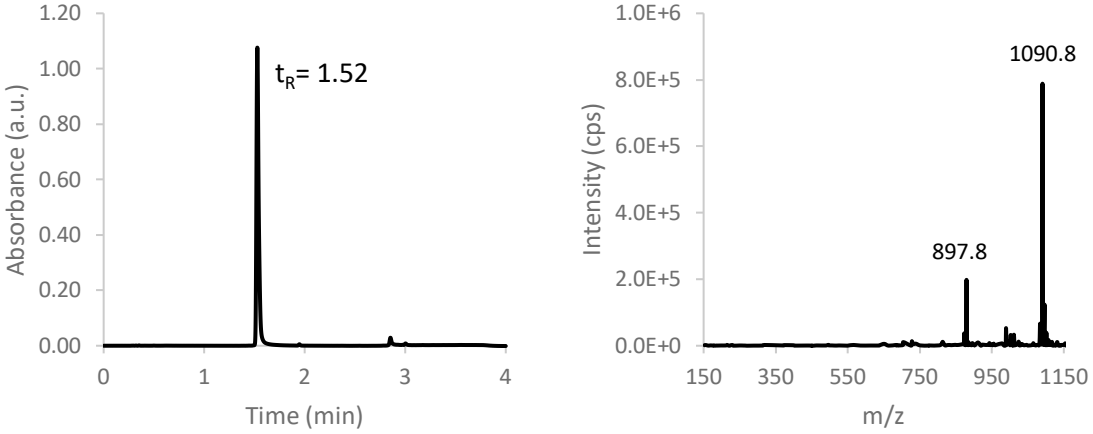

A14 **NH_2 – Gly Lys(Biotin) Lys ctt tgg tta tct ga Cys-NH_2**

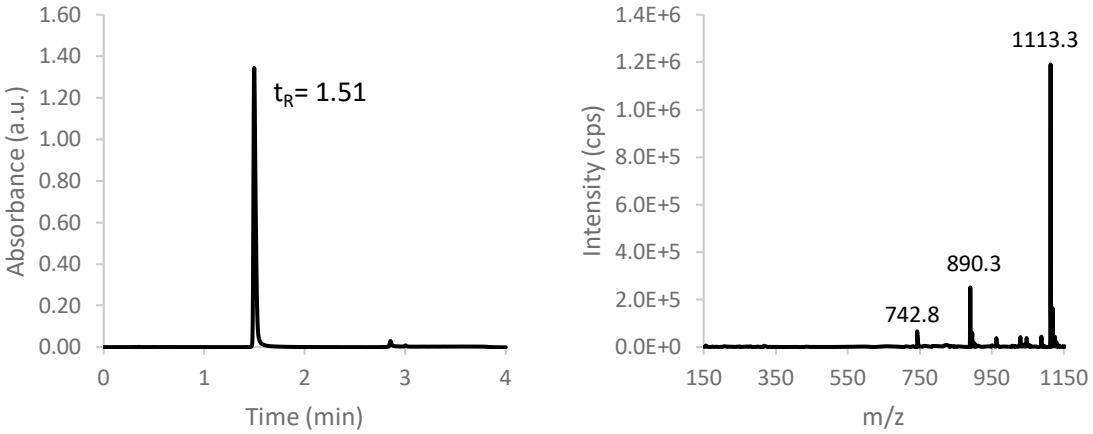

7.2.2. Donor probes

D1 **H_2N-Gly $OC(CH_2)_2$ S Gly cac ccc tt DOTA(Ho^{+3})**

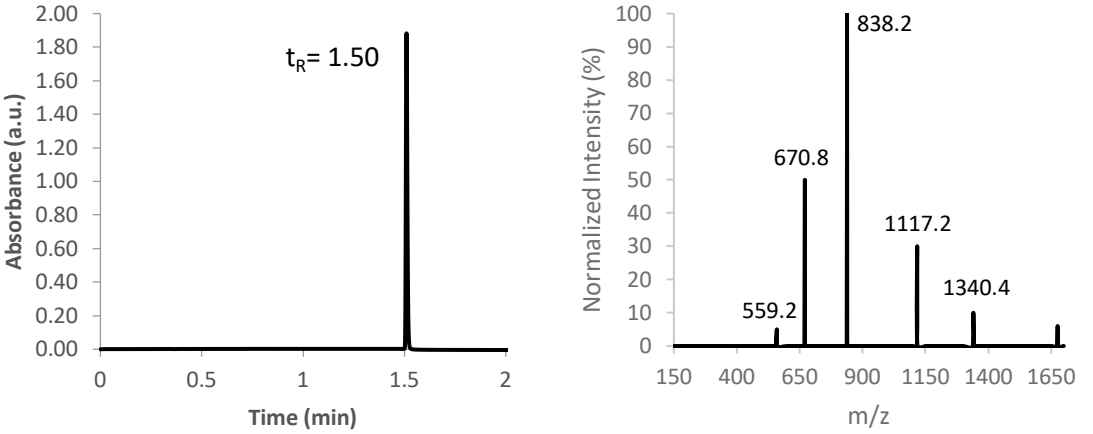

D2 **H_2N - Cys[Gly DOTA(Ho^{3+})] cac ccc tt - Ac**

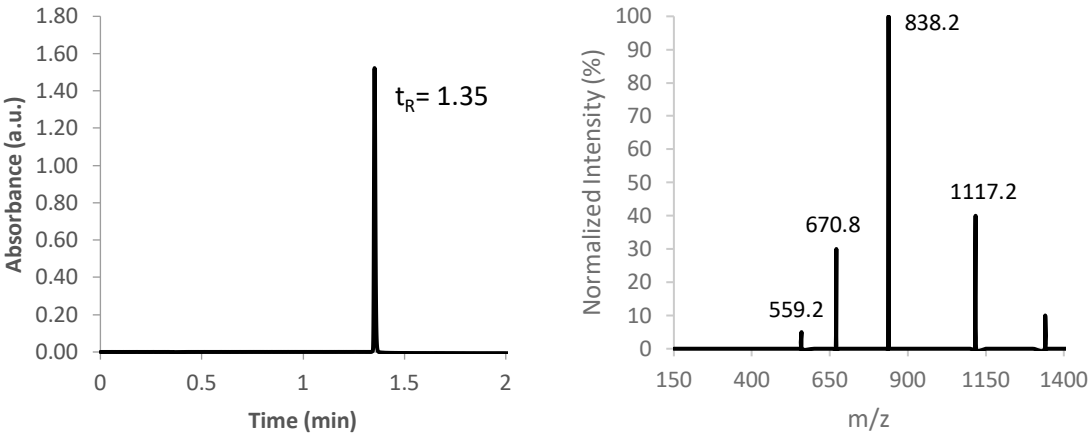

D3 **H_2N-Gly $OC(CH_2)_2$ S Gly cac ccc ttc tca DOTA(Ho^{+3})**

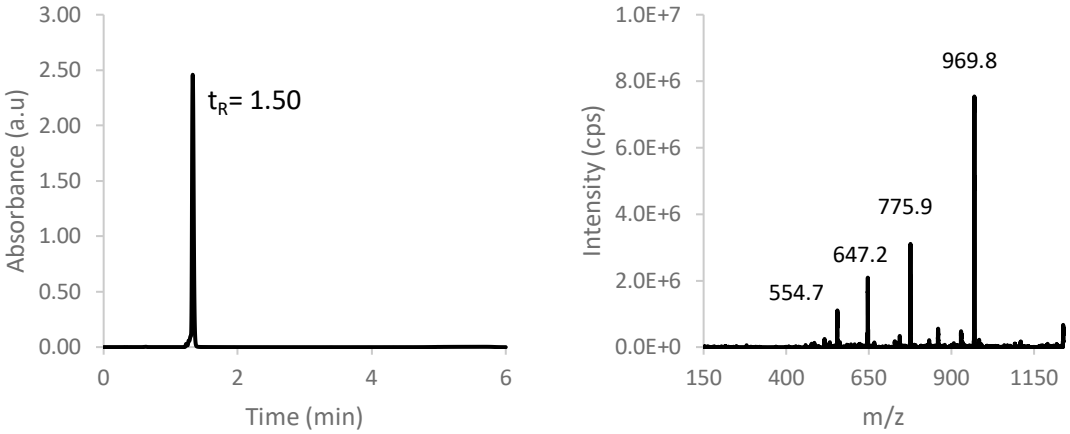

D4 **H_2N-Gly $OC(CH_2)_2$ S Gly cac ccc ttc* tc*a Lys DOTA(Ho^{+3})**

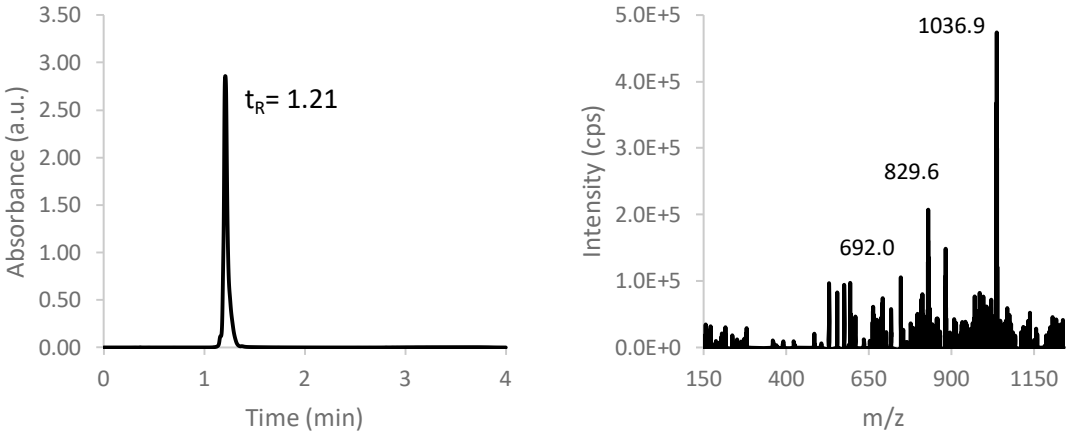

D5 **H_2N-Gly $OC(CH_2)_2$ S Gly cac ccc ttc tca Lys DOTA(Ho^{+3})**

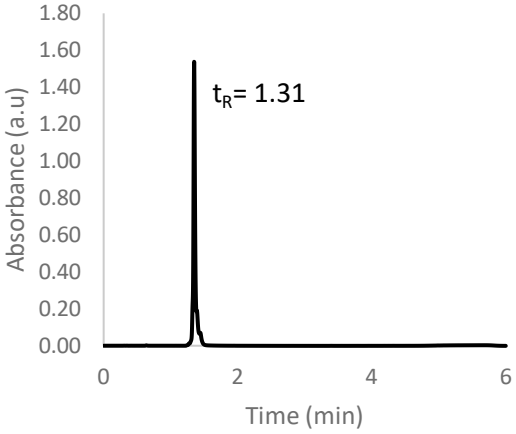

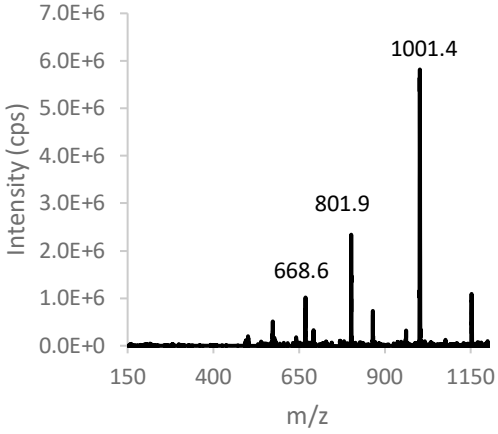

D6 **H_2N - Gly $OC(CH_2)_2$ S Gly ata ggt ctt ggt Lys DOTA(Tb^{+3})**

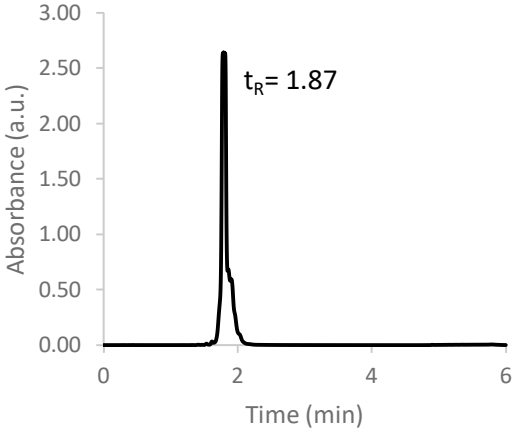

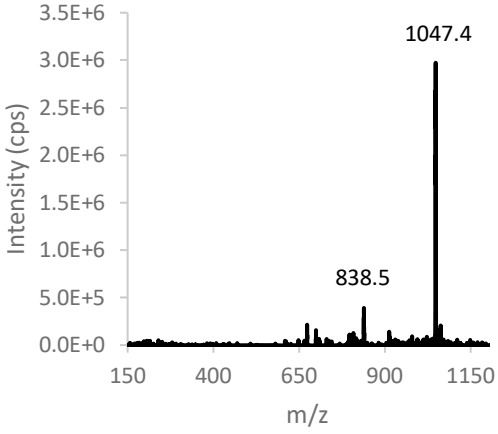

D7 **H_2N - Gly $OC(CH_2)_2$ S Gly tgc tgg ggt gg Lys DOTA(Tm^{+3})**

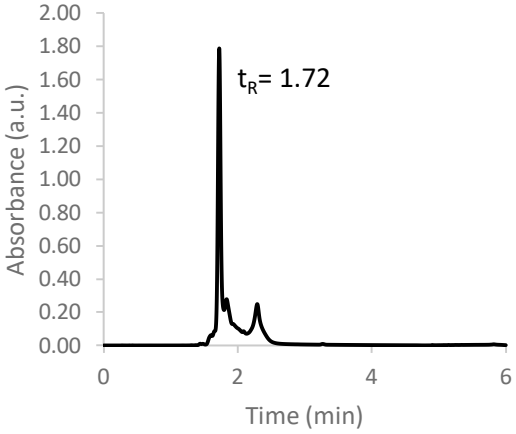

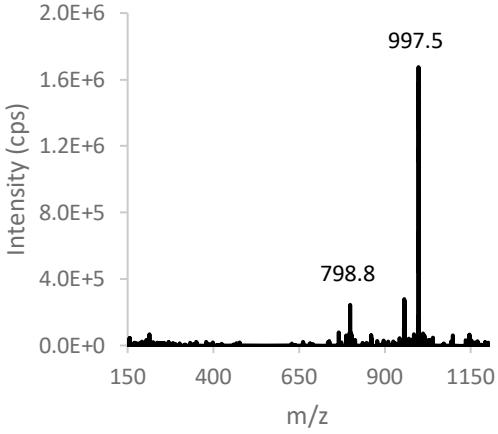

D8 **H_2N - Gly $OC(CH_2)_2$ S Gly ggc ctt cgt tc Lys DOTA(Lu^{+3})**

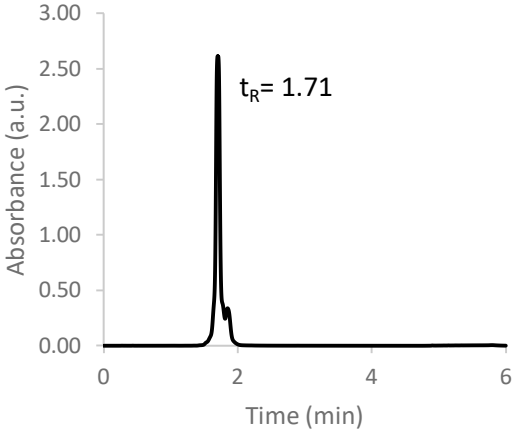

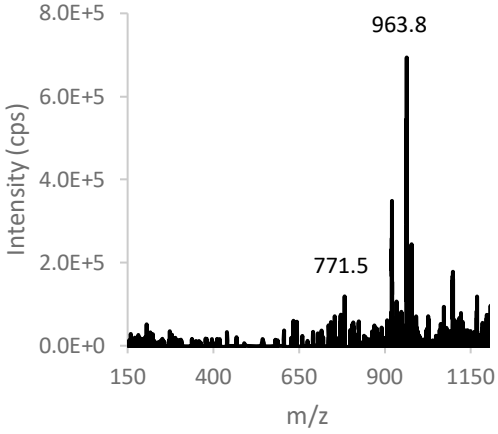

D9 **NH_2 – Gly $OC(CH_2)_2$S Gly agt gtg gac acc Lys DOTA (Tb^{+3})**

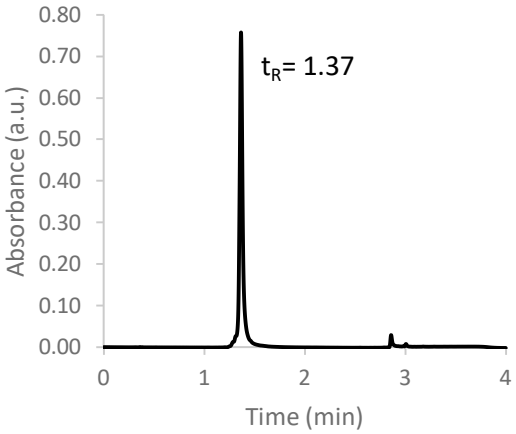

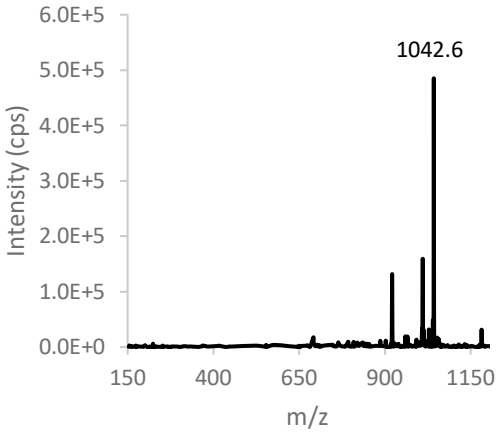

D10 **NH_2 – Gly $OC(CH_2)_2$S Gly ccc cgg gat ca Lys DOTA (Ho^{+3})**

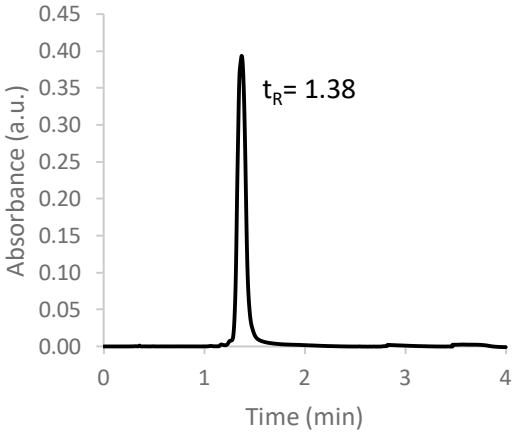

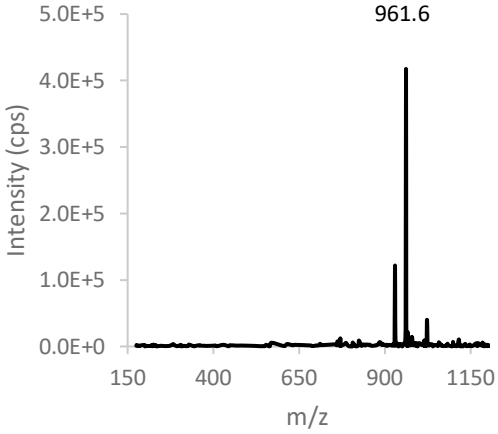

D11 **NH_2 – Gly $OC(CH_2)_2S$ Gly gat agt gaa tca ga Lys DOTA (Tm^{+3})**

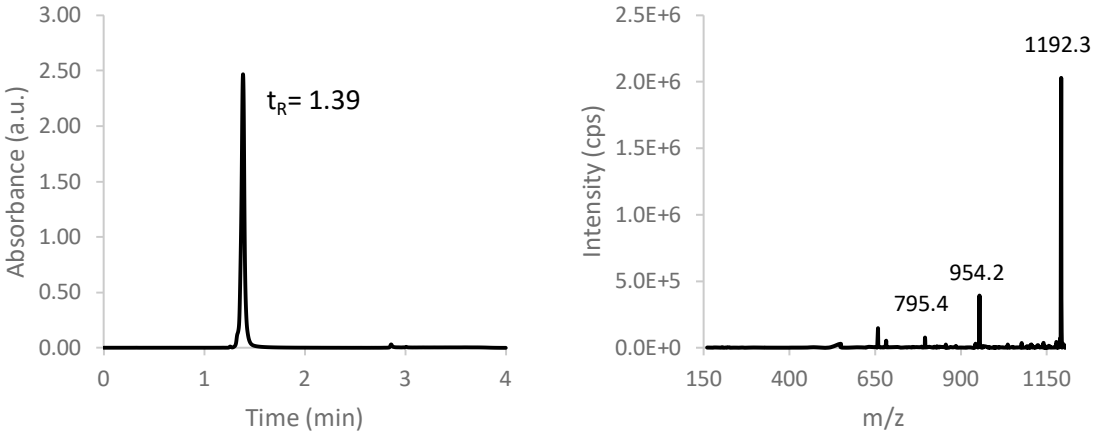

D12 **NH_2 – Gly $OC(CH_2)_2S$ Gly tta gat ggc agg Lys DOTA (Pr^{+3})**

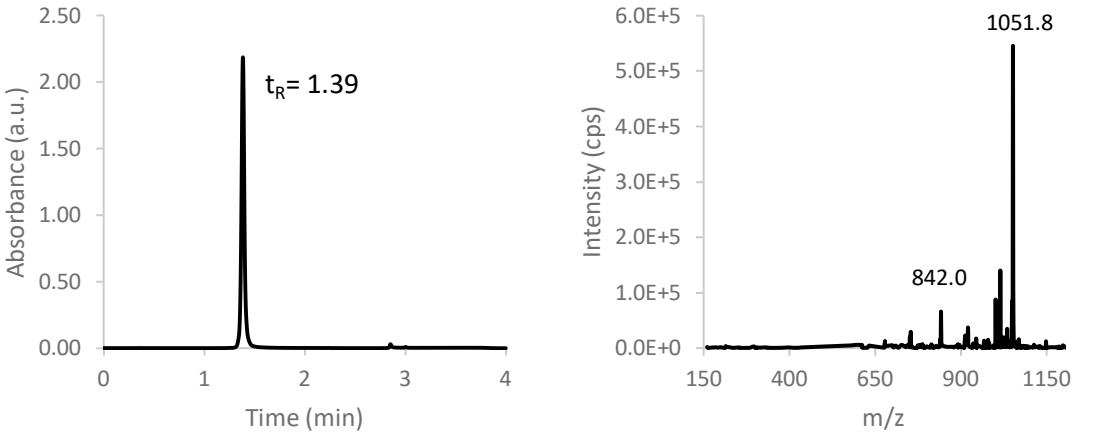

D13 **NH_2 – Gly $OC(CH_2)_2S$ Gly gtc aat gta atg tc Lys DOTA (Gd^{+3})**

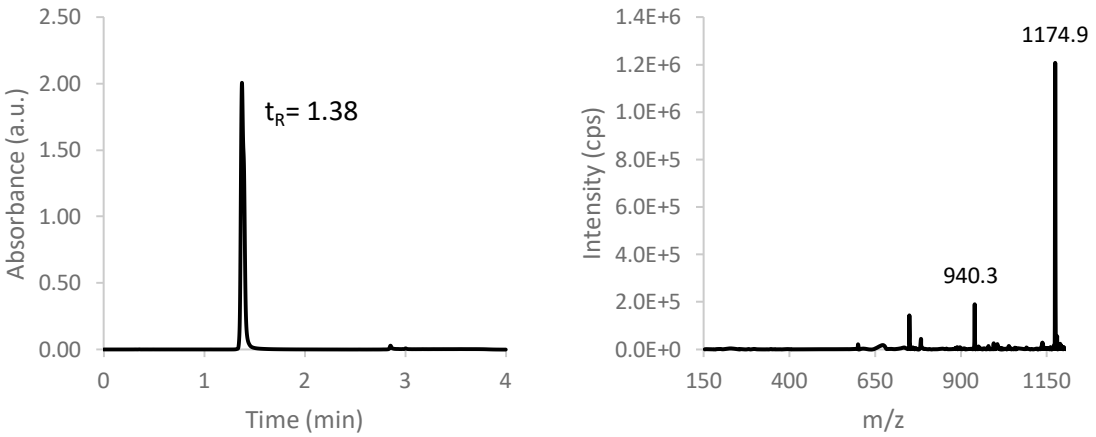

D14 **NH_2 – Gly $OC(CH_2)_2S$ Gly acc gaa aac ga Lys DOTA (Dy^{+3})**

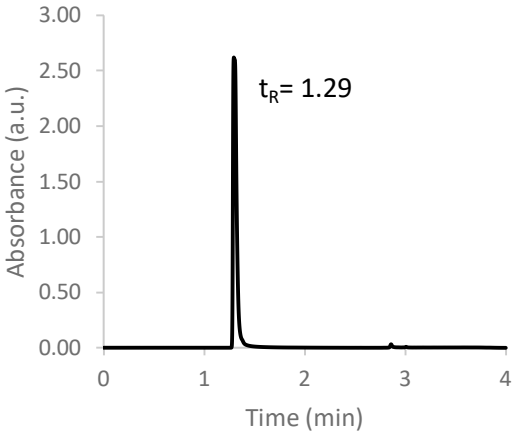

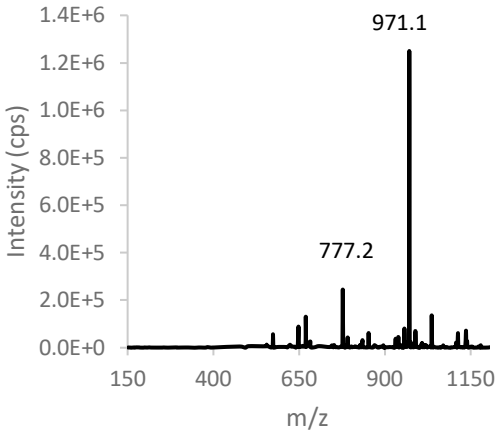

D16 **H_2N-Gly $OC(CH_2)_2$ S Gly cac ccc ttc tca Lys-NH_2**

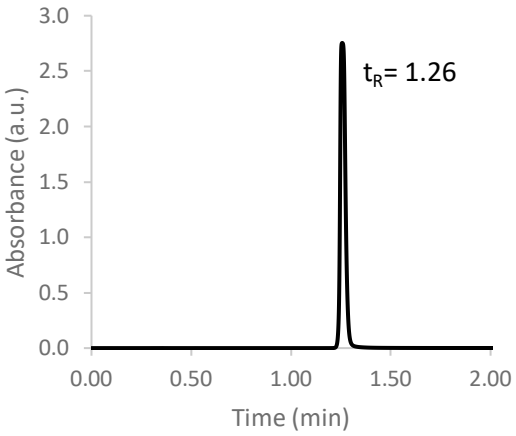

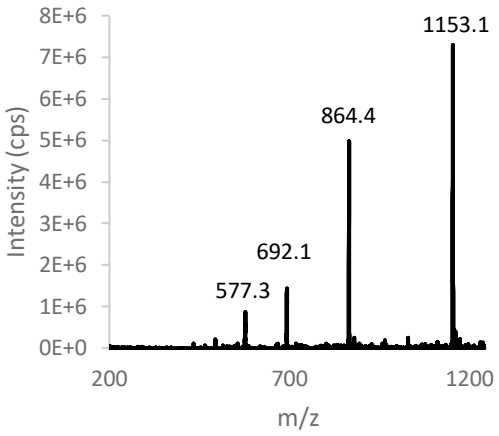

P1 **H_2N - Gly Lys(Biotin) gac ctc c Cys Gly cac ccc ttc t DOTA(Ho^{+3})**

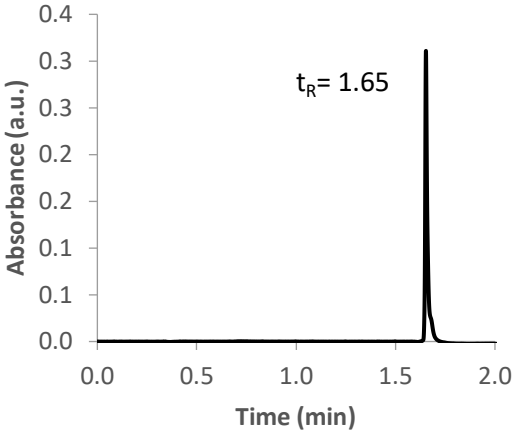

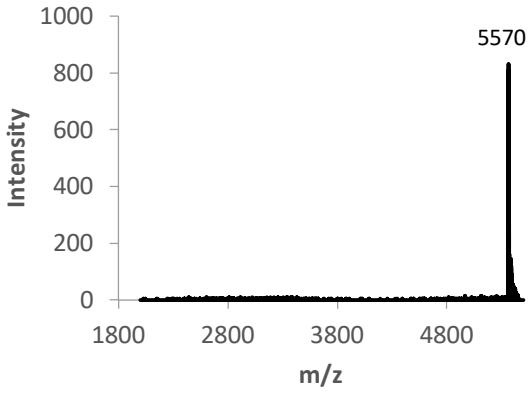

7.1.2. Characterization of γ-PNA synthesis

N^{ε}-(Benzyloxycarbonyl)-L-Lysine Hydrochloride

^{1}H-NMR Spectrum of compound S1

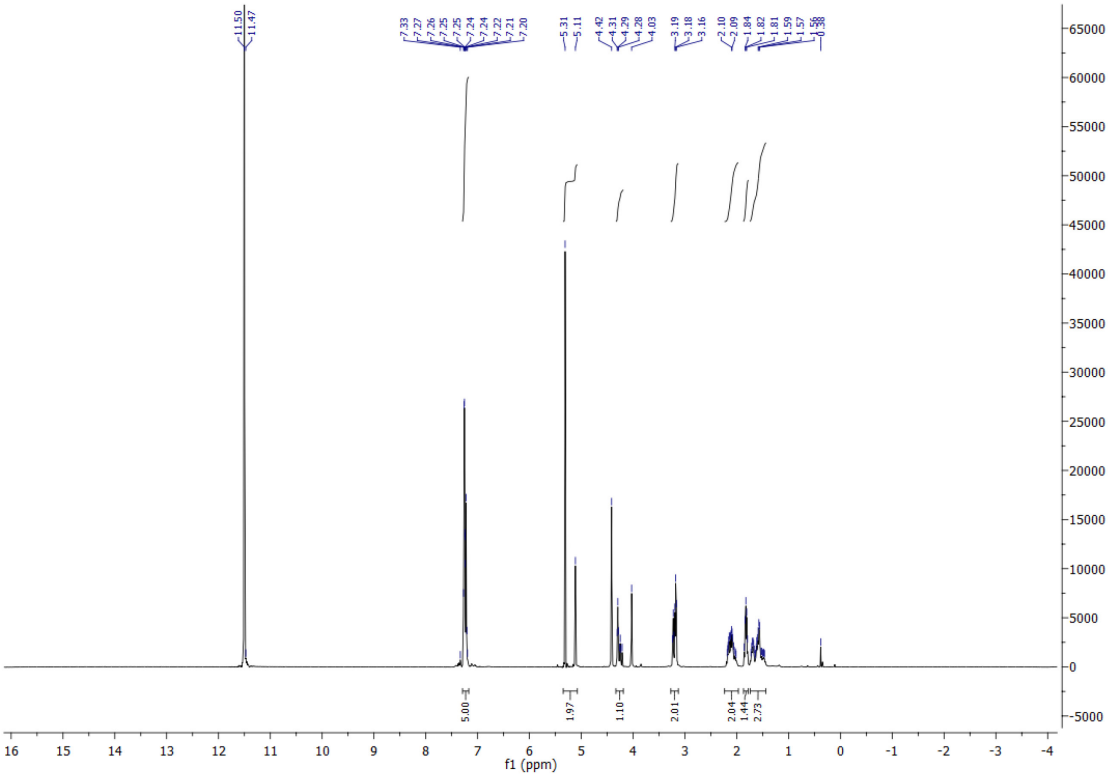

^{13}C-NMR Spectrum of compound S1

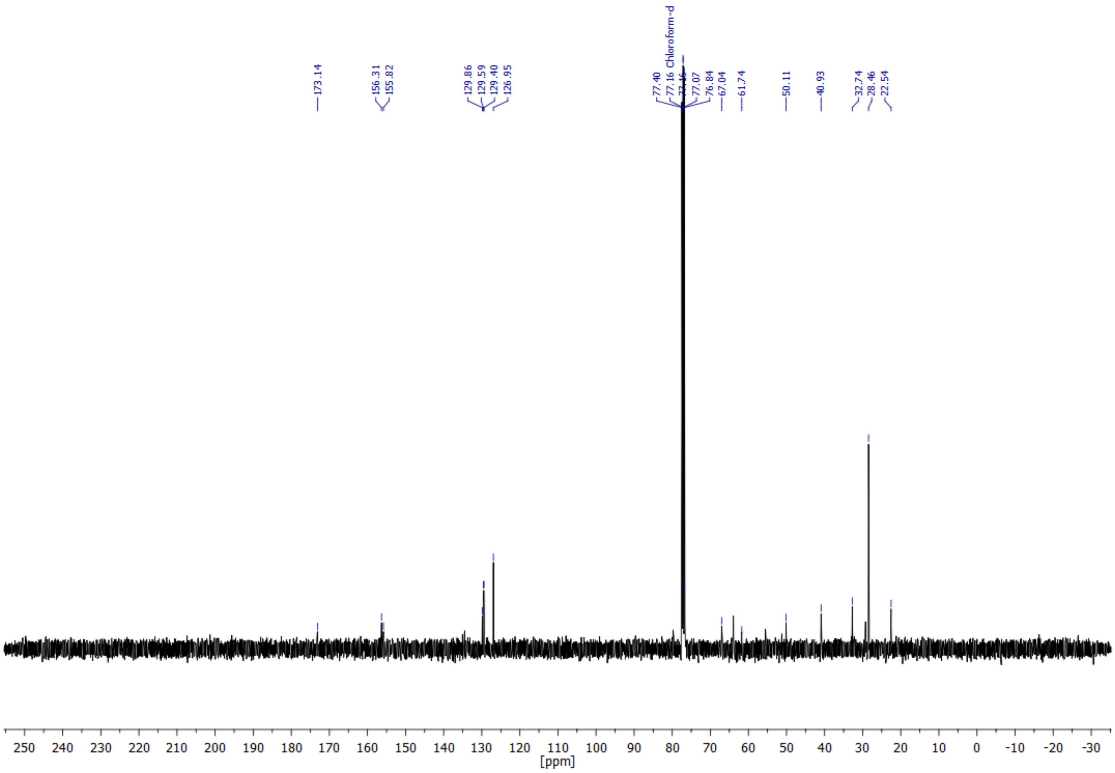

N^{α}-(tert-Butyloxycarbonyl,N^{ε}-(benzyloxycarbonyl)-lysin-Weinrebamide

^{1}H-NMR Spectrum of compound S3

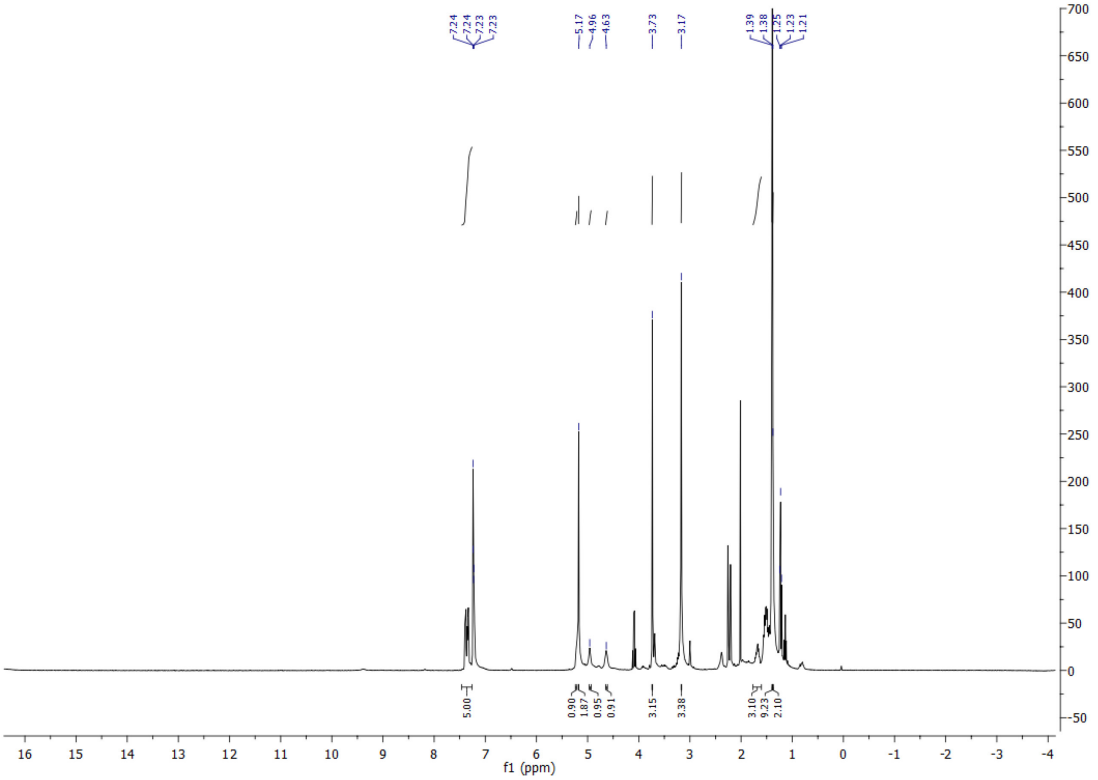

^{13}C-NMR Spectrum of compound S3

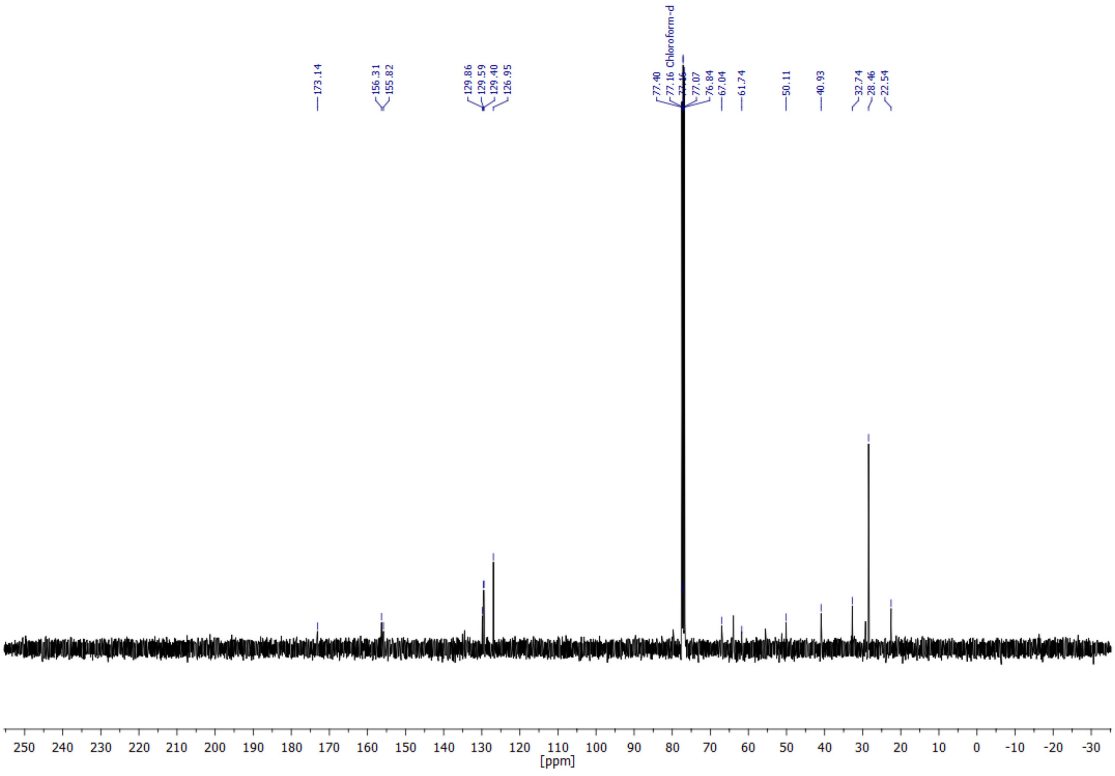

N^{α}-(*tert*-Butyloxycarbonyl)aminoethyl-N^{ε}-benzyloxycarbonyl)glycinmethylester

^{1}H-NMR Spectrum of compound S5

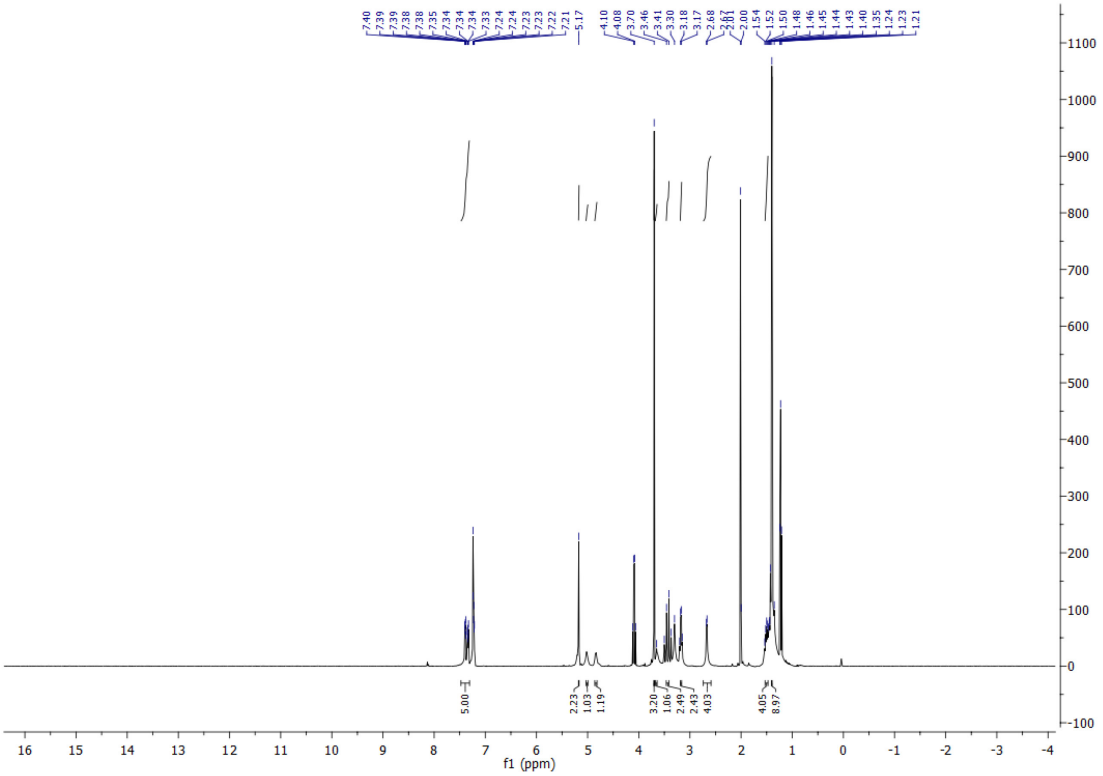

^{13}C-NMR Spectrum of compound S5

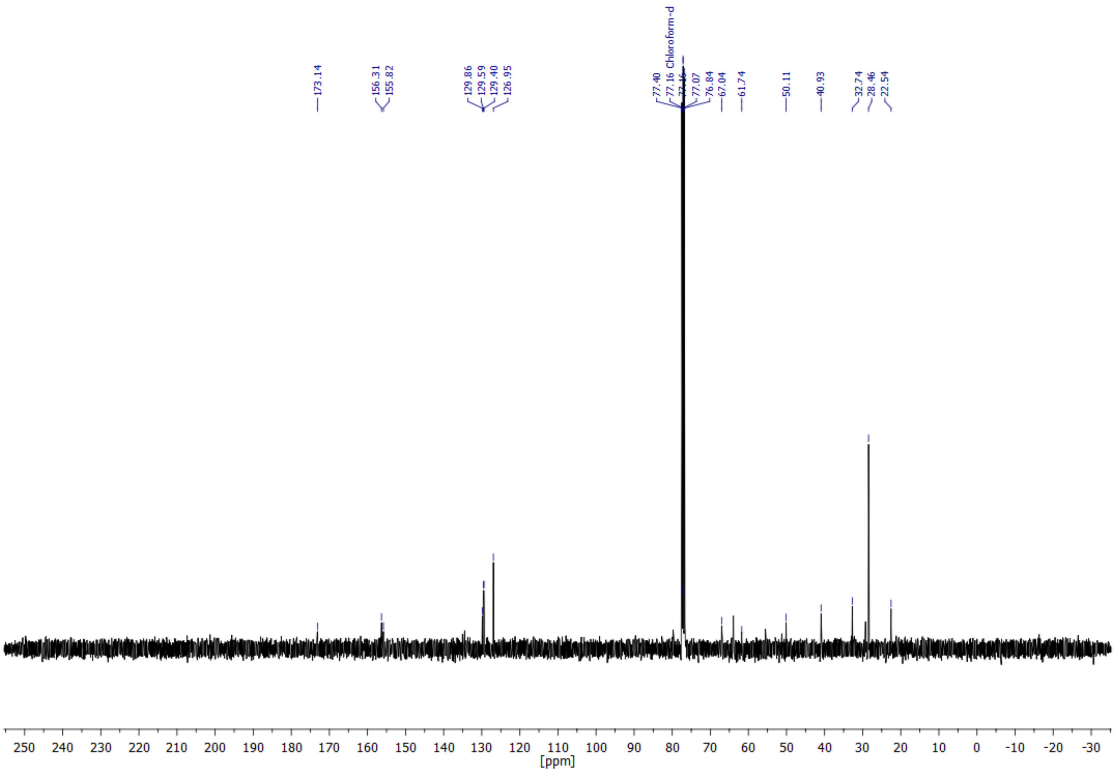

N^{α}-((N^{4}-benzyloxycarbonyl)cytosin-1-yl)acetyl)-N-(2-tert-butyloxycarbonyl)-aminoethyl)-Nε-benzyloxycarbonyl)-glycin

^{1}H-NMR Spectrum of compound S7

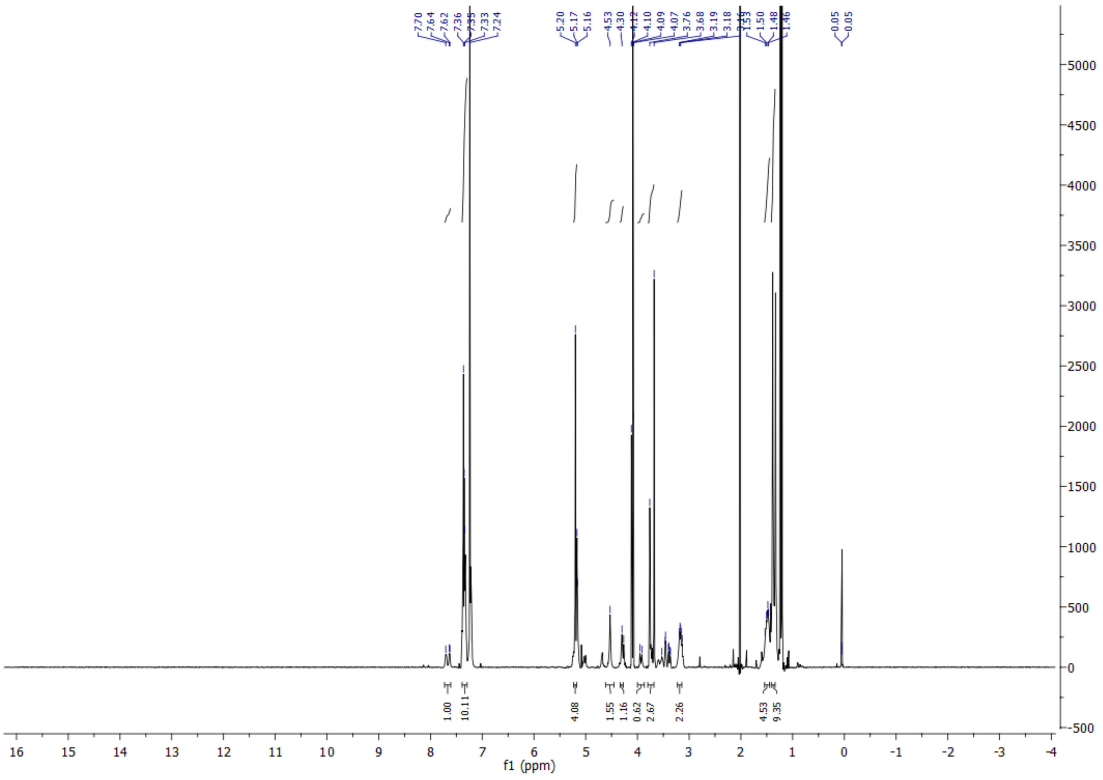

((N^4-Benzyloxycarbonyl)cytosine-1-yl) acetic acid

^{1}H-NMR Spectrum of compound S10

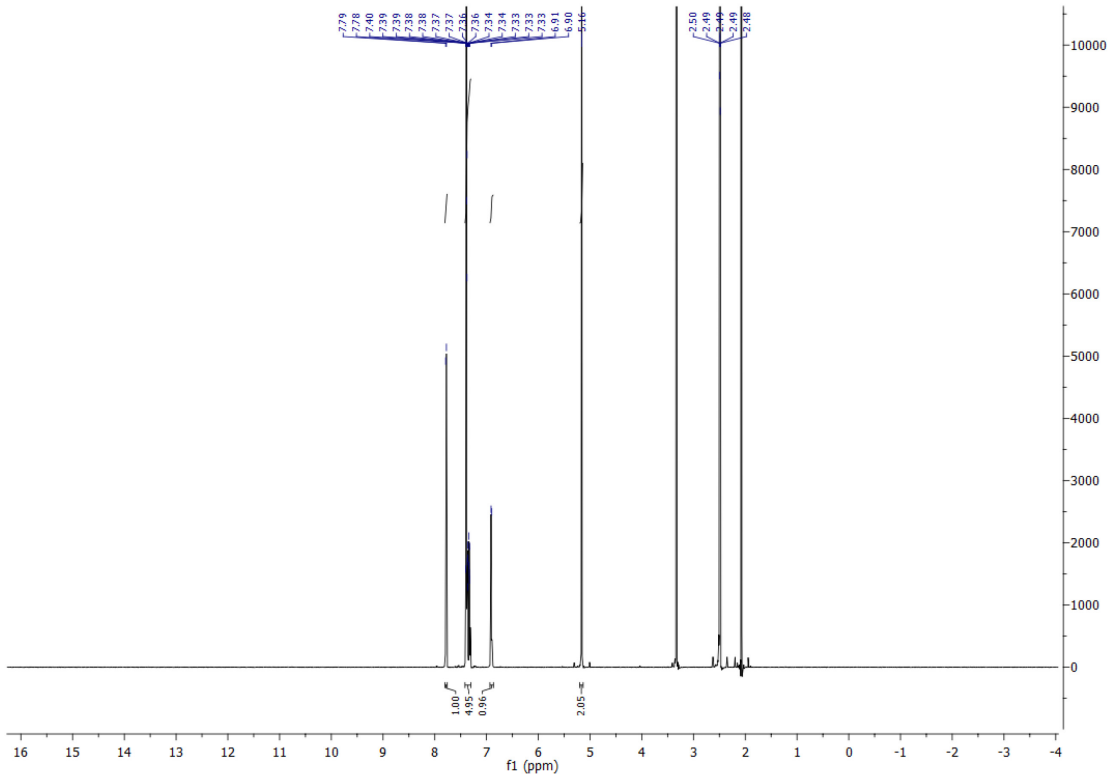

^{13}C-NMR Spectrum of compound S10

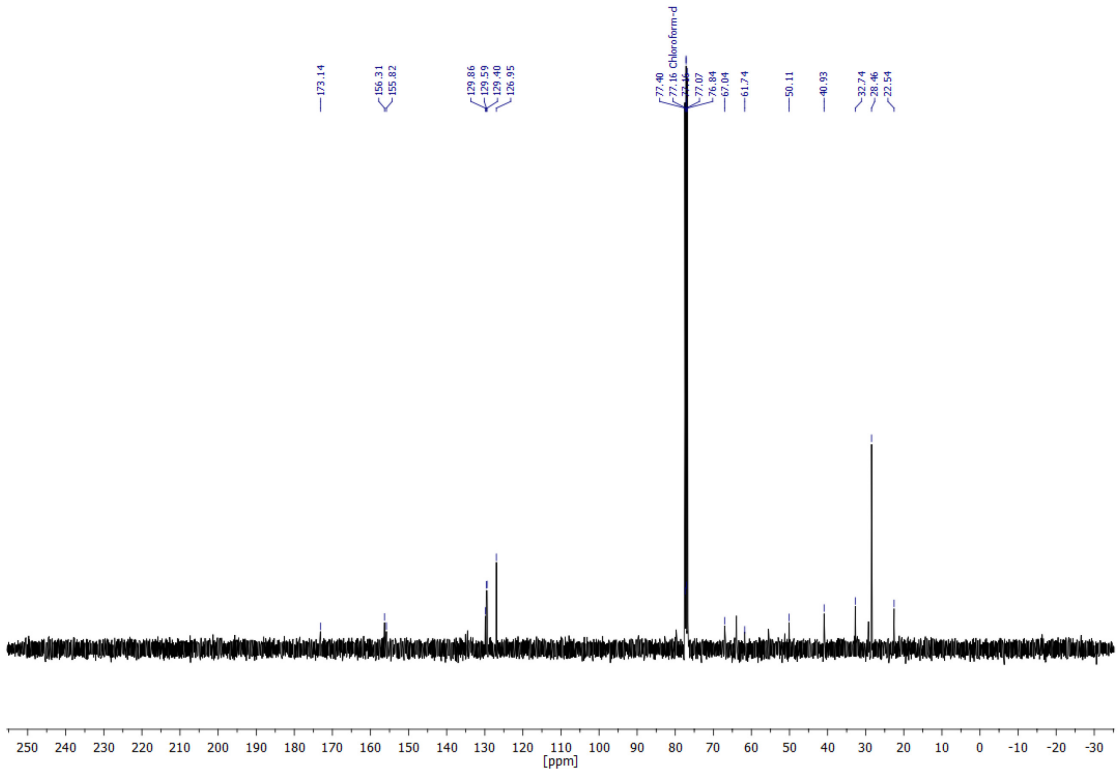

Appendix – Additional Figures

7.3. Acknowledgements

First, I would like to thank my PhD supervisors: Prof. Dr. Oliver Seitz and Prof. Dr. Michael W. Linscheid. Thank you for believing in me for the completion of this project, and thank you for the time that you have invested on my work and development. I appreciate the independency that I had during this time to pursue my own ideas.

I thank the School of Analytical Sciences Adlershof (SALSA) for the financial support for the PhD and after the PhD. Thank you for the interest that you have placed on me and in my development as a scientist. I am grateful for all the workshops, lectures, laboratory courses, and summer universities that the organizing team prepared for us.

Many thanks to Dr. Olalla Vázquez Vázquez, Dr. Gerbrand van der Heden, Dr. Margherita Di Pisa, Georgina Gavins, and Yannic Altrichter for the careful corrections of the first draft of my thesis. Your comments and insight really helped me deliver the thesis that I wanted.

Special thanks to the members of the laboratory 210 of the chemistry department: Georgina Gavins, Yannic Alrichter, Ziv Harpaz, and Oleksandr Zavoiura, as well as the whole Seitz and Linscheid group.

Y en este último párrafo me gustaría agradecer el esfuerzo de mi madre y mi padre. Me lo habéis dado todo incluso cuando no habéis tenido nada para vosotros. Gracias a mis hermanos Aleix y Heitor por animarme a superarme a mí mismo. Por último, gracias a Felipe Niño Duarte por apoyarme, por aguantar lo inaguantable y por ayudarme a ser mejor persona.

List of Publications

H. Faber, H. Lutze, P. Lores Lareo, L. Frensemeier, M. Vogel, T. C. Schmidt, and U. Karst; Liquid chromatography/mass spectrometry to study oxidative degradation of environmentally relevant pharmaceuticals by electrochemistry and ozonation. Journal of Chromatography A, 2014, 1343, 152-159.

P. Lores Lareo, M. W. Linscheid, and O. Seitz; Nucleic acids and SNPs detection via template-directed native chemical ligation and inductively coupled mass spectrometry. Journal of Mass Spectrometry, 2019, 54 (8), 676-683.

7.6. Statement of Authorship

I expressly declare that the work I have submitted was written independently and without external help.

I expressly declare that all sources used in the abovementioned work – including those from the Internet (including tables, graphic, and suchlike) – have been marked as such. In particular, I declare that I have without exception, stated the source for any statements quoted verbatim and/or unmodified tables, graphics etc. (i.e. quotations) of other authors.

I am aware that violations against the principles of academic independence are considered deception and are punished accordingly

Berlin, on November 21st, 2018

Pablo Lores Lareo